Terpenoids for medicine

Fischedick, J.

Terpenoids for Medicine

PROEFSCHRIFT

Ter verkrijging van

de graad van Doctor aan de Universiteit Leiden,

op gezag van Rector Magnificus Professor C.J.J.M. Stolker,

volgens besluit van het College voor Promoties

te verdedigen op 13-03-2013

door

Justin Fischedick

Geboren te New York, United States of America

In 1984

Promotiecommissie

Promotor	Prof. Dr. R. Verpoorte
Co-promotor	Dr. Y.H. Choi
Overige leden	Prof. Dr. P.G.L. Klinkhamer
	Prof. Dr. C.J. ten Cate
	Prof. Dr. I. Merfort
	Dr. T.A. van Beek

Dedicated to my parents!

Cover Photograph: Photographs of *Salvia officinalis*, *Rosmarinus officinalis*, and *Lavandula angustifolia* were taken by author. Photographs of Soxhlet and distillation apparatus were also taken by author. The *Inula Britannica* close up photograph was generously donated by Dr. Slađana Todorović from Institute for Biological Research "Siniša Stanković", University of Belgrade, Belgrade, Serbia.

ISBN: 978-94-6203-281-1

Printed by: WÖHRMANN PRINT SERVICE, 2013

Contents

Chapter 1

General Introduction

Terpenoids, also known as isoprenoids or terpenes, are a large class of natural products found in nearly all living organisms (Oldfield and Lin, 2012). Over 60,000 terpenoid structures have been identified from natural sources making them one of the largest classes of natural products known (Köksal et al., 2011; Berthelot et al., 2012). Terpenoids are perhaps most familiar to us as major components of essential oils produced by various aromatic plants, tree resins such as turpentine, or as cholesterol found in animal cell membranes. Essential oils are composed of mixtures of volatile compounds which are produced by physical processes such as distillation or pressing from the organisms producing them. Due to their volatile nature along with a wide variety of scents and flavors terpenoids are important ingredients in the cosmetic and flavor industries (Schmidt, 2010). It is the purpose of this thesis to investigate aspects of plant terpenoid chemistry relevant to medicine.

History of terpenoid chemistry

Humankind has for thousands of years made use of plants containing terpenoids as medicines, incenses, foods, intoxicants, and even natural rubber. Devices and documents that appear to resemble a water distillation apparatus have been dated back to ancient Mesopotamia from around 3,000 BCE. The ancient Egyptians adopted such primitive distillation practices however the Arabs in the middle ages are often credited as the inventors of distillation. Ad-Dimaschki a 13th century Arabian writer described the distillation of rose water and early improvements on condensation of the vapors. In the 15th century, German physician and scientist Hieronymus Brunschwyk in his book *Liber de Arte Distillandi* (The true art to distill) described the production of 25 essential oils (Figure 1). It should be noted that many of the products of such early distillation practices would not be considered essential oils but rather water or alcohol solutions enriched with volatile compounds (Schmidt, 2010). The medicinal use of aromatic plants is recorded in ancient herbal texts such as *De Materia Medica* written by the Greek herbalist Pedanius Dioscorides in the first century CE. Resins such as myrrh, from *Communphora* and *Balsamodendron* species as well as sandalwood oils from *Santalum* species have been used as far back as ancient Egypt for embalming and cleansing rituals. Aromatic plants are also featured in both traditional Chinese medicine and Ayurvedic medicine (Maffei et al., 2011). Systematic investigations into selection criteria of medicinal plants suggest that smell and taste are important characteristics for incorporation of a plant into traditional medicine systems (Leonti et al., 2003).

Modern terpenoid chemistry began in the 1800's. The German chemist Otto Wallach who was awarded the Nobel Prize in chemistry in 1910 for his achievements in the structure elucidation of monoterpenoids is often regarded as the father of terpenoid chemistry. Wallach began researching terpenoids while working under the direction of another Nobel Prize laureate, August Kekulé in Bonn, Germany (Christmann, 2010). At the time hydrocarbons isolated from plant essential oils with the molecular formula

$C_{10}H_{16}$ which stayed liquid even at low temperatures were known as terpenes, a term coined by Kekulé due to their presence in turpentine oil. Compounds with the molecular formulas $C_{10}H_{16}O$ or $C_{10}H_{14}O$ containing an alcohol or a ketone respectively and could be crystallized or precipitated as solids were known as camphors (Kubeczka, 2010). Through the use of distillation techniques, particularly vacuum and fractional distillation, Wallach and his contemporaries were able to isolate individual essential oil components. By synthesizing terpenoid derivatives which could be crystallized and physical properties such as melting point, optical rotation, boiling point etc., characterized a systematic way of identifying terpenoids was developed. It was also discovered that natural terpenoids could be converted into other natural terpenoids. This sort of chemistry made it possible for quality control of natural essential oils and for the development of the synthetic fragrance and flavor industry. Furthermore, this research revealed that plants within the same genus could produce essential oils of different composition and that species taxonomically far apart could produce the same compounds (Wallach, 1910).

Figure 1. Inside title page of Hieronymus Brunschwyk's *Liber de Arte Distillandi*. Image downloaded from National Library of Medicine website (http://www.nlm.nih.gov).

In 1887 Wallach proposed that monoterpenoids were constructed from two isoprene units (Figure 2). Further development of the isoprene rule was accomplished

by the work of L. Ruzicka, in Zurich, through the structure elucidation of higher terpenes for which he also won the Nobel Prize in 1939 (Kubeczka, 2010). Ruzicka described the main terpene chemical classes as monoterpenoids composed of two isoprene units, sesquiterpenes three isoprene units (C_{15}), diterpenes four isoprene units (C_{20}), and triterpenes six isoprene units (C_{30}) (Ruzicka, 1953). We now know that hemiterpenoids made up of a single isoprene unit (C_5), tetraterpenes (C_{40}), as well as isoprenoid polymers with thousands of units such as rubber are also classes of terpenoids (Berthelot et al., 2012). Since the development of chromatographic techniques and nuclear magnetic spectroscopy (NMR) in the 2nd half of the 20th century the isolation and structure elucidation of thousands of terpenoids has been accomplished. Through improvements in analytical techniques such as gas chromatography (GC), mass spectrometry (MS), GC and MS in tandem (GC-MS), and high performance liquid chromatography (HPLC) identification and quantification of terpenoids from natural sources has become routine.

Figure 2. Isoprene

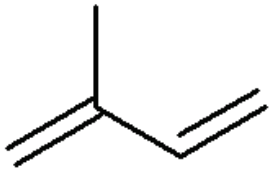

Biosynthesis

The isoprene used in the biosynthesis of terpenoids consists of isopentyl diphosphate (IPP) and dimethylallyl diphosphate (DMAPP). The enzyme isopentyl diphosphate isomerase (IDI), also known as IPP isomerase, converts IPP to DMAPP in a reversible isomerization reaction, regulating the pool of these 2 metabolites (Figure 3) (Berthelot et al., 2012). The mevalonate (MVA) pathway, discovered in the 1950's, was the first biosynthetic pathway elucidated that lead to IPP and DMAPP. The MVA pathway was first identified in yeast and mammals (Rodríguez-Concepción and Boronat, 2002). The MVA pathway is located in the cytosol of most eukaryotes, archaebacteria, as well as some gram positive and gram negative bacteria (Oldfield and Lin 2012; Berthelot et al., 2012). However in the 1990's, another pathway the 2-*C*-methyl-D-erythritol 4 phosphate (MEP) pathway was discovered. The MEP pathway is known to occur in the plastids of terrestrial plants, algae, some protozoa such as malaria parasites, and many eubacteria including *Escherichia coli* (Phillips et al., 2008). Both the MVA and MEP pathways leading to IPP and DMAPP are shown in Figure 4.

Terpenoid biosynthesis begins with the condensation of IPP and DMAPP, except in the case of the hemiterpenoids. The reaction occurs through a 1'-4 so called "head to tail" process beginning with the ionization of DMAPP to remove the diphosphate group forming a carbocation intermediate. The carbocation through nucleophilic attack with double bond in IPP and removal of H^+ forms geranyl diphosphate (GPP). Geranyl diphosphate can be further condensed with IPP to farnesyl

diphosphate (FPP), and again to geranylgeranyl disphosphate (GGPP) (Figure 5). Geranyl diphosphate, FPP, and GGPP are the precursors to the C_{10} monoterpenoids, C_{15} sesquiterpenoids and C_{20} diterpenoids respectively. Both FPP and GGPP can also be condensed in a 1'-2,3 so called "head to head" manner to form C_{30} triterpenoid and C_{40} tetraterpenoid precursors. The C_{30} is used in plants mainly for the production of sterols from squalene while C_{40} for the production of carotenoids from phytoene (Figure 6) (Oldfield and Lin, 2012; Chen et al., 2011). Monoterpenoids, diterpenoids, and tetraterpenoids are mainly synthesized by the MEP pathways while sesquiterpenoids and triterpenoids are mainly synthesized by the MVA pathway, although there are exceptions and cross talk between the 2 pathways occurs (Rodríguez-Concepción and Boronat, 2002; Maffei et al., 2011). The hemiterpene (C_5) isoprene is also biosynthesized in plants mainly from DMAPP by loss of diphosphate group. Terpenoids and their precursors can also be used to post translationally modify proteins (Oldfield and Lin, 2012).

Figure 3. Isopentyl diphosphate isomerase mediated isomerization of IPP and DMAPP.

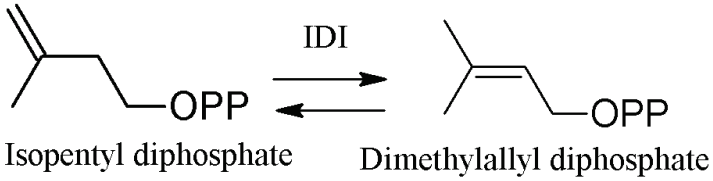

Terpene synthases, also known as terpene cyclases, catalyze the reactions which lead to the wide variety of terpenoid structures. Typically terpene synthases function by ionizing the respective terpenoid precursor, removing the phosphate groups leading to the formation of carbocation intermediates which undergo cyclizations, hydride shifts, or other rearrangements. The reaction is terminated by nucleophile capture often with water or deprotonation (Figure 7). An interesting aspect of terpene synthases is that a single enzyme can sometimes produce multiple terpenoid products and enantiomers (Chen et al., 2004; Degenhardt et al., 2009; Chen et al., 2011). Terpenoid structures can then be further enzymatically altered by hydroxylation, oxidation, reduction, isomerization, further cyclization, or be used as substrates to modify other compound classes (Dewick, 2002; Sell, 2010). Cytochrome P450 enzymes are an important class of proteins known to further modify terpenoids skeletons after they have been formed by terpene synthases (Keeling and Bohlmann, 2006; Mizutani, 2012).

Figure 4. MVA and MEP pathways. **1** Acetyl CoA, **2** acetoacetyl-CoA, **3** 3-hydroxy-3-methylglutaryl-CoA, **4** mevalonate, **5** mevalonate-5-phosphate, **6** mevalonate-5-diphosphate, **7** pyruvate, **8** D-glyceraldehyde 3-phosphate, **9** 1-deoxy-D-xylulose 5-phosphate, **10** 2-*C*-methyl-D-erythritol 4-phosphate, **11** 4-(cytidine 5'-diphospho)-2-*C*-methyl-D-erythritol, **12** 2-*C*-methyl-D-erythritol 2,4-cyclodiphosphate, **13** (*E*)-4-hydroxy-3-methylbut-2-enyl diphosphate. AACT: acetoacetyl-CoA thiolase, HMGS: 3-hydroxy-3-methylglutaryl-CoA synthase, HMGR: 3-hydroxy-3-methylglutaryl-CoA reductase, MVK: mevalonate kinase, PMK: 5-phosphomevalonate kinase, MVD: mevalonate-5-diphosphate decarboxylase, DXS: 1-deoxy-D-xylulose 5-phosphate synthase, DXR: 1-deoxy-D-xylulose 5-phosphate reductoisomerase, MCT: 2-*C*-methyl-D-erythritol 4-phosphate cytidylyltransferase, CMK: 4-(cytidine 5'-diphospho)-2-*C*-methyl-D-erythritol kinase, MDS: 2-*C*-methyl-D-erythritol 2,4-cyclodiphosphate synthase, HDS: (*E*)-4-hydroxy-3-methylbut-2-enyl diphosphate synthase, HDR: (*E*)-4-hydroxy-3-methylbut-2-enyl diphosphate reductase.

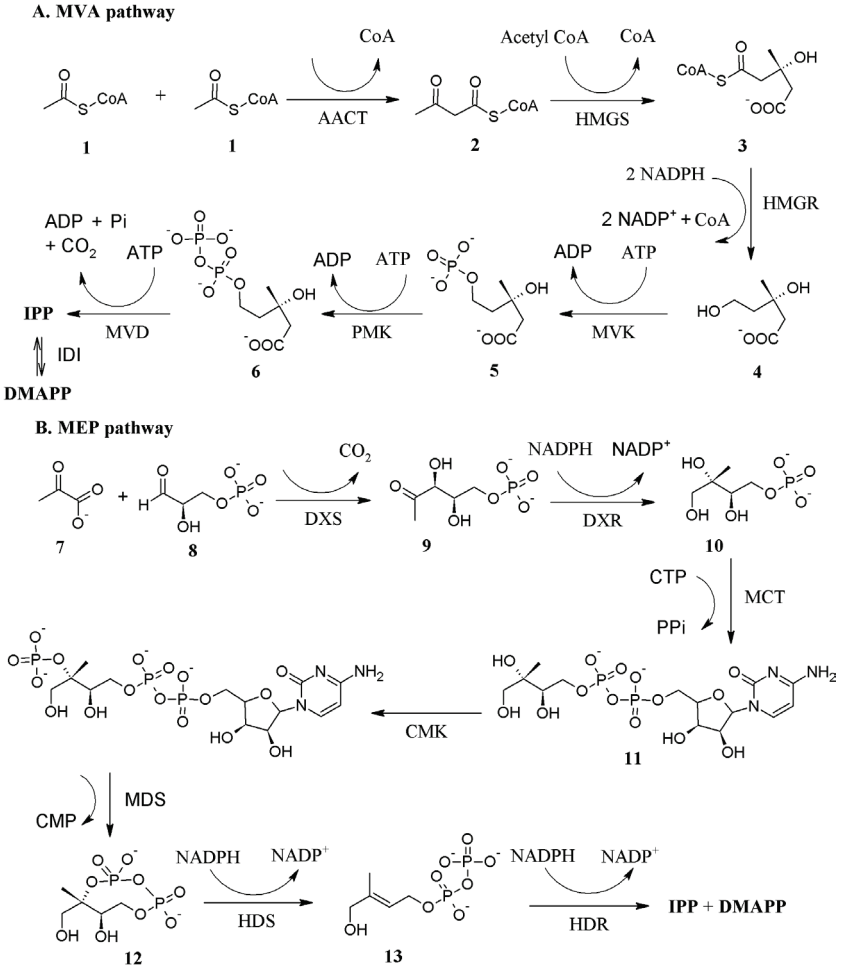

Terpenoid secondary metabolites are often produced and secreted by specialized plant cells in anatomical structures such as glandular trichomes, secretory cavities, and resin ducts. Glandular trichomes are made up of groups of cells which form an outgrowth of the epidermis. The morphology of glandular trichomes can vary considerably (Figure 8) (McCaskill and Croteau, 1998). Glandular trichomes can be divided into two groups peltate and capitate. Peltate trichomes contain a basal cell on the epidermis, a stalk or neck cell, and 4-16 cells on the head which secrete terpenoids into a large subcuticular space. Capitate trichomes contain a smaller subcuticular space and typically 1-4 secreting cells (Franz and Novak, 2010). Citrus fruits secrete essential oils into secretory cavities surrounded by isolated cells located beneath the epicarp. Similar secretory cavities are found in eucalyptus leaves which are located beneath the epidermis (Schmidt, 2010). Pine trees produce terpenoids in layers of cells found within the intercellular space of their bark which can be excreted through resin ducts (Keeling and Bohlmann, 2006).

Figure 5. Biosynthesis of important terpenoid precursors.

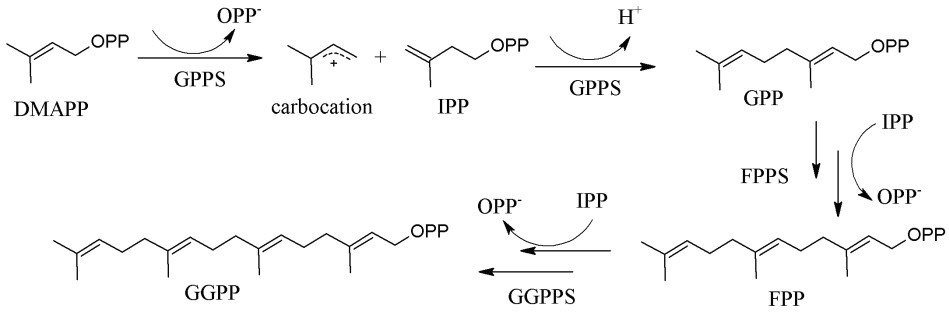

Roles in plant physiology

Certain terpenoids are ubiquitous in plants having essential functions in their physiology and are thus often considered part of primary metabolism. Protein prenylation by C_{15} and C_{20} units is important for transferring and anchoring of cytosol proteins to membranes. Carotenoids make up part of the photosynthetic apparatus and are important plant pigments. Chlorophylls contain a diterpene side chain derived from phytol (Figure 6). Ubiquinones, which are part of the mitochondrial electron transport chain and plastoquinone in the photosynthetic electron carrier chain, both contain polyprenyl isoprenoid units (Lohr et al., 2012). Sterols are important constituents of plant cell membranes and are required for various cellular processes including cell division, elongation, and polarity (Figure 6). Although the mechanisms of plant sterols function remain largely unknown. Plant sterols are also precursors to the steroid hormones, brassinosteroids which are involved in plant growth and development (Figure 6) (Boutte and Grebe, 2009). Another important group of plant hormones are the diterpenoid carboxylic acids known as gibberellins which act as endogenous plant growth regulators (Figure 6) (Hedden and Thomas, 2012).

Figure 6. Examples from terpenoid classes.

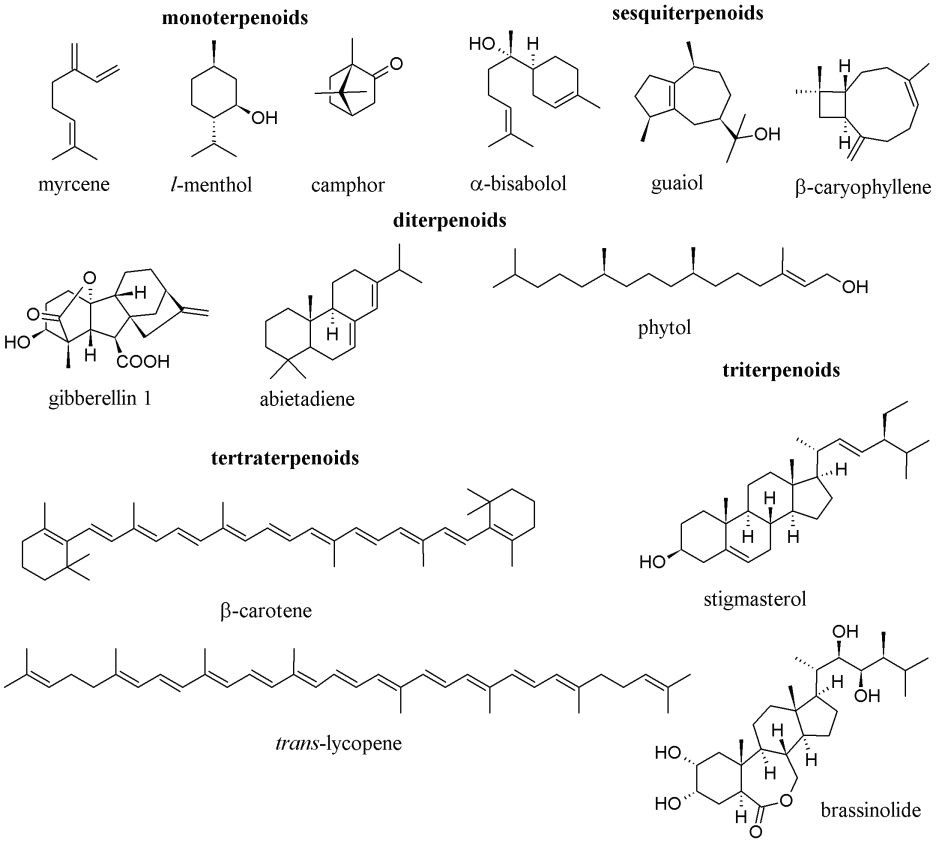

Chemical ecology

The majority of terpenoid chemical diversity found in nature is the result of secondary metabolism. Plants produce terpenoids and other volatile compounds to interact with the surrounding environment. Volatile terpenoids from flowering plants can serve as important environmental cues to attract or deter pollinators. Allelopathic effects from a terpenoid producing plant on other plants in the environment such as growth inhibition or inhibition of seed germination are also known (Maffei et al., 2011). Terpenoids and other plant volatiles can act as defense compounds against herbivores by either direct action against the attacking organism or by attracting natural predators of herbivores (Lucas-Barbosa et al., 2011).

Examples of direct terpenoid defenses against insects include the triterpene glycosides (eg. cardenolides) found in the latex of the milkweed *Asclepias curassavica*. The larvae of *Trichoplusia ni* (Lepidoptera) after feeding on *A. curassavica* have spasms resulting in immobility, taking around 3 days to recover. *Aradopsis thaliana*

genetically modified to produce large amounts of the monoterpene alcohol linalool are more resistant to *Myzus persicae* (aphids) then non-engineered plants which produce very low levels of linalool (Gershenzon and Dudareva, 2007). Conifer resins which often contain mixtures of monoterpenoids, sesquiterpenoids, and diterpenoids have been shown to have important roles in defending trees against bark beetles and pathogenic fungi (Langenheim, 1994; Keeling and Bohlmann, 2006). Saponins (triterpenoid glycosides) can act as detergents disrupting fungal cell membranes leading to toxicity. *Avena strigosa* an oat species which normally produces saponins has mutant varieties which do not produce saponins. Such plants are significantly more susceptible to fungal pathogens (Gershenzon and Dudareva, 2007).

Figure 7. Generalized scheme showing typical reaction mechanisms of monoterpene synthases and subsequent oxidation steps leading to monoterpenoids.

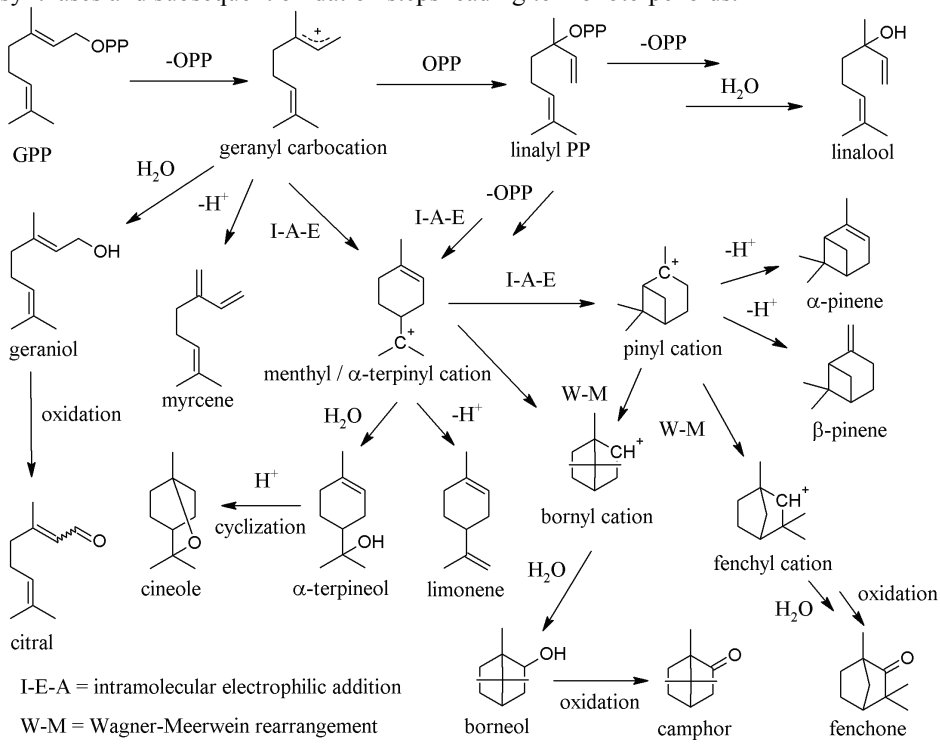

Biological activity

Due to the historical use of terpenoids in medicine and the evolutionary fine tuning of their interactions in natural systems it is no surprise that so many biological activities have been reported. Since there are hundreds of studies dealing with the biological activity of terpenoids the aim of the following sections is not to provide a comprehensive survey of their activity but rather to provide an overview of biological activities important to medicine and understanding subsequent discussions in later

chapters. Throughout the rest of this thesis the focus will be on monoterpenoids, sesquiterpenoids, and diterpenoids. Tripterpenoids and carotenoids are excluded because they are not discussed or studied in subsequent chapters. The term essential oil will be used to refer to essential oils dominated by monoterpenoid and sesquiterpenoid constituents while those containing mostly phenylpropanoids or other compounds will not be discussed. One common chemical feature of many but not all terpenoids is their lipophilic nature. Due to their hydrophobic nature it is often assumed that the biological activity of certain terpenoids is a result of their tendency to partition into cellular membranes and either disrupt membrane integrity or interact with membrane bound proteins (Edris, 2007; Maffei et al., 2011; Solórzano-Santos et al., 2012).

Figure 8. Scanning electron microscope photos of trichomes on floret surfaces of *Tanacetum parthenium* (left) and *Inula britannica* (right). Image generously donated by Dr. Slađana Todorović from Institute for Biological Research "Siniša Stanković", University of Belgrade, Belgrade, Serbia.

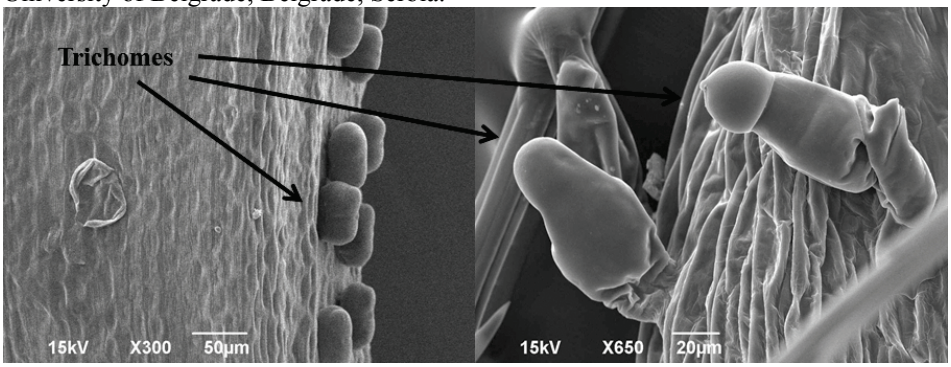

Antimicrobial

One of the most commonly reported biological activities of terpenoids and especially those found in essential oils is their *in-vitro* antimicrobial activity. Thymol and carvacrol, phenolic monoterpenoids commonly found in *Thymus vulgaris* and *Origanum vulgare* essential oils as well as menthol found in peppermint oils are among some of the best studied antimicrobial monoterpenoids (Pauli and Schilcher, 2010; Solórzano-Santos et al., 2012). Due to the fact that essential oils occur in mixtures and their chemical composition can vary so can their antimicrobial effects. This makes clinical trials and pharmaceutical research into essential oils difficult. For example rosemary oil's minimum inhibitory concentration (MIC) against *Staphylococcus aureus* in nine *in-vitro* studies ranged between 20-50,000 µg/mL (Pauli and Schilcher, 2010). Many diterpenoids also exhibit antibacterial and antifungal activities (Hanson, 2007). Antiviral effects of monoterpenoids, sesquiterpenoids, and diterpenoids have also been reported (Sun et al., 2003; Wang et al., 2005; Buchbauer, 2010).

One reason why so many essential oils have *in-vitro* antimicrobial activity is likely due to their non-specific membrane disrupting properties. *In-vitro* antimicrobial data of terpenoids must therefore be interpreted carefully (Maffei et al., 2011).

Furthermore weak or strong *in-vitro* antibacterial data of essential oils does not always correlate well with *in-vivo* results complicating the interpretation of *in-vitro* data even further (Pauli and Schilcher, 2010). While the complex chemical profile of essential oils and weak to moderate antimicrobial activity makes them unlikely candidates for systemic treatment of infections, essential oils do have uses as topical and gastrointestinal antimicrobial agents as well as antiseptics (Maffei et al., 2011). Clinical data regarding the antimicrobial activity of essential oils is unfortunately scarce. Regarding topical application of essential oils studies have shown positive effects against *Propionibacterium acnes* (acne) infections from treatment with *Ocimum gratissimum* (rich in thymol) and tea tree oil (*Melaleuca alternifolia*). A number of studies have also shown promising results against topical fungal infections from various essential oils. However the best clinically studied use of topically administered essential oils is against infectious bacteria of the oral cavity. The commercial mouthrinse Listerine contains 1,8-cineole (cineol), menthol, and thymol as active ingredients (Harris, 2010).

Artemisinin, a sesquiterpene lactone found in *Artemisia annua* (Asteraceae) is an example of a potent antimicrobial terpenoid with specific activity against the malaria parasite, *Plasmodium falciparum* (Figure 9). Artemisinin and its analogues can kill most stages of the parasites life cycle and are currently the main treatments against malaria worldwide (White, 2008). The endoperoxide functionality is necessary for artemisinin's antimalarial activity. Artemisinin's mechanism of action is not entirely understood although there is evidence that once inside the parasite the endoperoxide can be cleaved by an iron source, such as Fe^{2+}. This reaction leads to the formation of radical ion intermediates which bind to various proteins one of which is the sarco-endoplasmic reticulum Ca^{2+}-ATPase (SERCA) thereby killing the organism (O'Neill, 2010).

Inflammation and pain

Many plants containing terpenoids are used in traditional medicine for their anti-inflammatory and pain relieving properties. The Asteraceae family contains many species used traditionally against inflammatory conditions which produce sesquiterpene lactones. One well known example is parthenolide from *Tanacetum parthenium* commonly known as feverfew (Figure 9). The pro-inflammatory transcription factor, nuclear factor kappa B (NF-$_K$B) is inhibited by sesquiterpene lactones which may explain their mechanism of action (Salminen et al., 2008). Many essential oils have been evaluated for anti-inflammatory and analgesic activity in a variety of cellular and animal models (Buchbauer, 2010). Small clinical trials performed with essential oils have demonstrated positive effects against dysmenorrhea (menstrual pain), infantile colic, traumatic or surgical joint related pain, headaches, postherpetic neuralgia, and irritable bowel syndrome (Harris, 2010). Important anti-inflammatory diterpenoids include triptolide found in the traditional Chinese medicinal plant *Tripterygium wilfordii* (Figure 9). Traditionally the plant is used in the treatment of autoimmune conditions. Triptolide may also exert its effects via NF-$_K$B mediated mechanisms (Salminen et al., 2008). The labdane diterpenoid, andrographolide from *Andrographis panuculata,* exhibits anti-inflammatory effects through inhibition of pro-inflammatory mediators tumor necrosis factor α (TNF-α) and interleukin-12 (Figure 9) (Hanson,

2007). Abietane diterpenoids carnosic acid and carnosol found in *Rosmarinus officinalis* (rosemary) and *Salvia officinalis* (sage) also have anti-inflammatory properties. They have been shown to activate the peroxisome proliferator-activated receptor gamma (PPARγ) (Rau et al., 2006) as well as suppress pro-inflammatory responses of human polymorphonuclear leukocytes (Peockel et al., 2008).

Other potential protein targets of terpenoids are the transient receptor potential channels (TRP) also known as vanilloid or capsaicin receptors. These membrane bound receptors are known to be involved in sensing hot or cold temperatures and other noxious stimuli. Compounds such as (-)-menthol and camphor exhibit their cooling sensations by interacting with TRP's (Maffei et al., 2011). The TRP vanilloid-3 (TRPV3) is known to be involved in skin inflammation and peripheral nerve injuries. Camphor and cineol not only activate the TRPV3 but desensitize the receptor after long term exposure which may explain their mechanism as topical analgesics (Sherkheli et al., 2009). Sesquiterpene dialdehyes which are pungent ingredients in certain spices also activate vanilloid receptors (Szallasi et al., 1998). The cannabinoid receptors, CB1 and CB2 are G protein coupled receptors. They are the primary targets of cannabinoids, part terpenoid and part polyketide compounds found in *Cannabis sativa* L (cannabis). The CB1 receptor is located primarily on central and peripheral neurons while the CB2 receptor is located primary on immune cells. Many of the pain relieving, anti-inflammatory, and psyschoactive effects of cannabinoids are mediated through the CB1 and CB2 receptors (Pertwee, 2009). Interestingly the dietary sesquiterpenoid, β-caryophyllene is a potent and selective CB2 receptor agonist with anti-inflammatory properties. Many herbs and spices including cannabis, cinnamon, and black pepper contain significant amounts of β-caryophyllene (Gertsch, 2008).

Inflammation and pain

Many plants containing terpenoids are used in traditional medicine for their anti-inflammatory and pain relieving properties. The Asteraceae family contains many species used traditionally against inflammatory conditions which produce sesquiterpene lactones. One well known example is parthenolide from *Tanacetum parthenium* commonly known as feverfew (Figure 9). The pro-inflammatory transcription factor, nuclear factor kappa B (NF-$_K$B) is inhibited by sesquiterpene lactones which may explain their mechanism of action (Salminen et al., 2008). Many essential oils have been evaluated for anti-inflammatory and analgesic activity in a variety of cellular and animal models (Buchbauer, 2010). Small clinical trials performed with essential oils have demonstrated positive effects against dysmenorrhea (menstrual pain), infantile colic, traumatic or surgical joint related pain, headaches, postherpetic neuralgia, and irritable bowel syndrome (Harris, 2010). Important anti-inflammatory diterpenoids include triptolide found in the traditional Chinese medicinal plant *Tripterygium wilfordii* (Figure 9). Traditionally the plant is used in the treatment of autoimmune conditions. Triptolide may also exert its effects via NF-$_K$B mediated mechanisms (Salminen et al., 2008). The labdane diterpenoid, andrographolide from *Andrographis panuculata,* exhibits anti-inflammatory effects through inhibition of pro-inflammatory mediators tumor necrosis factor α (TNF-α) and interleukin-12 (Figure 9) (Hanson,

2007). Abietane diterpenoids carnosic acid and carnosol found in *Rosmarinus officinalis* (rosemary) and *Salvia officinalis* (sage) also have anti-inflammatory properties. They have been shown to activate the peroxisome proliferator-activated receptor gamma (PPARγ) (Rau et al., 2006) as well as suppress pro-inflammatory responses of human polymorphonuclear leukocytes (Peockel et al., 2008).

Figure 9. Structures of biologically active terpenoids.

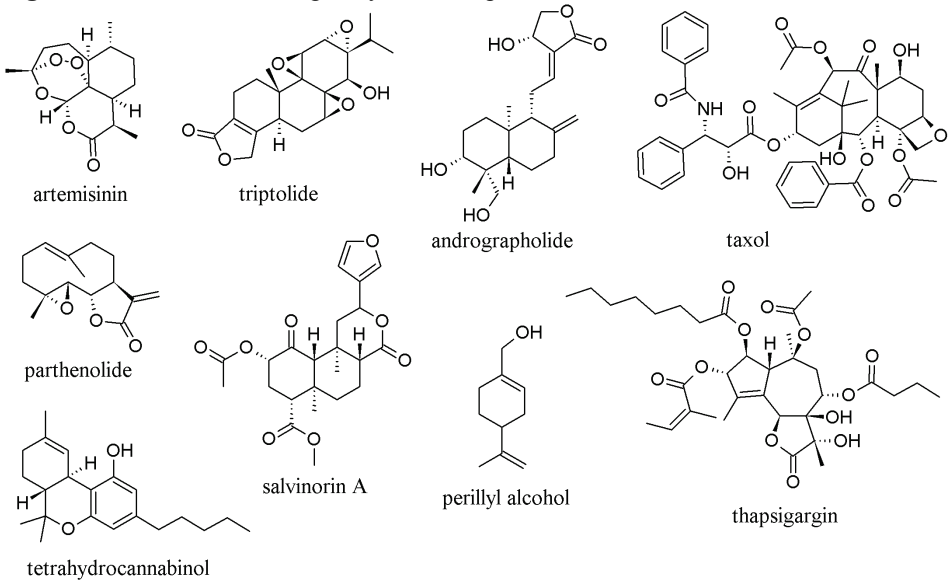

Other potential protein targets of terpenoids are the transient receptor potential channels (TRP) also known as vanilloid or capsaicin receptors. These membrane bound receptors are known to be involved in sensing hot or cold temperatures and other noxious stimuli. Compounds such as (-)-menthol and camphor exhibit their cooling sensations by interacting with TRP's (Maffei et al., 2011). The TRP vanilloid-3 (TRPV3) is known to be involved in skin inflammation and peripheral nerve injuries. Camphor and cineol not only activate the TRPV3 but desensitize the receptor after long term exposure which may explain their mechanism as topical analgesics (Sherkheli et al., 2009). Sesquiterpene dialdehyes which are pungent ingredients in certain spices also activate vanilloid receptors (Szallasi et al., 1998). The cannabinoid receptors, CB1 and CB2 are G protein coupled receptors. They are the primary targets of cannabinoids, part terpenoid and part polyketide compounds found in *Cannabis sativa* L (cannabis). The CB1 receptor is located primarily on central and peripheral neurons while the CB2 receptor is located primary on immune cells. Many of the pain relieving, anti-inflammatory, and psyschoactive effects of cannabinoids are mediated through the CB1 and CB2 receptors (Pertwee, 2009). Interestingly the dietary sesquiterpenoid, β-caryophyllene is a potent and selective CB2 receptor agonist with anti-inflammatory properties. Many herbs and spices including cannabis, cinnamon, and black pepper contain significant amounts of β-caryophyllene (Gertsch, 2008).

Cytotoxic, antitumor, and anticancer

In the following section cytotoxic compounds will refer to compounds which inhibit cancer cells *in-vitro*, antitumor to those which inhibit tumor growth *in-vivo*, and anticancer to those being used to treat cancer in humans. An important anticancer diterpene is taxol, also known as paclitaxel isolated from the bark of *Taxus* species (Figure 9). Taxol is used in the treatment of a variety of cancers such as ovarian, breast, and lung cancer (Wang et al., 2005). The anticancer effects of taxol are due to its ability to promote polymerization of tubulin into stable microtubules, which thereby prevent mitosis. Structure activity relationships of taxols anticancer properties revealed that the oxetane ring and aromatic substituents are important for the drugs activity (Kingston, 1994). Many other diterpenoids also exhibit cytotoxic or antitumor properties (Hanson, 2007). Interestingly many of the same diterpenoids mentioned above as having anti-inflammatory activity also have cytotoxic and antitumor activities. Andrographolide has antitumor properties which may also be mediated by inhibition of NF-$_{K}$B (Gunn et al., 2011; Kuttan et al., 2011). Carnosic acid and carnosol have cytotoxic and antitumor properties (Johnson, 2011; Ngo et al., 2011).

Many sesquiterpenoids have been reported to have cytotoxic activity (Modzelewska et al., 2005). Sesquiterpene lactones are among the most well studied cytotoxic sesquiterpenoids. Extensive structure activity relationships have demonstrated that the α-methylene-γ-lactone moiety is often, although not always necessary for cytotoxicity. Through a Michael addition reaction the α-methylene-γ-lactone functionality can act as a nucleophile reacting with cysteine residues on proteins forming a protein adduct. As with anti-inflammatory activity an important target protein for sesquiterpene lactones cytotoxic activity is NF-$_{K}$B. Parthenolide is an example of an antitumor sesquiterpene lactone containing the α-methylene-γ-lactone (Ghantous et al., 2010). However it is important to note that the α-methylene-γ-lactone group is also responsible for certain sesquiterpene lactones causing contact dermatitis (Lepoittevin et al., 2009) and toxicity in mammals (Robles et al., 1995). Thapsigargin, from *Thapsia garganica* and *Thapsia gymnesica* is an example of a sesquiterpene lactone that does not contain an unsaturated lactone yet still possesses antitumor activity (Figure 9). The main mechanism of inducing apoptosis by thapsigargin is inhibition of SERCA which causes an increase in cytoplasmic Ca^{2+} leading to cell death (Drew et al., 2009). Artemisinin also lacks the unsaturated lactone functionality yet also exhibits anti-tumor activity through a similar mechanism as against malaria. Interestingly parthenolide, thapsigargin, and artemisinin all seem to exhibit selectively towards cancer cells *in-vivo*. Analogues of all 3 compounds are being developed as anti-cancer drugs (Ghantous et al., 2010).

Monoterpenoids such as limonene and its main metabolite in humans, perillyl alcohol exhibit antitumor activities (Figure 9). Other monoterpenoid alcohols such as geraniol, linalool, carveol prevent tumor formation in chemically induced tumor animal models. Many essential oils have also been tested for cytotoxic and antitumor properties (Buchbauer, 2010). Despite much research *in-vitro* and in animals, clinical trials with

monoterpenoids are scarce. Perillyl alcohol has been tested in phase II clinical trials however no anti-cancer effects were observed in advanced ovarian, colorectal, or breast cancer. A reduction in tumor size was noted in a trial with recurrent malignant gliomas (Harris, 2010). A phase I and II trial to assess anticancer potential of limonene demonstrated that limonene was well tolerated however was only able to exhibit a partial response in one patient. The researchers note however that the dose which was the maximum tolerated dose for each patient may not be appropriate and suggested further research (Vigushin et al., 1998).

Central nervous system

The most obvious effect of terpenoids can have on the central nervous system (CNS) is odor perception. Why exactly humans maintain the evolutionary traits which allow us to sense and discriminate so many volatile terpenoids is not entirely clear. Terpenoids are not directly linked to the nutritional value of a plant when compared to other plant volatiles derived from essential nutrients such as fatty acids or carotenoids. The antimicrobial effects of many spices containing terpenoids suggest that cultural preferences for certain flavors may have developed throughout history due to health promoting or food preservation benefits (Goff and Klee, 2006). Olfactory receptors are located primarily on neurons in nasal cavities. About 380 genes encode for human olfactory receptors. Another, approximately 400 non-functional pseudogenes can be found in the human genome suggesting that olfactory genes were lost throughout primate evolution (Niimura and Nei, 2003; Schmiedeberg, 2007). In contrast with other senses, olfactory information can bypass the thalamus and directly link with areas of the brain involved in emotion and memory such as the amygdala, frontal cortex, hypothalamus, and hippocampus (Kandal et al., 2000). Furthermore due to their lipophilic nature terpenoids are able to pass the blood brain barrier (BBB) and interact directly with the brain. Both mechanisms are important because odorous terpenoids can have a direct pharmacological action in the brain, such as interaction with a neural receptor, and a psychological component through the olfactory system (Heuberger, 2010).

Essential oils used commonly in folk medicine and pure monoterpenoids have been demonstrated to cause sedative and stimulating effects in mice (Buchbauer et al., 1993). Psychopharmacological effects of essential oils and pure monoterpenoids in animals include anxiolytic, anticonvulsant, antidepressant, and hypnotic effects (Nunes et al., 2010). Mechanisms of action have been investigated. Lemon oil vapor increases metabolism of dopamine in the hippocampus and serotonin in the prefrontal cortex and striatum which may explain its anxiolytic and antidepressant effects in mice (Komiya et al., 2006). The anticonvulsant effects of linalool may be mediated by interactions with NMDA receptors (Brum et al., 2001). The effects of essential oils and pure fragrances on human cognition have also been investigated. Examples of higher cognitive functions studied include alertness and attention as well as learning and memory. Unfortunately most studies do not report chemical composition of the essential oil under investigation and dose response curves are not established. Therefore it is difficult to draw clear relationships between essential oils and their effects on higher cognitive functions in humans (Heuberger, 2010).

Terpenoids can also have profound effects on human consciousness. *Salvia divinorum* is used by Mazatec traditional healers for divination. The plant is often chewed or smoked to produce hallucinations necessary for their healing rituals. The main active ingredient is salvinorin A, a neoclerodane diterpenoid (Figure 9). Salvinorin A is one of the most potent non-nitrogenous natural hallucinogens known with doses as little as 200-500 μg inducing hallucinatory experiences. The psychoactive effects of salvinorin A are due to its ability to act as a selective K-opioid receptor agonist (Vortherms and Roth, 2006). The cannabinoid, Δ^9-tetrahydrocannabinol (THC) is the primary psychoactive ingredient in cannabis (Figure 9). The psychoactive effects of THC are mediated mainly through the CB1 receptor (Pertwee, 2009). Clinical studies demonstrate potential of cannabinoids and cannabis in treating chronic neuropathic pain, as appetite stimulants in cancer patients undergoing chemotherapy as well as AIDS patients, and treatment of multiple sclerosis (Amar, 2006; Hazekamp and Grotenhermen, 2010).

Thesis outline and goals

Throughout this discussion a number of issues become apparent with regards to complications in the development of terpenoids and plants containing them as drugs. One major issue is that plants and products derived from them such as essential oils or extracts are often of variable or unknown chemical composition. Another issue concerns administration forms of volatile terpenoids. Often protocols for administering essential oils vary between studies and controlled dosing is difficult. Finally for many terpenoids the mechanisms of action and structure activity relationships are still unknown. Therefore the major goals of this thesis are:

1. Investigate vaporization as an administration form for volatile terpenoids in various medicinal plants.
2. Determine if plants can be standardized to produce reproducible levels of active components in order to improve clinical research.
3. Isolate and study the biological activity of medically interesting sesquiterpenoids and diterpenoids.

In chapter 2 a device designed to administer plant volatile compounds called a vaporizer was investigated. Some common terpenoid producing plants with medicinal properties were selected and tested in the device. The essential oil content and terpenoid content of the vapor was analyzed with GC and GC-MS. In chapter 3, cannabis was used as a model plant to test the vaporizer in more detail, compare it with cannabis smoke, and test whether any components in the smoke or vapor altered the CB1 binding of THC *in-vitro*. In order to determine if plants producing terpenoids can be standardized for their chemical content cannabis was again chosen as a model plant. In chapter 4 a number of cannabis varieties grown in multiple batches under the same environmental conditions were analyzed with GC-FID and GC-MS. Multivariant data analysis was used to chemically classify the varieties. The reproducibility of the chemical profiles was determined. The plants studied in chapters 5-7 were investigated

as part of a larger projet to further study their biological activity and their biosynthesis called the Terpmed project (EU grant number 227448). Chapter 5 focuses on the isolation and biological activity of sesquiterpenoids from *T. parthenium*. The isolated compounds were tested as activators of a biological pathway emerging as a potential drug target for neurodegenerative disease, the nuclear factor E2-related factor 2 / Kelch-like ECH-associated protein 1 pathway. This same pathway is investigated for diterpenoids isolated from *S. officinalis* in chapter 7. In chapter 6 sesquiterpene lactones isolated from *Inula britannica* were studied for their cytotoxic activity in drug susceptible cancer cell lines and multi drug resistant cancer cell lines. Finally chapter 8 discusses the overall conclusions from these investigations and future perspectives.

References:

Ben Amar, M., 2006. Cannabinoids in medicine: A review of their therapeutic potential. Journal of Ethnopharmacology 105, 1–25.

Berthelot, K., Estevez, Y., Deffieux, A., Peruch, F., d&eacute, ric, 2012. Isopentenyl diphosphate isomerase: A checkpoint to isoprenoid biosynthesis. Biochimie 94, 1621–1634.

Boutté, Y., Grebe, M., 2009. Cellular processes relying on sterol function in plants. Current Opinion in Plant Biology 12, 705–713.

Brum, L.F., Elisabetsky, E., Souza, D., 2001. Effects of linalool on [(3)H]MK801 and [(3)H] muscimol binding in mouse cortical membranes. Phytotherapy Research 15, 422–425.

Buchbauer, G., 2010. Biological Activities of Essential Oils, in: Handbook of essential oils : science, technology, and applications. CRC Press/Taylor & Francis, Boca Raton.

Buchbauer, G., Jirovetz, L., Jäger, W., Plank, C., Dietrich, H., 1993. Fragrance compounds and essential oils with sedative effects upon inhalation. Journal of Pharmaceutical Sciences 82, 660–664.

Chen, F., Ro, D.-K., Petri, J., Gershenzon, J., Bohlmann, J., Pichersky, E., Tholl, D., 2004. Characterization of a Root-Specific Arabidopsis Terpene Synthase Responsible for the Formation of the Volatile Monoterpene 1,8-Cineole. Plant Physiology 135, 1956–1966.

Chen, F., Tholl, D., Bohlmann, J., Pichersky, E., 2011. The family of terpene synthases in plants: a mid-size family of genes for specialized metabolism that is highly diversified throughout the kingdom. The Plant Journal 66, 212–229.

Christmann, M., 2010. Otto Wallach: Founder of Terpene Chemistry and Nobel Laureate 1910. Angewandte Chemie International Edition 49, 9580–9586.

Degenhardt, J., Köllner, T.G., Gershenzon, J., 2009. Monoterpene and sesquiterpene synthases and the origin of terpene skeletal diversity in plants. Phytochemistry 70, 1621–1637.

Dewick, P.M., 2002. Medicinal Natural Products: A Biosynthetic Approach. John Wiley & Sons.

Drew, D., Krichau, N., Reichwald, K., Simonsen, H., 2009. Guaianolides in apiaceae: perspectives on pharmacology and biosynthesis. Phytochemistry Reviews 8, 581–599.

Edris, A.E., 2007. Pharmaceutical and therapeutic Potentials of essential oils and their individual volatile constituents: a review. Phytotherapy Research 21, 308–323.

Franz, C., Novak, J., 2010. Sources of Essential Oils, in: Handbook of essential oils : science, technology, and applications. CRC Press/Taylor & Francis, Boca Raton.

Gershenzon, J., Dudareva, N., 2007. The function of terpene natural products in the natural world. Nature Chemical Biology 3, 408–414.

Gertsch, J., Leonti, M., Raduner, S., Racz, I., Chen, J.-Z., Xie, X.-Q., Altmann, K.-H., Karsak, M., Zimmer, A., 2008. Beta-caryophyllene is a dietary cannabinoid. Proceedings of the National Academy of Sciences of the United States of America 105, 9099–9104.

Ghantous, A., Gali-Muhtasib, H., Vuorela, H., Saliba, N.A., Darwiche, N., 2010. What made sesquiterpene lactones reach cancer clinical trials? Drug Discovery Today 15, 668–678.

Goff, S.A., Klee, H.J., 2006. Plant Volatile Compounds: Sensory Cues for Health and Nutritional Value? Science 311, 815–819.

Gunn, E.J., Williams, J.T., Huynh, D.T., Iannotti, M.J., Han, C., Barrios, F.J., Kendall, S., Glackin, C.A., Colby, D.A., Kirshner, J., 2011. The natural products parthenolide and andrographolide exhibit anti-cancer stem cell activity in multiple myeloma. Leukemia & Lymphoma 52, 1085–1097.

Hanson, J.R., 2007. Diterpenoids. Natural Product Reports 24, 1332–1341.

Harris, B., 2010. Phytotherapeutic Uses of Essential Oils, in: Handbook of essential oils : science, technology, and applications. CRC Press/Taylor & Francis, Boca Raton.

Hazekamp, A., Grotenhermen, F., 2010. Review on clinical studies with cannabis and cannabinoids 2005-2009. Cannabinoids 5, 1–21.

Hedden, P., Thomas, S.G., 2012. Gibberellin biosynthesis and its regulation. The Biochemical Journal 444, 11–25.

Heuberger, E., 2010. Central Nervous System Effects of Essential Oils in Humans, in: Handbook of essential oils : science, technology, and applications. CRC Press/Taylor & Francis, Boca Raton.

Johnson, J.J., 2011. Carnosol: a promising anti-cancer and anti-inflammatory agent. Cancer Letters 305, 1–7.

Kandel, E.R., Schwartz, J.H., Jessell, T.M., 2000. Principles of Neural Science, Fourth Edition. McGraw-Hill.

Keeling, C.I., Bohlmann, J., 2006. Genes, enzymes and chemicals of terpenoid diversity in the constitutive and induced defence of conifers against insects and pathogens. The New Phytologist 170, 657–675.

Kingston, D.G., 1994. Taxol: the chemistry and structure-activity relationships of a novel anticancer agent. Trends in Biotechnology 12, 222–227.

Köksal, M., Hu, H., Coates, R.M., Peters, R.J., Christianson, D.W., 2011. Structure and mechanism of the diterpene cyclase ent-copalyl diphosphate synthase. Nature Chemical Biology 7, 431–433.

Kumiya, M., Takeuchi, T., Harada, E., 2006. Lemon oil vapor causes an anti-stress effect via modulating the 5-HT and DA activities in mice. Behavioural Brain Research 172, 240–259.

Kubeczka, K.-H., 2010. History and Sources of Essential Oil Research, in: Handbook of Essential Oils : Science, Technology, and Applications. CRC Press/Taylor & Francis, Boca Raton.

Kuttan, G., Pratheeshkumar, P., Manu, K.A., Kuttan, R., 2011. Inhibition of tumor progression by naturally occurring terpenoids. Pharmaceutical Biology 49, 995–1007.

Langenheim, J.H., 1994. Higher plant terpenoids: a phytocentric overview of their ecological roles. Journal of Chemical Ecology 20(6) p. 1223-1280.

Leonti, M., Fernando, R., Sticher, O., Heinrich, M., 2003. Medicinal Flora of the Popoluca, Mexico: A botanical systematical perspective. Economic Botany 57, 218–230.

Lepoittevin, J.-P., Berl, V., Giménez-Arnau, E., 2009. Alpha-methylene-gamma-butyrolactones: versatile skin bioactive natural products. Chemical Record 9, 258–270.

Lohr, M., Schwender, J., Polle, J.E.W., 2012. Isoprenoid biosynthesis in eukaryotic phototrophs: a spotlight on algae. Plant Science: An International Journal of Experimental Plant Biology 185-186, 9–22.

Lucas-Barbosa, D., van Loon, J.J.A., Dicke, M., 2011. The effects of herbivore-induced plant volatiles on interactions between plants and flower-visiting insects. Phytochemistry 72, 1647–1654.

Maffei, M.E., Gertsch, J., Appendino, G., 2011. Plant volatiles: Production, function and pharmacology. Natural Product Reports 28, 1359.

McCaskill, D., Croteau, R., 1999. Strategies for bioengineering the development and metabolism of glandular tissues in plants. Nature Biotechnology 17, 31–36.

Mizutani, M., 2012. Impacts of diversification of cytochrome P450 on plant metabolism. Biological & Pharmaceutical Bulletin 35, 824–832.

Modzelewska, A., Sur, S., Kumar, S.K., Khan, S.R., 2005. Sesquiterpenes: natural products that decrease cancer growth. Current Medicinal Chemistry. Anti-cancer Agents 5, 477–499.

Moss, M., Cook, J., Wesnes, K., Duckett, P., 2003. Aromas of rosemary and lavender essential oils differentially affect cognition and mood in healthy adults. The International Journal of Neuroscience 113, 15–38.

Ngo, S.N.T., Williams, D.B., Head, R.J., 2011. Rosemary and cancer prevention: preclinical perspectives. Critical Reviews in Food Science and Nutrition 51, 946–954.

Niimura, Y., Nei, M., 2003. Evolution of olfactory receptor genes in the human genome. Proceedings of the National Academy of Sciences 100, 12235–12240.

Nunes, D.S., Linck, V.M., Silva, A.L., Figueiro, M., Elisabetsky, E., 2010. Psychopharmacology of Essential Oils, in: Handbook of essential oils : science, technology, and applications. CRC Press/Taylor & Francis, Boca Raton.

O'Neill, P.M., Barton, V.E., Ward, S.A., 2010. The Molecular Mechanism of Action of Artemisinin—The Debate Continues. Molecules 15, 1705–1721.

Oldfield, E., Lin, F.-Y., 2012. Terpene biosynthesis: modularity rules. Angewandte Chemie International Edition English 51, 1124–1137.

Pauli, A., Schilcher, H., 2010. In vitro Antimicrobial Activities of Essential Oils Monographed in the European Pharmacopoeia 6th Edition, in: Handbook of essential oils : science, technology, and applications. CRC Press/Taylor & Francis, Boca Raton.

Pertwee, R.G., 2009. Emerging strategies for exploiting cannabinoid receptor agonists as medicines. British Journal of Pharmacology 156, 397–411.

Phillips, M.A., León, P., Boronat, A., Rodríguez-Concepción, M., 2008. The plastidial MEP pathway: unified nomenclature and resources. Trends in Plant Science 13, 619–623.

Poeckel, D., Greiner, C., Verhoff, M., Rau, O., Tausch, L., Hörnig, C., Steinhilber, D., Schubert-Zsilavecz, M., Werz, O., 2008. Carnosic acid and carnosol potently inhibit human 5-lipoxygenase and suppress pro-inflammatory responses of stimulated human polymorphonuclear leukocytes. Biochemical Pharmacology 76, 91–97.

Rau, O., Wurglics, M., Paulke, A., Zitzkowski, J., Meindl, N., Bock, A., Dingermann, T., Abdel-Tawab, M., Schubert-Zsilavecz, M., 2006. Carnosic acid and carnosol, phenolic diterpene compounds of the labiate herbs rosemary and sage, are activators of

the human peroxisome proliferator-activated receptor gamma. Planta Medica 72, 881–887.

Robles, M., Aregullin, M., West, J., Rodriguez, E., 1995. Recent studies on the zoopharmacognosy, pharmacology and neurotoxicology of sesquiterpene lactones. Planta Medica 61, 199–203.

Rodríguez-Concepción, M., Boronat, A., 2002. Elucidation of the Methylerythritol Phosphate Pathway for Isoprenoid Biosynthesis in Bacteria and Plastids. A Metabolic Milestone Achieved through Genomics. Plant Physiology 130, 1079–1089.

Ruzicka, L., 1953. The isoprene rule and the biogenesis of terpenic compounds. Cellular and Molecular Life Sciences 9, 357–367.

Salminen, A., Lehtonen, M., Suuronen, T., Kaarniranta, K., Huuskonen, J., 2008. Terpenoids: natural inhibitors of NF-kappaB signaling with anti-inflammatory and anticancer potential. Cellular and Molecular Life Sciences 65, 2979–2999.

Schmidt, E., 2010. Production of Essential Oils, in: Handbook of Essential Oils : Science, Technology, and Applications. CRC Press/Taylor & Francis, Boca Raton.

Schmiedeberg, K., Shirokova, E., Weber, H.-P., Schilling, B., Meyerhof, W., Krautwurst, D., 2007. Structural determinants of odorant recognition by the human olfactory receptors OR1A1 and OR1A2. Journal of Structural Biology 159, 400–412.

Sell, C., 2010. Chemistry of Essential Oils, in: Handbook of essential oils : science, technology, and applications. CRC Press/Taylor & Francis, Boca Raton.

Sherkheli, M.A., Benecke, H., Doerner, J.F., Kletke, O., Vogt-Eisele, A.K., Gisselmann, G., Hatt, H., 2009. Monoterpenoids induce agonist-specific desensitization of transient receptor potential vanilloid-3 (TRPV3) ion channels. Journal of Pharmacy & Pharmaceutical Sciences 12, 116–128.

Solórzano-Santos, F., Miranda-Novales, M.G., 2012. Essential oils from aromatic herbs as antimicrobial agents. Current Opinion in Biotechnology 23, 136–141.

Sun, I.-C., Kashiwada, Y., Morris-Natschke, S.L., Lee, K.-H., 2003. Plant-derived terpenoids and analogues as anti-HIV agents. Current Topics in Medicinal Chemistry 3, 155–169.

Szallasi, A., Bíró, T., Modarres, S., Garlaschelli, L., Petersen, M., Klusch, A., Vidari, G., Jonassohn, M., De Rosa, S., Sterner, O., Blumberg, P.M., Krause, J.E., 1998. Dialdehyde sesquiterpenes and other terpenoids as vanilloids. European Journal of Pharmacology 356, 81–89.

Vigushin, D.M., Poon, G.K., Boddy, A., English, J., Halbert, G.W., Pagonis, C., Jarman, M., Coombes, R.C., 1998. Phase I and pharmacokinetic study of D-limonene in patients with advanced cancer. Cancer Research Campaign Phase I/II Clinical Trials Committee. Cancer Chemotherapy and Pharmacology 42, 111–117.

Vortherms, T.A., Roth, B.L., 2006. Salvinorin A: from natural product to human therapeutics. Molecular Interventions 6, 257–265.

Wallach, O., 1910. Alicyclic Compounds. Nobel Lecture.

Wang, G., Tang, W., Bidigare, R.R., 2005. Terpenoids As Therapeutic Drugs and Pharmaceutical Agents, in: Zhang, L., Demain, A.L. (Eds.), Natural Products. Humana Press, pp. 197–227.

White, N.J., 2008. Qinghaosu (artemisinin): the price of success. Science 320, 330–334.

Chapter 2

Analysis of essential oil vapors produced by a vaporizing device

Justin Fischedick

Natural Products Laboratory, Institute of Biology, Leiden University, 2300 RA Leiden, The Netherlands

Abstract

In order to improve the ability to study the pharmacology of essential oils reproducible administration forms are needed. Vaporizers are devices that heat up plant material in order to release their volatile components from plant matrix for inhalation. In this study we analyzed the vapor produced by a vaporizing device from a selection of common herbs using gas chromatography. *Lavandula angustifolia, Thymus vulgaris, Matricaria recutita, Salvia officinalis*, *Eucalyptus globulus,* and *Melissa officinalis* were selected as model plants for this study because of their well studied essential oils. *Lavandula. angustifolia, T. vulgaris, M. recutita,* and *S. officinalis* all produced detectable (>0.1 mg/g) levels of essential oil components in the vapor. Levels of compounds increased with temperature. These results suggest that vaporizing devices may be useful for the controlled administration of plant essential oils.

Introduction

Many medicinal and food plants contain volatile compounds commonly known as essential oils. Essential oils have many practical uses ranging from herbal medicines to cosmetics and foodstuffs. Aromatherapy involves inhaling volatile compounds either from whole plant preparations or pure essential oils for therapeutic effects or relaxation (Lahlou, 2004a; Lahlou, 2004b). Potential therapeutic effects of inhaled essential oils include antimicrobial, antiviral, anti-carcinogenic, sedative, analgesic, anxiolytic, and anti-inflammatory effects (Edris, 2007). Despite a long history of using essential oils the molecular mechanisms of action and therapeutic efficacy of many plant volatiles are largely unknown (Maffei et al., 2011). Although some clinical trials have been performed on essential oils administered in an aromatherapy setting, most have weak experimental designs and thus the effectiveness of such approaches is questionable (Yim et al., 2009; Cooke and Ernst, 2000).

One approach to improve research into essentials oils is to use methodology that allows for controlled dosing and manipulation of the essential oil or herb under study. Safe and effective methods for administering essential oils may be possible with the use of vaporizing devices. Vaporizers are devices that heat plant material below combustion temperatures in order to volatilize plant compounds for inhalation, ideally without generating carcinogenic polynuclear aromatic hydrocarbons (PAH) associated with smoked plant material. The Volcano® is a sophisticated vaporizing device that utilizes a temperature controlled heat flow to fill a plastic bag with plant vapors. After filling the bag it is removed from the heat source and connected to a mouthpiece for inhalation. Vaporizer technology has been employed for the inhalation of cannabinoids, the main compounds found in *Cannabis sativa* in a clinical setting (Abrams et al., 2007).

The purpose of this study is to examine whether or not the volcano can reproducibly volatilize essential oil components found in 6 common medicinal plants. Gas chromatography with flame ionization detection (GC-FID) and mass spectrometry (GC-MS) was used to analyze the major components found in the essential oil and vapor of common herbs with well-known essential oils. *Lavandula angustifolia* (lavender), *Thymus vulgaris* (thyme), *Matricaria recutita* (chamomile), *Salvia officinalis* (sage), *Eucalyptus globulus,* and *Melissa officinalis* (lemon balm) were chosen for this study.

Thymus vulgaris is a popular herb used in cooking as well as industry. The essential oil has many interesting biological properties including antimicrobial, antifungal, and antioxidant activity. Monoterpenoids make up the majority of *T. vulgaris* essential oil with thymol being the major component as well as carvacrol, *p*-cymene, and γ-terpinene (Dawidowicz et al., 2008). Both thymol and carvacrol have been shown to be antimicrobial against oral bacteria. When utilized in combination they display a synergistic enhancement of antimicrobial activity (Didry et al., 1994).

The essential oil of *L. angustifolia* is well studied due to its extensive use in

foods and cosmetics as well as for its medicinal properties. Linalool is a major component of *L. angustifolia* essential oil along with eucalyptol and camphor (Da Porto et al., 2009). There is some clinical evidence that administration of *L. angustifolia* essential oil by aromatherapy has a significant relaxation effect (Shiina et al., 2008). Linalool has been shown to exhibit anticonvulsant properties (Silva Brum et al., 2001). Anti-inflammatory and analgesic effects have also been demonstrated in mice after administration of *L. angustifolia* essential oil (Hajhashemi et al., 2003). Anxiolytic effects have also been observed after the inhalation of *L. angustifolia* essential oils in rats (Shaw et al., 2007). The essential oil of *S. officinalis* has been shown to inhibit human acetylcholinesterase (AChE) and butyrylcholine esterase (BuChE) (Savelev et al., 2004). In a double blind clinical trial daily administration of a *S. officinalis* tincture significantly reduced cognitive impairment in patients with Alzheimer's disease which may be mediated by AChE or BuChE activity (Akhondzadeh and Abbasi, 2006).

Matricaria recutita is a popular herb used for a variety of minor ailments such as indigestion, inflammation, and for its antimicrobial action. The oil is composed of mostly sesquiterpenoids such as α-bisabolol, oxides of α-bisabolol, and chamazulene (Ganzera et al., 2006). *Matricaria recutita* may be helpful to women delivering birth for pain relief, as well as for relaxing and sedative effects (McKay and Blumberg, 2006). *Eucalyptus globulus* essential oil is mainly composed of eucalyptol a monoterpenoid and has been traditionally used for treatment of respiratory illnesses. The oil has analgesic, anti-inflammatory, and antimicrobial effects (Silva et al., 2003; Cermelli et al., 2008). *Melissa officinalis* essential oil contains the monoterpenoids citral and citronellal, as well as the biologically active sesquiterpenoid β-caryophyllene. The herb is often used for the treatment of digestive ailments and for its relaxing properties (Sadraei et al., 2003).

Materials and Methods

Chemicals and reagents

All organic solvents were of analytical reagent grade and purchased from Biosolve BV (Valkenswaard, The Netherlands). Camphor, carvacrol, 1,8-cineol (eucalyptol), (+)-borneol, (-)-linalool, α-humulene (humulene), α-bisabolol, β-pinene and thymoquinone were purchased from Sigma Aldrich (Steinheim, Germany). β-Caryophyllene (caryophyllene) ≥ 80% purity was purchased from SAFC Supply Solutions (Saint Louis MO, USA). Chamazulen, thymol and geraniol were purchased from Chromadex (Boulder CO, USA). Stock solutions of each compound were made in ethanol and stored in -20 °C.

Plant materials

Thymus vulgaris, *L. angustifolia*, *M. recutita*, *E. globulus* and *M. officinalis* were purchased from A.J. Van Der Pigge Drogisterij (Haarlem, The Netherlands). *Salvia officinalis* and an additional sample of *M. officinalis* were purchased from Jacob Hooy (Limmen, The Netherlands). *Lavandula angustifolia* and *M. recutita* were

supplied as dried mostly flower top material. *Thymus vulgaris, E. globulus* and *M. officinalis* were supplied as dried leaf material. *Salvia officinalis* was supplied as a mixture of dried leaves, flower material and stems.

The volcano vaporizer and vapor collection

The volcano was purchased from Storz & Bickel GmbH & Co (Tuttlingen, Germany). The device was used in a manner similar to that described in the manual provided by the manufacturer. In order to assess the effect of temperature on vaporization 3 different temperature settings were used 100, 150 and 200 °C. One gram of plant material was heated on the volcano vaporizer per sample until the bag was full, which took approximately 45 seconds. Once the bag was full it was removed from the heat flow. Vapors were collected immediately by placing the volcano mouth piece onto the bag and attaching it to a plastic filter holder which held a glass fiber filter (44 mm in diameter). Vapor was gradually sucked onto the glass fiber filter under vacuum. Each sample was performed in triplicate at each temperature setting with a new g of plant material and fresh glass fiber filter. Between each vapor collection volcano parts exposed to vapor and plant material were ultrasonicated for 30 seconds in EtOH, rinsed with EtOH and dried under a stream of air. The bag was also filled with hot air and emptied 3 times to ensure that no residual vapors remained from previous plant samples. Vapor samples were extracted by placing glass fiber filters into 15 ml falcon tubes and extracting the filter two times with 5 ml ethanol with 15 min of gentle shaking during each extraction. Both ethanol extracts were pooled to a volume total volume of 10 ml. Samples were then centrifuged for 5 min at 2000 rpm. Supernatant was transferred to a glass vial for GC-MS and GC-FID analysis.

Determination of plant essential oil content

In order to determine the total essential oil content of each plant 20 g of plant material was steam distilled in a Clevenger apparatus for 3 h. Plant essential oils yields were determined in samples with a volume ≥ 100 µl. Essential oils were diluted in EtOH or hexane to various concentrations and analyzed by GC-FID and GC-MS. The density of each essential oil was measured by weighing 10 µl of oil on an analytical balance (0.01 mg). Dilutions in ethanol for thymol, linalool, eucalyptol, and geraniol ranging from 0.05 mg/ml to 1 mg/ml and dilutions for chamazulen, carvacrol, camphor, and α-humulene ranging from 0.1 mg/ml to 1 mg/ml were used for quantitative analysis on the GC-FID. Reproducibility of the GC-FID was determined by injecting a *L. angustifolia* vapor sample (200 °C) 3 times and calculating % relative standard deviation (%RSD) of eucalyptol, linalool, and geraniol.

Gas chromatographic analysis

An Agilent gas chromatograph 6890 series with an FID detector was used for quantitative essential oil and vapor analysis (Agilent Technologies Inc., Santa Clara, CA, USA). The instrument was equipped with a 7683 series injector and autosampler, plus a 6890 series integrator. A Varian VA-5ms (5% phenyl polysiloxane) column with a length of 30 m, an I.D. of 0.25 mm and a film thickness of 0.25 µm was used for all

samples (Varian Inc., Walnut Creek, CA, USA). Injection volume was 2 µl and split ratio was 1:20. Temperature program was the following: injector 180 °C, FID detector 190 °C, oven start 60 °C, oven rise 3 °C/min, oven final 180 °C, final temperature hold 5 min and total run time was 45 min per sample.

A Varian 3800 GC equipped with an 8200 autosampler and a Saturn 2000 GC/MS ion trap mass detector was used for identification of essential oil and vapor components. The column was a DB-5ms with a length of 30 m, an I.D. of 0.25 mm and a film thickness of 0.25 µm. The split ratio was 1:20. Temperature program was the following; injector 230 °C, oven start 60 °C, oven rise 3 °C/min, oven final 240 °C, final temperature hold 5 min and total run time was 65 min. The ion trap temperature was 220 °C, the manifold 60 °C and the transfer line was 275 °C. Varian MS workstation version 6.9.1 software was used for instrument control and data analysis.

Table 1: Essential oil yield and % composition.

Plant	yield (% v/w)	Essential oil components
Thymus vulgaris	1.5	thymol (66%), cymene (12%), γ-terpinene (8%), carvacrol (3%), β-caryophyllene (1%)
Lavandula angustifolia	3.5	linalool (43%), eucalyptol (28%), geraniol (11%), γ-terpineol (5%), camphor (4%)
Salvia officinalis	1.5	camphor (29%), thujone (29%), eucalyptol (12%), camphene (8%), humulene (2%)
Matricaria recutita	< 1	bisabolol oxide A (77%), bisabolol oxide B (11%), α-bisabolol (8%), chamazulene (< 1%)
Eucalyptus globulus	1.7	eucalyptol (74%), α-pinene (10%)
Melissa officinalis	< 1	citronellal (5%), β-caryophyllene (10%), caryophyllene oxide (32%)

Results and Discussion

Essential oil and vapor components were identified on the basis of their mass spectrum and retention time comparison with authentic standards. Table 1 shows the yield of essential oils from each plant as well as the major components identified. The approximate percentage composition of essential oil components is based on peak area comparison in the FID detector. Standard curves were linear in the ranges analyzed (Table 2). The %RSD for eucalyptol, linalool, and geraniol from a *L. angustifolia* vapour sample (200 °C) after 3 injections was 2.1%, 1.0%, and 1.0% respectively suggesting that the GC-FID was reproducible for analysis of essential oil components. Identified essential oil components present in the vapor at levels > 0.1 mg/g were quantified in the essential oil and vapor samples (Figure 1).

Table 2. Response factor and r^2 value for standard curves.

Compound	Response factor	r^2
thymol	201550	0.996
eucalyptol	183907	0.999
linalool	200260	0.999
geraniol	191963	1.000
carvacrol	209572	0.998
camphor	198536	0.999
α-humulene	228170	1.000
chamazulene	174133	0.987

Figure 1. Quantitative analysis (mg/g of plant material) of major vapor and essential oil (EO) components.

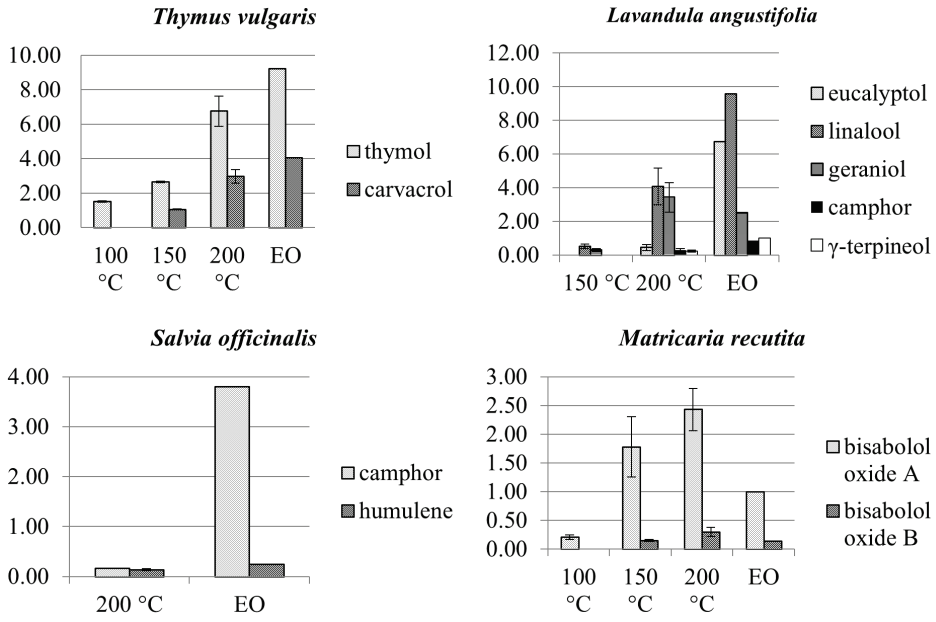

Thymus vulgaris, *L. angustifolia*, *S. officinalis*, and *M. recutita* all had major components of their essential oils enter the vapor with levels increasing with temperature (Figure 1). A representative GC-MS chromatogram comparing *L. angustifolia* vapor with its essential oil shows the 5 major components present in the essential oil are also present in the vapor at 200 °C (Figure 2). Although qualitatively similar the vapor samples differed both in absolute and relative quantitative terms from the total essential oil content. *Lavandula angustifolia* essential oil had eucalyptol as the 2nd major component while in the vapor at 200 °C geraniol is the 2nd major component. In *M. recutita*, bisabolol oxide A and B were present in higher concentrations in the

vapor than in the essential oil. The same was true for geraniol in *L. angustifolia*. Such quantitative variation could result from differences in efficiency of steam distillation versus the vaporizing technique or from chemical conversions of the essential oil components. Some compounds volatilized very efficiently from their plant matrix in the vaporizer. At 200 °C, 73% of the total thymol found in the essential oil of *T. vulgaris* was detected in the vapor and in *L. angustifolia* 43% of the linalool. No compound varied by more than 2 mg/g in vapor samples indicating that the volcano is capable of reproducibly delivering essential oil compounds.

Figure 2. GC-MS trace *Lavandula angustifolia* essential oil (top) compared to vapor collected at 200°C (bottom). 1 = eucalyptol, 2 = linalool, 3 = camphor, 4 = terpineol, 5 = geraniol.

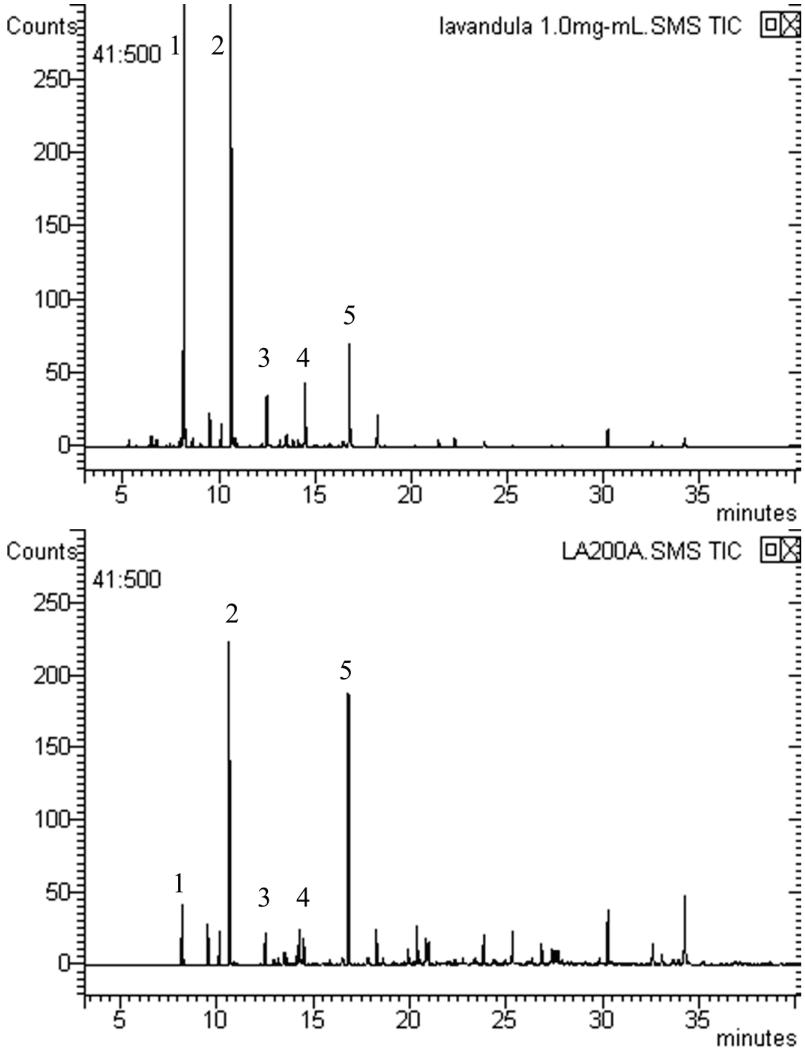

No essential oil components were detected at a concentration above 0.1 mg/g in vapor samples of *E. globulus* and *M. officinalis* on the GC-FID detector. *Melissa officinalis* had a low yield of essential oil (< 1%), which could explain why no components were detected in the vapor. A second batch of *M. officinalis* was purchased from a separate herb supplier and analyzed in the same manner. No essential oil components were detected in the vapor and the essential oil yield was again < 1%. This suggests that the lack of compounds detected was due to low amounts of terpenoids in the *M. officinalis* analyzed. *Eucalyptus globulus* had a higher yield of essential oil (1.7%) when compared to *M. officinalis* but no compounds were detected in vapor samples. An experiment was attempted where *E. globulus* leaves were soaked in water for 0.5 h and then vaporized in the same manner as the dry leaves but still no compounds were detected. Terpenoids in *E. globulus* are produced in secretory cavities beneath the epidermis (McCaskill and Croteau, 1998). This result suggests that the vaporizer is less efficient for volatiles from plants which are stored in secretory cavities as opposed to trichomes.

Overall these results demonstrate that volatile terpenoid components of aromatic plants can be produced by a vaporizing device. It is difficult to speculate whether or not the doses observed in the herb vapors would be enough to induce a clinical effect because so few well controlled clinical studies on monoterpenoids have been conducted. However, following oral administration of an equivalent of 1.08 mg thymol detectable levels of thymol metabolites were observed in human urine and blood (Kohlert et al., 2002). A pilot clinical trial conducted on dementia patients with orally administered *Salvia lavandulaefolia* (50 µl) 1-3 times daily was enough to produce significant improvements in cognition and inhibition of AChE *in-vivo* (Perry et al., 2003). Another recent study observed that different essential oils were capable of maintaining their antimicrobial activity in the vapor phase (Nedorostova et al., 2011). Based on such literature reports it is possible that the levels of terpenoid components produced by the vaporizer in this study are within a range that may be appropriate for further research into their effects on humans or animals.

References

Abrams, D.I., Vizoso, H.P., Shade, S.B., Jay, C., Kelly, M.E., Benowitz, N.L., 2007. Vaporization as a smokeless cannabis delivery system: a pilot study. Clinical Pharmacology and Therapeutics 82, 572–578.

Akhondzadeh, S., Abbasi, S.H., 2006. Herbal medicine in the treatment of Alzheimer's disease. American Journal of Alzheimer's Disease and Other Dementias 21, 113–118.

Cermelli, C., Fabio, A., Fabio, G., Quaglio, P., 2008. Effect of eucalyptus essential oil on respiratory bacteria and viruses. Current Microbiology 56, 89–92.

Cooke, B., Ernst, E., 2000. Aromatherapy: a systematic review. British Journal of General Practice 50, 493–496.

Da Porto, C., Decorti, D., Kikic, I., 2009. Flavour compounds of Lavandula angustifolia L. to use in food manufacturing: Comparison of three different extraction methods. Food Chemistry 112, 1072–1078.

Dawidowicz, A., Rado, E., Wianowska, D., Mardarowicz, M., Gawdzik, J., 2008. Application of PLE for the determination of essential oil components from Thymus vulgaris L. Talanta 76, 878–884.

Didry, N., Dubreuil, L., Pinkas, M., 1994. Activity of thymol, carvacrol, cinnamaldehyde and eugenol on oral bacteria. Pharmaceutica acta Helvetiae 69, 25–28.

Edris, A.E., 2007. Pharmaceutical and therapeutic potentials of essential oils and their individual volatile constituents: a review. Phytotherapy Research 21, 308–323.

Ganzera, M., Schneider, P., Stuppner, H., 2006. Inhibitory effects of the essential oil of chamomile (Matricaria recutita L.) and its major constituents on human cytochrome P450 enzymes. Life Sciences 78, 856–861.

Hajhashemi, V., Ghannadi, A., Sharif, B., 2003. Anti-inflammatory and analgesic properties of the leaf extracts and essential oil of Lavandula angustifolia Mill. Journal of Ethnopharmacology 89, 67–71.

Kohlert, C., Schindler, G., Marz, R.W., Abel, G., Brinkhaus, B., Derendorf, H., Grafe, E.U., Veit, M., 2002. Systemic availability and pharmacokinetics of thymol in humans. Journal of Clinical Pharmacology 42, 731–737.

Lahlou, M., 2004a. Essential oils and fragrance compounds: bioactivity and mechanisms of action. Flavour and Fragrance Journal 19, 159–165.

Lahlou, M., 2004b. Methods to study the phytochemistry and bioactivity of essential oils. Phytotherapy Research 18, 435–448.

Maffei, M.E., Gertsch, J., Appendino, G., 2011. Plant volatiles: production, function and pharmacology. Natural Product Reports 28, 1359–1380.

McKay, D.L., Blumberg, J.B., 2006. A Review of the bioactivity and potential health benefits of chamomile tea (Matricaria recutita L.). Phytotherapy Research 20, 519–530.

Nedorostova, L., Kloucek, P., Urbanova, K., Kokoska, L., Smid, J., Urban, J., Valterova,
I., Stolcova, M., 2011. Antibacterial effect of essential oil vapours against different strains of Staphylococcus aureus, including MRSA. Flavour and Fragrance Journal 26, 403–407.

Perry, N.S.L., Bollen, C., Perry, E.K., Ballard, C., 2003. Salvia for dementia therapy: review of pharmacological activity and pilot tolerability clinical trial. Pharmacology Biochemistry and Behavior 75, 651–659.

Sadraei H., Ghannadi A., Malekshahi K., 2003. Relaxant effect of essential oil of Melissa officinalis and citral on rat ileum contractions. Fitoterapia 74, 445–452.

Savelev, S.U., Okello, E.J., Perry, E.K., 2004. Butyryl- and acetyl-cholinesterase inhibitory activities in essential oils of Salvia species and their constituents. Phytotherapy Research 18, 315–324.

Shaw, D., Annett, J.M., Doherty, B., Leslie, J.C., 2007. Anxiolytic effects of lavender oil inhalation on open-field behaviour in rats. Phytomedicine 14, 613–620.

Shiina, Y., Funabashi, N., Lee, K., Toyoda, T., Sekine, T., Honjo, S., Hasegawa, R., Kawata, T., Wakatsuki, Y., Hayashi, S., Murakami, S., Koike, K., Daimon, M., Komuro, I., 2008. Relaxation effects of lavender aromatherapy improve coronary flow velocity reserve in healthy men evaluated by transthoracic Doppler echocardiography. International Journal of Cardiology 129, 193–197.

Silva Brum, L.F., Elisabetsky, E., Souza, D., 2001. Effects of Linalool on [3H] MK801 and [3H] Muscimol Binding in Mouse Cortical Membranes. Phytotherapy Research 15, 422–425.

Silva, J., Abebe, W., Sousa, S.M., Duarte, V.G., Machado, M.I.L., Matos, F.J.A., 2003. Analgesic and anti-inflammatory effects of essential oils of Eucalyptus. Journal of Ethnopharmacology 89, 277–283.

Yim, V.W.C., Ng, A.K.Y., Tsang, H.W.H., Leung, A.Y., 2009. A Review on the Effects of Aromatherapy for Patients with Depressive Symptoms. The Journal of Alternative and Complementary Medicine 15, 187–195.

Chapter 3

Cannabinoid Receptor 1 Binding Activity and Quantitative Analysis of *Cannabis sativa* L. Smoke and Vapor

Jusin T. Fischedick, Frank van der Kooy, Robert Verpoorte

Natural Products Laboratory, Institute of Biology, Leiden University, 2300 RA Leiden, The Netherlands

Abstract

Cannabis sativa L. (cannabis) extracts, vapor produced by the Volcano vaporizer, and smoke made from burning cannabis joints were analyzed by GC-hydrogen flame ionization detector (FID), GC-MS and HPLC. Three different medicinal cannabis varieties were investigated Bedrocan®, Bedrobinol®, and Bediol®. Cannabinoids plus other components such as terpenoids and pyrolytic by-products were identified and quantified in all samples. Cannabis vapor and smoke was tested for cannabinoid receptor 1 (CB1) binding activity and compared to pure Δ^9-tetrahydrocannabinol (Δ^9-THC). The top five major compounds in Bedrocan extracts were Δ^9-THC, cannabigerol (CBG), terpinolene, myrcene, and *cis*-ocimene in Bedrobinol Δ^9-THC, myrcene, CBG, cannabichromene (CBC), and camphene in Bediol cannabidiol (CBD), Δ^9-THC, myrcene, CBC, and CBG. The major components in Bedrocan vapor (>1.0 mg/g) were Δ^9-THC, terpinolene, myrcene, CBG, *cis*-ocimene and CBD in Bedrobinol Δ^9-THC, myrcene and CBD in Bediol CBD, Δ^9-THC, myrcene, CBC and terpinolene. The major components in Bedrocan smoke (>1.0 mg/g) were Δ^9-THC, cannabinol (CBN), terpinolene, CBG, myrcene and *cis*-ocimene in Bedrobinol Δ^9-THC, CBN and myrcene in Bediol CBD, Δ^9-THC, CBN, myrcene, CBC and terpinolene. There was no statistically significant difference between CB1 binding of pure Δ^9-THC compared to cannabis smoke and vapor at an equivalent concentration of Δ^9-THC.

Published:

Fischedick, J., Van der Kooy, F., Verpoorte, R., 2010 Cannabinoid receptor 1 binding activity and quantitative analysis of *Cannabis sativa* L. smoke and vapor. Chemical Pharmaceutical Bulletin 58, 201–207.

Introduction

More than 400 chemicals have been identified in *Cannabis sativa* L. (cannabis), of which 70 are a group of terpenophenolic compounds known as cannabinoids (Turner et al., 1980; ElSohly and Slade, 2005). Δ^9-Tetrahydrocannabinol (Δ^9-THC) is the main cannabinoid and is primarily responsible for the psychoactive and medicinal effects of cannabis. Δ^9-THC exhibits many of its effects by interacting with two G-protein coupled receptors known as the cannabinoid receptor 1 (CB1) and the cannabinoid receptor 2 (CB2) (Costa, 2007). A variety of compounds both endogenous to the human body and synthetic, can interact with the CB receptors including fatty acid amides, fatty acid esters, aminoalkylindoles and diarylpyrazoles (Howlett, 1995).

Despite the illegality of cannabis in most nations a renewed interest in the medicinal properties of cannabis has resulted in the development of a number of cannabinoid based medicines. Oral Δ^9-THC (Marinol®) and nabilone (Cesamet®) a synthetic analogue of Δ^9-THC have been available since the 1980's as prescription medicine for treatment of nausea and appetite stimulation for patients undergoing chemotherapy or for AIDS wasting syndrome. More recently Sativex® a cannabinoid based oral mucosal spray containing Δ^9-THC and cannabidiol (CBD) has become available in some countries for relief of neuropathic pain in multiple sclerosis (Pertwee, 2009). In the Netherlands cannabis can be legally prescribed by medical doctors for treatment of nausea (caused by chemotherapy and radiotherapy), for chronic pain, Tourette's syndrome and multiple sclerosis. Since March 2005, Bedrocan BV (The Netherlands) has been contracted by the Dutch Ministry of Health, Welfare and Sport for the growth and production of medicinal cannabis.

Cannabis is traditionally consumed by smoking, eating, or drinking in the form of a tea preparation. Heating the plant material plays an important role as this decarboxylates the naturally occurring non-psycho-active tetrahydrocannabinolic acid (THCA) into the psycho-active neutral cannabinoid Δ^9-THC (Russo, 2007). A relatively new method of administration is to heat cannabis plant material at a temperature high enough to volatilize the active compounds without reaching temperatures which could cause combustion of the plant material. This technique is known as vaporizing and shows promise as a safe alternative to smoking while maintaining pharmacokinetic advantages of pulmonary administration (Abrams et al., 2007).

The identification of components in cannabis smoke condensate has been extensively studied (Fentiman et al., 1973; Adams and Jones, 1973; Jones and Foote, 1975; Lee et al., 1976; Maskarinec et al., 1976; Kettenes-Van Den Bosch and Salemink, 1977; Novotný et al., 1982; Hiller et al., 1984; Van der Kooy et al., 2008; Van der Kooy et al., 2009). An excellent review on cannabis smoke condensate, its constituents and some biological effects is available (ElSohly, 2006). Recently, research has been undertaken to determine the safety and effectiveness of vaporization for the administration of cannabis and cannabinoids. Effectiveness in human subjects has been demonstrated (Abrams et al., 2007), the suppression of pyrolytic by-products has been shown (Gieringer et al., 2004), vaporization parameters of pure Δ^9-THC have been optimized (Hazekamp et al., 2006), and the effect of different samples sizes and

temperatures on Δ^9-THC levels has been studied (Pomahacova et al., 2009). However one shortcoming of the above studies is that other components delivered by cannabis smoke or vapor such as terpenoids were not investigated.

Therefore in order to continue to evaluate the effectiveness of vaporization versus smoking our research focused on the identification and quantification of the components of cannabis smoke and vapor as well as CB1 binding activity of the collected samples. The goal of the CB activity test was to observe whether or not levels of Δ^9-THC in cannabis smoke and vapor was equivalent to CB1 binding activity of pure Δ^9-THC.

Materials and Methods

Plant Material

The plant material was obtained from Bedrocan BV (Groningen, The Netherlands) under the opium regulation register number 105815 CO/w. It consisted of mature flower tops of three cannabis varieties Bedrocan (dried), Bedrobinol (dried) and Bediol (granular, dried). According to the producer Bedrocan contains 18% Δ^9-THC and <1% CBD, Bedrobinol contains 11% Δ^9-THC and <1% CBD, and Bediol contains 6% Δ^9-THC and 7% CBD. Upon receiving the plant material it was stored at 4° C in the dark until use.

Chemicals

All reference terpenoids were purchased from Sigma-Aldrich (Steinheim, Germany), Fluka (Steinheim, Germany) or Chromadex (California, USA) and included α-thujene, camphene, sabinene, 1-8-cineol, terpinene-4-ol, 1-4-cineol, α-humulene, camphor, α-bisabolol, β-pinene, linalool, myrcene, terpineol, α-pinene, γ-terpineol, limonene, caryophyllene-oxide, (-)-carvacrol, Δ3-carene, p-cymene, terpinolene, citronellal, geranyl acetate, pulegone, citral, α-terpinene, α-fenchyl alcohol, calamanene, γ-cadinene, bornyl acetate, cis-trans-ocimene, α-cedrene, α-phellandrene, nerol, β-phellendrene, nerolodol, piperitonoxide, β-caryophyllene and geraniol. The cannabinoid references for Δ^9-THC, THCA, Δ^8-tetrahydrocannabinol (Δ^8-THC), CBD, cannabigerol (CBG), cannabichromene (CBC), tetrahydrocannabivarin (THCV), and cannabinol (CBN) were purified and quantified as previously described (Hazekamp et al., 2004a; Hazekamp et al., 2004b) by PRISNA BV (Leiden, The Netherlands). All cannabinoids references were >98% pure. Organic solvents used for extraction and sample preparation were of analytical reagent (AR) grade. Solvents used for HPLC were of HPLC grade.

Sample Preparation

Cannabis plant material was extracted using previous validated methodology (Hazekamp, 2007). Extracts from each cannabis variety were prepared in triplicate. One gram of plant material was transferred to 50 ml falcon tubes for extraction. The amount

of ethanol was brought to 40 ml and the falcon tubes were placed on a shaker for 15 min at 300 rpm. After shaking the samples were centrifuged at 2500 rpm for 5 min and the supernatant was collected in a 100 ml volumetric flask. The same procedure was repeated two more times with 25 ml ethanol. The final volume of ethanol was made up to 100 ml and samples were filtered through a 25 mm PTFE membrane syringe filter (0.45 µm).

For the smoke experiments the procedure described by Van der Kooy et al., (2009) was followed. Each cannabis joint was separately weighed (1 g/joint) and numbered. For each sample 2 joints were prepared. The puff frequency was one puff (lasting 3 sec) every 30 sec while the puff volume was 35 ml. The smoke was collected in two gas traps connected in series containing each 50 ml of a 1:1 mixture of ethanol and hexane. The final volume for each sample was 100 ml. A total of 3 samples were collected for each variety.

For the vapor collection the procedures described by Pomahacova et al., 2009 were followed. The Volcano® was obtained from Storz & Bickel GmbH & Co. (Tuttlingen, Germany) and was used according to the manual as provided by the manufacturer. The volume of the plastic bag used was 8 L. For each vaporization 250 mg of plant material was used. This process was repeated with 5 (total) separate 250 mg portions per sample (1.25 g cannabis material/sample). Samples were prepared in triplicate for each of the cannabis varieties. At the start of each experiment the Volcano was preheated until the indicator light showed that the target temperature of 200 °C was reached. The bag, connected to the filling chamber, was then immediately placed onto the Volcano and the ventilation was started. When the bag was completely inflated, ventilation was stopped and the bag was removed and reattached to a tube connected to the solvent trap (ethanol: *n*-hexane 1:1, 100 ml). Using a pump connected to the solvent system *via* a tube, the smoke was collected into the solvents. All resulting samples were analyzed with GC-FID, GC-MS, and HPLC.

GC-FID Analysis

An Agilent GC 6890 series equipped with a 7683 autosampler and injector was used for quantification. The column used for separation was a VA5ms (0.25 mm x 30 m, film thickness 0.25 µm, Varian, Walnut Creek, CA, USA). The injector temperature was set to 230 °C with an injection volume of 4 µl, a split ratio of 10 and a N_2 flow of 2 ml/min. The oven temperature program began at 60 °C with a ramp rate of 3 °C/min. The final temperature was 240 °C which was held for 5 min making a total run time of 65 min/sample. The FID detector temperature was 250 °C. Five point standard curves of myrcene, α-humulene and Δ^9-THC (0.01-1.0 mg/ml) diluted in ethanol were measured for quantification. All samples were analyzed undiluted and reference compounds were run at a concentration of 1 mg/ml.

GC-MS Analysis

The GC-MS analyses for compound identification were performed on a Varian 3800 GC, Varian Saturn 2000 GC ms/ms with a Varian 8200 autosampler and injector.

The injection volume was 3 µl with a split ratio of 20. The column used for separation was a DB5ms. (0.25 mm x 30 m, film thickness 0.25 µm, J&W Scientific, Folsom, CA, USA). The oven temperature program was the same as GC-FID. The transfer line temperature was 275 °C, manifold temperature 60 °C, and ion trap temperature 220 °C. Electron impact was used at an ionization mode of 70 eV and a scan range of 41-500 amu. All samples were analyzed undiluted and reference compounds were analyzed at a concentration of 1 mg/ml. The NIST library (Standard Reference Data Program of the National Institute of Standards and Technology) was used to aid in compound identification when no reference standard was available.

HPLC Analysis

The quantification of acidic and neutral cannabinoids was performed on an Agilent 1200 HPLC system equipped with an autosampler and injector and a photodiode array detector. The column used for separation was a GraceVydac (Deerfield, IL, USA) (250 x 4.6 mm 5 µM C_{18}) equipped with a guard column containing the same material as the column (All-guard 7.5 x 4.6 mm 5 µM C_{18}). The mobile phase consisted of solvent A (50% MeOH and 0.1% formic acid) and solvent B (100% MeOH and 0.1 % formic acid). The gradient employed started with 70% solvent A at time 0 and increased to 100% solvent B in 25 min. At 26 min the system was returned to 70% solvent A and 4 min was allowed for re-equalibration. The total run time was 30 min/sample. The flow rate was 1.5 ml/min and the detection wave length was 228 nm. Quantitative HPLC analysis of all samples was performed based previously validated methodology (Hazekamp, 2007).

CB1 Radioactive Displacement Assay

The CB1 receptor containing membranes (0.63 pmol/mg membrane protein; 16.4 mg/ml protein concentration) from Sf9 cells coexpressed with $G\alpha_{i3}\beta_1\gamma_2$ were purchased from PerkinElmer (Boston, MA, USA). The radioactive ligand CP-55,940, [Side chain-2,3,4(N)-^{3}H] was purchased from PerkinElmer. The CB1 containing membranes were diluted at a ratio of 1:200 with assay buffer (20 mM Hepes, 5 nM $MgCl_2$, 1 mM ethylene-diamine-tetra-acetic acid (EDTA), 0.3% bovine serum albumin (BSA), pH 7.4). Receptor solutions were used on the same day and all buffers were freshly prepared. The total assay volume was 550 µl of which 500 µl was the receptor solution, 25 µl the radioactive ligand (0.5 nM final concentration) and 25 µl the sample. All vapor and smoke samples were diluted to a final concentration of 10 nM Δ^9-THC in the final assay solution and were assayed in triplicate. Samples containing 10 nM of pure Δ^9-THC were also assayed (n=6). To determine non-specific binding CP-55,940 was assayed at final concentration of 10 µM (n=6). Blank samples were assayed to determine total binding of the radioactive ligand (n=6). All samples including controls Δ^9-THC, CP-55,940, and blanks contained ≤0.3% ethanol in the final assay solution.

The radioactive displacement assay was performed according to the recommended assay conditions of PerkinElmer with an incubation time of 1 hour at 30 °C. After incubation samples were filtered with a Brandel harvester (Gaithersburg, MD,

USA) over GF/C filters. The harvester can handle 24 filters at a time. After filtration the filters were collected in plastic scintillation vials to which 3 ml scintillation fluid was added. The scintillation fluid (brand: 'emulsifier safe') contained ethoxylated phenol. After adding the scintillation fluid and a brief vortex the samples were counted in a PerkinElmer scintillation counter (Tri-carb 2900TR). A student t-test (two tailed; two sample unequal variance) was performed in order to compare statistical significance between pure Δ^9-THC and group of samples (variety and smoke or vapor). A p-value <0.05 was considered significant.

Results and Discussion

HPLC quantification

The results of HPLC quantification of THCA and Δ^9-THC are shown in Table 1. The amount of THCA in the extracted cannabis plant material was used to calculate the total theoretical amount of Δ^9-THC in the ethanol extracts taking into account the difference in molecular weight (Δ^9-THC% = THCA% x (314.47 / 358.48)). Δ^9-THC levels for Bedrocan were higher than claimed by the producer (21.7%). This difference could be due to the fact that Bedrocan material was supplied as intact dried flower buds rather then granulated as it is normally supplied to pharmacies. Granulating the plant material causes some trichomes which contain the most cannabinoids to fall off. As expected the amount of Δ^9-THC in the vapor and smoke declined with the original content of Δ^9-THC in the plant varieties. The smoke and vapor samples showed an inverse relationship between Δ^9-THC volatization efficiency compared to original Δ^9-THC content with the Bediol variety having the highest efficiency. Δ^9-THC volatization efficiency was higher for each variety when vaporized compared to smoked. The absolute quantities of Δ^9-THC in the smoke samples of the Bedrocan variety confirms earlier reports (Pomahacova et al., 2009) which found Δ^9-THC levels of around 40 mg/g in the smoke samples. Δ^9-THC levels in vaporized samples cannot be directly compared with previous research as differences in sample weights vaporized causes differences in Δ^9-THC levels (Pomahacova et al., 2009).

GC Identification and Quantification

All components identified and quantified by GC-FID and GC-MS are shown in tables 2-4. A representative chromatogram for a Bedrocan extract, smoke and vapor sample is shown in figure 1. Compound identification was based on mass spectra, retention times compared with authentic standards and retention indexes reported in literature (Ross and ElSohly, 1996; Adams, 1989). Mono-terpenoids were quantified using a linear calibration curve for myrcene ($y=6945.1x$; $r^2=0.997$), sesquiterpenoids with α-humulene ($y=7529.5x$; $r^2=0.998$), and cannabinoids with Δ^9-THC ($y=5873.4x$; $r^2=0.999$). The % difference in response coefficients between the above three compounds classes was 12.4%. Putative identification of pyrolytic by-products using a NIST library (2005) is reported in smoke samples. These compounds did not fit into the above 3 compound groups therefore they were quantified using the standard compound that was most similar in mass as response coefficients in FID detectors are mass sensitive. Standard curves were not generated for every compound quantified so the

data represents a normalized quantitation. A number of compounds had fragmentation patterns that were typical of cannabinoids or sesquiterpenoids but identification could not be confirmed based on available data. For such compounds mass ions were reported and they were labeled as unknown sesquiterpenoids or cannabinoids.

Table 1. HPLC Quantification of THC and THCA in the three cannabis varieties

Sample	Varieties	THC mg/g	%RSD n=3	Efficiency of THC volatilization	THCA mg/g	%RSD n=3
Extract	Bedrocan	217.0[a)]	2.4	-	240.9	2.5
	Bedrobinol	103.0 [a)]	3.5	-	114.8	3.5
	Bediol	62.0 [a)]	1.4	-	66.9	1.3
Vapor	Bedrocan	47.7	5.7	22.0%	2.3	17.4
	Bedrobinol	36.3	10.9	35.2%	2.2	6.3
	Bediol	24.5	22.2	39.5%	1.2	19.9
Smoke	Bedrocan	34.6	33.4	15.9%	ND[b)]	--
	Bedrobinol	26.3	6.4	25.5%	ND	--
	Bediol	18.5	12.4	29.8%	ND	--

a) THC equivalents based on the amount of THCA in the samples. b) ND = not detected.

Table 2 lists all the components which were identified and quantified in the cannabis extracts. No acidic cannabinoids were observed as expected because the high temperature used in GC decarboxylates them into their neutral forms. The concentration of Δ^9-THC determined by GC confirms the results obtained by HPLC. No CBN, a Δ^9-THC degradation product, was detected in any of the initial sample extracts. The top five major compounds in Bedrocan extracts were Δ^9-THC, CBG, terpinolene, myrcene, and *cis*-ocimene. In Bedrobinol Δ^9-THC, myrcene, CBG, CBC, and camphene were major components and in Bediol CBD, Δ^9-THC, myrcene, CBC, and CBG.

Table 3 lists the components identified and quantified in the vapor samples. Most of the components identified in the initial extracts can also be seen in the vapor samples. The major components of Bedrocan vapor (>1.0 mg/g) were Δ^9-THC, terpinolene, myrcene, CBG, *cis*-ocimene, and CBD. Bedrobinol contained mostly Δ^9-THC, myrcene, and CBD. Note that the levels of CBD were higher in Bedrocan and Bedrobinol vapor samples than they were in the original extracts. We suspect this observation is a result of the degradation of another cannabinoid, perhaps Δ^9-THC, into CBD. Since the %RSD was also very high (>50%) and the effect was not observed in cannabis smoke (Table 4) we suspect that such degradation is not reproducible. In Bediol vapor the major components (>1.0 mg/g) were CBD, Δ^9-THC, myrcene, CBC, and terpinolene. Only a small amount of CBN (<0.1 mg/g) was formed in vapor samples. No new compounds that were not observed in the cannabis extracts were detected in cannabis vapor.

In contrast to vapor samples smoked cannabis contained many compounds not observed in extracts or vapor (Table 4). In total 23 unknown cannabinoids, various

hydrocarbons, phenolic compounds, nitrogen containing compounds, Δ^8-THC, 1-oxo-cannabinol and significant amounts of CBN (>2.0 mg/g) were observed in cannabis smoke. These results suggest a much higher degree of pyrolytic degradation in cannabis smoke when compared to cannabis vapor and is consistent with previous literature (Gieringer et al., 2004). The major compounds in Bedrocan smoke (>1.0 mg/g) were Δ^9-THC, CBN, terpinolene, CBG, myrcene and *cis*-ocimene. In Bedrobinol Δ^9-THC, CBN and myrcene were the major compounds. In Bediol CBD, Δ^9-THC, CBN, myrcene, CBC and terpinolene were the major compounds.

CB1 binding activity

Cannabis smoke and vapor samples were diluted to a concentration of 10 nM which is very near the EC_{50} of Δ^9-THC. This was done to maximize the ability of the assay to show an increase or decrease in binding. The EC_{50} of Δ^9-THC was determined to be 9.9 nM with a K_i of 3.8 nM from a dose response curve performed under the same assay conditions using the same batches of ligands and receptors (data not shown). The K_i and EC_{50} for Δ^9-THC is comparable with literature reports (Pertwee, 2008). Figure 2 shows the % displacement of CP-55,940, [Side chain-2,3,4(N)-^{3}H] caused by binding to the CB1 receptor. No significant difference was found between smoke and vapor samples when compared with pure Δ^9-THC (Figure 2). This suggests that no additional CB1 binding is taking place in cannabis smoke or vapor samples when compared with pure Δ^9-THC.

Conclusions

Our CB1 binding results verify previous reports in humans which showed that the subjective psychoactive effects of cannabis are primarily due to Δ^9-THC content (Wachtel et al., 2002; Ilan et al., 2005). Our results demonstrate that any non-Δ^9-THC components in cannabis smoke and vapor are too diluted to have any significant effects *in vitro* on CB1 binding. However there still exists evidence that other components in cannabis extracts play a role in the plant's overall therapeutic effects (Pickens, 1981; Fairbairn and Pickens, 1981; Zuardi et al., 1982; Wilkinson et al., 2003; Whalley et al., 2004; Ryan et al., 2006). There has even been considerable controversy over this issue (ElSohly et al., 2003; Russo and McPartland, 2003). We propose that any additional beneficial effects observed by patients using cannabis are due to effects other than CB1 agonism. Such benefits could come from other components in cannabis that interact with the CB2 receptors or new potential cannabinoid receptors such as the transient receptor potential vanilloid 1 (Begg et al., 2005).

Figure 1. Typical GC-FID chromatograms of a Bedrocan extract, vapor and smoke sample

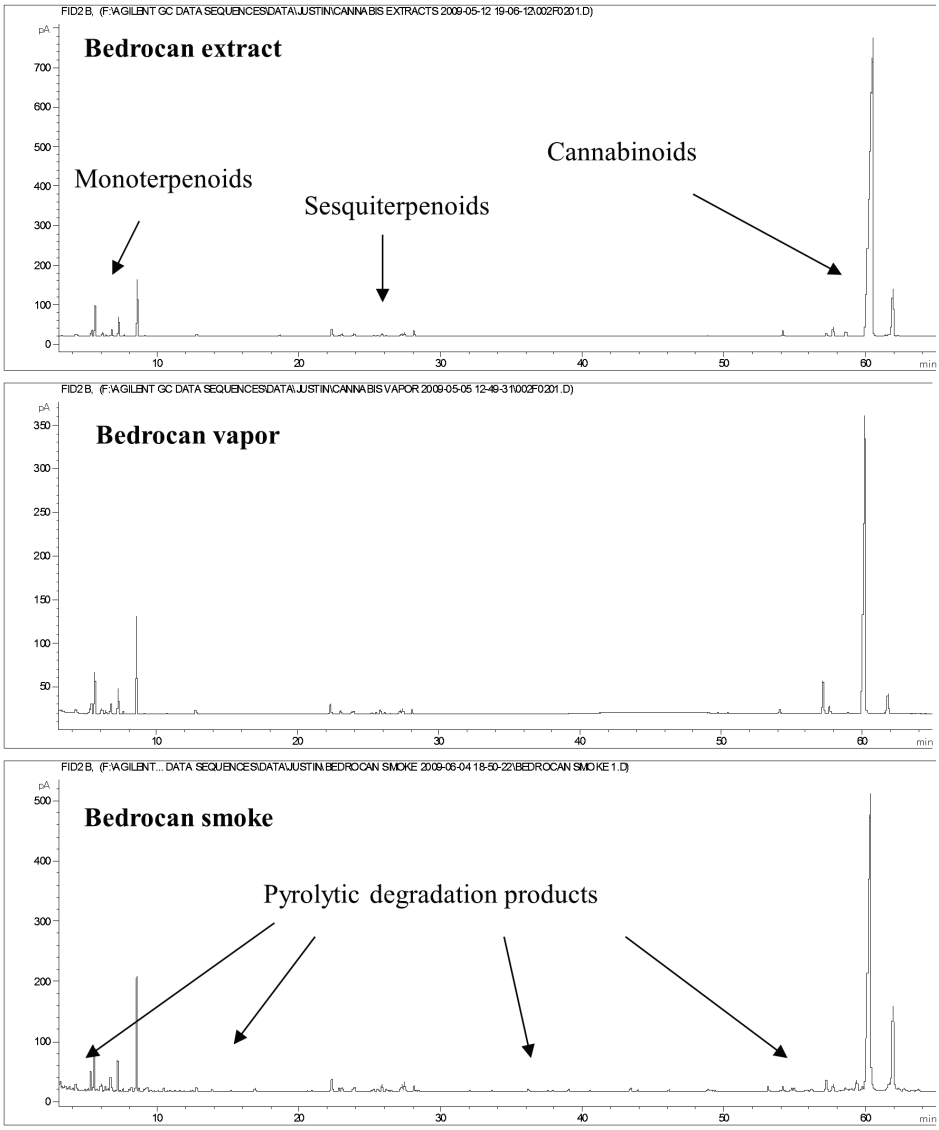

Quantitative comparison of cannabis smoke and vapor shows that vaporizing cannabis with the Volcano is a more reliable and safer administration form for the delivery of Δ^9-THC due to the lack of pyrolytic degradation and more efficient Δ^9-THC volatilization. Analysis of cannabis smoke and vapor showed for the first time in a quantitative manner that terpenoids are major components of the smoke and vapor of 3 medicinal cannabis varieties. Myrcene has analgesic and anti-inflammatory properties which may contribute to the medical benefits of cannabis. Other compounds identified

in our samples terpineol, terpinene-4-ol, γ-terpinene, limonene and α-pinene are acetylcholine esterase inhibitors that may act by reducing acetylcholine deficits in the hippocampus induced by Δ^9-THC (McPartland and Russo, 2001). Further research should be done to determine whether or not terpenoids and other non-Δ^9-THC components of cannabis are contributing to the overall medical benefits of herbal cannabis.

Figure 2. CB1 activity of Cannabis Smoke and Vapor

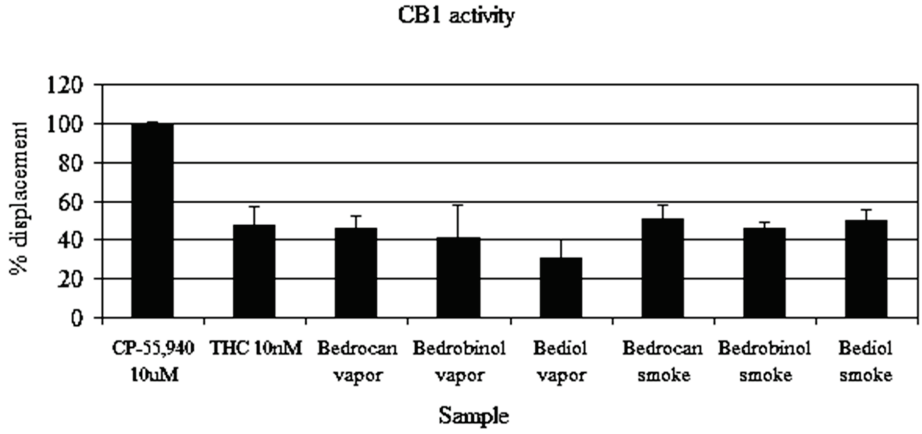

Table 2. GC Identification and Quantification of Components in Cannabis Extracts

RT min[a)]	Compound	Bedrocan mg/g	%RSD n=3	Bedrobinol mg/g	%RSD n=3	Bediol mg/g	%RSD n=3
4.20	α-pinene	0.4	5	0.9	8	0.6	6
4.34	camphene	0.4	4	1.1	8	0.7	7
5.23	sabinene	0.5	8	ND		0.2	10
5.35	β-pinene	0.9	1	0.3	4	0.4	9
5.60	myrcene	5.0	10	12.0	8	11.3	3
6.08	α-phellandrene	0.5	4	ND		ND	
6.14	Δ^3-carene	0.3	6	ND		0.2	0.0
6.37	α-terpinene	0.2	7	ND		ND	
6.75	β-phellandrene	0.9	4	ND		0.2	2
6.77	limonene	0.7	1	ND		0.2	4
7.25	*cis*-ocimene	3.0	13	0.7	4	0.7	3
7.64	γ-terpineol	0.2	0.4	ND		ND	
8.56	terpinolene	8.9	4	ND		1.9	17
9.15	linalool	0.3	15	ND		0.3	0.0
10.70	camphor	ND		ND		0.2	18
12.49	terpinene-4-ol	0.2	10	ND		0.2	0.0
12.74	terpineol	0.7	8	ND		0.6	1
22.30	β-caryophyllene	1.7	13	0.6	8	0.8	2
22.82	*trans*-α-bergomotene	0.2	6	ND		ND	
23.03	α-guaiene	0.6	16	ND		0.5	3
23.82	α-humulene	0.6	13	0.4	33	0.3	23
23.95	*cis*-β-farnesene	0.5	23	ND		0.5	5
25.24	β-selinene	0.2	32	0.2		0.3	0.0
25.55	α-selinene	0.2	30	0.3	32	0.2	45
25.83	ST *m/z*: 204 (M+) 189, 107, 91, 77	0.5	14	ND		0.3	25
26.14	γ-cadinene	0.2	13	0.3	26	0.4	6
27.11	ST *m/z*: 204 (M+) 189, 161, 133	0.2	0.0	ND		ND	
27.24	ST *m/z*: 204 (M+) 161, 133, 105	0.5	15	0.2	20	0.2	16
27.42	ST *m/z*: 204 (M+) 161, 122, 102	0.7	16	0.2	10	0.2	5
28.10	γ-elemene	1.1	9	0.3	62	0.3	58
48.85	CB *m/z*: 258 (M+) 243, 215, 275	ND		ND		0.3	0.0
51.19	CB *m/z*: 286 (M+) 271, 243, 203	ND		ND		0.3	10
54.16	THCV	1.5	7	0.8	6	0.5	13
57.31	CBD	0.8	2	0.4	4	85.6	2
57.71	CBC	2.6	7	1.7	6	6.5	2

58.58	CB *m/z*: 313 (M+) 297, 272, 244	1.8	12	0.7	9	0.5	5
59.02	CB *m/z*: 314 (M+) 299, 272, 244	ND		ND		1.4	2
60.36	Δ^9-THC	220.8	4	110.1	5	67.6	2
61.38	CB *m/z*: 314 (M+) 297, 232	0.3	25	ND		ND	
61.86	CBG	16.0	11	2.7	22	3.1	3
63.91	CB *m/z*: 314 (M+) 294, 272, 232	ND		ND		0.5	14

ND= not detected. ST= unknown sesquiterpenoid. CB= unknown cannabinoid. a) Retention time in GC-FID.

Table 3. GC Identification and Quantification of Components in Cannabis Vapor

RT min[a)]	Compound	Bedrocan mg/g	% RSD n=3	Bedrobinol mg/g	% RSD n=3	Bediol mg/g	% RSD n=3
4.26	α-pinene	0.2	34	0.7	12	0.3	3
4.33	camphene	0.2	7	0.9	10	0.4	9
5.26	Sabinene	0.3	3	0.2	3	0.1	4
5.35	β-pinene	0.6	6	0.3	5	0.2	10
5.60	Myrcene	2.8	10	7.1	4	5.6	6
6.08	α-phellandrene	0.3	13	ND		ND	
6.13	Δ^3-carene	0.2	7	ND		ND	
6.37	α-terpinene	0.2	8	ND		ND	
6.74	β-phellandrene	0.7	35	0.1	6	ND	
6.77	limonene	0.4	8	ND		0.2	11
7.25	*cis*-ocimene	1.7	13	0.6	5	0.4	5
7.64	γ-terpinene	0.2	7	ND		ND	
8.55	terpinolene	6.5	10	0.6	83	1.9	3
12.74	terpineol	0.3	24	0.2	2	0.3	31
22.30	β-caryophyllene	0.9	16	0.6	13	0.6	12
23.02	α-guaiene	0.2	20	0.2	12	0.3	19
23.83	α-humulene	0.3	16	0.2	10	0.2	11
23.95	*cis*-β-farnesene	0.2	19	0.1	18	0.2	20
25.55	α-selinene	0.1	11	ND		0.1	0.0
25.83	ST *m/z*: 204 (M+) 189, 107, 91, 77	0.4	19	0.2	24	0.4	17
26.13	γ-cadinene	0.1	11	0.1	0.0	0.1	15
27.24	ST *m/z*: 204 (M+) 161, 133, 105	0.2	19	0.2	18	0.2	33
27.42	ST *m/z*: 204 (M+) 161, 122, 102, 91	0.4	17	0.3	14	0.3	15
28.10	γ-elemene	0.4	23	0.2	43	0.2	26
51.19	CB *m/z*: 286 (M+) 271, 243, 203	ND		ND		0.2	0.0
54.16	THCV	0.4	8	0.3	8	0.1	3
57.27	CBD	1.5	109	1.6	70	28.0	20
57.69	CBC	0.6	8	0.7	8	1.9	22

59.00	CB *m/z*: 314 (M+) 299, 272, 244	ND		ND		0.4	21
60.18	Δ^9-THC	46.5	6	35.4	10	23.5	22
61.81	CBG[b)]	2.3	11	0.7	20	0.9	20
61.81	CBN[b)]	0.1	5	0.1	8	<0.1	27

ND= not detected. ST= unknown sesquiterpenoid. CB= unknown cannabinoid. a) Retention time in GC-FID. b) Values determined by HPLC due to overlap in GC-FID.

Table 4. GC Identification and Quantification of Components in Cannabis smoke

RT min[a)]	Compound	Bedrocan mg/g	%RSD n=3	Bedrobinol mg/g	%RSD n=3	Bediol mg/g	%RSD n=3
3.10	ethyl benzene[b)]	0.2	30	0.1	19	0.2	16
3.14	*ortho*-xylene[b)]	0.2	12	0.1	27	0.2	22
3.47	1, 3, 5, 7-cyclooctatetraene[b)]	0.1	12	0.1	36	0.2	8
3.75	Ethanone, 1-(2-furanyl)[b)]	ND		0.1	17	0.1	10
3.84	1,3-benzenediamine[b)]	ND		0.1	9	0.1	13
3.78	unknown *m/z*: 110 (M+) 95, 58	0.1	22	ND		ND	
4.08	α-thujene	0.1	8	ND		ND	
4.23	α-pinene	0.4	7	0.7	5	0.3	8
4.92	1,3,5-trimethylbenzene[b)]	ND		ND		0.1	7
5.13	sabinene	0.1		ND		ND	
5.27	β-pinene	0.8	9	0.6	14	0.5	13
5.53	β-myrcene	2.1	8	1.9	4	1.9	8
5.99	α-phellandrene	0.3	10	ND		0.5	14
6.14	Δ^3-carene	0.2	7	ND		0.1	4
6.30	α-terpinene	0.2	21	ND		ND	
6.53	cymene	0.1	18	0.1	40	0.9	8
6.68	β-phellandrene	0.5	12	0.1	4	0.3	7
6.70	limonene	0.4	21	ND		ND	
7.20	*cis*-ocimene	1.4	7	0.2	3	0.2	3
7.41	phenol, 3-methyl[b)]	ND		0.1	15	0.1	17
7.58	γ-terpineol	0.1	1	ND		ND	
8.17	phenol, 4-methyl[b)]	0.2	24	0.3	37	0.2	0.4
8.51	terpinolene	5.4	11	0.2	24	1.3	9
8.69	*para*-cymene	0.1	25	0.1		0.4	10
9.06	linalool	0.1	16	ND		ND	
9.28	4-pyridinol[b)]	0.4	21	0.4	36	0.4	19
9.51	1,3,8-*p*-menthatriene[b)]	ND		ND		0.9	18
10.32	cycloheptane, 1,3,5-tris(methylene)[b)]	ND		ND		0.1	11
10.44	benzene, 1-isocyano-2-methyl[b)]	0.1	28	0.1	13	0.2	23
11.68	phenyl, 4-ethyl[b)]	ND		0.1	6	ND	

12.72	unknown *m/z*: 134 (M+) 89, 71, 56	0.2	4	ND		0.4	6
12.76	terpineol	0.2	11	ND		ND	
13.88	benzaldehyde, 2-methyl [b)]	ND		0.2	21	0.2	21
16.88	indole [b)]	0.1	26	0.2	17	0.2	7
20.88	1H-indole, 3-methyl [b)]	ND		0.1		0.1	16
22.30	β-caryophyllene	0.8	14	0.5	14	0.5	5
22.81	*trans*-α-bergomotene	0.2	16	ND		ND	
23.03	α-guaiene	0.3	4	ND		0.4	5
23.82	α-humulene	0.3	8	0.2	17	0.2	1
23.95	*cis*-β-farnesene	0.2	11	ND		0.3	5
25.24	β-selinene	0.1	36	0.1	11	0.1	9
25.55	α-selinene	0.1	39	0.1	21	0.1	4
25.84	ST *m/z*: 204 (M+) 189, 107, 91, 77	0.4	15	ND		0.4	5
26.14	γ-cadinene	0.1		0.1	20	0.2	13
26.52	β-gurjunene [b)]	0.1		ND		ND	
27.10	ST *m/z*: 204 (M+) 189, 161, 133, 105	0.1		0.1	17	ND	
27.24	ST *m/z*: 204 (M+) 161, 133, 105, 91	0.3	19	0.2	17	0.2	2
27.42	ST *m/z*: 204 (M+) 161, 122, 102, 91	0.5	18	0.3	16	0.3	3
28.10	γ-elemene	0.3	21	0.1	15	0.1	6
28.47	ST *m/z*: 204 (M+) 161, 107, 91, 69	0.1		ND		0.1	9
32.02	Δ-selinene [b)]	ND		ND		ND	
36.21	olivitol [b)]	0.1	34	0.1		0.6	6
37.57	1-(3-methylbutyl)-2,3,5,6-tetramethylbenzene [b)]	0.1		ND		0.1	
39.04	7-octadecyne, 2-methyl [b)]	0.2	7	0.2	11	0.3	3
40.54	3, 7, 11, 15-tetramethyl-2-hexadecen-1-ol [b)]	0.1	3	0.1	19	0.1	4
43.42	CB *m/z*: 232 (M+) 231, 174	0.2	36	0.3	33	0.3	17
43.94	CB *m/z*: 246 (M+) 232, 231, 190, 175	0.1	23	ND		0.4	6
47.95	CB *m/z*: 258 (M+) 244, 243, 215, 175	0.1	2	0.2	24	0.1	
48.90	CB *m/z*: 248 (M+) 206, 193. 136	ND		ND		0.2	13
49.07	CB *m/z*: 258 (M+) 243, 215, 175	ND		ND		0.2	10
51.23	CB *m/z*: 286 (M+) 271, 243, 203	ND		ND		0.1	5
53.12	CB *m/z*: 314 (M+) 299, 271, 258, 232	0.3	29	0.3	16	0.8	3
54.24	THCV	0.3	34	0.2	6	0.1	7
54.79	CB *m/z*: 314 (M+) 299, 258, 243, 232	0.2	11	0.1	22	0.3	9
54.99	CB *m/z*: 312 (M+) 270, 256, 257, 214	0.2	4	ND		0.1	6

55.87	CB *m/z*: 310 (M+) 295, 238, 223	0.1	8	0.1		0.2	
56.25	CB *m/z*: 316 (M+) 274, 260, 232	0.1		0.1	35	0.2	44
56.73	CB *m/z*: 314 (M+) 246, 231, 175	ND		ND		0.4	11
57.35	CBD	0.5	80	0.1		21.1	7
57.82	CBC	0.4	34	0.3	36	1.3	11
58.48	CB *m/z*: 313 (M+) 297, 272, 244, 231	0.2		0.2	59	0.1	3
58.68	CB *m/z*: 314 (M+) 299, 272, 244, 232	0.1		ND		ND	
59.02	CB *m/z*: 314 (M+) 299, 272, 243, 232	0.2		ND		ND	
58.99	Δ^8-THC	1.0	17	0.2	12	0.5	4
59.39	CB *m/z*: 352 (M+) 314, 282, 259, 232	ND		ND		0.5	4
59.67	CB *m/z*: 299 (M+) 300	0.4	18	0.3	41	0.1	
60.23	Δ^9-THC	36.2	39	26.7	9	17.6	12
60.80	CB *m/z*: 314 (M+) 299, 272, 256, 243	ND		ND		0.3	
61.71	CB *m/z*: 312 (M+) 298, 270, 257, 232	0.4	97	0.2	41	0.2	9
61.94	CBG[c)]	2.5	16	0.9	25	1.0	3
61.94	CBN[c)]	6.9	2	3.5	25	2.9	4
62.33	CB *m/z*: 312 (M+) 296, 272, 270, 257	0.1	17	ND		ND	
62.70	CB *m/z*: 337 (M+) 312, 298, 282	0.2	18	ND		ND	
63.22	1'-oxo-cannabinol [b)]	0.1	12	ND		ND	
63.56	CB *m/z*: 334 (M+) 319, 300, 263	0.1	13	ND		ND	
63.74	CB *m/z*: 352 (M+) 338, 310, 270	0.2	38	ND		ND	

ND= not detected. ST= unknown sesquiterpenoid. CB= unknown cannabinoid. a) Retention time in GC-FID. b) Compounds putatively identified on NIST (2005) library search >80% match. c) Values determined by HPLC due to overlap in GC-FID.

Acknowledgments

We wish to thank the STW foundation for the financial support of this study. We also thank Bedrocan BV for supplying plant material and PRISNA BV for cannabinoid references.

References

Abrams, D.I., Vizoso, H.P., Shade, S.B., Jay, C., Kelly, M.E., Benowitz, N.L., 2007. Vaporization as a smokeless cannabis delivery system: a pilot study. Clinical pharmacology and therapeutics 82, 572–578.

Adams, R.P., 1989. Identification of essential oils by ion trap mass spectroscopy. Academic Press, San Diego, California.

Adams, T.C., Jones, L.A., 1973. Long-chain hydrocarbons of Cannabis and its smoke. Journal of Agriculture and Food Chemistry 21, 1129–1131.

Begg, M., Pacher, P., Bátkai, S., Osei-Hyiaman, D., Offertáler, L., Mo, F.M., Liu, J., Kunos, G., 2005. Evidence for novel cannabinoid receptors. Pharmacology & Therapeutics 106, 133–145.

Costa, B., 2007. On the Pharmacological Properties of Δ^9-Tetrahydrocannabinol (THC). Chemistry & Biodiversity 4, 1664–1677.

ElSohly, H.N., ElSohly, M.A., 2006. Marijuana Smoke Condensate, in: Marijuana and the Cannabinoids. Humana Press, Totowa, New Jersey

ElSohly, M.A., Slade, D., 2005. Chemical constituents of marijuana: The complex mixture of natural cannabinoids. Life Sciences 78, 539–548.

ElSohly, M.A., Wachtel, S.R., de Wit, H., 2003. Cannabis versus THC: response to Russo and McPartland. Psychopharmacology 165, 433–434.

Fairbairn, J.W., Pickens, J.T., 1981. Activity of cannabis in relation to its delta'-trans-tetrahydro-cannabinol content. British Journal of Pharmacology 72, 401–409.

Fentiman, A.F., Foltz, R.L., Kinzer, G.W., 1973. Identification of noncannabinoid phenols in marihuana smoke condensate using chemical ionization mass spectrometry. Analytical Chemistry 45, 580–583.

Gieringer, D., St. Laurent, J., Goodrich, S., 2004. Cannabis Vaporizer Combines Efficient Delivery of THC with Effective Suppression of Pyrolytic Compounds. Journal of Cannabis Therapeutics 4, 7–27.

Hazekamp, A., 2007. Cannabis; extracting the medicine (Doctoral thesis). Universiteit Leiden, Leiden, The Netherlands.

Hazekamp, A., Choi, Y.H., Verpoorte, R., 2004. Quantitative Analysis of Cannabinoids from Cannabis sativa Using 1H-NMR. Chemical and Pharmaceutical Bulletin 52, 718–721.

Hazekamp, A., Ruhaak, R., Zuurman, L., van Gerven, J., Verpoorte, R., 2006. Evaluation of a vaporizing device (Volcano®) for the pulmonary administration of tetrahydrocannabinol. Journal of Pharmaceutical Sciences 95, 1308–1317.

Hazekamp, A., Simons, R., Peltenburg-Looman, A., Sengers, M., van Zweden, R., Verpoorte, R., 2004. Preparative Isolation of Cannabinoids from Cannabis sativa by Centrifugal Partition Chromatography. Journal of Liquid Chromatography & Related Technologies 27, 2421–2439.

Hiller, F.C., Wilson Jr., F.J., Mazumder, M.K., Wilson, J.D., Bone, R.C., 1984. Concentration and particle size distribution in smoke from marijuana cigarettes with different Δ9-tetrahydrocannabinol content. Fundamental and Applied Toxicology 4, 451–454.

Howlett, A.C., 1995. Pharmacology of Cannabinoid Receptors. Annual Review of Pharmacology and Toxicology 35, 607–634.

Ilan, A.B., Gevins, A., Coleman, M., ElSohly, M.A., de Wit, H., 2005. Neurophysiological and subjective profile of marijuana with varying concentrations of cannabinoids. Behavioural Pharmacology 16, 487–496.

Jones, L.A., Foote, R.S., 1975. Cannabis smoke condensate. Identification of some acids, bases, and phenols. Journal of Agriculture and Food Chemistry 23, 1129–1131.

Kettenes-Van Den Bosch, J.J., Salemink, C.A., 1977. Cannabis : XVI. Constituents of marihuana smoke condensate. Journal of Chromatography A 131, 422–424.

Lee, M.L., Novotny, M., Bartle, K.D., 1976. Gas chromatography/mass spectrometric and nuclear magnetic resonance spectrometric studies of carcinogenic polynuclear aromatic hydrocarbons in tobacco and marijuana smoke condensates. Analytical Chemistry 48, 405–416.

Maskarinec, M.P., Alexander, G., Novotný, M., 1976. Analysis of the acidic fraction of marijuana smoke condensate by capillary gas chromatography-mass spectrometry. Journal of Chromatography A 126, 559–568.

McPartland, J.M., Russo, E.B., 2001. Cannabis and Cannabis Extracts. Journal of Cannabis Therapeutics 1, 103–132.

Novotný, M., Merli, F., Wiesler, D., Fencl, M., Saeed, T., 1982. Fractionation and capillary gas chromatographic—mass spectrometric characterization of the neutral components in marijuana and tobacco smoke condensates. Journal of Chromatography A 238, 141–150.

Pertwee, R.G., 2008. The diverse CB1 and CB2 receptor pharmacology of three plant cannabinoids: delta9-tetrahydrocannabinol, cannabidiol and delta9-tetrahydrocannabivarin. British Journal of Pharmacology 153, 199–215.

Pertwee, R.G., 2009. Emerging strategies for exploiting cannabinoid receptor agonists as medicines. British Journal of Pharmacology 156, 397–411.

Pickens, J.T., 1981. Sedative activity of cannabis in relation to its delta'-trans-tetrahydrocannabinol and cannabidiol content. British Journal of Pharmacology 72, 649–656.

Pomahacova, B., Van der Kooy, F., Verpoorte, R., 2009. Cannabis smoke condensate III: The cannabinoid content of vaporized Cannabis sativa. Inhalation Toxicology 21, 1108–1112.

Ross, S.A., ElSohly, M.A., 1996. The volatile oil composition of fresh and air-dried buds of Cannabis sativa. Journal of Natural Products 59, 49–51.

Russo, E.B., 2007. History of Cannabis and Its Preparations in Saga, Science, and Sobriquet. Chemistry & Biodiversity 4, 1614–1648.

Russo, E.B., McPartland, J.M., 2003. Cannabis is more than simply Δ^9-tetrahydrocannabinol. Psychopharmacology 165, 431–432.

Ryan, D., Drysdale, A.J., Pertwee, R.G., Platt, B., 2006. Differential effects of cannabis extracts and pure plant cannabinoids on hippocampal neurones and glia. Neuroscience Letters 408, 236–241.

Turner, C.E., Elsohly, M.A., Boeren, E.G., 1980. Constituents of Cannabis sativa L. XVII. A review of the natural constituents. Journal of Natural Products 43, 169–234.

van der Kooy, F., Pomahacova, B., Verpoorte, R., 2008. Cannabis Smoke Condensate I: The Effect of Different Preparation Methods on Tetrahydrocannabinol Levels. Inhalation Toxicology 20, 801–804.

van der Kooy, F., Pomahacova, B., Verpoorte, R., 2009. Cannabis smoke condensate II: influence of tobacco on tetrahydrocannabinol levels. Inhalation Toxicology 21, 87–90.

Wachtel, S.R., ElSohly, M.A., Ross, S.A., Ambre, J., de Wit, H., 2002. Comparison of the subjective effects of Delta(9)-tetrahydrocannabinol and marijuana in humans. Psychopharmacology 161, 331–339.

Whalley, B.J., Wilkinson, J.D., Williamson, E.M., Constanti, A., 2004. A novel component of cannabis extract potentiates excitatory synaptic transmission in rat olfactory cortex in vitro. Neuroscience Letters 365, 58–63.

Wilkinson, J.D., Whalley, B.J., Baker, D., Pryce, G., Constanti, A., Gibbons, S., Williamson, E.M., 2003. Medicinal cannabis: is Δ^9–tetrahydrocannabinol necessary for all its effects? Journal of Pharmacy and Pharmacology 55, 1687–1694.

Zuardi, A.W., Shirakawa, I., Finkelfarb, E., Karniol, I.G., 1982. Action of cannabidiol on the anxiety and other effects produced by δ9-THC in normal subjects. Psychopharmacology 76, 245–250.

Chapter 4

Metabolic fingerprinting of *Cannabis sativa* L., cannabinoids and terpenoids for chemotaxonomic and drug standardization purposes

Justin Thomas Fischedick[a], Arno Hazekamp[a], Tjalling Erkelens[b], Young Hae Choi[a], Rob Verpoorte[a]

[a] *Natural Products Laboratory, Institute of Biology, Leiden University, 2300 RA Leiden, The Netherlands*
[b]*Bedrocan BV, PO box 2009, 9640CA, Veendam, The Netherlands*

Abstract

Cannabis sativa L. is an important medicinal plant. In order to develop cannabis plant material as a medicinal product quality control and clear chemotaxonomic discrimination between varieties is a necessity. Therefore in this study 11 cannabis varieties were grown under the same environmental conditions. Chemical analysis of cannabis plant material used a gas chromatography flame ionization detection method that was validated for quantitative analysis of cannabis monoterpenoids, sesquiterpenoids, and cannabinoids. Quantitative data was analyzed using principal component analysis to determine which compounds are most important in discriminating cannabis varieties. In total 36 compounds were identified and quantified in the 11 varieties. Using principal component analysis each cannabis variety could be chemically discriminated. This methodology is useful for both chemotaxonomic discrimination of cannabis varieties and quality control of plant material.

Published:

Fischedick, J. T., Hazekamp, A., Erkelens, T., Choi, Y. H., Verpoorte, R., 2010. Metabolic fingerprinting of *Cannabis sativa* L., cannabinoids and terpenoids for chemotaxonomic and drug standardization purposes. Phytochemistry 71, 2058–2073.

Introduction

Cannabis sativa L., (cannabis) is an annual dioecious plant belonging to the family Cannabaceae. Cannabis has a long history of human use as a medicinal plant, intoxicant, and ritual drug (Russo, 2007). Today most nations worldwide regard cannabis as an illegal drug of abuse. Despite the abuse potential of cannabis research into its chemistry and pharmacology has demonstrated that it also has medical properties. Chemical analysis of cannabis in the 1940's and 60's led to the discovery of a unique group of terpenophenolic secondary metabolites, known as cannabinoids, of which *trans*-(-)-Δ^9-tetrahydrocannabinol (Δ^9-THC) was shown to be the primary psychoactive ingredient (Pertwee, 2006). At least 90 plant cannabinoids, also known as phytocannabinoids, have been isolated from cannabis (Ahmed et al, 2008; ElSohly and Slade, 2005; Radwan et al, 2009). In the early 1990's the G-protein coupled cannabinoid receptors (CB) were discovered. Two types of cannabinoid receptors CB_1 and CB_2 revealed a receptor based mechanism for the action of Δ^9-THC (Pertwee, 2009).

Clinical trials into cannabis, pure cannabinoids, and synthetic analogues have demonstrated some effectiveness as analgesics for chronic neuropathic pain, appetite stimulants' for cancer or AIDS patients, and multiple sclerosis. The increased medical interest in these substances has prompted the development of various cannabis based medicines such as the oral Δ^9-THC preparation Marinol® (Solvay Pharmaceuticals, Belgium), a synthetic analogue of Δ^9-THC Nabilone® (Valeant Pharmaceuticals International, USA), and Sativex® (GW Pharmaceuticals, UK) an oral mucousal spray containing 1:1 ratio of Δ^9-THC and CBD (Ben Amar, 2006; Hazekamp and Grotenhermen, 2010). Since 2003 The Netherlands has allowed the distribution of standardized herbal cannabis in pharmacies to patients with a prescription (Hazekamp, 2006). In the USA 14 states have legalized under state law the use of medical cannabis. In order to facilitate research into clinical safety and effectiveness the American Medical Association (AMA) has recently called for the rescheduling of cannabis's legal status from Schedule I to Schedule II (Hoffmann and Weber, 2010). These developments highlight the urgency to define the criteria necessary for the chemotaxonomic classification of medicinal cannabis for drug standardization and clinical research purposes.

There has been considerable debate over whether or not whole herbal cannabis has any additional therapeutic benefits when compared to pure cannabinoids (ElSohly et al., 2003; Llan et al., 2005; McPartland and Russo, 2001; Russo and McPartland, 2003; Wachtel et al., 2002). However, there is some evidence that certain cannabis preparations exhibit different effects when compared to pure cannabinoids (Fairbarin and Pickens, 1981; Johnson et al., 1984; Pickens, 1981; Ryan et al., 2006; Segelman et al., 1974; Whalley et al., 2004; Wilkinson, 2003). Both the terpenes and minor cannabinoids present in cannabis are known to have various biological activities (McPartland and Russo, 2001). A lack of detailed chemical characterization beyond Δ^9-THC, CBD or cannabinol (CBN) quantification is shown in the above mentioned preclinical as well as clinical research making it difficult to compare results across studies (Ben Amar, 2006; Hazekamp and Grotenhermen, 2010). It is not possible to

draw any strong conclusions about what components other than Δ^9-THC and occasionally, depending on the study design CBD, present in cannabis preparations may have an influence on the drug's effects.

Cannabinoids are produced biosynthetically in cannabis as their carboxylic acid derivatives and are known as cannabinoid acids. Cannabinoid acids degrade into their neutral counterparts through the action of heat, sunlight, and storage (Taura et al., 2007). Cannabis is most commonly administered by smoking the dried flower buds due to the avoidance of first pass metabolism of orally administered Δ^9-THC as well as ease of self titration by the user or patient (Williamson and Evans, 2000). In a recent study we demonstrated that cannabis ethanol extracts, smoke, and vapor produced by a vaporizing device are composed of a complex mixture of terpenoids and cannabinoids (Fischedick et al., 2010). Therefore quality control methods for the major volatile compounds in cannabis should be utilized prior to and during clinical studies of cannabis administered with a vaporizing device or by smoking.

Two morphological types of cannabis are commonly recognized, *C. sativa* being taller and more highly branched typically representing fiber type varieties and *Cannabis indica* being shorter with broader leaves typically representing strains used for recreational or medicinal purposes. Whether or not these two morphotypes are different species is still a matter of debate (Russo, 2007). A third subtype, *Cannabis ruderalis* has also been recognized, and is described as having low levels of cannabinoids with a bushy appearance (Hillig and Mahlberg, 2004). Today many cannabis varieties used recreationally and for medical purposes are hybrids of the various cannabis morphotypes mostly *C. sativa* and *C. indica*. Chemotaxonomic evaluation of cannabis has led to the recognition of 3 chemotypes, a drug type with higher levels of Δ^9-THC, a fiber type with higher CBD, and an intermediate type with similar levels of each (Fetterman et al., 1971; Small and Beckstead, 1973a; Small and Beckstead, 1973b). More recent studies using gas chromatography (GC) analyzing cannabinoids (Hillig and Mahlberg, 2004) or terpenoids (Hillig, 2004) have been performed for chemotaxonomic purposes. ^{1}H-NMR has been used to fingerprint cannabis aqueous extracts and tinctures (Politi et al., 2008) as well as to chemically differentiate cannabis cultivars (Choi et al., 2004). However, none of these methods offer validated quantitative methods for the analysis of cannabis terpenoids and cannabinoids simultaneously. Furthermore the sample preparation used by Hillig (2004) for terpenoid analysis utilized extensive sample drying (2 months at room temperature) and heating at 30 °C prior to analysis. This would have resulted in a higher rate of volatilization for the monoterpenoids thus biasing the chemotaxonomic evaluation towards the less volatile sesquiterpenoids.

Metabolic fingerprinting, also known as metabolic profiling, is a targeted analytical approach which aims to quantify a group or groups of compounds found in an organism or group of organisms. Metabolic fingerprinting with GC, HPLC, coupled with mass spectrometry, or ^{1}H-NMR is useful for studying plant biochemistry, chemotaxonomy, ecology, pharmacology, and quality control of medicinal plants (van der Kooy et al., 2009). To metabolically fingerprint cannabis we validated a GC-flame

ionization detection (GC-FID) method for monoterpenoids, sesquiterpenes, and cannabinoids. The analytical method was used to study the chemical composition and variability of terpenoids and cannabinoids in 11 cannabis varieties grown under standardized environmental conditions. Principal component analysis (PCA) was used to identify the compounds most important in distinguishing cannabis varieties. We also studied the variation on cannabis chemical profiles as a result of growing plants in different batches and with deviations in growth time. This study establishes useful criteria for quality control and standardization of cannabis varieties for clinical studies as well as chemotaxonomy.

Materials and Methods

Chemicals

Reference terpenoids of caryophyllene-oxide, camphor, α-bisabolol, β-pinene, myrcene, α-pinene, γ-terpineol, (*R*)-limonene (limonene), (*S*)-limonene, 1-8-cineol, carvacrol, and β-caryophyllene were purchased from Sigma-Aldrich (Steinheim, Germany). Terpineol mixture of isomers, α-humulene, and linalool were purchased from Fluka (Steinheim, Germany). Geraniol was purchased from Chromadex (Irvine, California, U.S.A). Camphene, α-thujene, sabinene, terpinene-4-ol, 1-4-cineol, Δ^3-carene, *p*-cymene, terpinolene, citronellal, geranyl acetate, pulegone, citral, α-terpinene, α-fenchyl alcohol, calamanene, γ-cadinene, bornyl acetate, a mixture of *cis/trans*-ocimene, α-cedrene, α-phellandrene, nerol, β-phellandrene, nerolidol, and piperitone-oxide were from a chemical bank of the authors. The cannabinoid references for Δ^9-THC, Δ^8-THC, CBD, cannabigerol (CBG), cannabichromene (CBC), *trans*-(-)-Δ^9-tetrahydrocannabivarin (THCV), and cannabinol (CBN) were purified and quantified by PRISNA BV as previously described (Leiden, The Netherlands) (Hazekamp et al., 2004a; Hazekamp et al., 2004b). All cannabinoids references were > 98% pure, except THCV. Absolute ethanol (EtOH) used for extraction and sample preparation was of analytical reagent (AR) grade (Biosolve BV, Valkenswaard, The Netherlands). 1-Octanol (HPLC grade) was purchased from Sigma Aldrich (Steinheim, Germany).

Plant material

Cannabis plant material was grown indoors. The plant material was produced by taking cuttings from standardized plants (mother plants) kept under vegetative conditions. Cannabis plants were grown in two growth cycles. First a vegetative period in which plants are grown under 18 h of uninterrupted light per day producing only roots, stems, and leaves. After an optimized vegetative period plants are switched to 12 h of uninterrupted light per day which induces flowering. The period for which each variety exists in each phase can differ and has been optimized by Bedrocan BV for efficient growth.

Environmental conditions for all varieties were the same. Plants were harvested after a standardized amount of days when the pistils faded from white to brown and the branches started to hang. The plants were then dried under the same environmental conditions. After one week drying the plant material lost 73% of its

weight. The plants were then processed by removing leaves from the buds and clipping buds from the main stems. Remaining plant material (buds) was packaged into 50 ml Falcon® tubes and stored at -20 °C until extraction.

Sample preparation

Cannabis plant material was weighed to the nearest mg with a typical weight range of 0.9-1.1 g. The plant material was crushed with a metal spoon within a falcon tube and the spoon was rinsed with a few ml of EtOH into the falcon tube. The volume was then brought up to 45 ml with ethanol. Falcon tubes were placed on a Yellow Line Orbital Shaker OS 2 Basic (IKA GmbH, Staufen, Germany) at 400 revolutions per minute (rpm) for 15 min. Samples were centrifuged briefly for 30 s at 2000 rpm. Supernatant was collected in a 100 ml glass volumetric flask. Samples were extracted two more times with 25 ml ethanol. As an internal standard 1 ml of an EtOH soln. containing 1-octanol (1%) was added to the volumetric flasks. Samples were finally brought to a volume of 100 ml with ethanol. Samples were filtered into 20 ml glass vials with a PTFE syringe filter (0.45 µM, 25 mm diameter). Samples were stored air tight in the dark at -20 °C until analysis.

GC-FID

An Agilent GC 6890 series equipped with a 7683 autosampler, a DB5 (30 m length, 0.25 mm internal diameter, film thickness 0.25 µm, J&W Scientific Inc, Folsom, CA, USA) column and a flame ionization detector (FID) was used for quantitative analysis. The injector temperature was set to 230 °C, an injection volume of 4 µl, a split ratio of 1:20 and a carrier gas (N_2) flow rate of 1.2 ml/min. The oven temperature program began at 60 °C with a ramp rate of 3 °C/min. The final temperature was set to 240 °C which was held for 5 min making a total run time of 65 min/sample. The FID detector temperature was set to 250 °C. The GC-FID was controlled by GC Chemstation software version B.04.01 (Agilent Technologies Inc, Santa Clara, CA, USA).

GC-MS

GC-MS analysis was performed on an Agilent 7890A series gas chromatograph equipped with a 7693 autosampler, an HP5-ms column (30 m length, 0.25 mm internal diameter, film thickness 0.25 µm, Agilent Technologies Inc, Santa Clara, CA, USA), and a single quadropole mass spectrometer 5975C. The MS source was set to 230 °C, the single quad temperature was 150 °C, and the transfer line temperature was set to 280 °C. The GC-column was linked to the MS via a quickswap (Agilent Technologies Inc, Santa Clara, CA, USA) and restrictor (0.11 mm internal diameter, Agilent Technologies Santa Clara USA). The injector temperature was 230 °C with an injection volume of 2 µl, a split ratio of 1:20, and a carrier gas (He) flow rate of 1.2 ml/min. The oven temperature program was the same as the GC-FID. The mass range analyzed by the mass spectrometer was 50-500 amu. The GC-MS was controlled by Enhanced Chemstation software version E.02.00.493 (Agilent Technologies Inc,

Santa Clara, CA, USA). The NIST library version 2.0f (Standard Reference Data Program of the National Institute of Standards and Technology, Distributed by Agilent Technologies) was used to assist compound identification.

Standards preparation

Mono and sesquiterpenoid references were weighed to 50 mg in a tarred volumetric flask using a Satorius analytical balance A200S 0.01 mg (Satorius Mechatronics, Utrecht, The Netherlands). Volume was brought to 25 ml with EtOH to make 2 mg/ml stock solutions. Stock solutions were used to make dilutions for standard curves. Stocks were stored at -20 °C in sealed glass vials in the dark until needed. Cannabinoid references were supplied already quantified in EtOH. References were diluted in EtOH to make standard curves. Cannabinoid references were stored at -20 °C in amber sealed glass vials in the dark until needed.

Method validation

Reproducibility

Intra-day reproducibility was determined by injecting an aliquot of a cannabis extract 5 times from the same vial in a single day and a reference sample of γ-terpinene (1 mg/ml) 5 times from the same vial in a single day (n = 5). Inter-day reproducibility was determined by taking a fresh aliquot of the same cannabis extract and γ-terpinene reference and injecting 5 times for an additional two days (n = 15) using fresh aliquots on each day. All injections performed on the GC-FID.

Extraction efficiency

Three 1 g samples of a batch of Bedrocan that had been used in previous studies (Fischedick et al., 2010) and stored for 7 months at 4 °C in the dark were extracted with the procedure outlined above. After 3 extractions a 4th extraction was performed on each Bedrocan sample with an additional 25 ml of ethanol and analyzed for residual compounds by GC-FID.

Accuracy

Accuracy was determined by checking the recovery of the extraction method with spiked monoterpenoids and sesquiterpenoids. Five 1 g samples of a batch of Bedrobinol used in previous studies (Fischedick et al., 2010) and stored for 7 months at 4 °C in the dark were extracted as outlined above. Five 1 g samples of the same batch of Bedrobinol were spiked with 50 µl of the pure references of β-pinene, linalool and β-caryophyllene while in falcon tubes then extracted as described above. Five volumetric flasks were spiked with 50 µl of the pure references of β-pinene, linalool, and β-caryophyllene and brought to 100 ml with EtOH. All samples analyzed by GC-FID. Percent recovery was calculated by subtracting the peak area of each terpenoid from the spiked samples minus the un-spiked controls. This number was then divided by the peak area of pure references diluted in 100 ml ethanol and multiplied by 100.

Linear range, LOD, LOQ, and RF

The linear range was determined empirically by injecting standard compounds in a range of 0.01 mg/ml to 2 mg/ml. The LOD and LOQ were determined empirically and using signal to noise calculations with Chemstation software. The detector response for monoterpenoids, sesquiterpenoids, and cannabinoids was determined by running standard curves (0.02 mg/ml – 1.0 mg/ml) of γ-terpinene, limonene, α-pinene, β-pinene, (*S*)-limonene, camphor, linalool, 1,8-cineol, β-caryophyllene, humulene, caryophyllene oxide, Δ^9-THC, Δ^8-THC, CBD, CBN, and CBG in duplicate.

Instrumental precision

The variation in peak area of the internal standard 1-octanol for all cannabis samples was used to determine precision of the GC-FID.

Data analysis

Principal component analysis (PCA) was performed on SIMCA-P+ version 12.0.0.0 (Umetrics, Umeå Sweden). Unit variance scaling was used. Hierarchical clustering analysis was also done on SIMCA-P+ software and used PC's 1-6 with the Ward method sorted by size.

Results and discussion

Plant material

Bedrocan BV (Groningen, The Netherlands) is a company licensed and contracted by the Dutch government to produce standardized cannabis plant material under Good Agricultural Practice (GAP) conditions to be supplied to patients on prescription, through pharmacies (OMC, 2010). All plant material in these experiments was grown by Bedrocan BV. The varieties Bedrocan® (Bedrocan), Bedropuur® (Bedropuur), and Bediol® (Bediol), have been bred by Bedrocan BV for use in medicine or research. All other varieties grown in this study are currently used for research purposes only. In total 11 cannabis varieties were grown (Table 1). Standard growth conditions are defined as the optimum vegetative and flowering growth times for each variety. The morphological type classification for each variety is based on morphological traits as well as knowledge Bedrocan BV has of the varieties origin and breeding history. Hybrids are described as having either equal morphological traits from *C. indica* or *C. sativa* (ie. hybrid indica/sativa) or having traits of both but mostly having traits representative of one of the morphotypes (ie. hybrid mostly sativa). The letter codes have no meaning other than to distinguish between varieties. All plants were grown from clones of a 'motherplant'. A motherplant is defined as a female cannabis plant from one distinct variety used for cloning (vegetative propagation) only.

Table 1: Cannabis plant information and growth conditions. Vegetative and flowering columns show the number of days each sample was grown in each stage under standard conditions.

Variety	Vegetative	Flowering	Morphological type	Growth conditions
AG (1,2,3)	37	54	hybrid indica/sativa	1 and 2- standard 3- veg[a] +1 wk[b], fl[c] +1 wk
AE (1,2,3)	37	54	hybrid mostly sativa	1 and 2- standard 3- veg +1 wk, fl +1 wk
Ai94 (1,2,3)	37	54	hybrid mostly sativa	1 and 2- standard 3- veg +1 wk, fl +1 wk
AO (1,3,5,6,7)	37	47	indica	1,3,5,6- standard(4 seeds) 7- fl +1 wk
AN	37	54	indica	standard
AD	37	47	indica	standard
AM	37	40	indica	standard
AF	37	54	indica	standard
Bedropuur (A,B,C,D)	37	40	indica	A- veg -1 wk fl +1 wk B- standard C- veg +1 wk D- veg +1 wk fl +1 wk
Bedrocan (C)	37	54	hybrid indica/sativa	bedrocan- standard C- lower branches clipped
Bediol	29	54	indica/sativa/ruderalis	standard

[a]Veg = vegetative, [b]wk = week, [c]fl = flowering.

Two female cannabis plants were grown for each batch and each growth treatment. Five random samples of dried flower material were selected for the analysis of each batch and each growth treatment. The purpose of growing plants in different batches and with deviations from standard growth conditions was to test the robustness of our chemical classification as well as determine the reproducibility of a cannabis varieties chemical profile. The AO variety was grown in 5 batches at the same time. Each batch originated from a different seed from the same cannabis variety. Seeds were grown and female plants were selected for cloning. Each number for the AO variety thus denotes a different original seed and its subsequent female clones. Therefore each AO batch was not genetically identical. For all other varieties the plants grown were genetically identical. The AO7 batch was grown for an extra week in the flowering state. The varieties AG, AE, Ai94 were each grown in 3 separate batches (1, 2, and 3). Batches 1 and 2 were grown about a month apart while batch 3 was grown at the same time as 2 except with an extra week of vegetative growth and an extra week of flowering (Table 1). Bedrocan was grown in 2 batches at the same time. One batch had its lower branches clipped (c) while the other batch was grown under standard conditions (Table 1). Bedropuur was grown in 4 batches at the same time with 1 batch grown under standard conditions and the other 3 batches grown with deviations from standard conditions (Table 1).

Method validation

Results of GC method validation are summarized in Table 2. For precision the percent relative standard deviation (RSD) of the peak area of 1-octanol from the 120 cannabis samples analyzed was calculated. The low RSD of 1-octanol (2.8%) indicates that the method was precise in terms of needle injections and FID response over the duration of the analytical period. This period consisted of 130 h of GC time excluding calibration curves and other validation analyses. Reproducibility was determined by comparing peak areas of each compound in a Bedropuur extract for both intraday and interday analyses. All compounds had a RSD of <5%. The reproducibility of a pure compound, γ-terpinene had a RSD of <2%. These low RSD values indicate that the method is reproducible for the analysis of cannabis terpenoids and cannabinoids.

The extraction method chosen for this study had previously been demonstrated to be exhaustive and exhibit a high recovery for the quantitative analysis of cannabinoids by HPLC (Hazekamp, 2007). Therefore we sought to determine whether or not the extraction procedure utilized for cannabinoids was also exhaustive for the terpenoids present in cannabis. Bedrocan was selected because it has been shown to contain high levels of Δ^9-THC and terpenoids (Fischedick et al., 2010). By the fourth ethanol extract only 2% Δ^9-THC compared to the total peak area of Δ^9-THC in the first 3 extracts remained. This was consistent with previous results concerning the recovery of cannabinoids with this extraction method (Hazekamp, 2007). No other residual compounds were detected in the fourth extract indicating that the method is also exhaustive for the extraction of terpenoids in cannabis. Accuracy of the extraction method was demonstrated by determining the recovery of spiked terpenoids. We selected Bedrobinol plant material for this experiment because in previous studies (Fischedick et al., 2010) this plant material was shown to have low levels of β-pinene and β-caryophyllene with no detectable levels of linalool. All terpenoids were completely recovered indicating that the method is accurate for the analysis of cannabis terpenoids (Table 2).

Linear standard curves (r^2> 0.99) for all compounds tested could be generated in the range of 0.01 mg/ml to 1 mg/ml. For Δ^9-THC linear standard curves up to 2 mg/ml could be generated. The limit of quantification (LOQ) for monoterpenoids with a molecular weight (M_r) of 136 was 0.4 mg/g, monoterpenes with oxygen was 0.5 mg/g, sesquiterpenoids with a M_r of 204 was 0.4 mg/g, sesquiterpenoids with oxygen was 0.5 mg/g, and for cannabinoids was 0.6 mg/g. The signal to noise ratio was greater then 1:10 for all compounds present at a concentration above their LOQ. A signal to noise ratio of 1:5 was selected as the limit of detection (LOD) and is therefore half that of the LOQ for each compound group. The response factor (RF) for each compound is shown in table 2. The low variability in RF among compounds with similar mass and chemical structure using the FID is consistent with other research done on the quantification of essential oils with GC-FID (Bicchi et al., 2008). Therefore terpenoids or cannabinoids for which no reference is available could be accurately quantified with components of similar or identical molecular mass/formula.

Qualitative and quantitative analysis of cannabis varieties

Compounds were identified by comparing their mass spectra, and retention times with authentic references as well as literature reports (Adams, 1989; Hillig, 2004; Komori et al., 1968; Ross and ElSohly, 1996; Rothschild et al., 2005). The NIST library was also used to assist in compound identification. A summary of quantitative data for all compounds in all 11 cannabis varieties is shown in Table 3. The compounds γ-terpinene, limonene, α-pinene, β-pinene, linalool, β-caryophyllene, humulene, Δ^9-THC, *trans*-(−)-Δ^8-tetrahydrocannabinold (Δ^8-THC), CBD, and cannabigerol (CBG) were quantified using their standard curve RF values. All other compounds were quantified using the average RF for compounds with the closest molecular mass/formula. In total 36 compounds were quantified.

The sesquiterpenoids δ-guaiene and bulnesol are reported as putatively identified because they have not been reported in cannabis previously and a reference compound was not available for structural confirmation. Five compounds could not be identified so we report their characteristic mass ions. Unknown monoterpenoid TP(1) *m/z*: 152 [M^+], 91, 84, 69 (base). The unknown sesquiterpenoids (SQ) SQ(1) *m/z*: 204 [M^+], 161 (base), 133, 105; SQ(2) *m/z*: 236 [M^+], 204, 161, 119, 93 (base); SQ(3) *m/z*: 204 [M^+], 161 (base), 122, 93. The unknown cannabinoid CB(1) *m/z*: 356 [M^+], 313, 297 (base), 243, 231. The monoterpenoid TP(1), we suspect is oxygen substituted due to its M_r of 152. The unknown sesquiterpenoids SQ(1) and SQ(3) appear to have been reported as unknowns in previous studies (Hillig, 2004; Ross and ElSohly, 1996). SQ(2) is a sesquiterpenoid with unknown substitution. No detectable levels of the Δ^9-THC breakdown product CBN were detected in any samples. This indicates that the drying and storage process used in this study resulted in no significant amount of Δ^9-THC degradation except perhaps that of *trans*-(-)-Δ^9-tetrahydrocannabinolic acid A (THCA) into Δ^9-THC.

Figure 1 Correlation of cannabinoid versus terpenoid levels

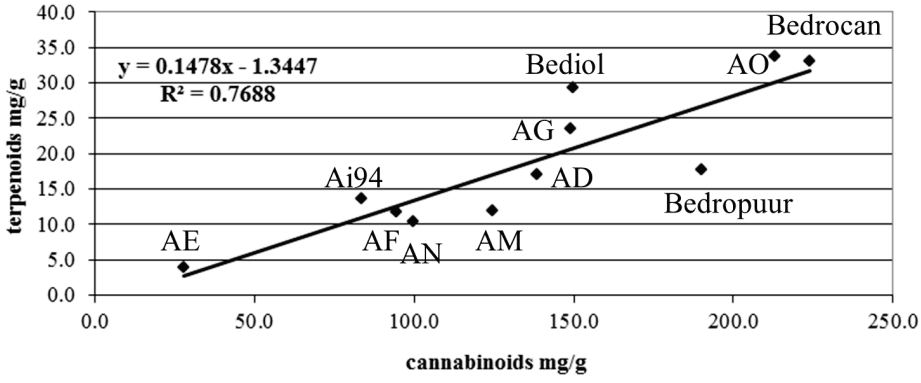

Table 2: Validation results.

Reproducibility			**Comparison RF**	
Extract	**Intraday (n=5) RSD**	**Interday (n=15) RSD**	**TP[a] M_r = 136**	**RF**
β-pinene	0.4	0.5	γ-terpinene	4604
myrcene	0.5	0.4	(*R*)-limonene	4598
limonene	0.7	0.5	α-pinene	4625
1-octanol	1.3	0.6	β-pinene	4753
linalool	1.2	0.6	(*S*)-limonene	4649
β-caryophyllene	1.3	0.5	average	4646
humulene	1.3	0.5	RSD	1.4
δ-guaiene	4.2	1.6	**TP with oxygen**	
SQ(1)	1.9	0.6	camphor	3894
SQ(2)	4.9	1.1	linalool	3936
elemene	1.7	0.6	1,8-cineol	3827
guaiol	1.5	0.7	average	3886
γ-eudesmol	1.4	1.3	RSD	1.4
THCV	1.1	1.6	**SQ[b] M_r = 204**	
CBC	2.6	1.3	β-caryophyllene	4754
CBGM	1.9	0.4	humulene	4661
Δ^9-THC	1.6	0.9	average	4708
CBG	2.0	0.8	RSD	1.4
Pure compound			**SQ with oxygen**	
γ-terpinene	0.5	1.9	caryophyllene-oxide	4285
Precision	**RSD (n=120)**		**Cannabinoids**	
1-octanol	2.8		Δ^9-THC	3490
Extraction efficiency	**% Remaining (n=3)**		Δ^8-THC	3674
Δ^9-THC	2		CBD	3502
Accuracy	**% Recovery (n=5)**	**RSD**	CBN	3521
β-pinene	102	3.2	CBG	3614
linalool	102	2.2	average	3560
β-caryophyllene	100	3.5	RSD	2.2

[a]TP = terpenoid. [b]Sesquiterpenoid.

Table 3: Quantitative data for cannabis strains (mg/g plant material). Compounds with no ± had standard deviations of < 100 µg.

Compound	RR_t[a]	AO	Bedropuur	Bedrocan	Bediol	AG	AE	Ai94	AN	AF	AM	AD
number of samples		25	20	10	5	15	15	15	5	5	5	5
α-pinene	0.26	6.7±2.4	0.5	0.8±0.1	1.7±0.1	2.8±0.4	Tr[c]	0.8±0.5	Tr	0.5	3.2±0.1	ND[b]
β-pinene	0.31	1.9±0.6	0.7±0.1	1.2±0.2	0.8±0.1	1.4±0.2	Tr	0.5±0.1	Tr	0.7	1.2	Tr
myrcene	0.33	14.8±7.3	1.6±0.7	6.1±1	19±1.9	13±1.6	0.4±0.1	7.1±0.8	0.8±0.2	3.4±0.1	6.7±0.6	13.8±0.9
α-phellandrene	0.35	ND	ND	0.6±0.1	Tr	ND	Tr	Tr	ND	Tr	ND	ND
Δ3-carene	0.36	ND	ND	0.5±0.2	Tr	ND	Tr	Tr	ND	Tr	ND	ND
α-terpinene	0.36	ND	ND	0.4	Tr	ND	Tr	Tr	ND	Tr	ND	ND
β-phellandrene	0.38	ND	ND	2.1±0.3	0.7±0.1	ND	Tr	0.5	ND	1.0	ND	Tr
limonene	0.38	2.5±0.7	4.9±0.8	ND	ND	2.4±0.4	ND	ND	2.3±0.3	ND	0.7±0.1	ND
cis-ocimene	0.40	1.4±0.4	ND	3.9±0.6	1±0.1	0.6±0.1	0.7±0.1	1±0.1	ND	1.0±0.1	ND	ND
terpinolene	0.47	ND	ND	11.3±1.7	3.7±0.4	ND	1.9±0.9	2.9±0.3	ND	5.4±0.2	ND	ND
linalool	0.48	0.9±0.1	1.2±0.2	Tr	ND	Tr	ND	Tr	Tr	Tr	Tr	Tr
terpineol	0.63	Tr	Tr	0.7±0.1	0.6	ND	Tr	Tr	Tr	Tr	Tr	ND
TP(1)	0.86	ND	ND	0.7±0.2	Tr	ND	Tr	ND	ND	Tr	ND	ND
β-caryophyllene	1.00	3.5±2.4	2.6±0.2	1.6±0.2	0.8±0.1	1.4±0.4	0.5±0.3	0.8±0.4	1.4±0.2	0.5	0.5	2.0±0.1
α-guaiene	1.03	ND	Tr	Tr	Tr	0.5	ND	Tr	ND	Tr	Tr	Tr
humulene	1.05	1.2±0.9	0.8±0.1	0.9±0.1	0.6±0.1	0.7±0.1	Tr	0.7±0.1	Tr	Tr	ND	0.6
δ-guaiene[P]	1.13	ND	0.7±0.1	0.8±0.1	0.8	0.7±0.2	ND	ND	ND	ND	ND	0.6
SQ(1)	1.18	0.5±0.1	0.6±0.1	0.6±0.1	Tr	Tr	ND	ND	1.3±0.1	Tr	ND	ND
SQ(2)	1.19	0.6±0.2	ND	ND	ND	ND	ND	ND	ND	ND	ND	ND
SQ(3)	1.19	ND	1.0±0.2	0.6±0.1	Tr	0.5±0.1	Tr	ND	1.8±0.1	ND	ND	ND
elemene	1.21	1.1±0.3	2.3±0.4	1.3±0.3	Tr	0.6±0.1	0.8±0.2	ND	2.7±0.6	Tr	Tr	ND

guaiol	1.27	0.6±0.2	0.6	ND	ND	ND	0.4	ND	ND	Tr	ND	ND
γ-eudesmol	1.30	0.7±0.2	0.6	ND	ND	ND	0.4	ND	ND	Tr	ND	ND
β-eudesmol	1.34	0.4	Tr	ND	ND	ND	Tr	ND	ND	Tr	ND	ND
agarospirol	1.35	0.5±0.1	Tr	ND	ND	ND	Tr	ND	ND	Tr	ND	ND
bulnesol[P]	1.37	0.5	ND	ND	ND	ND	ND	ND	ND	ND	ND	ND
α-bisabolol	1.39	0.5±0.1	Tr	ND	ND	ND	ND	ND	0.5±0.1	ND	ND	Tr
CBDV	2.04	ND	ND	ND	Tr	ND	ND	1.5	ND	ND	ND	ND
THCV	2.15	1.3±0.4	1.3±0.3	1.3±0.2	Tr	0.7±0.1	Tr	ND	0.6	0.7±0.1	1±0.1	0.6
CBD	2.27	Tr	Tr	Tr	79.8±1.8	ND	ND	73.6±2.1	ND1	ND	Tr	ND
CBC	2.27	2.1±0.4	2.1±0.3	2.3±0.1	5.4±0.1	1.4±0.1	1.6±0.8	4.6±0.3	0.9±0.1	0.9	1.4±0.1	2.2±0.2
CB(1)	2.32	0.8±0.5	1.1±0.2	1.6±0.3	1.2	0.7	ND	ND	Tr	Tr	Tr	Tr
CBGM	2.32	ND	1.1±0.1	ND	ND	ND	ND	ND	1.8±0.3	2.6±0.1	Tr	Tr
Δ8-THC	2.33	Tr	0.7±0.1	Tr	Tr	ND	ND	1.2±0.1	ND	0.6	Tr	Tr
Δ9-THC	2.37	199.2 ±33	181 ±21	207.5 ±19	61.5 ±1.9	144.1 ±16	26 ±7	3.4 ±0.6	95.2 ±6.7	87.2 ±3.4	120.1 ±5.5	134.9 ±6.6
CBG	2.42	10±1.6	4.1±1.3	11.2±2	1.7±0.2	2.8±0.6	1±0.4	ND	1.9±0.2	3.0±0.3	2.1±0.1	1.2±0.1

[a]*RRt* relative retention time to β-caryophyllene. [b]ND = not detected (< LOD). [c]Tr = trace levels detected (< LOQ). [p]Putative identification.

Higher levels of cannabinoids were positively correlated to higher levels of terpenoids (Figure 1). Both the cannabinoids and terpenoids of cannabis are localized primarily in glandular trichomes (Malingre et al., 1975; Taura et al., 2007). This may explain why in some varieties their levels are correlated, however it does not prove that their biosynthesis is necessarily correlated. This is demonstrated by the Bedropuur variety whose Δ^9-THC levels are high but its terpenoid levels are similar to the varieties AD and AG. This suggests that it is possible to breed cannabis that contains high levels of Δ^9-THC but not necessarily higher levels of terpenoids.

Figure 2 PCA of all cannabis varieties. PC1 versus PC2, scatter plot (top) and loading plot (bottom). (1) AO, (2) Bedropuur, (3) Bedrocan, (4) Bediol, (5) AG, (6) AE, (7) Ai94, (8) AN, (9) AF, (10) AM, and (11) AD.

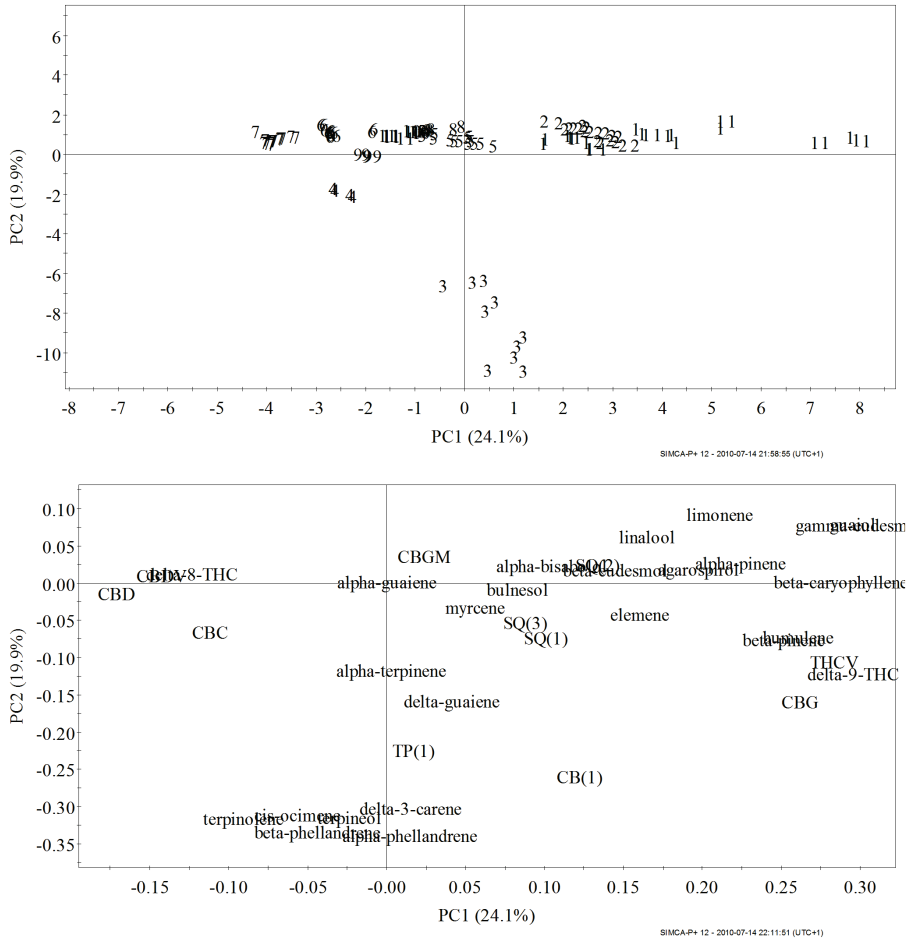

Figure 3 PCA of all cannabis varieties. PC1 versus PC3, scatter plot (top) and loading plot (bottom). (1) AO, (2) Bedropuur, (3) Bedrocan, (4) Bediol, (5) AG, (6) AE, (7) Ai94, (8) AN, (9) AF, (10) AM, and (11) AD.

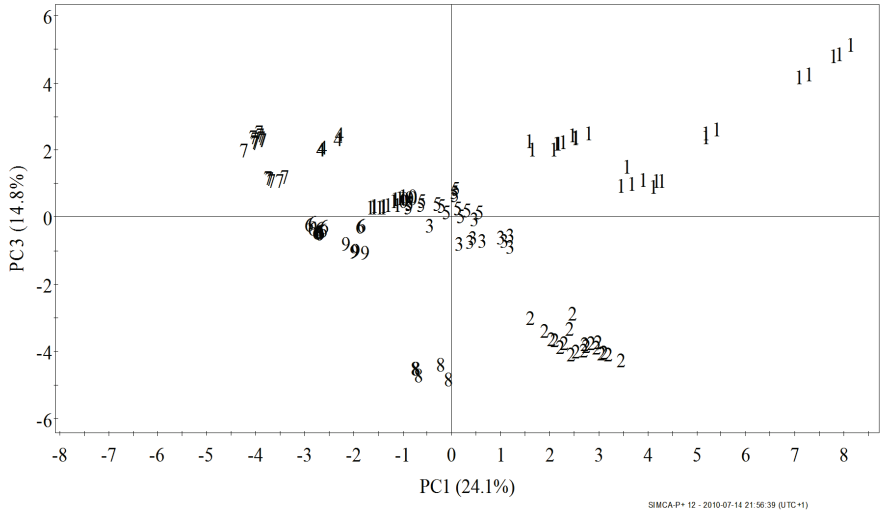

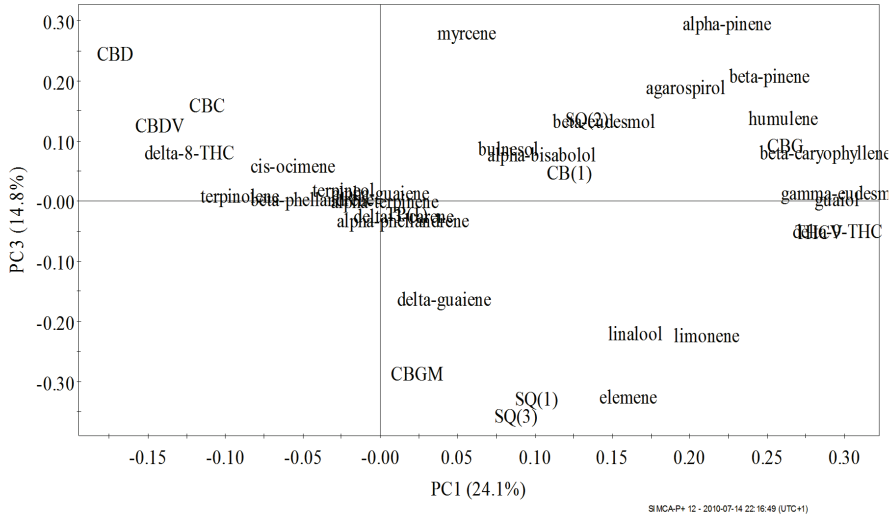

Metabolic fingerprinting of cannabis

It's clear from the data that each cannabis variety is both qualitatively and quantitatively different (Table 3). The levels of Δ^9-THC ranged from 20.8% (Bedrocan) to 0.3% (Ai94). Bedrocan, Bedropuur, and AO all contained high levels of Δ^9-THC (>15%). AG, AM, AD, AN, and AF all contained a medium level of Δ^9-THC (<15%, >5%). Bediol also contained a medium level of Δ^9-THC (6%) however its relatively

high level of CBD (8%) makes it unique compared to the other varieties. AE and Ai94 contained low amounts of Δ^9-THC (<5%). Ai94 contained a relatively high level of CBD (7.4%) compared to the other varieties. Ai94 also contained the C_3 side chain variant of CBD, (-)-cannabidivarin (CBDV). Bediol only contained trace levels of CBDV. The levels of propyl side chain analogues of cannabinoids have been reported to be of chemotaxonomic significance. It has been hypothesized that the enzymes involved in enhancing the levels of these compounds originate from *C. indica* and are not commonly present in *C. sativa* subtype (Hillig and Mahlberg, 2004). CBD was only detected in trace amounts (<0.6 mg/g) or not at all among the high, medium, and low Δ^9-THC varieties making them representatives of the drug/Δ^9-THC chemotype. Bediol is representative of the intermediate chemotype and Ai94 is representative of the fiber/CBD chemotype. The levels of Δ^9-THC and CBD alone do not chemically distinguish the high or medium Δ^9-THC containing varieties well from one another.

Therefore to further chemically classify cannabis principle component analysis (PCA) was used. PCA is a multivariate projection method which extracts and displays systemic variation from a set of matrix data consisting of observations and variables (Eriksson et al.,, 2006). The 36 compounds were the variables and their mg/g levels the observations. Initially all the cannabis samples were analyzed by PCA (Figure 2). Principal component 1 (PC1) and PC2 explains 44% of the variance. The highest Δ^9-THC containing varieties Bedropuur, Bedrocan, and AO are separated along the positive PC1. The Bedrocan variety was also well separated along negative PC2. The compounds responsible for making Bedrocan different according to the loading plot are terpinolene, β-phellandrene, α-phellandrene, terpineol, *cis*-ocimene, and Δ^3-carene. Bedrocan contained higher levels of these compounds compared with other varieties. Terpinolene was a very dominant monoterpenoid (11.3 mg/g) in the Bedrocan variety (Table 3). Bediol partially separated along the negative PC2 also contained terpinolene, β-phellandrene, α-phellandrene, terpineol, and Δ^3-carene but in lower levels than Bedrocan. This observation is interesting because the Bediol variety was bred by hybridizing the Bedrocan variety with higher CBD containing varieties.

The loading plot along the positive PC1 and positive PC2 shows that Bedropuur and AO contained more of the sesquiterpene alcohols guaiol, γ-eudesmol, β-eudesmol (Figure 2). The study by Hillig (2004) reported that guaiol, γ-eudesmol, and β-eudesmol were characteristic terpenoid compounds of the *C. indica* varieties originating from Afghanistan. These sesquiterpenoid alcohols appear to be important in distinguishing *C. indica* varieties from one another because the AG, AN, AM, and AD varieties which are also *C. indica* morphotypes did not contain detectable levels of these compounds. AF another *C. indica* only contained trace amounts of these compounds (Table 3). In order to distinguish Bedropuur and AO further PC1 and PC3 were compared (Figure 3). PC3 was able to explain an additional 15% of the variance. The Bedropuur variety contained higher levels of limonene as well as the sesquiterpenoid elemene while the AO variety contained higher levels of myrcene and α-pinene. Also along PC3 information was obtained about the AN variety which contains a medium level of Δ^9-THC (95.2 mg/g) but higher levels of the sesquiterpenoids SQ(1), SQ(3), and elemene when compared to all other varieties.

The medium Δ^9-THC varieties AG, AF, AM, and AD were not well separated along PC1, 2, or 3. Therefore these varieties were reanalyzed by PCA with all other varieties excluded (Figure 4). AG and AD had higher and very similar levels of Δ^9-THC, myrcene, and β-caryophyllene compared with AM and AF. AG and AD were distinguished along PC2. AG contained more α-pinene, β-pinene, limonene, α-guaiene, elemene, and SQ(3). AD however contained low levels of monoterpenoids and sesquiterpenoids in general and only slightly higher levels (<1.0 mg/g) of myrcene, β-caryophyllene, and CBC compared to AG. AF contained the highest levels of cannabigerol monomethyl ether (CBGM) while AM contained higher levels of myrcene and α-pinene.

Hierarchical cluster analysis (HCA) was used to confirm the PCA analysis (Figure 5). The AO batches are all clustered together and each genotype (different seed) is also grouped together. The Bedropuur batches are clustered together and AN was the next similar variety. Both Bedropuur and AN were separated along the negative PC3 (Figure 3) because of the presence of the cannabinoid CBGM as well as numerous similarities in monoterpenoids and sesquiterpenoids (Table 3). Bedrocan was in its own group which is consistent with PCA analysis. The clipped Bedrocan batch exhibits some differences according to HCA when compared to unclipped. Bediol and Ai94 are related due to higher levels of CBD but each clustering on their own. Ai94(2) however was clustered closer too AE and AF most likely because of small differences caused by growing this variety in different batches. The medium Δ^9-THC varieties are all clustered close to one another except AF. AF was closer to AE and Ai94(2) most likely because it has the lowest amount of Δ^9-THC compared to the other medium varieties. Each medium Δ^9-THC variety is clustered with itself except AG because it was grown in different batches which caused small differences in chemical profile. The morphotype of each medium Δ^9-THC variety does not seem important in relating these varieties.

These observations represent a significant improvement compared with other methodologies, discussed in the introduction, using chemotaxonomy to discriminate cannabis varieties. By using quantitative data on cannabinoid and terpenoid levels it was possible to chemically distinguish each variety from one another with the aid of PCA. Both Hillig (2004) and Hillig and Mahlberg (2004) had difficulty discriminating drug type cannabis accessions from one another. Furthermore the conclusion in the study of Hillig (2004) that sesquiterpenoids were more important than monoterpenoids in chemically differentiating cannabis varieties is not accurate. In this study monoterpenoids were able to distinguish varieties which had similar sesquiterpenoid levels and similar cannabinoid levels such as AO and Bedropuur as well as a number of the medium Δ^9-THC varieties.

Effect of growing cannabis in different batches and growth cycle deviations

The effect on chemical profile from growing cannabis varieties in separate batches about a month apart as well 1 week extra vegetative and flowering periods was studied in the AG, AE, and Ai94 varieties. A comparison of the compounds within the AG varieties batches is shown in Figure 6. The differences between each batch were

minor with no clear distinction between them. The largest differences are between AG(1) and AG(2) with the level of myrcene being 1.8 mg/g higher on average in AG(1) compared with AG(2), β-caryophyllene being 0.5 mg/g higher on average in AG(2) compared to AG(1), CBG being 0.8 mg/g higher in AG(2) compared to AG(1), and Δ^9-THC being 17.3 mg/g higher in AG(2) compared to AG(1). Most compounds in the AE batches did not differ much in concentration (<1.0 mg/g), except terpinolene and Δ^9-THC (Figure 7). The Ai94 batches also only had minor differences (Figure 8). These results importantly demonstrate that genetically identical cannabis plants grown in batches at separate times under standardized environmental conditions are reproducible in terms of terpenoid and cannabinoid concentrations.

Figure 4 PCA of the varieties AG, AD, AM, and AF. PC1 versus PC2 scatter plot (top) and loading plot (bottom).

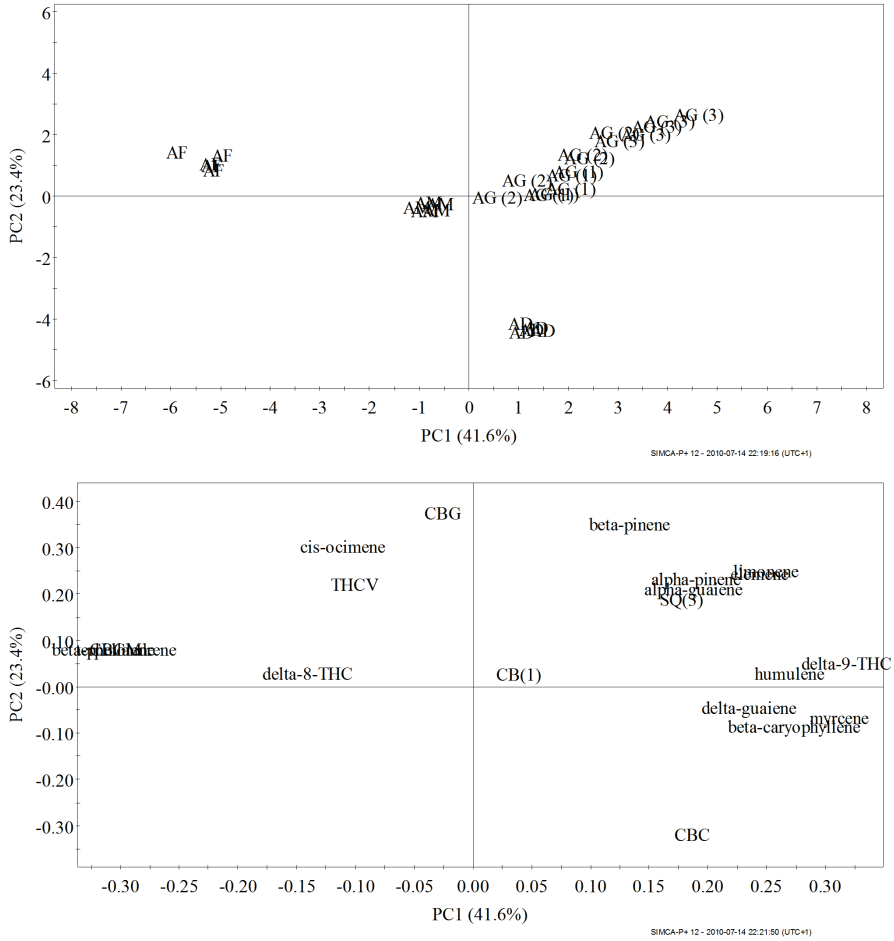

Figure 5 Hierarchical clustering analysis of all cannabis samples.

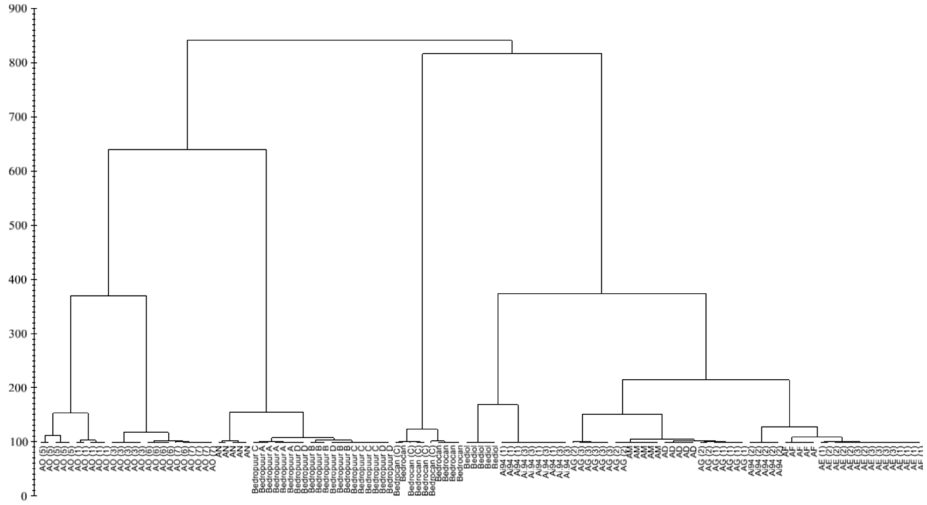

A detailed look into the chemical variation among the Bedropuur batches is shown in Figure 9. Batches A, C, and D differed in the concentrations of certain compounds compared with the standard batch B. The levels of limonene were lower in A, C, and D. Myrcene was lower in A and D compared with B and C. The levels of Δ^9-THC were about 30 mg/g higher in Bedropuur C compared to the other 3 batches. Bedropuur D had the lowest amount of Δ^9-THC. Bedropuur A had lower concentrations of the β-caryophyllene, elemene, and CBG when compared to batches B and C. These results demonstrate that alterations in growth cycle time can cause changes in the chemical profile of cannabis plants grown under environmental conditions that were otherwise the same. Alterations in growth cycle time appear to cause more differences in a cannabis varieties chemical profile then growing the plant material in different batches. However more experiments with more varieties, grown with more deviations in growth cycle time, and more replicates would be needed to confirm these observations.

Clipping the lower branches on the Bedrocan variety caused some compounds to be present at lower concentrations (Figure 10). These compounds include myrcene, *cis*-ocimene, β-caryophyllene, elemene, CBG, and Δ^9-THC. This suggests that by clipping the lower branches, which would allow more water and nutrients to flow to the upper parts of the plant closest to the light, does causes some changes in the chemical profile. Further experiments would be needed to determine if this represents a consistent pattern and explain why it occurs.

The different AO batches exhibited the greatest quantitative differences in chemical profile compared with all other varieties (Figure 11). AO batches exhibited a wide range of concentrations for α-pinene, myrcene, β-caryophyllene, and Δ^9-THC. The different AO batches could even be clearly distinguished by PCA (Figure 12). This observation shows that by metabolically profiling cannabis strains based on cannabinoid

and terpenoid levels it is also possible to distinguish separate genotypes of the same variety.

Overall these experiments demonstrate that the best way to grow reproducible batches of cannabis is by using genetically identical plant material grown from clones, under standardized environmental conditions, with the same growth cycle. Deviations in growth cycle and clipping of lower branches can cause quantitative differences, although minor in absolute terms, in chemical profile. These deviations can obscure their chemical classification as was observed in the HCA. Cannabis plants from seeds representing different genotypes but the same variety can differ considerably in quantitative chemical profile. Future research should aim to determine if cannabis could be grown in such a reproducible manner for many years. As a preliminary indication of chemical profile reproducibility a previous study in our laboratory using similar methodology analyzed the Bedrocan variety. This plant material was grown about 1 year previously to the batches analyzed in this study. This batch had similar levels of the main compounds observed in the present study (Fischedick et al., 2010).

Conclusions

In this study a simple quantitative GC-FID method was validated for the quantitative analysis of cannabis monoterpenoids, sesquiterpenoids, and cannabinoids. Quantitative GC data was used to chemically discriminate cannabis varieties with the aid of principal component analysis. Our results show for the first time using validated methodology the absolute (mg/g) levels of cannabinoids and terpenoids in cannabis simultaneously. This data can be useful for guiding pharmacological or clinical studies that want to examine the potential interactions of the volatile constituents of cannabis. The chemical profile of cannabis varieties could potentially be more closely correlated to therapeutic effectiveness. The reported methodology could be implemented in the quality control of medicinal cannabis. Our methodology also appears to be able to overcome the difficulties in chemotaxonomic analysis of cannabis observed by other researchers in distinguishing drug type cannabis varieties from one another. These techniques should be applied on a wider range of cannabis samples representing both geographically and morphologically distinct varieties. By combining genomic approaches with metabolic fingerprinting it may be possible to elucidate exactly which biochemical pathways differ in various cannabis varieties and how these differences lead to the observed chemical profile.

Figure 6 Comparison of AG batches. Compounds that are missing in certain batches were present at levels < LOQ.

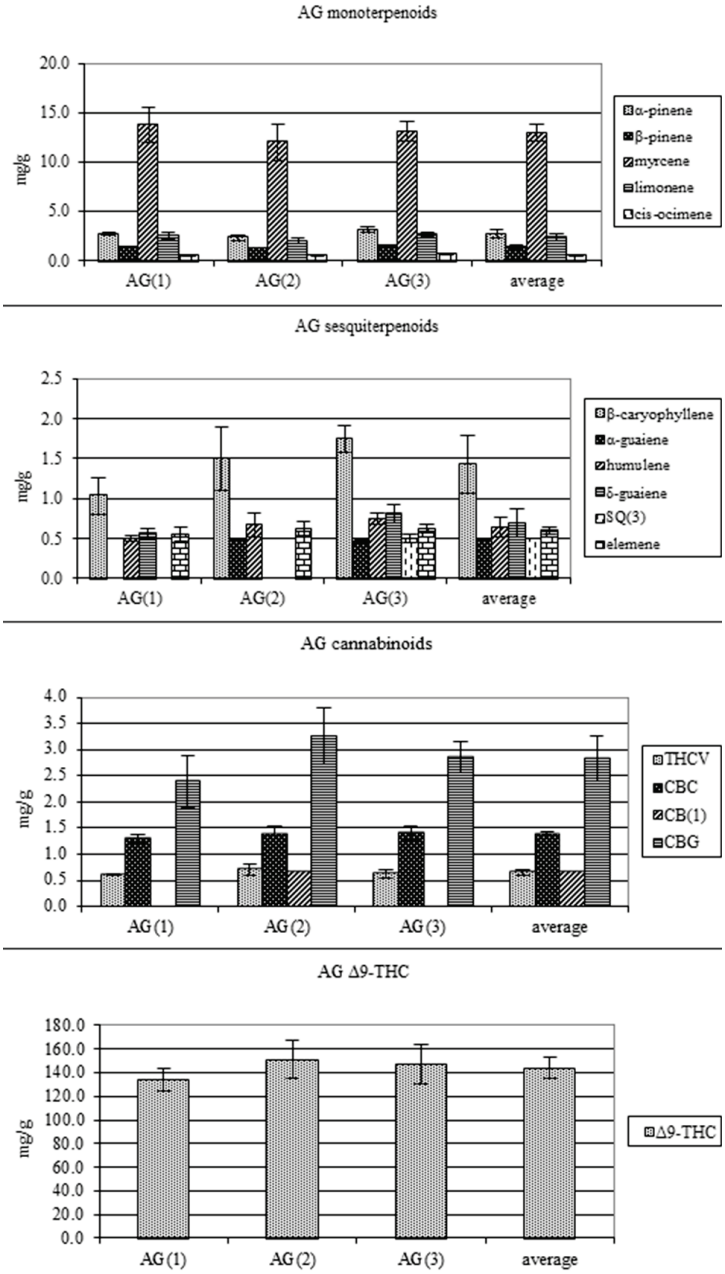

Figure 7 Comparison of AE batches. Compounds that are missing in certain batches were present at levels < LOQ.

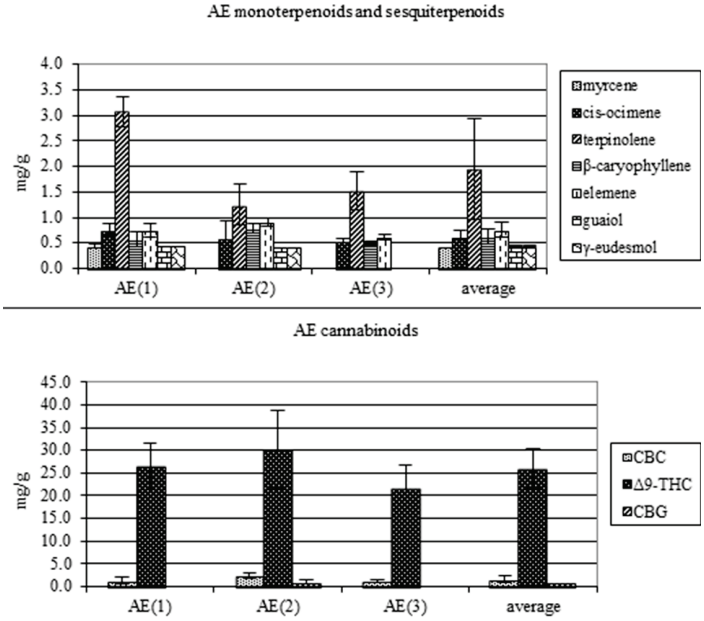

Figure 8 Comparison of Ai94 batches. Compounds that are missing in certain batches were present at levels < LOQ.

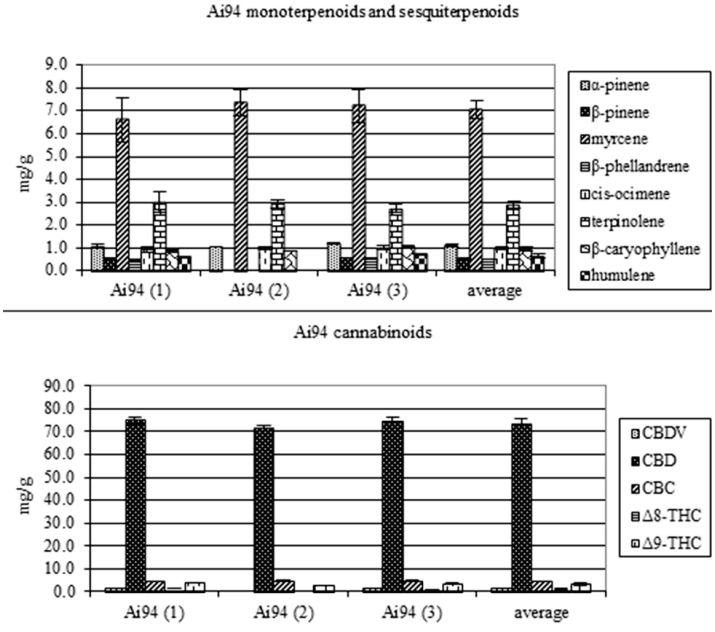

Figure 9 Comparison of Bedropuur batches. Compounds that are missing in certain batches were present at levels < LOQ.

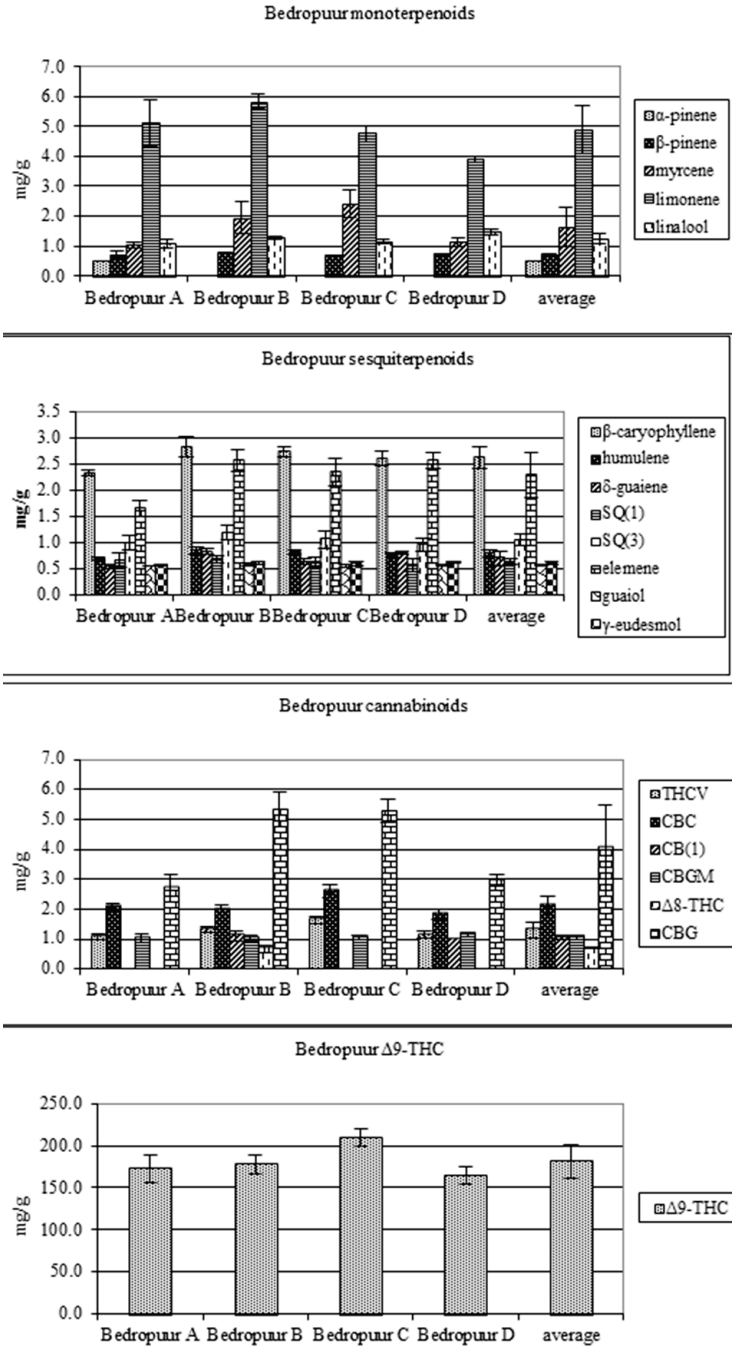

Figure 10 Comparison of Bedrocan batches. Compounds that are missing in certain batches were present at levels < LOQ.

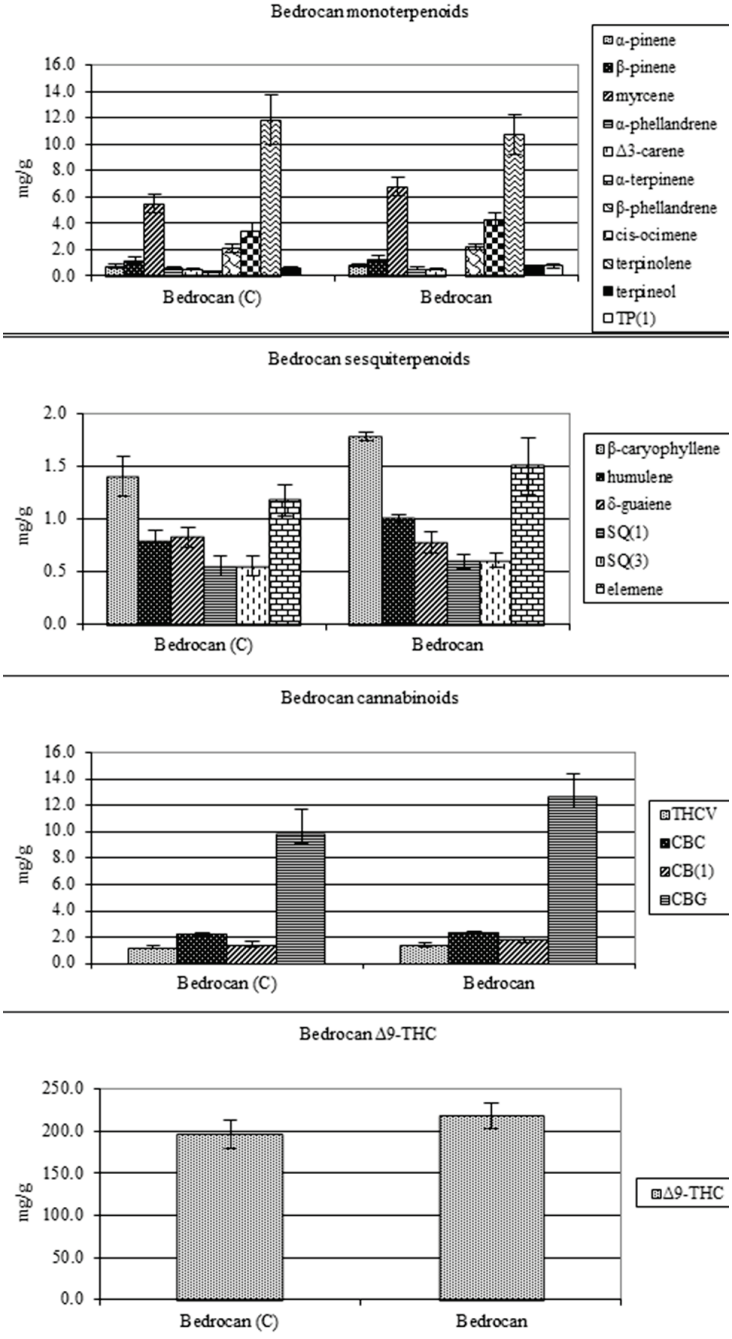

Figure 11 Comparison of AO seed batches. Compounds that are missing in certain batches were present at levels < LOQ.

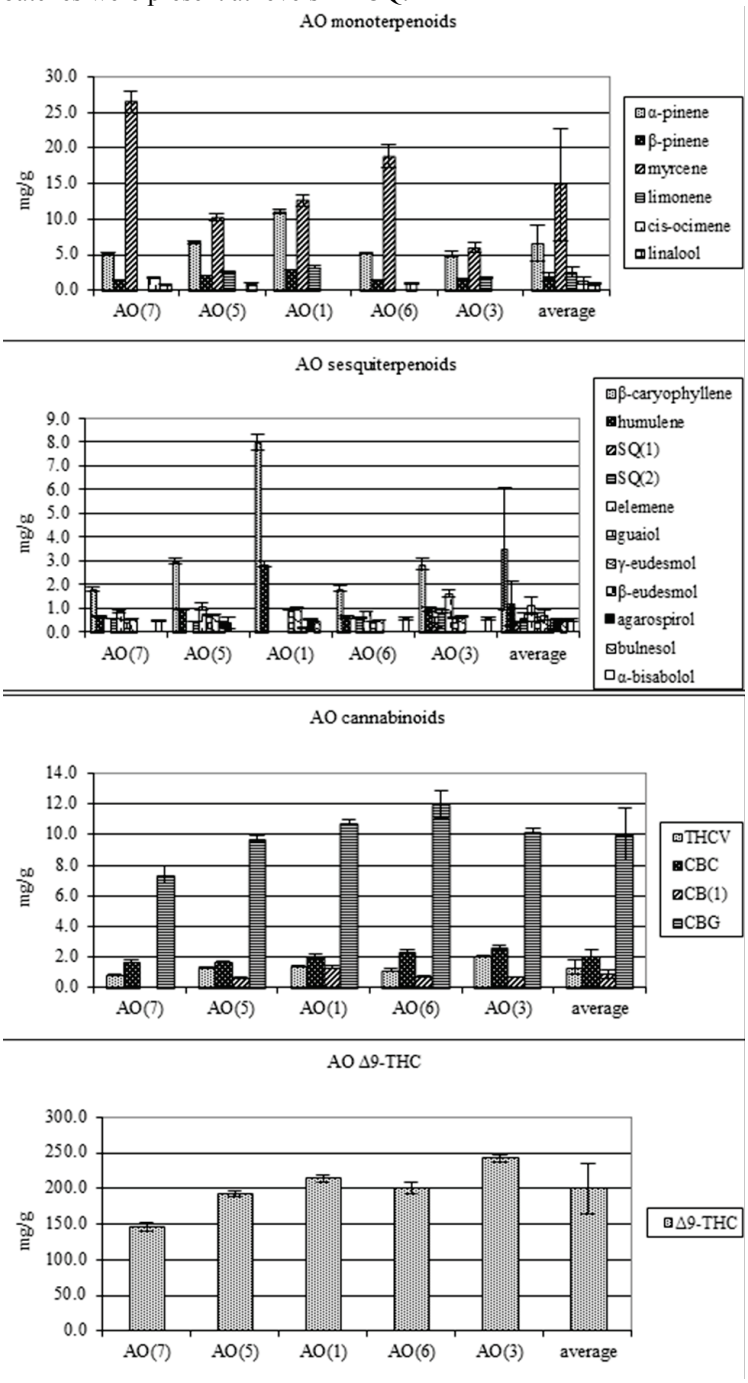

Figure 12 PCA loading plot PC1 versus PC2 of AO seed batches.

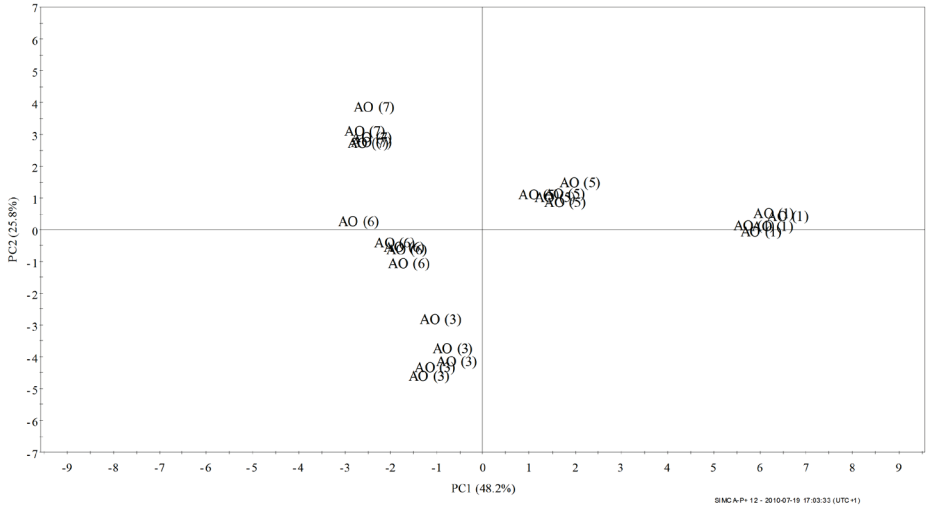

Acknowledgements

We thank Bedrocan BV for supplying the plant material used in this study. We also thank the STW foundation for financial support of this study.

References

Adams, R.P., 1989. Identification of Essential Oils by Ion Trap Mass Spectrometry. Academic Press Inc, New York.

Safwat, S.A., Ross, S.A., Slade, D., Radwan, M.M., Zulfiqar, F., ElSohly, M.A., 2008. Cannabinoid ester constituents from high-potency *Cannabis sativa*. Journal of Natural Products 71, 536-542.

Ben Amar, M., 2006. Cannabinoids in medicine: a review of their therapeutic potential. Journal of Ethnopharmacology 105, 1-25.

Bicchi, C., Liberto, E., Matteodo, M., Sgorbini, B., Mondello, L., Zellner, B.A., Costa, R., Rubiolo, P., 2008. Quantitative analysis of essential oils: a complex task. Flavour and Fragrance Journal 23, 382-391.

Choi, Y.H., Kim, H.K., Hazekamp, A., Erkelens, C., Lefeber, A.W.M., Verpoorte, R., 2004. Metabolic differentiation of *Cannabis sativa* cultivars using ^{1}H-NMR spectroscopy and principal components analysis. Journal of Natural Products 67, 953-957.

ElSohly, M.A., Wachtel, S.R., de Wit, H., 2003. Cannabis versus THC: response to Russo and McPartland. Psychopharmacology 165, 433-434.

ElSohly, M.A., Slade, D., 2005. Chemical constituents of marijuana: The complex mixture of natural cannabinoids. Life Sciences 78, 539-548.

Fairbairn, J.W., Pickens, J.T., 1981. Activity of cannabis in relation to its Δ'-*trans*-tetrahydrocannabinol content. British Journal of Pharmacology 72, 401-409.

Fetterman, P.S., Keith, E.S., Waller, C.W., Guerrero, O., Doorenbos, N.J., Quimby, M.W., 1971. Mississippi-grown *Cannabis sativa* L. preliminary observation on chemical definition of phenotype and variations in tetrahydrocannabinol content versus age, sex, and plant part. Journal of Pharmaceutical Sciences 60, 1246-1477.

Fischedick, J., Van der Kooy, F., Verpoorte, R., 2010. Cannabinoid receptor 1 binding activity and quantitative analysis of *Cannabis sativa* L. smoke and vapor. Chemical Pharmaceutical Bulletin 58, 201-207.

Hazekamp, A., Choi, Y.H., Verpoorte, R., 2004a. Quantitative analysis of cannabinoids from *Cannabis sativa* using ^{1}H-NMR. Chemical Pharmaceutical Bulletin 52, 718-721.

Hazekamp, A., Simons, R., Peltenburg-Looman, A., Sengers, M., Van Zweden, R., Verpoorte, R., 2004b. Preparative isolation of cannabinoids from *Cannabis sativa* by centrifugal partition chromatography. Journal of Liquid Chromatography and Related Technologies 27, 2421-2439.

Hazekamp, A., 2006. An evaluation of the quality of medicinal grade cannabis in the Netherlands. Cannabinoids 1, 1-9.

Hazekamp, A., 2007. Cannabis extracting the medicine. Doctoral thesis, Universiteit Leiden, Leiden, The Netherlands.

Hazekamp, A., Grotenhermen, F., 2010. Review on clinical studies with cannabis and cannabinoids 2005-2009. Cannabinoids 5, 1-21.

Hillig, K.W., 2004. A chemotaxonomic analysis of terpenoid variation in *cannabis*. Biochemical Systematics and Ecology 32, 875-891.

Hillig, K.W., Mahlberg, P.G., 2004. A chemotaxonomic analysis of cannabinoid variation in *cannabis* (cannabaceae). American Journal of Botany 91, 966-975.

Hoffmann, D.E., Weber E., 2010. Medical marijuana and the law. New England Journal of Medicine 362, 1453-1457.

Johnson, J.M., Lemberger, L., Novotny, M., Forney, R.B., Dalton, W.S., Maskarinec, M.P., 1984. Pharmacological activity of the basic fraction of marihuana whole smoke condensate alone and in combination with delta-9-tetrahydrocannabinol in mice. Toxicology and Applied Pharmacology 72, 440-448.

Komori, T., Nohara, T., Hosokawa, I., Kawasaki, T., 1968. Cannabigerol monomethyl ether, a new component of hemp. Chemical Pharmaceutical Bulletin 16, 1164-1165.

Llan, A.B., Gevins, A., Coleman, M., ElSohly, M.A., de Wit, H., 2005, Neurophysiological and subjective profile of marijuana with varying concentrations of cannabinoids. Behavioral Pharmacology 16, 487-496.

Malingre, T., Hendricks, H., Batterman, S., Bos, R., Visser, J., 1975. The essential oil of *Cannabis sativa*. Planta Medica 28, 56-61.

McPartland, J.M., Russo, E.B., 2001. Cannabis and cannabis extracts: greater then the sum of their parts? Journal of Cannabis Therapeutics 1, 103-132.

Office of Medicinal Cannabis [WWW Document], 2010. . Ministerie van Volksgezondheid Welzijn en Sport. URL http://www.cannabisbureau.nl/en/

Pertwee, R.G., 2006. Cannabinoid pharmacology: the first 66 years. British Journal of Pharmacology 147, 163-171.

Pertwee, R.G., 2009. Emerging strategies for exploiting cannabinoid receptor agonists as medicines. British Journal of Pharmacology 156, 397-411.

Pickens, J.T., 1981. Sedative activity of cannabis in relation to its Δ'-*trans*-tetrahydrocannabinol and cannabidiol content. British Journal of Pharmacology 72, 649-656.

Politi, M., Peschel, W., Wilson, N., Zloh, M., Prieto, J.M., Heinrich, M., 2008. Direct NMR analysis of cannabis water extracts and tinctures and semi-quantitative data on Δ^9-THC and Δ^9-THC-acid. Phytochemistry 69, 562-570.

Radwan, M.M., ElSohly M.A., Slade, D., Admed, S.A., Khan, I.A., Ross, S.A., 2009. Biologically active cannabinoids from high-potency *Cannabis sativa*. Journal of Natural Products 72, 906-911.

Ross, S.A., ElSohly, M.A., 1996. The volatile oil composition of fresh and air-dried buds of *Cannabis sativa*. Journal of Natural Products 59, 49-51.

Rothschild, M., Bergström, G., Wångberg, S., 2005. *Cannabis sativa*: volatile compounds from pollen and entire male and female plants of two variants, Northern lights and Hawaian indica. Botanical Journal of the Linnean Society 147, 387-397.

Russo, E.B., McPartland, J.M., 2003. Cannabis is more than simply Δ^9-tetrahydrocannabinol. Psychopharmacology 165, 431-432.

Russo, E.B., 2007. History of cannabis and its preparations in saga, science, and sobriquet. Chemistry & Biodiversity 4, 1614-1648.

Ryan, D., Drysdale, A.J., Pertwee, R.G., Platt, B., 2006. Differential effects of cannabis extracts and pure plant cannabinoids on hippocampal neurones and glia. Neuroscience Letters 408, 236-241.

Segelman, A.B., Sofia, R.D., Segelman, F.P., Harakal, J.J., Knobloch, L.C., 1974. *Cannabis sativa* L. (marijuana) V: pharmacological evaluation of marijuana aqueous extract and volatile oil. Journal Pharmaceutical Sciences 26, 962-964.

Small, E., Beckstead, H.D., 1973a. Cannabinoid phenotypes in *Cannabis sativa*. Nature 245, 147-148.

Small, E., Beckstead, H.D., 1973b. Common cannabinoid phenotypes in 350 stocks of *cannabis*. Lloydia 36, 144-165.

Taura, F., Sirikantaramas, S., Shoyama, Y., Shoyama, Y., Morimoto, S., 2007. Phytocannabinoids in *Cannabis sativa*: recent studies on biosynthetic enzymes. Chemistry & Biodiversity 4, 1649-1663.

Eriksson, L., Johansson, E., Kettaneh-Wold, N., Tyrgg, J., Wikström, C., Wold, S., 2006. Multi- and megavariate data analysis part 1: Basic principles and applications, second ed. Umetrics, Umeå, Sweden.

van der Kooy, F., Maltese, F., Choi, Y.H., Kim, H.K., Verpoorte, R., 2009. Quality control of herbal material and phytopharmaceuticals with MS and NMR based metabolic fingerprinting. Planta Medica 75, 763-775.

Wachtel, S.R., ElSohly, M.A., Ross, S.A., Ambre, de Wit, J.H., 2002. Comparison of the subjective effects of Δ^9-tetrahydrocannabinol and marijuana in humans. Psychopharmacology 161, 331-339.

Whalley, B.J., Wilkinson, J.D., Williamson, E.M., Constanti, A., 2004. A novel component of cannabis extracts potentiates excitatory synaptic transmission in rat olfactory cortex *in vitro*. Neuroscience Letters 365, 58-63.

Wilkinson, J.D., Whalley, B.J., Baker, D., Pryce, G., Constanti, A., Gibbons, S., Williamson, E.M., 2003. Medicinal cannabis: is Δ^9-tetrahydrocannabinol necessary for all its effects? Journal of Pharmacy and Pharmacology 55, 1687-1694.

Williamson, E.M., Evans, F.J., 2000. Cannabinoids in clinical practice. Drugs 60, 1303-13.

Chapter 5

Activation of antioxidant response element in mouse primary cortical cultures with sesquiterpene lactones isolated from *Tanacetum parthenium*

Justin T Fischedick[a,b], Miranda Standiford[c], Delinda A. Johnson[c], Ric C.H. De Vos[d,e,f], Slađana Todorović[g], Tijana Banjanac[g], Rob Verpoorte[b], Jeffrey A. Johnson[c]

[a] *PRISNA BV, Einsteinweg 55, 2300 RA Leiden, The Netherlands*
[b] *Natural Products Laboratory, Institute of Biology, Leiden University, 2300 RA Leiden, The Netherlands*
[c] *Division of Pharmaceutical Sciences, School of Pharmacy, University of Wisconsin, Madison, WI, USA*
[d] *Plant Research International, BU Biosciences, Wageningen University and Research Centre, Wageningen, The Netherlands*
[e] *Centre for BioSystems Genomics, Wageningen, The Netherlands*
[f] *Netherlands Metabolomics Centre, Leiden, The Netherlands*
[g] *Institute for Biological Research "Siniša Stanković", University of Belgrade, Belgrade, Serbia*

Abstract

Tanacetum parthenium (Asteraceae) produces biologically active sesquiterpene lactones (SL). Nuclear factor E2-related factor 2 (Nrf2) is a transcription factor known to activate a series of genes termed the antioxidant response element (ARE). Activation of Nrf2/ARE may be useful for the treatment of neurodegenerative disease. In this study we isolated 11 SL from *T. parthenium* with centrifugal partition chromatography and semi-preparative HPLC. Compounds were screened *in-vitro* for their ability to activate the ARE on primary mouse cortical cultures as well as for their toxicity towards the cultures. All SL containing the α-methylene-γ-lactone moiety were able to activate the ARE and cause cellular toxicity. The structure activity relationship among the SL isolated indicates that the guaianolides were more active and when lacking the endoperoxide functionality less toxic then the germacranolides.

Published:

Fischedick, J., Standiford, M., Johnson, D., De Vos, R., Todorović, S., Banjanac, T., Verpoorte, R., Johnson, J., 2012. Activation of Antioxidant Response Element in Mouse Primary Cortical Cultures with Sesquiterpene Lactones Isolated from *Tanacetum parthenium*. Planta Medica 78, 1725–1730.

Introduction

Tanacetum parthenium L. (syn. *Chrysanthemum parthenium*), commonly known as feverfew, is a member of the Asteraceae family containing various sesquiterpene lactones (SL) from the germacranolide, eudesmanolide, and guaianolide groups. In European traditional medicine, *T. parthenium* has been used for the treatment of migraine and rheumatism. The germacranolide, 4α,5β-epoxy-germacra-1-(10),11-(13)-dien-12,6α-olide (parthenolide (**1**)) is often regarded as the primary active ingredient in *T. parthenium* (Abed et al., 1995). Parthenolide exhibits numerous biological activities such as cytotoxicity, anti-viral, anti-leishmanial, and anti-inflammatory action (Hwang et al., 2006; Tiuman et al., 2005; Salminen et al., 2008). In past decades **1** and other SL have been the subject of cancer clinical trials (Ghantous et al., 2010).

Nrf2 is a transcription factor known to induce genes encoding cytoprotective and antioxidant enzymes by binding to the cis-acting enhancer element called ARE, in the promoter of these genes. Activation of Nrf2/ARE pathway with small molecules is a potential strategy to treat neurodegenerative diseases (Calkins et al., 2009; de Vries et al., 2008). Nrf2 localization and degradation is regulated by its cytoplasmic repressor protein the Kelch-like ECH-associated protein 1 (Keap1). Various compounds or reactive oxygen species (ROS) can interfere with the ability of Keap1 to bind Nrf2 and thereby up-regulate activation of ARE (de Vries et al., 2008). A series of conserved cysteine residues on Keap1 are important for compounds like tert-buytlhydroxyquinone (*t*BHQ) or ROS to liberate Nrf2 from Keap1 (Zhang and Hannink, 2003; Itoh et al., 2004).

The biological activity of many SL such as **1** is often attributed to the presence of the α-methylene-γ-lactone moiety. The nucleophilic methylene can react with biological thiols, such as cysteine residues on proteins, by a Michael addition type reaction (Mathema et al., 2012). Mild activation of Nrf2/ARE by **1** has been demonstrated using human hepatoma (HepG2) cells and SL from *Calea urticifolia* along with **1** in rat pheochromocytoma (PC12) cells (Jeong et al., 2005; Umemura et al., 2008). Neither study however investigated 11,13-dihydro versions of the compounds to confirm importance of α-methylene-γ-lactone moiety nor the toxicity of **1**. Another study demonstrated a neuroprotective effect of the SL isoatriplicolide tiglate against glutamate induced toxicity on primary rat cortical cells, however molecular mechanisms and toxicity were not investigated (Kim et al., 2010). Neurotoxic effects of SL such as repin from *Centaurea* species, which causes a disease in horses called equine nigropallidal enchalomalacia, have also been reported (Tukov et al., 2004).

Therefore in order to gain further insight into the structure activity relationships of SL for Nrf2/ARE activation, a variety of SL were isolated from *T. parthenium*. Due to difficulties reported in the isolation of certain SL from *T. parthenium* (Bohlmann and Zdero, 1982), a centrifugal partition chromatography (CPC) method was developed to improve their isolation. Isolated compounds were screened *in vitro* for ARE activation using primary mouse cortical cultures derived from ARE-human placental alkaline phosphatase (hPAP) transgenic reporter mice (Johnson et al.,

2002). Since SL are potentially neurotoxic, the compounds toxicity towards the cultures was also evaluated using the 3-(4,5-dimethylthiazol-2-yl)-5-(3-carboxymethoxyphenyl)-2-(4-sulfophenyl) 2H tetrazoluim inner salt (MTS) assay.

Materials and Methods

Chemicals

Ethylacetate (EtOAc), n-heptane (Hept), methanol (MeOH), ethanol (EtOH), n-hexane (Hex), diethylether (Et_2O), acetone, dichloromethane (DCM) of analytical reagent grade, and MeOH HPLC grade were purchased from Biosolve BV (Valkenswaard, The Netherlands). Et_2O was distilled at 35 °C prior to use. Vanillin, parthenolide (90% purity), and chloroform ($CHCl_3$) were from Sigma-Aldrich Inc. (St. Louis, Missouri, USA). Sulfuric acid 95-97% from Fluka GmbH (Buchs, Switzerland), magnesium sulfate ($MgSO_4$) from Brocacef BV (Maarssen, The Netherlands), silica gel 60 (0.063 - 0.2 mm) for column chromatography, and silica gel 60 F_{254} 10 x 20 cm TLC plates (Merck, Darmstadt, Germany) were used. $CDCl_3$ was purchased from Eurisotop SA (Gif-Sur-Yvette, France).

Plant material

One kg of the dried aerial parts of *T. parthenium* was purchased from De Groene Luifel BV (Sluis, The Netherlands) referred to as NL and 2 kg of the dried flower heads of *T. parthenium* was grown at the University of Belgrade Institute for Biological Research referred to as IBRSS. Plant material was identified by Wout Holverda and voucher specimens were deposited in the economic botany collection of the National Herbarium Nederland in Leiden under the following barcodes 0991399 J. Fischedick No. 132010 and 0991384 J. Fischedick No. 172010.

Crude extraction preparation

Two hundred and fifty g of NL plant material was extracted 3 times with 4, 3, and 3 L of EtOH with stirring for 24 h each with an initial 30 min of ultra-sonication. EtOH extracts were combined and solvent removed under reduced pressure at 40 °C. The extract was then dissolved in 500 mL EtOAc and rinsed 3 times with 500 mL H_2O. The EtOAc fraction was dried over $MgSO_4$, filtered, and EtOAc removed under reduced pressure at 40 °C yielding 8.0 g of a dark green extract (Extract 1). Extract 2 was prepared in the same way as extract 1 except 250 g of IBRSS plant material, flower heads only, was used and yielded 17.3 g of a dark golden extract.

CPC apparatus and solvent system selection

CPC experiments were carried out on a Fast Centrifugal Partition Chromatograph with a 1 L internal volume rotor (Kromaton Technologies, Angers, France). The CPC was connected to a Rheodyne injector equipped with a 30 mL injection loop (Rheodyne Inc, Cotati, CA, USA), an AP100 Armen instruments pump (Saint-Avé, France), and a LKB Bromma Fraction Collector 2211 SuperRac (Bromma, Sweden). A Tamson Instruments BV (Bleiswijk, The Netherlands) Low Temperature

Circulator TLC15 set at 21 °C was used to maintain a constant temperature inside the rotor chamber. The CPC solvent system was selected by screening 3 and 4 solvent bi-phasic mixtures described in (Foucault, 1995) for the ability to solubilize a crude *T. parthenium* extract and evenly partition compounds between the upper (↑) and lower (↓) layers. Partitioning of compounds was assessed visually by TLC ($CHCl_3$: EtOAc; 7: 3; vanillin/sulfuric acid reagent) analysis of ↑ and ↓ layers. Finally a solvent system composed of Hept: EtOAc: MeOH: H_2O, 1:1:1:1 (HEMW) solvent system was selected for fractionation of extract 1 and 2.

CPC experiments

Extract 1 could be dissolved in 90 mL of 1:1 mixture of ↑:↓ layer of the HEMW system while extract 2 could be dissolved in 110 mL. In total six CPC experiments were performed to process extracts 1 (CPC1-3) and 2 (CPC4-6). Each CPC experiment consisted of the following procedure. Four L HEMW was prepared by mixing for 1 h, settling for 1 h, and separating into ↑ and ↓ layer. Initially 1.1 L of the ↓ layer was pumped into the CPC system to act as the stationary phase. The CPC was equilibrated by pumping the ↑ layer in ascending mode, at a flow rate of 10 mL/min, and rotor speed of 1000 rpm. The system was in equilibrium when the ↑ layer began to elute and the volume of ↓ layer displaced was recorded (void volume). Thirty mL of sample was injected for all experiments except for experiment 6 which was 50 mL. The 50 mL injection was performed by first injecting 30 mL of the sample, allowing 10 mL/min flow rate to run for 3 min, flow stopped while remaining 20 mL of sample was injected, and the run was continued as normal.

Initially during each CPC experiment 400 mL of the eluent was collected in a glass bottle (FrI) then 85 x 10 mL fractions (Fr) were collected in glass test tubes. After the 85^{th} fraction was collected the ↓ layer was pumped into the system. The remaining ↑ layer was collected in a glass bottle and the fraction labeled Fr↑. Finally 800 mL of the ↓ layer was eluted and this fraction labeled Fr↓. Some ↓ layer bleeding was observed in each experiment however it was confined to FrI. Fractions were analyzed by TLC in the same way as above and combined based on similarity of chemical profile.

HPLC

An Agilent 1200 series HPLC was used for analyzing purity of combined fractions and isolated compounds. The system consisted of a G1322A degasser, G1311A quaternary pump, G1367B Hip automated liquid sampler, and G1315D diode-array (DAD) detector (Agilent technologies Inc, Santa Clara, CA, USA). The software used was Chemstation Rev. B03.02. A 150 x 4.6 mm Luna 5 micron C18 (2) 100A column equipped with a guard column containing C18 4 x 3 mm cartridges was used for separation (Phenomenex Inc, Torrance, CA, USA). Gradient elution with a flow of 0.5 mL/min consisted initially of 50% H_2O and 50% MeOH which increased to 100% MeOH over 40 min and remained at 100% MeOH for 10 min. The DAD detector was set at 210 nm with a UV spectrum scan from 190-390 nm.

Semi-preparative HPLC general procedure

Semi-preparative HPLC (pHPLC) was performed with 2 LC-10ADvp liquid chromatograph pumps, a SPD-10Avp UV-vis detector, a SCL-10Avp system controller, a FRC-10A Fraction Collector, and controlled by software LCsolution Version 1.21 SP1 all manufactured by Shimadzu (Kyoto, Japan). A Luna C18 (2) 100 A 5 micron 250 x 10 mm column was used for reverse phase pHPLC (RP) and a Luna Silica (2) 100 A 5 micron 250 x 10 mm column equipped with a security guard cartridge holder (10 mm internal diameter) containing a security guard semiprep cartridge silica (10 x 10 mm) was used for normal phase pHPLC (NP) (Phenomenex, Torrance, CA, USA). Flow rates were 5 mL/min, UV 210 and 254 nm, and 10 mL fractions were collected. After filtration over a 25 mm 0.45 µm PTFE syringe filter samples were injected manually into the pHPLC system using a Rheodyne injector equipped with a 5 mL injection loop. NP samples were dissolved in 5 mL DCM for injection. After each NP experiment column was rinsed with 100 mL of acetone or EtOAc (rinse fraction) and fractions were combined based on similarity of TLC profile. RP samples were dissolved in 1-5 mL mobile phase or pure MeOH. RP fractions were combined based on UV chromatograms, MeOH removed under reduced pressure at 40 °C, remaining H_2O frozen at -20 °C, and sample lyophilized to dryness.

Purification

CPC experiments 1-3 Fr_{43-70} (540 mg) was fractionated by NP (Hept: EtOAc, 9:1). Fr_{13-26} were combined and solvent removed to yield of **1 (**408 mg, 96% pure) as a clear gum which can be crystallized to white needles using cyclohexane. Fr_{27-33} (11 mg) was further purified with RP (H_2O: MeOH, 1:1, isocratic) yielding 11,13-dihydroparthenolide (**2**) (4.9 mg, >99%). CPC 1-3 Fr_{71-85} (55 mg) was fractionated by NP (Hept: EtOAc, gradient) with Fr_{29} (1.9 mg) and Fr_{44} (0.8 mg) being purified with RP (H_2O: MeOH, 1:1, isocratic) yielding anhydroverlotorin (**3**) (0.2 mg, 82%) and santamarine (**4**) (0.4 mg, >99%) respectively. CPC 1-3 Fr↑ (78 mg) was fractionated by NP (Hept: EtOAc, gradient) with Fr_7 being purified with RP (H2O: MeOH, 3:7, isocratic) yielding **3** (0.8 mg, 87%) and Fr_{34-35} (0.4 mg) purified with RP (H2O: MeOH, 1:1, isocratic) yielding reynosin (**5**) (0.3 mg, 88%). CPC 1-3 Fr↓ (2.2 g) was fractionated with an additional CPC experiment (7) using a 200 mL rotor, HEMW 4:6:4:6 solvent system, with all other CPC conditions same as described above. Seventy 10 mL fractions were collected. CPC 7 fractions Fr_{10-20} (508 mg), Fr_{21-42} (506 mg), Fr_{43-50} (78 mg), and Fr_{51-70} (130 mg) were each further separated by NP (Hept: EtOAc, 7:3) with subsequent fractions being purified with repeated RP to yield 3β-hydroxycostunolide (**6**) (4.8 mg, 94%), costunolide diepoxide (**7**) (13 mg, 90%), 3-hydroxyparthenolide (**8**) (20.2 mg, 94%), artemorin (**9**) (4.6 mg, 98%), and artecanin (**10**) (1.1 mg, 95%).

CPC 4-6 Fr_{40-70} was dissolved in 30 mL EtOAc, loaded onto 10 g of silica gel, eluted with 200 mL EtOAc, and solvent removed to yield **1** (2.3 g, 98%), which was crystallized from Et_2O: Hex to white/yellow needles. CPC 4-6 Fr_{71-85} and Fr↑ were combined (490 mg) and separated with NP (Hept: EtOAc, gradient) with Fr_{15-16} (44 mg) and Fr_{22-24} (22 mg) further purified with RP (H_2O: MeOH, gradient) to yield **3** (1.5 mg, 99%) and **6** (3.6 mg, 74%) respectively. CPC 4-6 Fr↓ (4 g) was separated by flash chromatography (150 g silica) using Hex with increasing proportion EtOAc followed by

EtOAc with increasing proportions of acetone into 17-100 mL fractions. Flash Fr_{8-9} (434 mg) was further purified with repeated RP to yield **8** (1.7 mg, 90%), **6** (27.5 mg, 86%), and tanaparthin-β-peroxide (**11**) (3.9 mg, 76%). Flash Fr_{10-17} (2.6 g) was again fractionated by flash chromatography (100 g silica) using Hex with increasing proportion of acetone. Subsequent fractions were purified with repeated RP to yield **7** (18 mg, 99%), **10** (13.3 mg, 82%), **9** (32.1 mg, 96%), and **11** (2.3 mg, 87%).

Structure elucidation

^{1}H-NMR and COSY spectra were acquired on a Bruker DMX 500 MHz NMR (Karlsruhe, Germany). The solvent was $CDCl_3$ and chemical shift was calibrated to residual solvent (7.26 ppm). High resolution mass spectrometry was performed on an LC-LTQ-Orbitrap FTMS system (Thermo Scientific, Waltham, Massachusetts, USA). The instrument consisted of an Accela HPLC, an Accela photodiode array detector, connected to a LTQ/Orbitrap hybrid mass spectrometer equipped with an ESI source. Chromatographic separation took place on a Phenomenex Luna C18(2) analytical column (150 x 2.0 mm, 3 µm particle size), using H_2O and acetonitrile, both containing 0.1 % v/v formic acid, at a flow rate of 0.19 mL/min and a column temperature at 40 °C. A linear gradient from 5 to 75% acetonitrile in 45 min was applied, which was followed by 15 min of washing and equilibration. FTMS full scans (*m/z* 100−1200) were recorded with a resolution of 60.000, whereas for MS^n scans a resolution of 15.000 was used. The FTMS was externally calibrated in negative mode using sodium formate clusters in the range *m/z* 150-1200 and automatic tuning was performed on *m/z* 384.93.

Primary Cortical Neuronal Cultures

Cultures were derived from ARE-hPAP reporter mice as previously described (Johnson et al., 2002; Kraft et al., 2004). Briefly, cortices from E15 mouse pups were pooled in 10 mL ice-cold Ca^{2+} and Mg^{2+} free HBSS (Life Technologies, Carlsbad, CA, USA). Tissue was minced, centrifuged and digested in 0.05% trypsin without EDTA in HBSS for 15 min at 37 °C. Following trypsinization, cells were rinsed 3 times with HBSS. Cells were then washed with CEMEM (minimum essential media with Earle's salts; (Life Technologies), 2 mM glutamine, 1% penicillin/streptomycin, and 10% each of heat inactivated fetal bovine serum and horse serum (Atlanta Biologicals, Inc., Lawrenceville, GA, USA) and triturated to a single-cell suspension and strained through a 70 µM cell strainer (BD Biosciences, San Jose, CA, USA). Cells were counted, assayed for viability using trypan blue, and plated at a density of 3 x 105 cell/cm^2 on poly-D-lysine coated plates. Cells were maintained in CEMEM for 45 min, followed by a medium change with CEMEM. After two days, medium was changed from CEMEM to NBM (Neurobasal media; Life Technologies) supplemented with B27 with antioxidants and 2 mM glutamine. These mixed cultures (~ 40% astrocytes and 60% neurons), were left for at least 48 hours in NBM prior to initiating experiments. Cells were incubated at 37 °C in a tri-gas incubator with 5% O_2, 5% CO_2, and 90% N_2.

Compounds were dissolved in 100% DMSO and administered to cells for 48 hours (final concentration of DMSO was 0.1%) after 6 days in culture. Nrf2 activation was determined by measuring for hPAP activity. The hPAP activity assay has been

described previously (Kraft et al., 2004). Briefly, cells were lysed in TMNC lysis buffer (50 mM Tris, 5 mM $MgCl_2$, 100 mM NaCl, 1% 3-[(3-cholamidopropyl)dimethylammonio]-1-propanesulfonate (CHAPS)) and freeze-thawed at -20 ^oC. Extracts were incubated with 200 mM diethanolamine (DEA) buffer at 65 ^oC to inactivate endogenous alkaline phosphatase activity. hPAP activity was quantified in 200 mM DEA with 0.8 mM CSPD [disodium 3-(4-methoxyspiro (1,2-dioxetane-3,2'-(5'-chloro)tricycle(3.3.1.1^{3,7})decan)-4-yl)phenyl phosphate) (Life technologies), 2x Emerald and 5 mM $MgCl_2$]. Luminescence was measured on a Berthold Orion microplate luminometer with one-second integration. Baseline signal from hPAP negative control culture samples was subtracted from all values. Cell viability was assayed using the MTS (3-(4,5-Dimethylthiazol-2-yl)-5-(3-carboxymethoxyphenyl)-2-(4-sulfophenyl)-2H-tetrazolium salt) assay from Promega (Madison, WI, USA) following the manufacturer's suggested protocol.

Statistical analysis

All data are represented as mean ± SEM (n = 5). Statistical analysis was performed using one-way ANOVA followed by Newman-Keuls multiple comparison (GraphPad prism version 4).

Appendix

Detailed *T. parthenium* growth conditions, NMR data, and high resolution MS, are available in chapter 5 appendix.

Results and Discussion

For CPC experiments the void volume ranged from 210-250 mL and the pressure ranged from 51-57 bar between runs. Up to 7.9 g of extract 2 could be injected without destabilizing the CPC system while maintaining a good separation of **1**. Compound **1** eluted in similar fractions between NL and IBRSS plant material. These results indicate that the CPC method is robust and reproducible for the isolation of **1**. IBRSS flower heads of *T. parthenium* yielded higher amounts of **1** (0.9% dry weight) then NL material which can be explained by observations that **1** accumulates mostly in the flower heads compared to other plant parts (Majdi et al., 2011). With CPC the yields of **1** from IBRSS material are higher then those using low pressure or open column chromatography with silica (Bohlmann and Zdero, 1982; Milbrodt et al., 1997; Rey et al., 1992). In total 11 SL were isolated (Figure 1). All compounds were identified based on ^{1}H-NMR comparison with literature, COSY, and high resolution MS (Bohlmann and Zdero, 1982; El-Feraly and Chan, 1978; Parodi et al., 1989; Sanz et al., 1989; Romo De Vivar and Jiménez 1965; Yoshioka et al., 1970; Asakawa et al., 1981; El-Feraly and Chan, 1977; Geissman, 1970; Begley et al., 1989).

The purest samples of each SL were selected for hPAP assay (Figure 2) and MTS assay (Figure 3). Compound **2** lacks the α-methylene-γ-lactone moiety and did not increase hPAP levels, while all other SL displayed some level of significant activation confirming the importance of this functional group. Compounds **4**, **5**, **6**, and **10** showed

a linear dose response, although they were weaker compared to the positive control *t*BHQ. Compounds **1**, **7**, **8**, and **9** at higher doses decreased or eliminated activation. This observation can be explained by the MTS results for **1**, **7**, **8**, and **9** which show increasing cellular toxicity at increasing doses (Figure 3A).

Figure 1. Structures of isolated SL. Germacranolides - **1**, **2**, **3**, **6**, **7**, **8**, **9**; eudesmanolides - **4**, **5**; guaianolides – **10**, **11**.

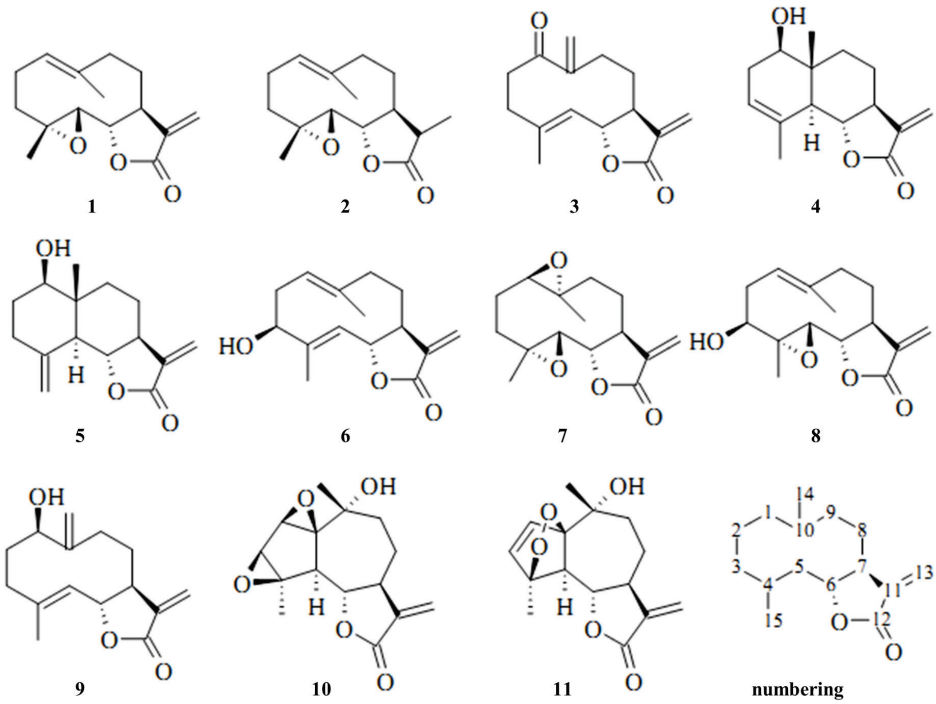

Compounds **3** and **11** at 12.5 µM had nearly 100 fold and >200 fold hPAP activation respectively with considerable toxicity at higher doses (data not shown). Therefore both compounds were assayed at lower doses until a linear dose response was observed and toxicity was lowered (Figure 2B and Figure 3B). Both the α-methylene-γ-lactone and endoperoxide moieties are present in **11**. The related compound **10,** which lacks the endoperoxide group but contains 2 epoxides, had weaker hPAP activity suggesting that the endoperoxide also contributes to the activity of **11**. The potent compound **3** had 2 exocyclic methylene groups at C-11,13 and C-10,14 neighboring a carbonyl. The replacement of the carbonyl with a hydroxyl group at position 1 as in **9** weakens activity. The presence of an extra methylene group could provide an additional reactive alkylating center in the molecule leading to more activity. Similar observations were reported in a previous study (Umemura et al., 2008).

Figure 2. Fold increase in hPAP luminescence over negative controls. *Statistically significant increase, $p < 0.05$.

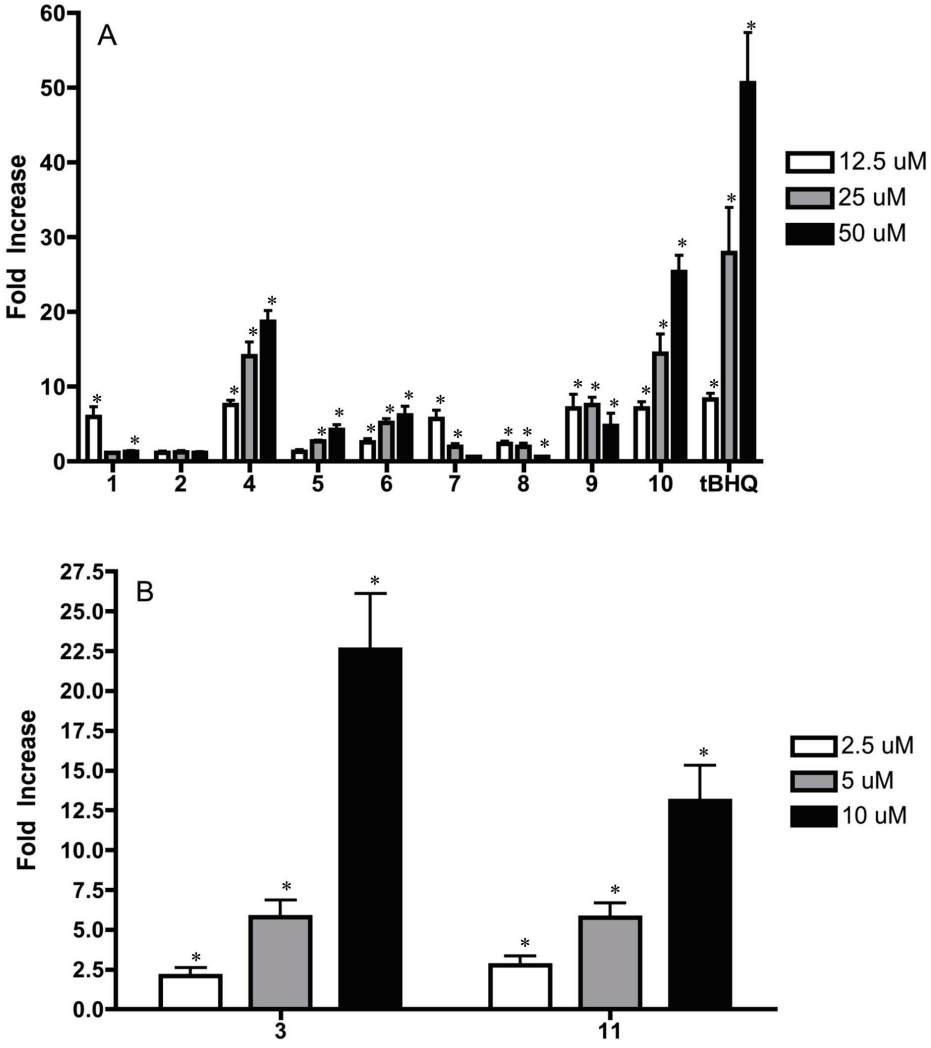

A common structural feature for the germacranolides **1**, **7**, and **8** is the presence of epoxides at positions 4 and 5 as well as 1 and 10 in the case of **7.** Compounds **1**, **7**, and **8** were among the most toxic compounds in the MTS assay and had both low and non-linear activity in the hPAP assay. Elimination of the epoxide as in **6,** eliminated toxicity at 5 and 12.5 μM and reduced it at 50 μM when compared with **1**, **7**, and **8** confirming the importance of epoxide functionality for toxicity. The guaianolide **10** also contains epoxide groups, however it is the least toxic of the most active SL's containing α-methylene-γ-lactone moiety, with a potency of about half that of *t*BHQ. This suggests that the differences between the open, germacranolide ring and

the bridged, guaianolide ring plays an important role in the activity of these compounds. Lewis-acid catalyzed intramolecular cyclization reactions of germanacranolides into guaianolides are known to occur (Castaneda-Acosta and Fischer, 1993; Parodi et al., 1989). Other biological activities such as anti-cancer activity and anti-inflammatory action are known to differ between various SL skeletons (Ghantous et al., 2010; Neukirch et al., 2003). Whether or not intramolecular cyclizations of germacranolides to guaianolides occur *in-vivo* is worth further investigation. With regards to the eudesmanolides **4** and **5**, these compounds could only be isolated in very low amounts and therefore we were unable to fully evaluate their toxicity (Figure 3A). Compound **4** was the second most potent germacranolide for hPAP activation (Figure 2A), although even at low doses toxicity was observed (Figure 3A). Compound **5** mildly stimulated hPAP activation and no toxicity was observed at the doses tested.

From these results, we can conclude that the guaianolides tested were generally more potent activators of Nrf2/ARE in mouse primary cortical cultures then the germacranolides and eudesmanolides tested. Furthermore **10**, which lacked the endoperoxide functionality was the most potent Nrf2/ARE activator and among the least toxic SL. Further structure activity studies with guaianolides may lead to interesting compounds for drug development or biological research tools for studying the Nrf2/ARE pathway. A deeper understanding of the mechanism of SL for Nrf2/ARE activity is also required to determine if SL activity is due to direct binding with cysteine residues on Keap1 or an indirect mechanism such as depletion of glutathione. Finally, whether or not toxicity of SL *in vivo* is a problem should be investigation in more detail as well as toxicity on other cell types.

Acknowledgements

We thank the European Union Seventh Framework Program for funding the Terpmed project of which this research is a part of. Grant number 227448. The work was also funded by R01ES08089 and R01ES10042 from the National Institute of Environmental Health Sciences (JAJ). Finally, we would like to thank Young Hae Choi and the Leiden University Chemistry Department for helping acquire NMR spectra.

Figure 3. Percent Cell viability in MTS assay. *Statistically significant cellular toxicity, $p < 0.05$.

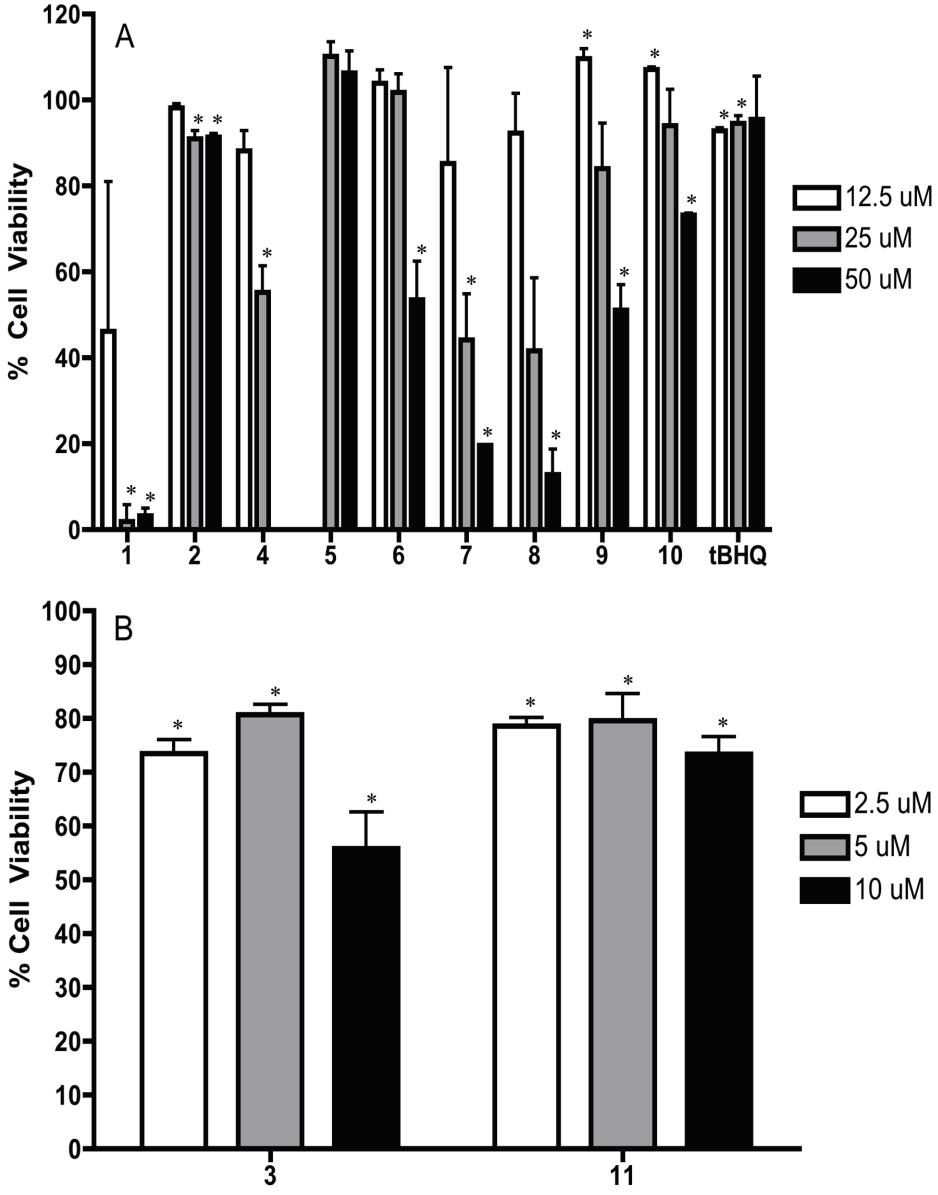

References

Abad, M.J., Bermejo, P., Villar, A., 2006. An approach to the genus Tanacetum L. (Compositae): Phytochemical and pharmacological review. Phytotherapy Research 9, 79–92.

Asakawa, Y., Toyota, M., Takemoto, T., 1981. Two guaiane-type sesquiterpene lactones and their related sesquiterpene lactones from Porella japonica. Phytochemistry 20, 257–261.

Begley, M.J., Hewlett, M.J., Knight, D.W., 1989. Revised structures for guaianolide α-methylenebutyro-lactones from feverfew. Phytochemistry 28, 940–943.

Bohlmann, F., Zdero, C., 1982. Naturally-Occurring Terpene Derivatives .454. Sesquiterpene Lactones and Other Constituents from Tanacetum-Parthenium. Phytochemistry 21, 2543–2549.

Calkins, M.J., Johnson, D.A., Townsend, J.A., Vargas, M.R., Dowell, J.A., Williamson, T.P., Kraft, A.D., Lee, J.-M., Li, J., Johnson, J.A., 2009. The Nrf2/ARE pathway as a potential therapeutic target in neurodegenerative disease. Antioxidants & Redox Signaling 11, 497–508.

Castañeda-Acosta, J., Fischer, N.H., Vargas, D., 1993. Biomimetic transformations of parthenolide. Journal of Natural Products 56, 90–98.

de Vries, H.E., Witte, M., Hondius, D., Rozemuller, A.J.M., Drukarch, B., Hoozemans, J., van Horssen, J., 2008. Nrf2-induced antioxidant protection: a promising target to counteract ROS-mediated damage in neurodegenerative disease? Free Radical Biology & Medicine 45, 1375–1383.

El-Feraly, S., Chan, Y.-M., Fairchild, E.H., Doskotch, R.W., 1977. Peroxycostunolide and peroxyparthenolide: two cytotoxic germacranolide hydroperoxides from magnolia grandiflora. Structural revision of verlotorin and artemorin. Tetrahedron Letters 18, 1973–1975.

El-Feraly, F.S., Chan, Y.M., 1978. Isolation and characterization of the sesquiterpene lactones costunolide, parthenolide, costunolide diepoxide, santamarine, and reynosin from Magnolia grandiflora L. Journal of Pharmaceutical Sciences 67, 347–350.

Foucault, A.P., 1995. Centrifugal Partition Chromatography. Marcel Dekker Inc, New York.

Geissman, T.A., 1970. Sesquiterpene lactones of Artemisia— A. verlotorum and A. vulgaris. Phytochemistry 9, 2377–2381.

Ghantous, A., Gali-Muhtasib, H., Vuorela, H., Saliba, N.A., Darwiche, N., 2010. What made sesquiterpene lactones reach cancer clinical trials? Drug Discovery Today 15, 668–678.

Hwang, D.-R., Wu, Y.-S., Chang, C.-W., Lien, T.-W., Chen, W.-C., Tan, U.-K., Hsu, J.T.A., Hsieh, H.-P., 2006. Synthesis and anti-viral activity of a series of sesquiterpene lactones and analogues in the subgenomic HCV replicon system. Bioorganic & Medicinal Chemistry 14, 83–91.

Itoh, K., Tong, K.I., Yamamoto, M., 2004. Molecular mechanism activating Nrf2-Keap1 pathway in regulation of adaptive response to electrophiles. Free Radical Biology & Medicine 36, 1208–1213.

Jeong, W.-S., Keum, Y.-S., Chen, C., Jain, M.R., Shen, G., Kim, J.-H., Li, W., Kong, A.-N.T., 2005. Differential expression and stability of endogenous nuclear factor E2-related factor 2 (Nrf2) by natural chemopreventive compounds in HepG2 human hepatoma cells. Journal of Biochemistry and Molecular Biology 38, 167–176.

Johnson, D.A., Andrews, G.K., Xu, W., Johnson, J.A., 2002. Activation of the antioxidant response element in primary cortical neuronal cultures derived from transgenic reporter mice. Journal of Neurochemistry 81, 1233–1241.

Kim, S.-K., Cho, S.-B., Moon, H.-I., 2010. Neuroprotective effects of a sesquiterpene lactone and flavanones from Paulownia tomentosa Steud. against glutamate-induced neurotoxicity in primary cultured rat cortical cells. Phytotherapy Research 24, 1898–1900.

Kraft, A.D., Johnson, D.A., Johnson, J.A., 2004. Nuclear factor E2-related factor 2-dependent antioxidant response element activation by tert-butylhydroquinone and sulforaphane occurring preferentially in astrocytes conditions neurons against oxidative insult. Journal of Neuroscience 24, 1101–1112.

Majdi, M., Liu, Q., Karimzadeh, G., Malboobi, M.A., Beekwilder, J., Cankar, K., de Vos, R., Todorovic, S., Simonovic, A., Bouwmeester, H., 2011. Biosynthesis and localization of parthenolide in glandular trichomes of feverfew (Tanacetum parthenium L. Schulz Bip.). Phytochemistry 72, 1739–1750.

Mathema, V.B., Koh, Y.-S., Thakuri, B.C., Sillanpää, M., 2012. Parthenolide, a sesquiterpene lactone, expresses multiple anti-cancer and anti-inflammatory activities. Inflammation 35, 560–565.

Milbrodt, M., Schröder, F., König, W.A., 1997. 3,4-β-Epoxy-8-deoxycumambrin B, A sesquiterpene lactone from Tanacetum parthenium. Phytochemistry 44, 471–474.

Neukirch, H., Kaneider, N.C., Wiedermann, C.J., Guerriero, A., D'Ambrosio, M., 2003. Parthenolide and its photochemically synthesized 1(10)Z isomer: chemical reactivity and structure–activity relationship studies in human leucocyte chemotaxis. Bioorganic & Medicinal Chemistry 11, 1503–1510.

Parodi, F.J., Fronczek, F.R., Fischer, N.H., 1989. Biomimetic Transformations of 11,13-Dihydroparthenolide and Oxidative Rearrangements of a Guai- 1(10)-en-6,12-olide. Journal of Natural Products 52, 554–566.

Rey, J.-P., Levesque, J., Louis Pousset, J., 1992. Extraction and high-performance liquid chromatographic methods for the γ-lactones parthenolide (Chrysanthemum parthenium Bernh.), marrubiin (Marrubium vulgare L.) and artemisinin (Artemisia annua L.). Journal of Chromatography A 605, 124–128.

Romo de Vivar, A., Jiménez, H., 1965. Structure of santamarine, a new sesquiterpene lactone. Tetrahedron 21, 1741–1745.

Salminen, A., Lehtonen, M., Suuronen, T., Kaarniranta, K., Huuskonen, J., 2008. Terpenoids: natural inhibitors of NF-kappaB signaling with anti-inflammatory and anticancer potential. Cellular and Molecular Life Sciences 65, 2979–2999.

Sanz, J.F., Barbera, O., Marco, J.A., 1989. Sesquiterpene lactones from Artemisia hispanica. Phytochemistry 28, 2163–2167.

Tiuman, T.S., Ueda-Nakamura, T., Garcia Cortez, D.A., Dias Filho, B.P., Morgado-Díaz, J.A., De Souza, W., Nakamura, C.V., 2005. Antileishmanial Activity of Parthenolide, a Sesquiterpene Lactone Isolated from Tanacetum Parthenium. Antimicrobial Agents and Chemotherapy 49, 176–182.

Tukov, F.F., Anand, S., Gadepalli, R.S.V.S., Gunatilaka, A.A.L., Matthews, J.C., Rimoldi, J.M., 2004. Inactivation of the cytotoxic activity of repin, a sesquiterpene lactone from Centaurea repens. Chemical Research in Toxicology 17, 1170–1176.

Umemura, K., Itoh, T., Hamada, N., Fujita, Y., Akao, Y., Nozawa, Y., Matsuura, N., Iinuma, M., Ito, M., 2008. Preconditioning by sesquiterpene lactone enhances H2O2-induced Nrf2/ARE activation. Biochemical and Biophysical Research Communications 368, 948–954.

Yoshioka, H., Renold, W., Fischer, N.H., Higo, A., Mabry, T.J., 1970. Sesquiterpene lactones from Ambrosia confertiflora (Compositae). Phytochemistry 9, 823–832.

Zhang, D.D., Hannink, M., 2003. Distinct cysteine residues in Keap1 are required for Keap1-dependent ubiquitination of Nrf2 and for stabilization of Nrf2 by chemopreventive agents and oxidative stress. Molecular and Cellular Biology 23, 8137–8151.

Appendix Chapter 5

Tanacetum parthenium (IBRSS) growth conditions

The seeds stock (Item No. CA474) was purchased from Jelitto Trade Company GmbH (Schwarmstedt, Germany). Seeds were germinated in the greenhouse on FLORADUR Fine soil seed starting mixture (*Floragard*, Vertriebs GmbH, Oldenburg, Germany), under long day conditions, 16 h light and 8 h darkness. Four week old seedlings were transferred to FLORADUR B soil (*Floragard*, Vertriebs GmbH, Oldenburg, Germany), in separate pots. After 2 months seedlings were transferred from the greenhouse to an open-air garden. After several days adaptation to the open air environmental conditions seedlings were planted in the cultivation field. Plants were grown from spring to autumn 2010. During flowering time, flowers were subsequently harvested and dried at the room temperature.

Table A1. ^{1}H-NMR data ($CDCl_3$, 500 MHz)

	Parthenolide	**11,13-Dihydroparthenolide**	**3-Hydroxyparthenolide**
H-1	5.21 br dd (2.6, 12.1)	5.17 br dd (2.3, 12.2)	5.14 br dd (4, 12)
H-2α	2.12-2.23 m	2.11-2.21 m	2.35-2.52 m
H-2β	2.35-2.46 m	2.34-2.44 m	2.35-2.52 m
H-3α	1.20-1.28 m	1.22 td (5.7, 12.9)	3.43 dd (7, 11)
H-3β	2.12-2.23 m	2.11-2.21 m	
H-5	2.78 d (8.9)	2.70 d (9)	2.79 d (9)
H-6	3.86 t (8.6)	3.81 t (9.1)	3.92 t (9)
H-7	2.76-2.81 m	1.81-1.93 m	2.74 ddddd (3, 4, 6, 9, 9)
H-8α	2.12-2.23 m	1.81-1.93 m	2.53-2.52 m
H-8β	1.69-1.77 m	1.61-1.69 m	1.68 m
H-9α	2.12-2.23 m	2.05 br t (12.5)	2.13 m
H-9β	2.35-2.46 m	2.25-2.34 m	2.35-2.52 m
H-11		2.25-2.34 m	
H-13α	6.34 d (3.7)		6.34 d (4)
H-13β	5.62 d (3.3)	1.28 d (7.2)	5.63 d (3)
H-14	1.72 br s	1.7 br s	1.73 s
H-15	1.31 s	1.29 s	1.32 s

Table A2. ^{1}H-NMR data ($CDCl_3$, 500 MHz)

	3β-Hydroxycostunolide	**Costunolide diepoxide**
H-1	4.90 br dd (2.9, 12)	2.85 dd (1, 11)
H-2α	2.41-2.48 m	1.51 tdd (5, 11, 14, 14)
H-2β	2.28 td (10.3, 12, 12.1)	2.16-2.3 m
H-3α	4.28 m	1.20-1.29 m
H-3β		2.48 dd (8, 14)
H-5	4.79 br d (9.9)	2.91 d (9)
H-6	4.61 dd (8.7, 9.9)	3.94 t (9)
H-7	2.53 m	2.73 tq (3, 3, 3, 9, 9)
H-8α	2.06-2.13 m	1.20-1.29 m
H-8β	1.65-1.73 m	1.61 m
H-9α	2.41-2.48 m	2.16-2.30 m
H-9β	2.06-2.13 m	2.16-2.30 m
H-13α	6.29 d (3.6)	6.34 d (4)
H-13β	5.54 d (3.2)	5.62 d (3)
H-14	1.46 br s	1.40-1.35*
H-15	1.74 d (1.4)	1.40-1.35*

*Interchangeable

Table A3. ^{1}H-NMR data ($CDCl_3$, 500 MHz)

	Anhydroverlotorin	**Artemorin***
1α		3.96 br
H-2α	2.34-2.65 m	1.9-2.9 br m
H-2β	3.15 br m	1.9-2.9 br m
H-3α	2.34-2.65 m	1.9-2.9 br m
H-3β	2.34-2.65 m	1.9-2.9 br m
H-5	5.09 br d (10)	5.22 br d (10)
H-6	4.33 t (10)	4.39 br
H-7	2.56 m	2.75 m
H-8α	2.26 m	1.9-2.9 br m
H-8β	1.41 m	1.9-2.9 br m
H-9α	2.33-2.62 m	1.9-2.9 br m
H-9β	2.33-2.62 m	1.9-2.9 br m
H-13α	6.22 d (3.5)	6.16 d (3)
H-13β	5.48 d (3.2)	5.44 d (3)
H-14	5.48 s	5.20 br s
H-14	5.66 s	4.86 br s
H-15	1.75 d (1)	1.71 br s

*Peak broadening

Table A4. ^{1}H-NMR data ($CDCl_3$, 500 MHz)

	Santamarine	Reynosin
H-1α	3.68 ddd (5, 5, 10)	3.53 dd (5, 11)
H-2α	2.4 dddd (3, 5, 10, 16)	1.50-1.88 m*
H-2β	1.97 ddd (3, 10, 17)	1.50-1.88 m*
H-3	5.34 m	2.04-2.16 m
H-3		2.34 ddd (2, 5, 14)
H-5	2.35 br d (11)	2.19 br dd (2, 11)
H-6	3.95 t (11)	4.03 t (11)
H-7	2.50 ddddd (3, 3, 3, 10, 14)	2.54 m
H-8	1.65 qd (3, 13.5, 14, 14)	2.04-2.16 m
H-8	2.02-2.13 m	1.50-1.88 m*
H-9	1.31 td (4, 13, 13)	1.32-1.40 m*
H-9	2.02-2.13 m	2.04-2.16 m
H-13α	6.08 d (3)	6.09 d (3)
H-13β	5.41 d (3)	5.41 d (3)
H-14	0.88 s	0.82 s
H-15	1.83 br s	4.99 d (1)
H-15		4.87 d (1)

*Signals obscured by H_2O

Table A5. ^{1}H-NMR data ($CDCl_3$, 500 MHz)

	Tanaparthin-β-peroxide	**Artecanin**
H-2	6.33 d (6)	3.55 d (1)
H-3	6.29 d (6)	3.30 d (1)
H-5	2.65 d (10)	2.86 d (11)
H-6	3.75 t (10)	4.09 t (11)
H-7	3.36 ddddd (3, 3.5, 7, 10, 10)	3.26-3.33 m
H-8	1.52*	1.64-2.13
H-8	2.36 dddd (7, 9, 10, 14)	1.64-2.13
H-9	1.74 m	1.64-2.13
H-9	2.03 ddd (2, 8, 16)	1.64-2.13
H-13α	6.15 d (3.5)	6.20 d (3.5)
H-13β	5.42 d (3)	5.43 d (3)
H-14	1.39 s	1.14 s
H-15	1.71 s	1.56 s

*Signals obscured by H_2O

Table A6. High resolution MS data

Number	compound name	observed $[M+H]^+$	calculated [M+H]+	Formula	Δ ppm
1	parthenolide	249.1489	249.1485	$C_{15}H_{20}O_3$	1.69
2	11,13-dihydroparthenolide	251.1644	251.1642	$C_{15}H_{22}O_3$	1.04
3	anhydroverlotorin	247.1332	247.1329	$C_{15}H_{18}O_3$	1.38
4	santamarine	249.1488	249.1485	$C_{15}H_{20}O_3$	1.08
5	reynosin	249.1487	249.1485	$C_{15}H_{20}O_3$	0.84
6	3β-hydroxycostunolide	249.1487	249.1485	$C_{15}H_{20}O_3$	0.72
7	costunolide diepoxide	265.1435	265.1434	$C_{15}H_{20}O_4$	0.30
8	3-hydroxyparthenolide	265.1436	265.1434	$C_{15}H_{20}O_4$	0.68
9	artemorin	249.1486	249.1485	$C_{15}H_{20}O_3$	0.16
10	artecanin	279.1228	279.1227	$C_{15}H_{18}O_5$	0.25
11	tanaparthin-β-peroxide	279.1226	279.1227	$C_{15}H_{18}O_5$	-0.29

Figure A1. Parthenolide ^{1}H-NMR.

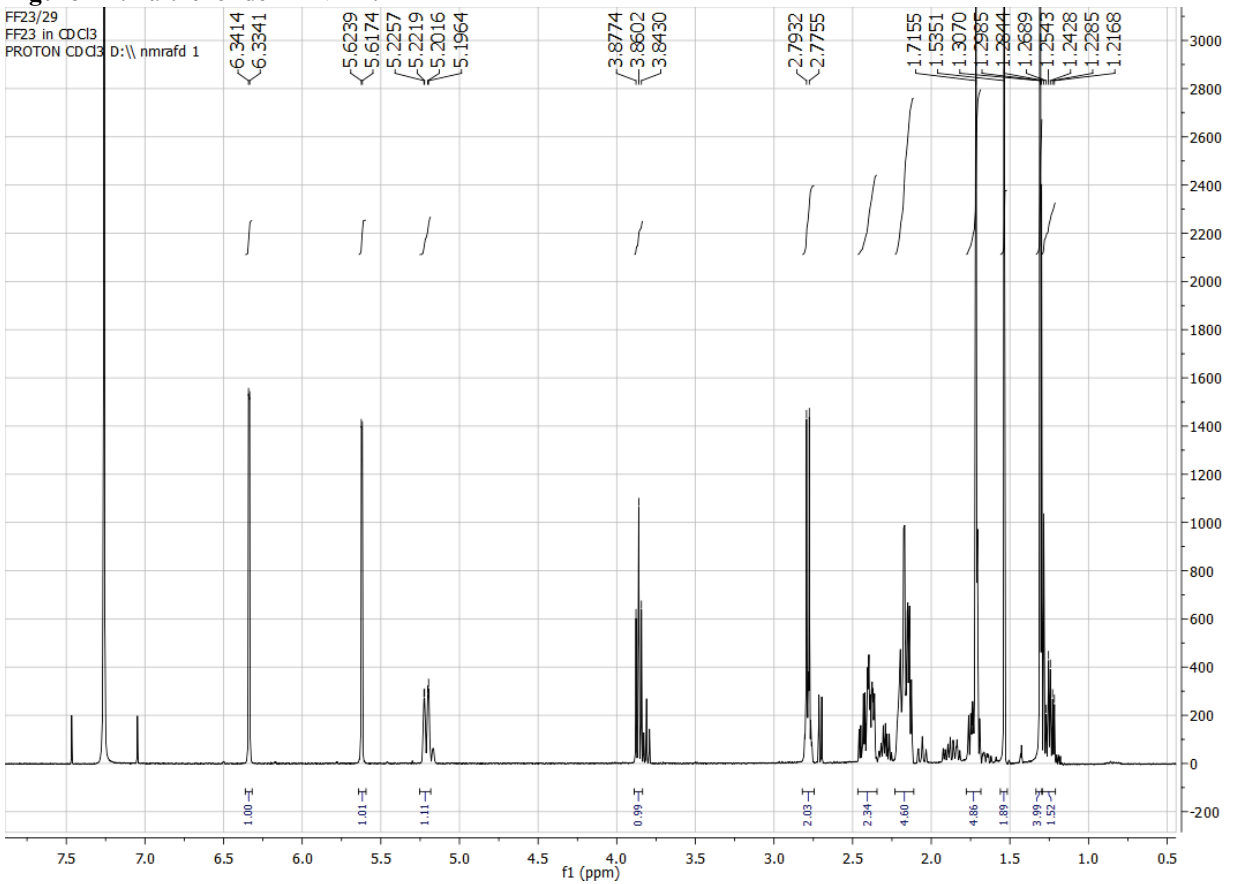

Figure A2. 11,13-Dihydroparthenolide ^{1}H-NMR.

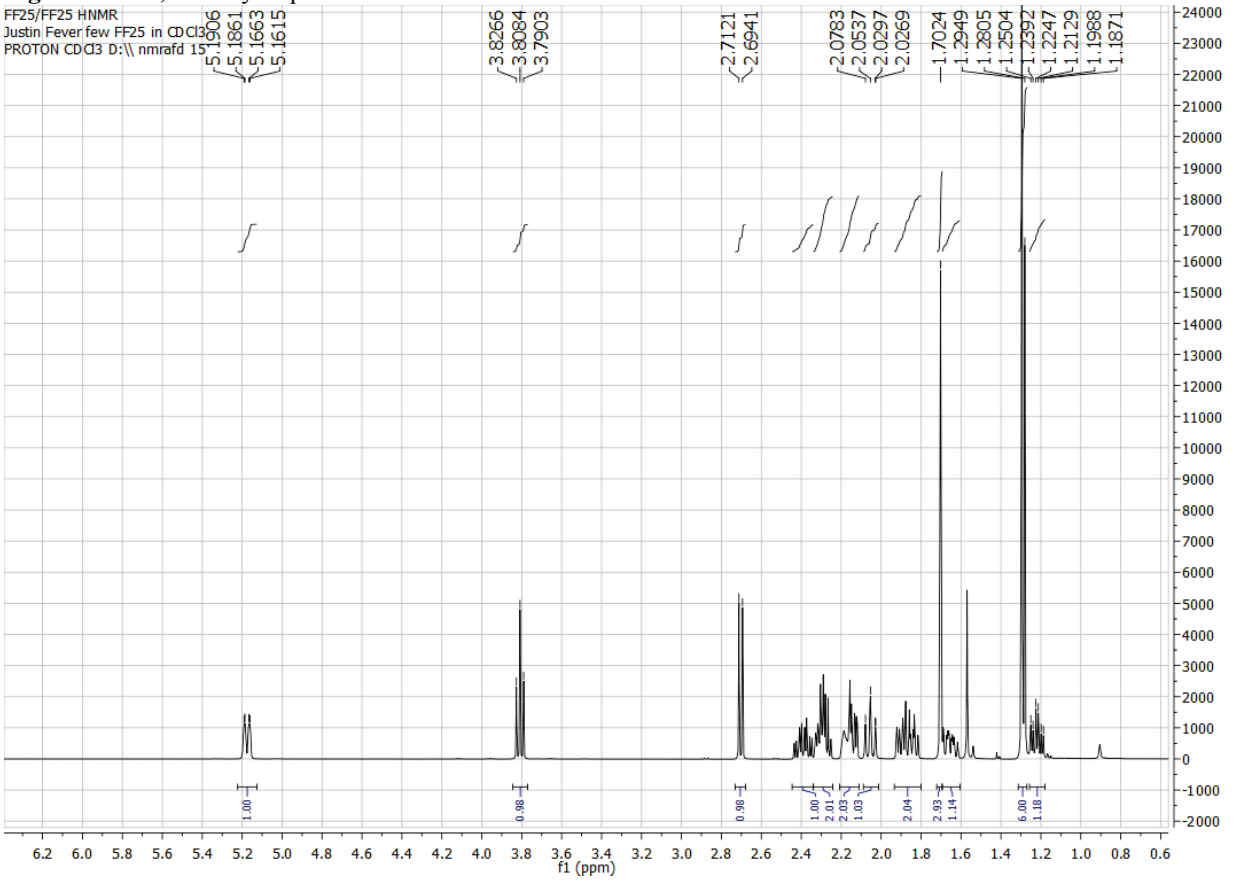

Figure A3. 3-Hydroxyparthenolide ^{1}H-NMR.

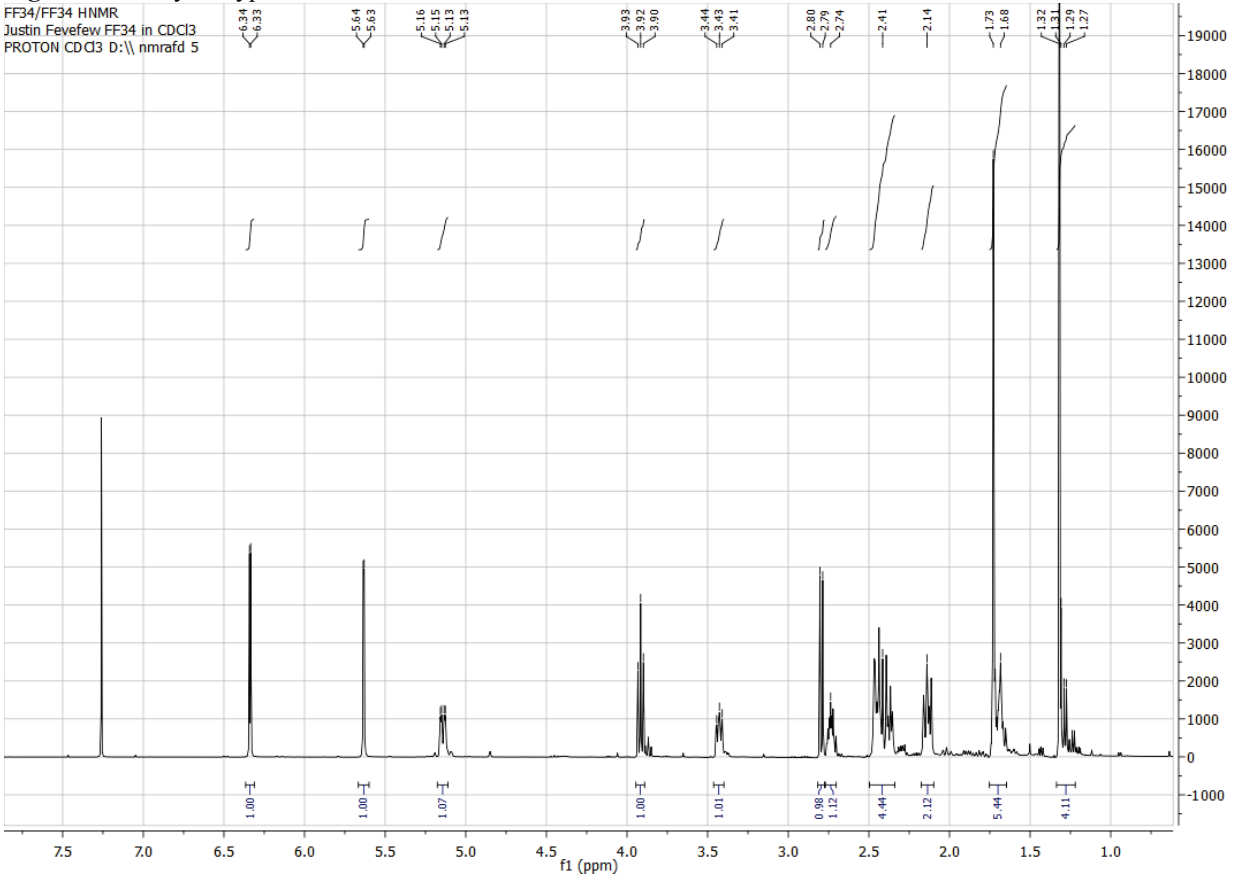

Figure A4. 3β-Hydoxycostunolide ^{1}H-NMR.

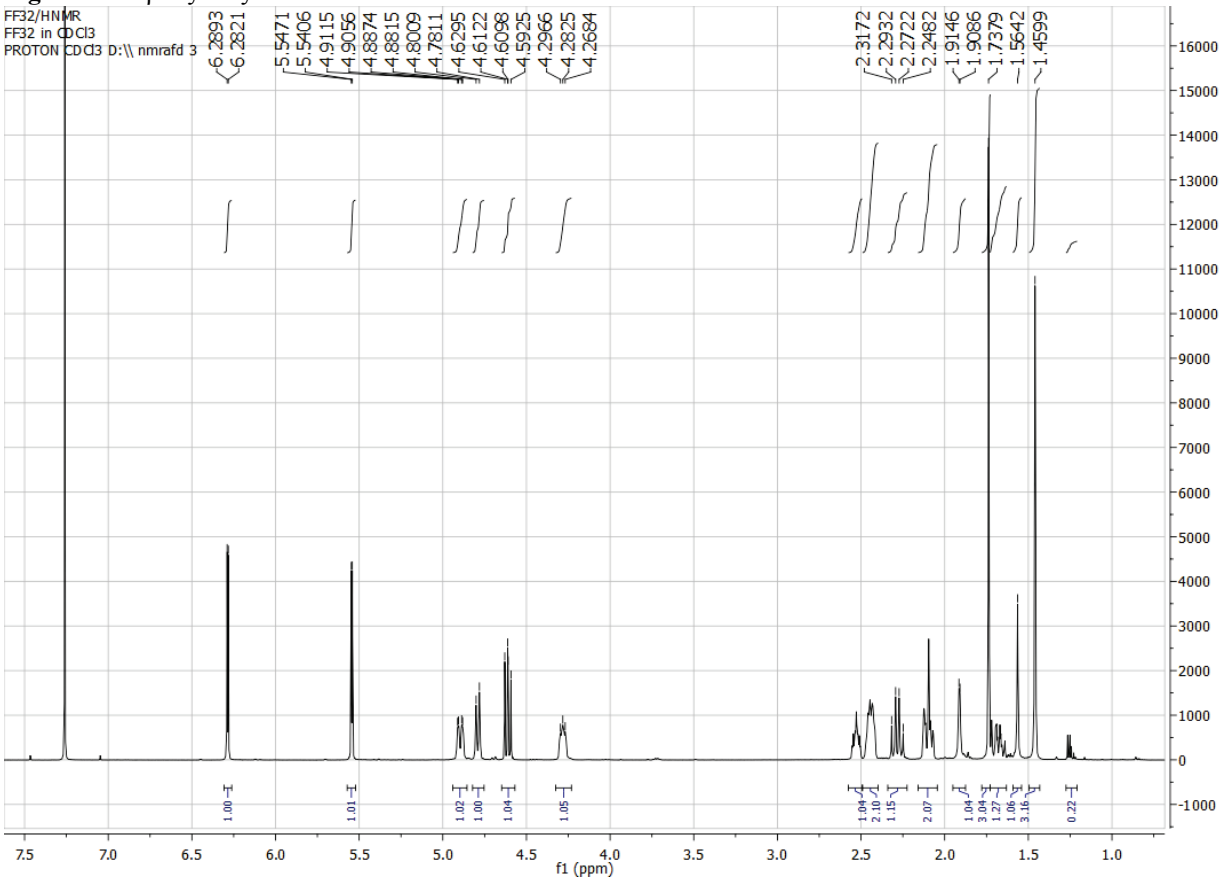

Figure A5. Costunolide diepoxide ^{1}H-NMR.

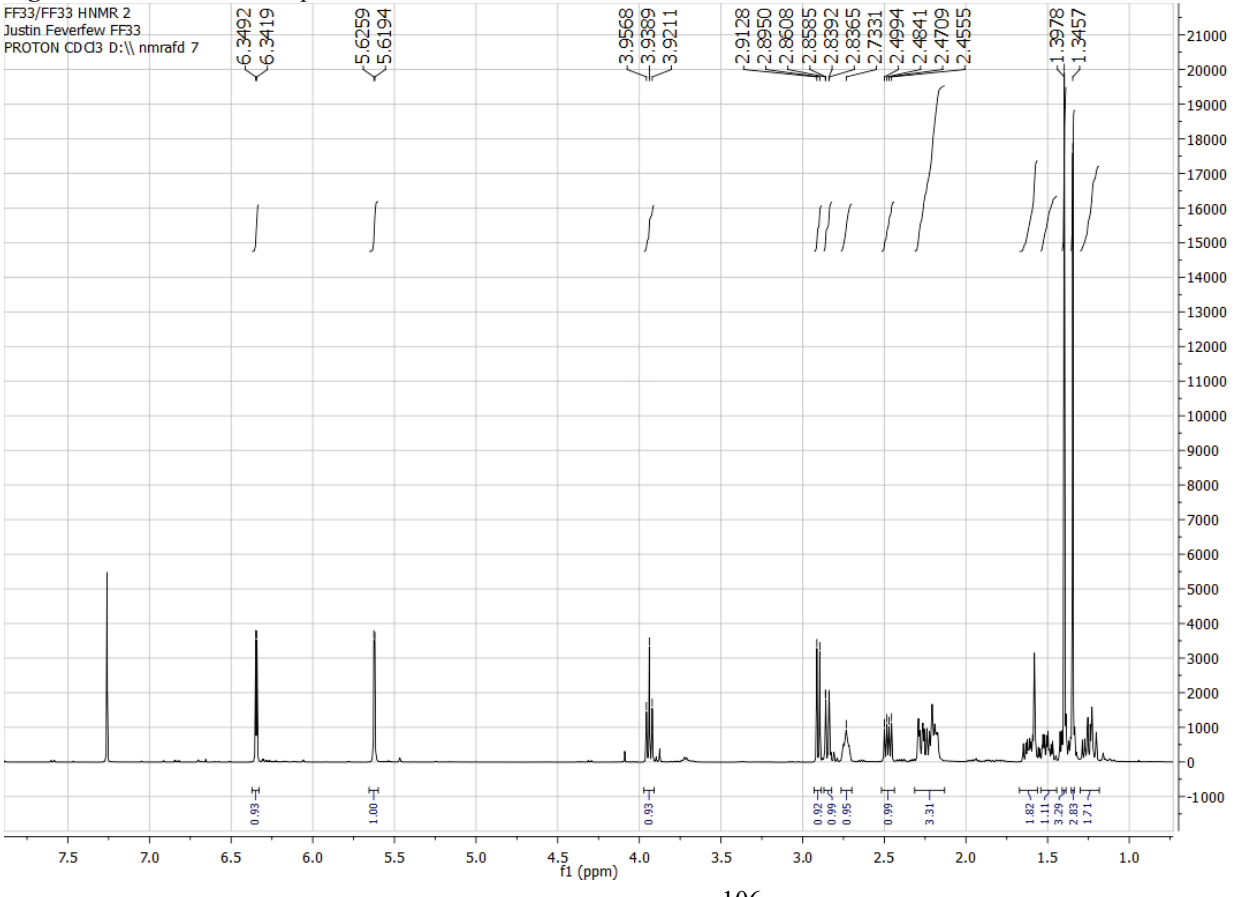

Figure A6. Anhydroverlotorin ^{1}H-NMR.

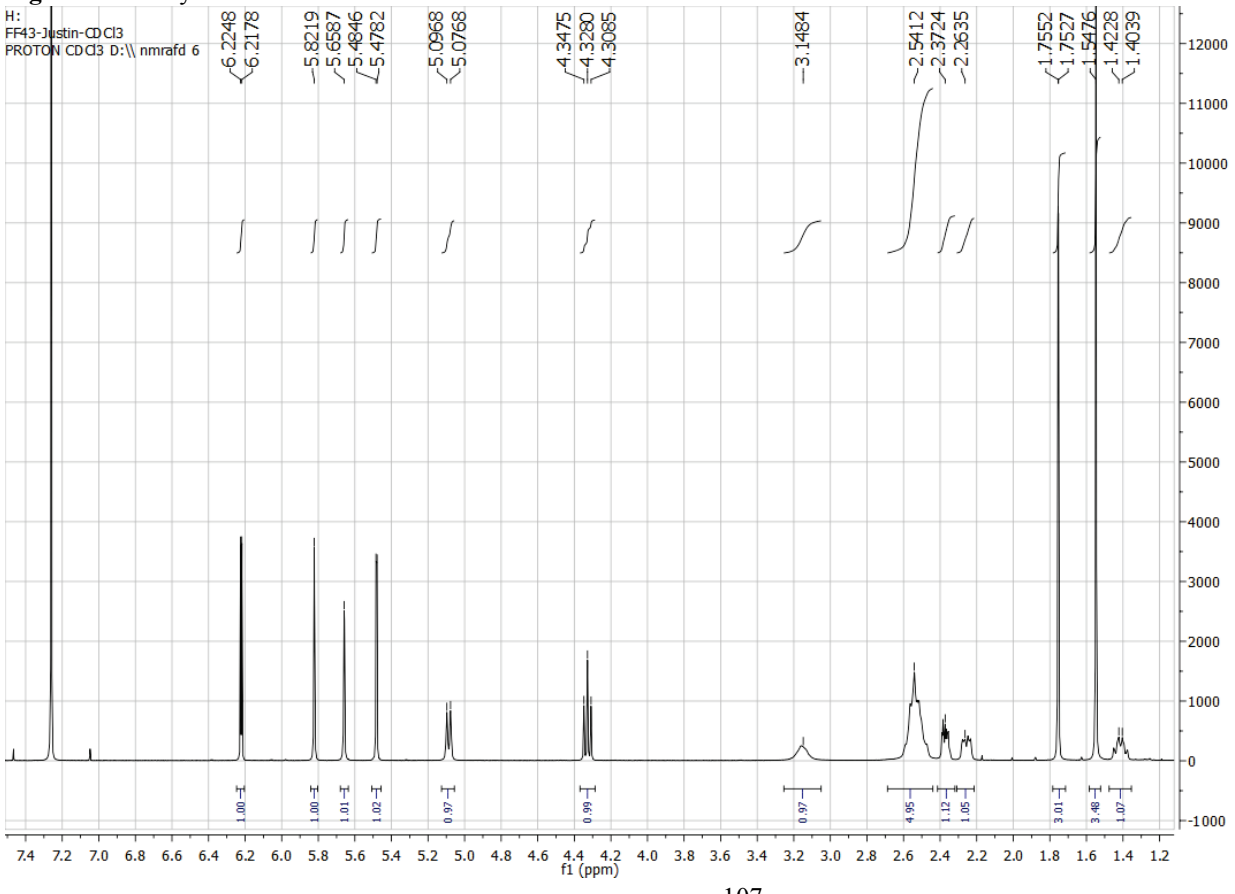

Figure A7. Artemorin ^{1}H-NMR.

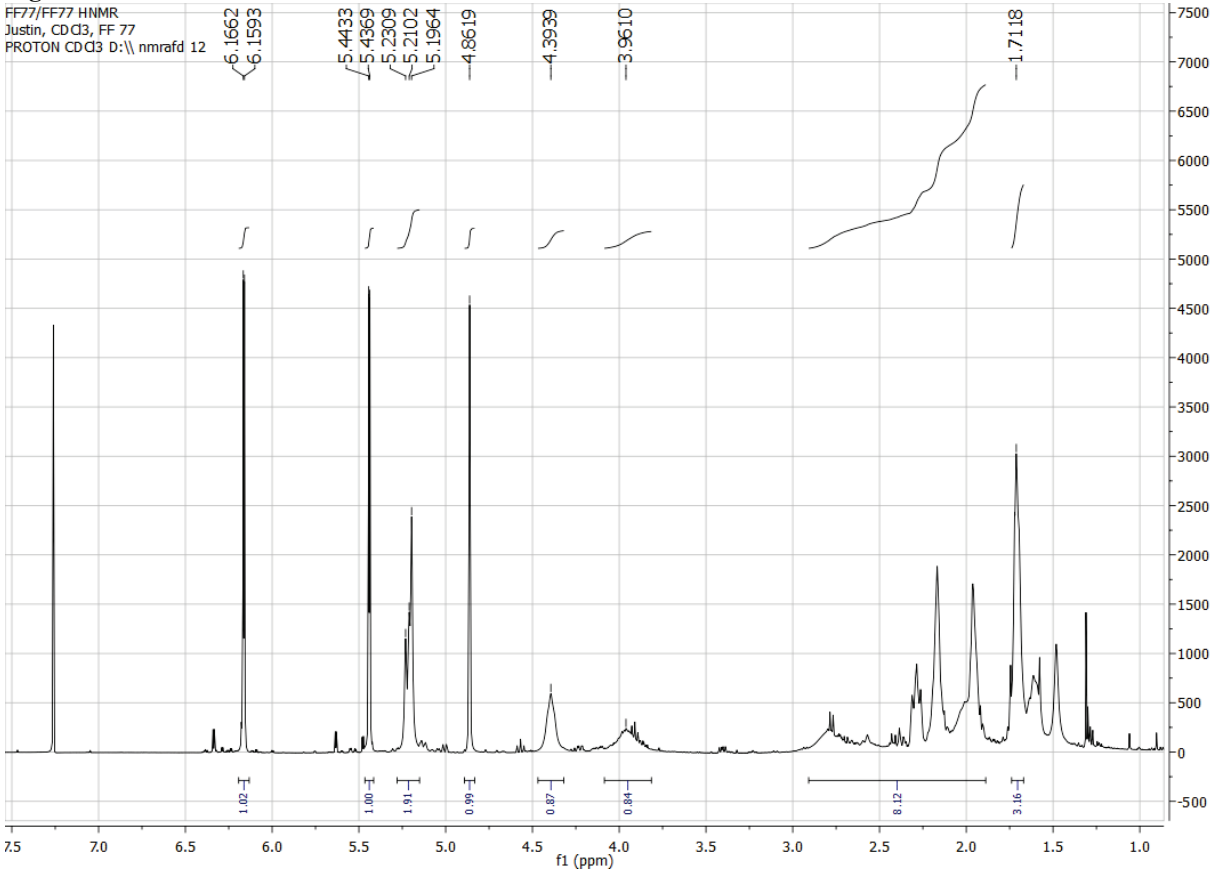

Figure A8. Santamarine ^{1}H-NMR.

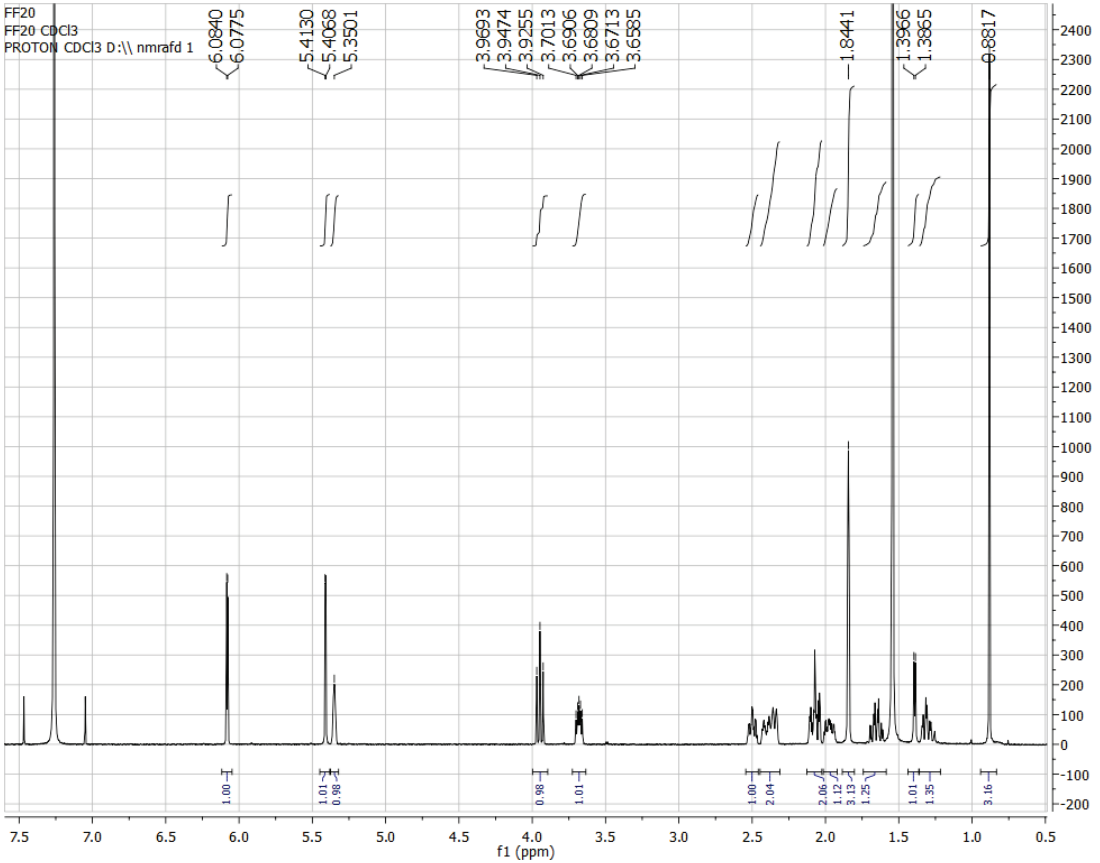

Figure A9. Reynosin ^{1}H-NMR

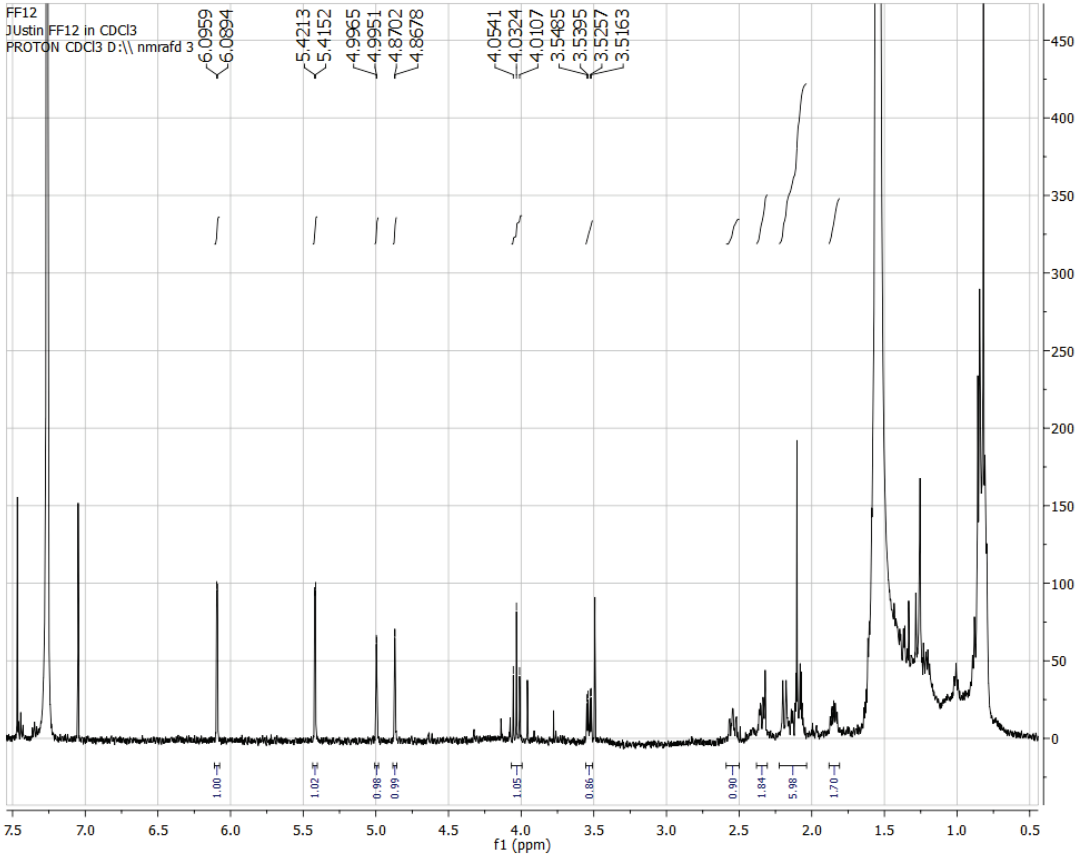

Figure A10. Tanaparthin-β-peroxide ^{1}H-NMR

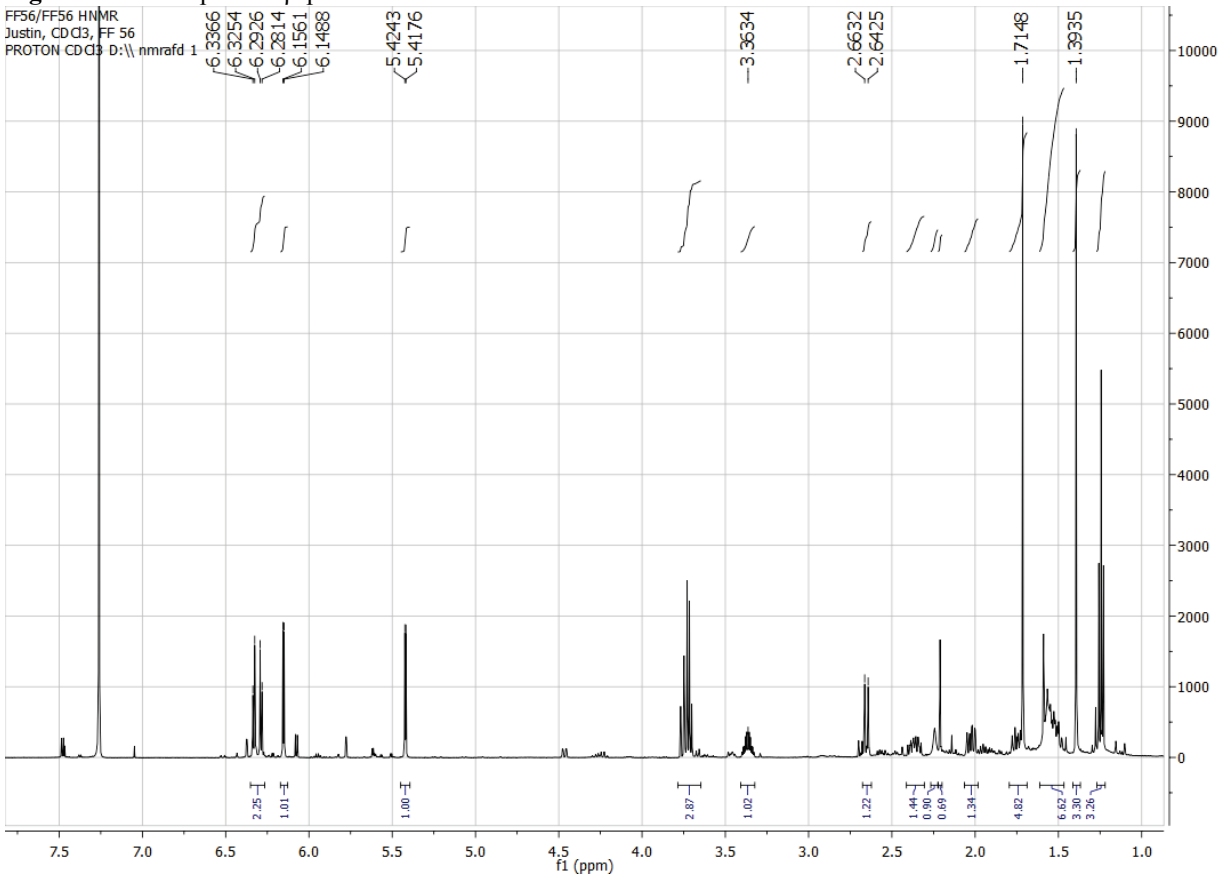

Figure A11. Artecanin ^{1}H-NMR

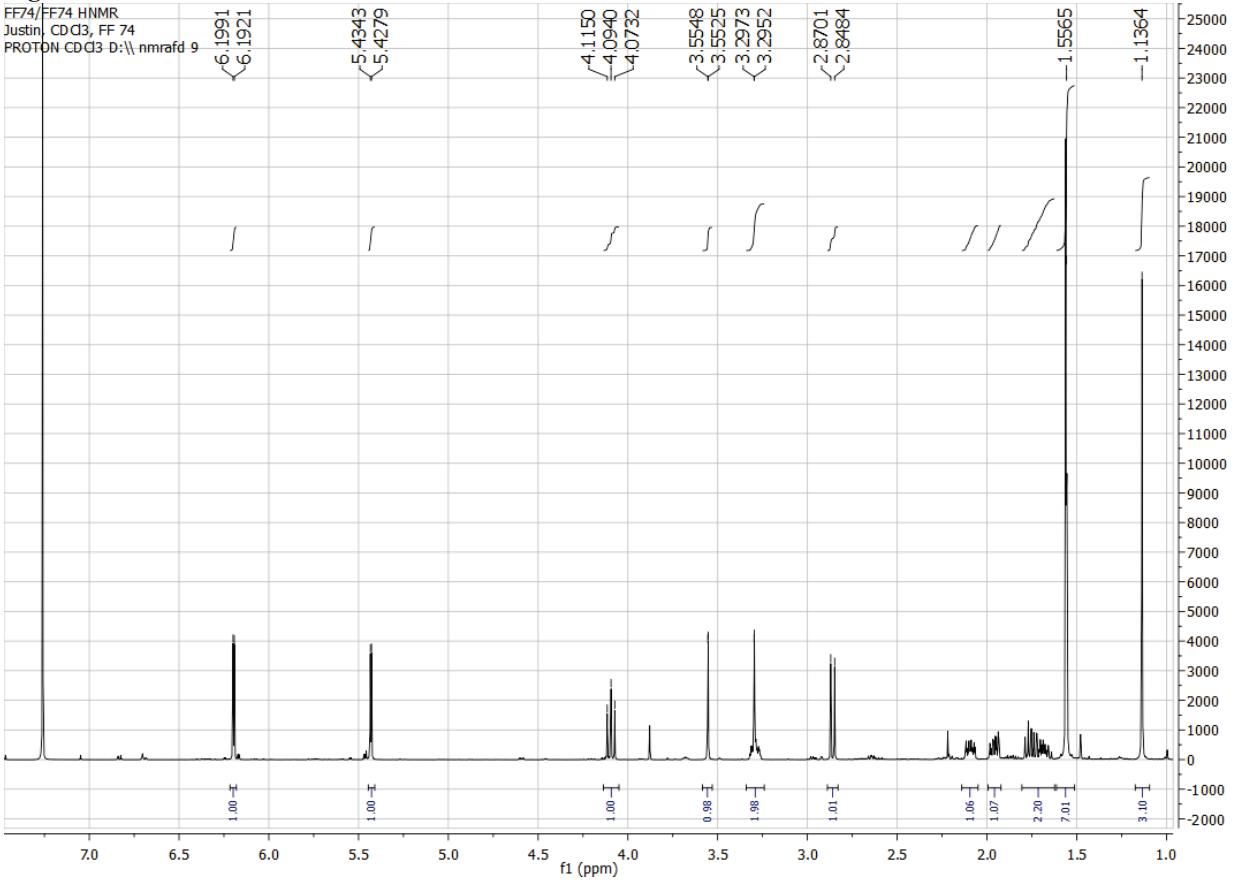

Chapter 6

Cytotoxic Activity of Sesquiterpene Lactones from *Inula britannica* on Multi-Drug Resistant Human Cancer Cell Lines

Justin T Fischedick,[a,b] Milica Pesic,[c] Jasna Bankovic,[c] Marija Perić,[d] Slađana Todorović,[e] Nikola Tanic[c]

[a]*PRISNA BV, Einsteinweg 55, 2300 RA Leiden, Netherlands*
[b]*Natural Products Laboratory, Institute of Biology, Leiden University, 2300 RA Leiden, The Netherlands*
[c]*Department of Neurobiology, Institute for Biological Research "Sinisa Stankovic", University of Belgrade, Bul. Despota Stefana 142, 11060 Belgrade, Serbia*
[d]*Faculty of Biology, Institute of Botany and Botanical Garden "Jevremovac", University of Belgrade, Takovska 43, 11000 Belgrade, Serbia*
[e]*Institute for Biological Research "Siniša Stanković", University of Belgrade, Belgrade, Serbia*

ABSTRACT

Five new sesquiterpene lactones (**1** – **5**) were isolated from *Inula britannica* collected in the wild from Serbia along with five known compounds (**6** – **10**). Sesquiterpene lactones were isolated using centrifugal partition chromatography followed by combination of flash chromatography and semi-preparative HPLC. Isolated compounds were screened for cytotoxic activity on human cancer cell line, their derived multi-drug resistant cell lines, and normal human keratinocytes. Sesquiterpene lactones showed similar cytotoxic activity towards drug sensitive and drug resistant cancer cell lines.

Submitted for publication: Phytochemistry letters

Introduction

Inula britannica L. (Asteraceae) produces a variety of secondary metabolites including sesquiterpene lactones, diterpenes, triterpenes, and flavonoids (Khan et al., 2010). *Inula britannica* extracts have been reported to possess anti-inflammatory, hepatoprotective, anti-bacterial, and cytotoxic activity (Zhao et al., 2006). Sesquiterpene lactones of the germacranolide, eudesmanolide, 1,10-seco-eudesmanolide, and pseudoguaianolide groups, isolated mainly from flowers of the Chinese herb *I. britannica* var. *chinensis* are known to display cytotoxic effects against several human cancer cell lines (Zhou et al., 1993; Park and Kim, 1998; Bai et al., 2006; Qi et al., 2008). Although sesquiterpene lactones are present in *I. britannica* ecotypes growing in Europe as well, (Rybalko et al., 1968; Chugunov et al., 1971; Serkerov and Mir-Babaev, 1988) no investigation regarding the cytotoxicity of the European samples constituents has been reported so far. Therefore, we investigated the cytotoxic activity of a series of sesquiterpene lactones isolated from *I. britannica* plants collected in the wild around Belgrade, Serbia. This led to the isolation and identification of 10 sesquiterpene lactones, five of which have never been reported before. The isolated compounds were subsequently tested for their cytotoxicity against human cancer cell lines, their multi-drug resistant (MDR) counterparts, and normal human keratinocytes (HaCaT).

Materials and Methods

General Experimental Procedures

FT-IR was measured on a Perkin-Elmer FT-IR Spectrometer Paragon 1000. Optical rotations were obtained using a Propol Automatic Polarimeter. UV measurements were performed using a Shimadzu UV mini-1240. NMR spectra were recored in $CDCl_3$ or MeOD on a Bruker DMX 500 MHz NMR calibrated to residual $CDCl_3$ (7.26 ppm ^{1}H; 77.16 ppm ^{13}C) or MeOD (3.31 ppm). High resolution mass data (HRESIMS) were collected on a Thermo LC-LTQ-Orbitrap FTMS system. LC-APCI mass data (APCIMS) were collected in both positive and negative mode on an Agilent 1100 series HPLC connected to G1956 LC/MSD SL single quadropole mass spectrometer. Centrifugal partition chromatography (CPC) was carried out with a Kromaton Fast Centrifugal Partition Chromatograph with 1 L internal rotor volume and 30 mL Rheodyne injector loop. Semi-preparative HPLC (pHPLC) was performed with a Shimadzu HPLC system and a 5 mL Rheodyne manual injection loop. Normal phase (NP) separation used a Phenomenex Luna Silica (2) 100 A 5 micron 250 x 10 mm column with 10 x 10 mm silica guard cartridge while reverse phase (RP) separation used a Phenomenex Luna C18 (2) 100 A 5 micron 250 x 10 mm column. All pHPLC experiments used 5 mL/min flow rate and 10 mL fractions were collected unless otherwise noted. TLC was performed with silica gel 60 (Merck) plates using $CHCl_3$: EtOAc 1:1 and visualized with vanillin/sulfuric acid reagent. Flash chromatography used silica gel 60 (0.063- 0.2 mm, Merck). All solvents were of analytical and HPLC grade.

Plant Material

Inula britannica plant material was collected in Serbia from several natural localities: from the edge of Lipovica forest and from meadows nearby Mladenovac and Kragujevac. Species identification was confirmed by Wout Holverda at the Leiden Nationaal Herbarium Nederland and a voucher specimen was deposited in the economic botany collection under the following barcode: AsteraceaeInulabritannicaL.L 0991383J. FischedickNo. 172010.

Extraction and Isolation

Inula britannica (200 g) dried flowers were extracted with 4 L EtOH for 24 hours. Solvent removed in vacuo to yield 14 g yellow solid/syrup. Crude extract was re-dissolved in 400 mL ethyl acetate (EtOAc) and 400 mL H_2O. The H_2O layer was drained off and EtOAc rinsed 2 additional times with 250 mL H_2O. The EtOAc layer was dried over $MgSO_4$, filtered, and solvent removed in vacuo to yield 6 g yellow solid/syrup. The EtOAc extract was further fractionated with CPC. A 2 phase solvent system composed of 4: 6: 4: 6 heptane: EtOAc: MeOH: H_2O (5 L) was prepared and split into upper (2.3 L) and lower layer (2.7 L). The EtOAc extract was dissolved in 30 mL upper and lower layer (1:1). The CPC system was first filled with lower layer to act as stationary phase. Upper layer was then pumped in at flow rate of 10 mL/min and rotor rotation speed of 1000 rpm. The CPC system was considered in equilibrium when upper layer began to elute and amount of lower layer displaced recorded as void volume (220 mL). The entire sample was then injected and initial 200 mL eluent discarded after which 120 x 10 mL fractions (CPC $Fr_{\#}$) were collected (pressure 52 bar). After the 120th fraction the CPC system was rinsed with lower layer which was collected as an additional rinse fraction (Fr_R). Fractions were analyzed by TLC, combined based on profile, and solvent removed in vacuo.

CPC $Fr_{11\text{-}30}$ (318 mg) was further separated by NP pHPLC ($CHCl_3$: EtOAc, 9:1) with subsequent fractions 3-8 (110 mg) run on RP pHPLC (H_2O: acetonitrile (ACN), 8:2) to yield **1** (11.6 mg) from fractions 11-13 and an impure sesquiterpene lactone in fractions 7-9 (88.9 mg). CPC $Fr_{31\text{-}45}$ (110 mg) was separated by NP pHPLC ($CHCl_3$: EtOAc, 9:1) with subsequent fractions 1-8 (52 mg) run on RP pHPLC (H_2O: ACN, 1:1) to yield 3 additional fractions. Fractions 1-2 (27.2 mg) were combined and fractionated by RP pHPLC (H_2O: ACN, 8:2, gradient to 100% ACN) to yield **10** (8.1 mg) and **3** (2.9 mg). Fraction 3 (13.5 mg) was combined with fractions 7-9 from CPC $Fr_{11\text{-}30}$ RP pHPLC and purified with RP pHPLC (H_2O: ACN, 6:4) to yield **2** (67.8 mg). CPC $Fr_{46\text{-}65}$ (368 mg) was separated by NP pHPLC ($CHCl_3$: EtOAc, 9:1, 3 mL/min, 6 mL fractions) with **9** (127 mg) crystallized from fractions 4-16 with hexane/Et_2O while fractions 17-20 were further purified with RP pHPLC (H_2O: ACN, 1:1) to yield **3** (2.7 mg). CPC $Fr_{66\text{-}120}$ (914 mg) was separated by flash chromatography (100 g silica, $CHCl_3$ increasing ratio of acetone), with 100 mL fractions collected. Flash fractions 2-6 were combined (576 mg) and run on NP pHPLC ($CHCl_3$: EtOAc, 7:3) with subsequent fractions 7-28 further separated by NP pHPLC ($CHCl_3$: EtOAc, 9:1) to yield **8** (98 mg) as white needles (hexane/Et_2O) from fractions 12-28. CPC Fr_R (478 mg) was further separated by flash chromatography (50 g silica) using hexane with increasing ratio of acetone followed by acetone with increasing ratio of ethanol. Flash fractions 4-5 (100

mg) were purified with RP pHPLC (H_2O: ACN, 8: 2) to yield **7** (8.3 mg) from fractions 16-17 while fractions 18-23 (22.4 mg) were again separated by RP pHPLC (H_2O: ACN, gradient to 100% ACN) to yield **5** (16.8 mg) from fraction 9. Flash fractions 6-7 (118 mg) were separated by RP pHPLC (H_2O: ACN, 8: 2) from which fractions 1-3 were again separated by RP pHPLC (H_2O: ACN, 9: 1) to yield **4** (8.8 mg) from fractions 22-25 and an impure sesquiterpene lactone in the rinse fraction. The impure sesquiterpene lactone was re-purified under the same conditions to yield **6** (18.2 mg).

14-(3-Methylpentanoyl)-6-deoxybritannilactone (**1**): amorphous colorless solid; $[\alpha]^{20}_D$ +109.5 (*c* 0.15, $CHCl_3$); UV (MeOH) λ_{max} (log ε) 212.0 (3.95) nm; IR (film) ν_{max} 3503.7, 2961.4, 2360.4, 2342.7, 1759.4, 1733.6, 1268.3 cm^{-1}; ^1H and ^{13}C NMR data, see Table1; APCIMS *m/z* 347 $[M - H_2O]^+$ (100), 363 $[M - H]^-$ (100); HRESIMS *m/z* 365.2321 $[M + H]^+$ (calcd for $C_{21}H_{33}O_5$ 365.2328).

14-(3-Methylbutanoyl)-6-deoxybritannilactone (**2**): amorphous colorless solid; $[\alpha]^{20}_D$ +112.6 (*c* 0.19, $CHCl_3$); UV (MeOH) λ_{max} (log ε) 209 (4.06) nm; IR (film) ν_{max} 3428.1, 2959.5, 2360.3, 2343.7, 1759.6, 1734, 1267.3, 1187.8, 996 cm^{-1}; ^1H and ^{13}C NMR data, see Table1; APCIMS *m/z* 333 $[M - H_2O]^+$ (100), 349 $[M - H]^-$ (100); HRESIMS *m/z* 351.2166 (calcd for $C_{20}H_{31}O_5$ 351.2172).

14-(2-Methylpropanoyl)-6-deoxybritannilactone (**3**): amorphous colorless solid; $[\alpha]^{20}_D$ +122.9 (*c* 0.07, $CHCl_3$); UV (MeOH) λ_{max} (log ε) 204.5 (4.29) nm; IR (film) ν_{max} 3440, 2961.5, 2360, 2343.3, 1759.1, 1734, 1268.4, 1191.7, 1157.8, 996 cm^{-1}; ^1H and ^{13}C NMR data, see Table1; APCIMS *m/z* 319 $[M - H_2O]^+$ (100), 335 $[M - H]^-$ (100); HRESIMS *m/z* 337.2011 (calcd for $C_{19}H_{29}O_5$ 337.2015).

1,3-Epi-granilin (**4**): amorphous white solid; $[\alpha]^{20}_D$ +146.0 (*c* 0.1, MeOH); UV (MeOH) λ_{max} (log ε) 226.5 (3.26) nm; IR (film) ν_{max} 3424, 2359.8, 2343.2, 1740, 1262, 1220, 772 cm^{-1}; ^1H NMR (MeOD, 500 MHz) δ 6.08 (1H, br s, H-13a), 5.71 (1H, br s, H-13b), 5.18 (1H, br s, H-15a), 4.67 (1H, br s, H-15b), 4.58 (1H, td, *J* = 4.8, 1.6 Hz, H-8), 4.02 (1H, dd, *J* = 11.8, 5.3 Hz, H-3), 3.42 (1H, dd, *J* = 11.9, 4.3 Hz, H-1), 3.07 (1H, m, H-7), 2.52 (1H, dd, *J* = 15.8, 1.6 Hz, H-9β), 2.09 (1H, m, H-2α), 1.80 (1H, m, H-5), 1.80 (1H, m, H-6α), 1.54 (1H, m, H-9α), 1.51 (1H, m, H-2β), 1.42 (1H, ddd, *J* = 13, 12.9 Hz, H-6β), 0.74 (3H, s, H-14); APCIMS *m/z* 265 $[M + H]^+$ (100), 263 $[M - H]^-$ (100); HRESIMS *m/z* 265.1436 $[M + H]^+$ (calcd for $C_{15}H_{21}O_4$ 265.1440).

11,13-Dihydro-inuchinenolide B (**5**): amorphous colorless solid; $[\alpha]^{20}_D$ -46.1 (*c* 0.26, $CHCl_3$); UV (MeOH) λ_{max} (log ε) 208 (4.05) nm; IR (film) ν_{max} 3428.5, 2976.1, 2360.3, 2343.7, 1733.8, 1239.6 cm^{-1}; ^1H-NMR ($CDCl_3$, 500 MHz) δ 5.55 (1H, m, H-2β), 4.71 (1H, ddd, *J* = 10.1, 7.2, 2.5 Hz, H-8), 2.78 (1H, m, H-7), 2.76 (1H, m, H-11), 2.66 (1H, m, H-9β), 2.63 (1H, br d, H-5), 2.49 (1H, dd, *J* = 15.9, 2.5 Hz, H-9α), 2.33 (1H, dd, *J* = 13.4, 7.4 Hz, H-3β), 2.05 (3H, s, $COOCH_3$, H-2'), ~1.88 (1H, s, OH-4α), 1.77 (1H, m, H-3α), 1.77 (1H, m, H-6α), 1.68 (3H, d, *J* = 1.6 Hz, H-14), 1.33, (1H, m, H-6β), 1.26 (3H, d, *J* = 7.5 Hz, H-13β), 1.11 (3H, s, H-15); ^{13}C-NMR ($CDCl_3$, 125.8 MHz) δ 180.1 (C, $COOCH_3$, C-1'), 170.7 (C, C12), 137.6 (C, C-1), 132.4 (C, C-10), 79.4 (CH, C-8), 78.3 (C, C-4), 72.7 (CH, C-2), 52.7 (CH, C-5), 46.7 (CH_2, C-3), 41.0 (CH, C-7), 38.8

(CH, C-11), 37.4 (CH_2, C-9), 23.4 (CH_2, C-6), 23.0 (CH_3, C-15), 22.0 (CH_3, C-14), 21.2 (CH_3, $COOCH_3$, C-2'), 12.8 (CH_3, C-13); APCIMS *m/z* 307 $[M - 1]^-$ (20); HRESIMS *m/z* 309.1701 $[M + H]^+$ (calcd for $C_{17}H_{25}O_5$ 309.1702).

Pulchellin C (**6**): amorphous yellow solid; $[\alpha]^{20}_D$ +119.8 (c 0.21, MeOH); ^{1}H-NMR (MeOD, 500 MHz) δ 6.08 (1H, s, H-13a), 5.72 (1H, s, H-13b), 5.27 (1H, d, *J* = 1.2 Hz, H-15a), 4.71 (1H, d, *J* = 1.4 Hz, H-15b), 4.55 (1H, m, H-8), 3.75 (1H, br d, H-3α), 3.44 (1H, ddd, *J* = 11.6, 9.2, 4.9 Hz, H-2β), 3.11 (1H, m, H-7), 2.21 (1H, dd, *J* = 15.6, 1.3 Hz, H-9α), 1.98 (1H, br d, *J* = 12.6 Hz, H-5), 1.83 (1H, m, H-1β), 1.83 (1H, m, H-6α), 1.61 (1H, dd, *J* = 15.6, 4.6 Hz, H-9β), 1.35 (IH, m, H-6β), 1.31 (1H, m, H-1α) 0.81 (3H, s, H-14); APCIMS *m/z* 265 $[M + H]^+$ (100), 263 $[M - H]^-$ (100); HRESIMS *m/z* 265.1438 $[M + H]^+$ (calcd for $C_{15}H_{21}O_4$ 265.1440).

6-Deacetylbritanin (**7**): amorphous colorless solid; $[\alpha]^{20}_D$ +5.2 (c 0.12, $CHCl_3$); ^{1}H-NMR ($CDCl_3$, 500 MHz) δ 6.25 (1H, br d, H-13a), 6.16 (1H, br d, H-13b), 4.91 (1H, ddd, *J* = 8.8, 6.6, 1.5 Hz, H-2β), 4.61 (1H, ddd, *J* = 12.1, 8.3, 4.6 Hz, H-4α), 4.28 (1H, ddd, *J* = 12.1, 9.7, 2.8 Hz, H-8), 3.76 (1H, dd, *J* = 9.8, 3.6 Hz, H-6β), ~2.88 (1H, m, OH-6α), 2.85 (1H, m, H-7), 2.35 (1H, m, H-9β), 2.05 (1H, m, H-3a), 2.04 (3H, s, $COOCH_3$, H-2'), 1.90 (1H, m, H-1), 1.84 (1H, m, H-10α), 1.82 (1H, m, H-3b), ~1.79-1.93 (1H, m, OH-4β), 1.42 (1H, m, H-9α), 0.95 (3H, d, *J* = 6.3 Hz, H-14), 0.95 (3H, s, H-15); ^{13}C-NMR ($CDCl_3$, 125.8 MHz) δ 170.6 (C, $COOCH_3$, C-1'), 170.1 (C, C-12), 139.0 (C, C-11), 123.3 (CH_2, C-13), 77.1 (CH, C-6), 76.7 (CH, C-8), 75.4 (CH, C-2), 73.8 (CH, C-4), 52.1 (CH, C-7), 51.2 (C, C-5), 51.1 (CH, C-1), 44.0 (CH_2, C-9), 36.8 (CH_2, C-3), 29.7 (CH, C-10), 21.4 (CH_3, $COOCH_3$, C-2'), 20.2 (CH_3, C-14), 17.7 (CH_3, C-15); APCIMS m/z 325 $[M + H]^+$ (100), 323 $[M - H]^-$ (95); HRESIMS m/z 325.1649 $[M + H]^+$ (calcd for $C_{17}H_{25}O_6$ 325.1651).

4H-Tomentosin (**10**): amorphous colorless solid; $[\alpha]^{20}_D$ +18.4 (*c* 0.10, $CHCl_3$); ^{1}H-NMR ($CDCl_3$, 500 MHz) δ 6.26 (1H, d, *J* = 3.2 Hz, H-13a), 5.52 (1H, d, *J* = 2.8 Hz, H-13b), 5.49 (1H, dd, *J* = 9.2, 5.3 Hz, H-5), 4.64 (1H, ddd, *J* = 11.7, 8.5, 2.8 Hz, H-8), 3.78 (1H, m, H-4), 3.34 (1H, m, H-7), 2.45 (1H, m, H-6β), 2.37 (1H, m, H-10), 2.18 (1H, m, H-6α), 2.14 (1H, m, 2a), 2.00 (1H, m, H-9α), 1.99 (1H, m, H-2b), 1.90 (1H, m, H-9β), 1.57 (1H, m, H-3a), 1.46 (1H, m, H-3b), 1.33 (1H, br s, OH-4), 1.21 (3H, d, *J* = 6.2 Hz, H-15), 1.14 (3H, d, *J* = 6.9 Hz, H-14); ^{13}C-NMR ($CDCl_3$, 125.8 MHz) δ 170.4 (C, C-12), 145.7 (C, C-1), 139,2 (C, C-11), 122.2 (CH_2, C-13), 120.0 (CH, C-5), 79.8 (CH, C-8), 67.7 (CH, C-4), 42.4 (CH, C-7), 38.1 (CH_2, C-3), 36.8 (CH_2, C-9), 35.2 (CH, C-10), 33.0 (CH_2, C-2), 26.9 (CH_2, C-6), 24.0 (CH_3, C-15), 21.1 (CH_3, C-14); APCIMS *m/z* 251 $[M + H]^+$ (100), 249 $[M - H]^-$ (100); HRESIMS *m/z* 251.1642 $[M + H]^+$ (calcd for $C_{15}H_{23}O_3$ 251.1647).

Cell lines and Cell Culture

The NCI-H460, DLD1, and U87 cell lines were purchased from the American Type Culture Collection (ATCC), while COR-L23 and COR-L23/R cell lines were purchased from European Collection of Cell Cultures (ECACC). Human normal

keratinocytes – HaCaT were obtained from Cell Lines Service (CLS). NCI-H460/R cells were selected originally from NCI-H460 cells and cultured in a medium containing 100 nM doxorubicin (Pešić et al., 2006). DLD1-TxR and U87-TxR cells were selected from DLD1 and U87 cells, respectively, and cultured in a medium containing 300 nM paclitaxel (Podolski-Renić et al., 2011). All cell lines were sub-cultured at 72 h intervals using 0.25% trypsin/EDTA and seeded into a fresh medium at the following densities: 8,000 cells/cm^2 for NCI-H460, DLD1, DLD1-TxR, COR-L23 and COR-L23/R, 16,000 cells/cm^2 for U87 and NCI-H460/R, and 32,000 cells/cm^2 for U87-TxR and HaCaT.

Cytotoxicity assays

Cells grown in 25 cm^2 tissue flasks were trypsinized, seeded into flat-bottomed 96-well tissue culture plates, and incubated overnight. Treatment with all compounds (10 μM) lasted 72 h. The cellular proteins were stained with Sulforhodamine B assay (SRB), following a slightly modified protocol (Skehan et al., 1990). To further assess the cytotoxic effects of the most potent sesquiterpene lactones in NCI-H460 and NCI-H460/R cells, beside SRB assay, the MTT assay based on the reduction of 3-(4,5-dimethyl-2-thizolyl)-2,5-diphenyl-2H-tetrazolium bromide into formazan dye by active mitochondria of living cells was applied as well. The cells were incubated with indicated compounds for 72 h. Afterwards, 100 μl of MTT solution (1 mg /ml) was added to each well and plates were incubated at 37°C for 4 h. Formazan product was dissolved in 200 μl of DMSO. The absorbance of obtained dye after SRB or MTT assay was measured at 540 nm using an automatic microplate reader (LKB 5060-006 Micro Plate Reader, Vienna, Austria).

Appendix

Detailed LC-MS conditions, NMR parameters, ^{1}H-NMR data for compounds **6** and **7**, and NMR spectra of all isolated compounds are available in the chapter 6 appendix.

Results and Discussion

An EtOH extract from dried *I. britannica* flowers was partitioned between EtOAc and H_2O. The EtOAc fraction was further purified with CPC followed by combination of flash chromatography and pHPLC to yield 10 sesquiterpene lactones. Three of these compounds were new 1,10-seco-eudesmanolides assigned the trivial names; 14-(3-methylpentanoyl)-6-deoxybritannilactone (**1**), 14-(3-methylbutanoyl)-6-deoxybritannilactone (**2**), and 14-(2-methylpropanoyl)-6-deoxybritannilactone (**3**). In addition, a new stereoisomer of granillin, 1,3-epi-granillin (**4**), and a new pseudoguaianolide, 11,13-dihydro-inuchinenolide B (**5**), were isolated. Five known sesquiterpene lactone compounds; pulchellin C (**6**) (Serkerov and Mir-Babaev, 1988; Adekenov et al., 1990), 6-deacetylbritannin (**7**) (Dzhazin and Adekenov, 1996; Yang et al., 2010), gaillardin (**8**) (Kupchan et al., 1965; Kupchan et al., 1966; Ito and Iida, 1981), britannin (**9**) (Adekenov et al., 1990; Rybalko et al., 1968), and 4H-tomentosin

(**10**) (Bohlmann et al., 1978; Kim et al., 2004) were also isolated, with **10** being reported in *I. britannica* for the first time.

Chemical structures (1 – 10)

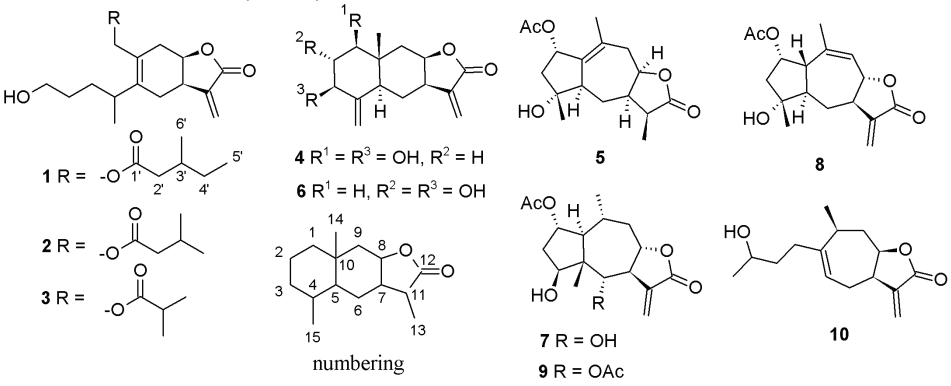

Compounds **1-3** were isolated as amorphous colorless solids. Complete ^{1}H and ^{13}C-NMR assignments are shown in table 1. Carbon atom multiplicity was confirmed with ^{13}C-APT and HSQC. Complete HMBC correlations are shown in table 2. Similarity of ^{1}H and ^{13}C-NMR with literature (Zhou et al., 1993; Bai et al., 2006; Qi et al., 2008) suggested that **1-3** contained a 1,10-seco-eudesmanolide skeleton. A mass of 364 was suggested by the APCIMS spectrum of **1**. The molecular formula $C_{21}H_{32}O_5$ was established for **1** by HRESIMS (obsd 365.2321, calcd 365.2328, $[M + H]^+$). The IR suggested the presence of a hydroxyl group (3507.7 cm^{-1}), a γ unsaturated lactone (1759.4 cm^{-1}), and an ester (1733.6 cm^{-1}). The terminal methylene functionality of the α-methylene-γ-lactone was confirmed by the pair of 1H doublets appearing at δ_H 5.64 and 6.27, both attached to δ_C 122.0 (C-13). Furthermore the carbonyl carbon at δ_C 170.5 (C-12) and the quaternary carbon at δ_C 140.1 (C-11) correlated in HMBC to H-13. Correlations in COSY between H-13a and H-13b with δ_H 3.23 (H-7) were observed. The rest of the spin system connectivity was easily deduced by COSY showing correlations between H-7 with δ_H 4.90 (H-8), 2.25 (H-6), and 2.09 (H-6) as well as correlations in COSY between H-8 with δ_H 2.43 (H-9) and 2.62 (H-9). HSQC was used to unambiguously assign proton containing carbons on the bicyclic ring and HMBC confirmed connectivity of the entire spin system. The dd splitting pattern of protons at position 6 and 9 indicated that carbons at C-5 and C-10 were quaternary. Through analysis of HMBC spectra 2 alkene region quaternary carbons at δ_C 139.6 and δ_C 129.2 were assigned as C-5 and C-10 respectively (C-5→ 2H-6, 2H-9; C-10→ 2H-6, H-8, 2H-9). An additional HMBC correlation from C-5 to the methyl protons at δ_H 0.97 (CH_3-15) confirmed connectivity of side chain. Connectivity of C-5 to C4, C-15 to C4, C-4 to C-3, C-3 to C-2, and C-2 to C-1 was established through analysis of COSY, HSQC spectra, and confirmed by HMBC. The chemical shift of protons at position 1 (δ_H 3.98) and carbon (δ_C 64.0) confirmed the presence of hydroxyl functionality at position 1. Alkyl ester substitution connected to C-14 was suggested by the IR, remaining $C_6H_{11}O_2$, and the deshielded protons and carbon at C-14 (δ_C 61.4; δ_H 4.13, 4.19). Connectivity

from C-1' (δ_C 173.7) to C-2' (δ_C 41.6, CH_2) and C-3' (δ_C 32.1, CH) was established by HMBC. The methine at H-3' (δ_H 1.86) COSY spectrum showed correlations to H-2a' (δ_H 2.29), H-2b' (δ_H 2.09), CH_3-6' (δ_H 0.92), H-4a' (δ_H 1.34), and H-4b' (δ_H 1.22). The remaining methyl group was assigned to 5' (δ_H 0.88) and confirmed with COSY. The ester substituent was thus identified as a 3-methylpentanoyl group. The *cis* and axial relative configuration of protons H-7 and H-8 was confirmed by correlation in NOESY spectrum (Figure 1). Correlations were observed between H-7 and both H-6 as well as between H-8 and both H-9 (not shown in figure 1) and thus could not be used to establish their relative configuration. However due to the *cis* configuration of H-7 and H-8 as well as a cross peak between H-13b and H-6 (δ_H 2.09) confirmed β configuration. A NOESY correlation from H-6β (δ_H 2.09) to H-9β (δ_H 2.62) confirmed β configuration of H-9β. A NOESY correlation between H-6 (δ_H 2.25) and H-9 (δ_H 2.43) was also observed and confirmed α configuration of these protons. Compound **1** was therefore identified as 14-(3-methylpentanoyl)-1-hydroxy-1,10-seco-5(10),11(13)-eudesadien-12,8β-olide.

The same 1,10-seco-eudesmanolide skeleton as **1** was recognized in compounds **2** and **3** by ^{1}H-NMR, COSY, ^{13}C-APT, HSQC and HMBC spectra. A mass of 350 was suggested by APCIMS of **2**. The molecular formula $C_{20}H_{30}O_5$ was established for **2** by HRESIMS (obsd 351.2166, calcd 351.2172, $[M + H]^+$). The difference between **1** and **2** was therefore due to a different functional group at the C-14 position. Alkyl ester substitution was again suggested from IR (1734 cm^{-1}) and remaining $C_5H_9O_2$. Connectivity from the carbonyl C-1' (δ_C 177.5) to 2'-H (δ_H 2.17) and 3'-H (δ_H 2.08) was determined by HMBC and 2' correlated in COSY with 3'. The 2 overlapping methyl groups (δ_H 0.94) showed correlations in COSY with 3' and were assigned at the 4' and 5' positions. The substituent was therefore established as a 3-methylbutanoyl group. The relative configuration was the same as **1**, confirmed by NOESY. Therefore compound **2** was identified as 14-(3-methylbutanoyl)-1-hydroxy-1,10-seco-5(10),11(13)-eudesadien-12,8β-olide.

The mass of compound **3** was suggested to be 336 based on APCIMS. Confirmation of the molecular formula as $C_{19}H_{28}O_5$ was established by HRESIMS (obsd 337.2011, calcd 337.2015, $[M + H]^+$). Alkyl ester substitution at C-14 was suggested by IR (1734 cm^{-1}) and remaining $C_4H_7O_2$. In HMBC correlations between carbonyl C-1', 2'-H (δ_H 2.53) and 2 overlapping methyl groups (δ_H 1.16). Connectivity between 2'-H and the methyl groups at 3' and 4' was confirmed by coupling constant (J = 7.0 Hz) and COSY. The substituent was therefore established as a 2-methylpropanoyl group. NOESY established that the relative configuration for **3** was the same as in **1** and **2**. Compound **3** was thus identified as 14-(2-methylpropanoyl)-1-hydroxy-1,10-seco-5(10),11(13)-eudesadien-12,8β-olide.

Table 1. ^{1}H and ^{13}C-NMR data for compounds **1** – **3** ($CDCl_3$)

	1		**2**		**3**	
position	δ_C type	δ_H (J in Hz)	δ_C type	δ_H (J in Hz)	δ_C type	δ_H (J in Hz)
1	64.0, CH_2	3.98, m	64.0, CH_2	3.98, m	64.1, CH_2	3.97, m
2	27.0, CH_2	1.32, m 1.42, m	27.0, CH_2	1.31, m 1.41, m	27.0, CH_2	1.32, m 1.41, m
3	30.8, CH_2	1.16, m 1.31, m	30.7, CH_2	1.15, m 1.29, m	30.7, CH_2	1.17, m 1.30, m
4	33.6, CH	2.76, m	33.5, CH	2.76, m	33.6, CH	2.77, m
5	139.6, C		139.4, C		139.6, C	
6α	29.0, CH_2	2.25, dd (15.0, 6.6)	28.9, CH_2	2.24, dd (15.0, 6.7)	29.0, CH_2	2.25, dd (15.0, 7.1)
6β		2.09, m		2.08, m		2.09, dd (15.0, 4.5)
7	37.5, CH	3.23, m	37.5, CH	3.23, m	37.5, CH	3.24, m
8	77.1, CH	4.90, m	77.1, CH	4.90, m	77.1, CH	4.91, m
9α	31.8, CH_2	2.43, dd (15.3, 4.4)	31.8, CH_2	2.42, dd (15.4, 4.3)	31.8, CH_2	2.43, dd (15.0, 4.4)
9β		2.62, dd (15.3, 4.6)		2.61, dd (15.3, 4.6)		2.64, dd (15.0, 4.5)
10	129.2, C		129.2, C		129.2, C	
11	140.1, C		140.1, C		140.1, C	
12	170.5, C		170.5, C		170.5, C	
13b	122.0, CH_2	5.64, d (2.3)	122.9, CH_2	5.64, d (2.3)	122.0, CH_2	5.65, d (2.3)
13a		6.27, d (2.7)		6.27, d (2.7)		6.28, d (2.7)
14	61.4, CH_2	4.13, d (11.9) 4.19, d (11.9)	61.3, CH_2	4.13, d (11.9) 4.19, d (11.9)	61.5, CH_2	4.14, d (12) 4.19, d (12)
15	19.5, CH_3	0.97, d (6.8)	19.5, CH_3	0.97, d (6.8)	19.5, CH_3	0.98, d (6.8)
1’	173.7, C		173.4, C		177.5, C	
2’	41.6, CH_2	2.09, m 2.29, dd (14.7, 6.1)	43.5, CH_2	2.17, d (7.1)	34.16, CH	2.53, septet (7)
3’	32.1, CH	1.86, m	25.8, CH	2.08, m	19.2, CH_3	1.16, d (7)
4’	29.8, CH_2	1.22, m 1.34, m	22.5, CH_3	0.94, d (6.6)	19.2, CH_3	1.16, d (7)
5’	11.4, CH_3	0.88, t (7.5)	22.5, CH_3	0.94, d (6.6)		
6’	19.4, CH_3	0.92, d (6.7)				
OH		~1.51, br s		~1.50, br s		~1.43, m

Figure 1. NOESY correlations of **1** – **3**.

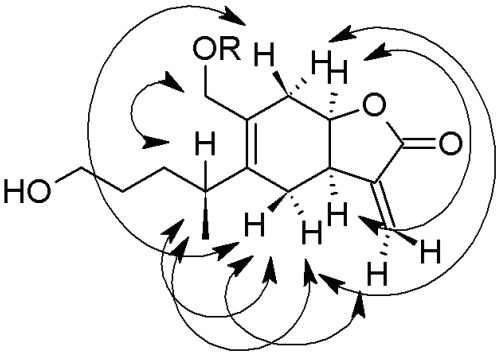

Table 2. HMBC correlations **1** - **3**

position	**1** (C→ H#)	**2** (C→ H#)	**3** (C→ H#)
1		2, 3	2, 3
2	1, 3	1, 3	1, 3
3	1, 15	1, 2, 4, 15	1, 15
4	6β, 15	2, 3, 6, 15	6β, 15
5	6, 9, 15	3, 6, 9, 15	6, 9, 14, 15
6	8, 13a	8, 13	8, 13a
7	6, 9, 13	6, 9, 13	6, 9, 13
8	6, 9	6, 9	6, 9
9	6, 14	4	14
10	6, 8, 9, 14	6, 8, 9	6, 8, 9, 14
11	6, 13a	13	13a
12	8, 13	8, 13	8, 13
13			
14	9	9	9
15		3	
1’	2’, 3’	2’, 3’	2’, 3’, 4’
2’	4’, 6’	3’, 4’, 5’	3’, 4’
3’	2’, 5’	2’, 4’, 5’	2’, 4’
4’	2’, 5’	2’, 3’, 5’	2’, 3’
5’	4’	2’, 3’, 4’	
6’	2’, 4’		

A mass of 264 was suggested from the APCIMS spectrum of **4** and HRESIMS (obsd 265.1436, calcd 265.1440 $[M + H]^+$) confirmed $C_{15}H_{20}O_4$ as the molecular formula. Compound **4** had very similar ^{1}H-NMR and IR spectra as that of granilin (Nikonova and Nikonov, 1972; Maruyama and Shibata, 1975; Vichnewski et al., 1976). However differences were noted in the δ and *J* values for protons at position 1, 2, and 3 suggesting a different relative configuration of the hydroxyl groups. The spin system connecting 2H-13 to H-7, H-7 to 2H-6 and H-8, H-8 to 2H-9, H-6 (δ_H 1.42) to H-5, and H-5 to 2H-15 was confirmed by COSY. Protons at δ_H 3.42 and δ_H 4.02 were assigned to H-1 and H-3 respectively due to deshielding from hydroxyl groups and for H-3 a correlation in COSY with methylene protons 2H-15. Connectivity between H-1 to 2H-2 (δ_H 2.09; δ_H 1.51) to H-3 was confirmed by COSY. In the NOESY spectrum a correlation between H-7 and H-8 was observed confirming a *cis* and axial configuration (Figure 4). Further correlations in NOESY between H-7 and H-6 (δ_H 1.80) as well as H-8 and H-9 (δ_H 1.54) confirmed α configuration for these protons. Both H-6β (δ_H 1.42) and H-9β (δ_H 2.52) correlated in NOESY with the methyl group at position 14 (δ_H 0.74) confirming β configuration. The α configuration of H-1 was confirmed by a correlation in NOESY with H-9α. Further correlations from H-1 to H-2α (δ_H 2.09) and H-2α to H-3 confirmed the hydroxyl groups at 1 and 3 as β oriented. Finally a correlation from H-2β (δ_H 1.51) to the β oriented methyl group at C-14 was also observed in the NOESY spectrum. Compound **4** was therefore identified as 1β,3β-dihydroxy-4(15),11(13)-eudesmadien-12,8β-olide.

Figure 2. NOESY correlations of **4**.

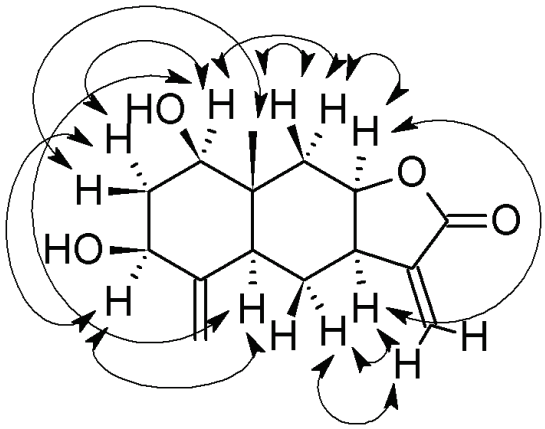

Figure 3. NOESY correlations of **5**.

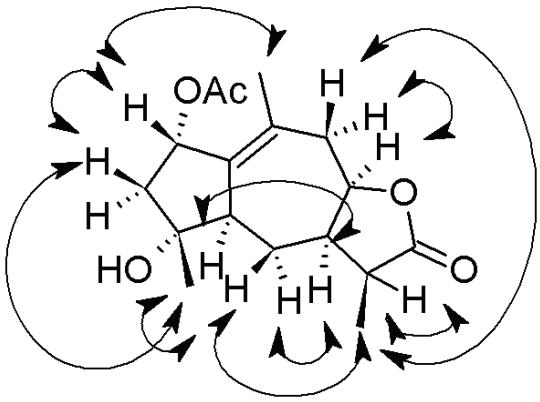

The molecular formula of compound **5** was established as $C_{17}H_{24}O_5$ by HRESIMS (obsd 365.2321, calcd 365.2328 $[M + H]^+$). The ^1H and ^{13}C-NMR spectra of **5** resembled inuchinenolide B, previously reported from *I. Britannica* (Ito and Iida, 1981), however the methylene H-13 doublets were lacking and an additional methyl group (δ_H 1.26) was present. The connectivity of the spin system H-2 (δ_H 5.55) and 2H-3 (δ_H 2.33; 1.77) was confirmed with COSY. Correlations in COSY from H-8 (δ_H 4.71) to 2H-9 (δ_H 2.66; 2.49), H-8 to H-7 (δ_H 2.78), H-7 to 2H-6 (δ_H 1.77; 1.33), and H-6 (δ_H 1.33) to H-5 (δ_H 2.63) were observed. The methyl groups at positions 14 (δ_H 1.63), 15 (δ_H 1.11), and 2' (δ_H 2.05) were assigned based on typical δ_H from neighboring functional groups and similarity with inuchinenolide B (Ito and Iida, 1981). The remaining methine proton and methyl group were assigned to H-11 (δ_H 2.76) and 3H-13 (δ_H 1.26) respectively with correlation in COSY confirming connectivity. Carbon resonances containing protons were unambiguously assigned with ^{13}C-APT and HSQC.

Remaining quaternary carbons were assigned based on similarity to inuchinenolide B (Ito and Iida, 1981). This data confirmed that **5** was the 11,13-dihydro version of inuchinenolide B. A correlation in NOESY between H-7 and H-8 was observed confirming axial and *cis* configuration (Figure 3). Correlations in NOESY from H-7 to H-6 (δ_H 1.77) and H-5 as well as H-8 to H-9 (δ_H 2.49) and H-5 confirmed α configuration of these protons. Both H-6β and H-9β correlated with 3H-13 in NOESY confirming the methyl group was in β orientation. Correlations in NOESY from H-6β to 3H-15 confirmed the methyl group was β orientated and hydroxyl group at position 4 α orientated. The methyl group at 15 also correlated with H-3 (δ_H 2.33) and H-2 confirming their β configuration. Therefore compound **5** was identified as 2α-acetoxy-4α-hydroxy-1(10)-guaiadien-12,8β-olide.

Figure 4. NOESY correlations of **6**.

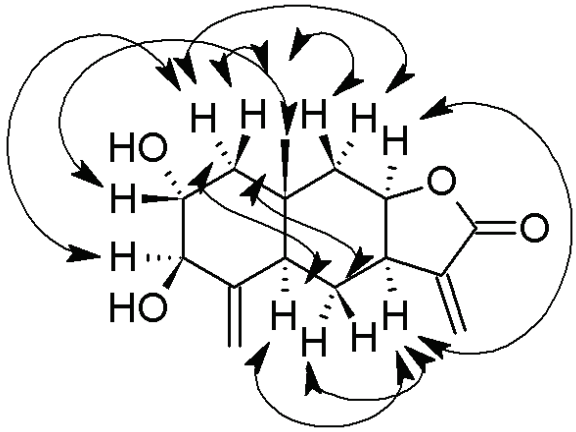

Previously literature concerning **6** did not complete all proton assignments (Serkerov and Mir-Babaev, 1988; Adekenov et al., 1990). By measuring **6** in MeOD with ^{1}H-NMR, COSY, and NOESY all protons and their relative configuration was completed (see experimental) (Figure 4). For **7** it was noted that no ^{13}C-NMR data was available (Dzhazin and Adekenov, 1996). Using ^{13}C-APT and HSQC carbon resonances for **7** were assigned. Close inspection of previous NMR data regarding **10** (Bohlmann et al., 1978; Kim et al., 2004) compared with ^{1}H-NMR, COSY, HMBC, and NOESY spectra obtained revealed incorrect assignments of 2H-2 and 2H-6 (Figure 5). Furthermore no complete ^{13}C-NMR assignments were found for **10**. Therefore the corrected proton assignments, relative configuration based on NOESY, and ^{13}C-NMR assignments are reported for **10** (see experimental).

Figure 5. HMBC (C → H) and NOESY correlations of **10**.

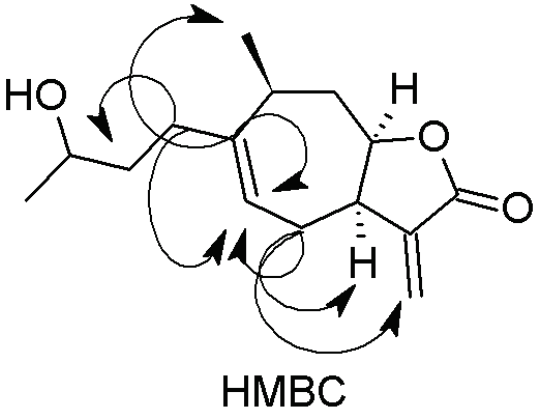

HMBC

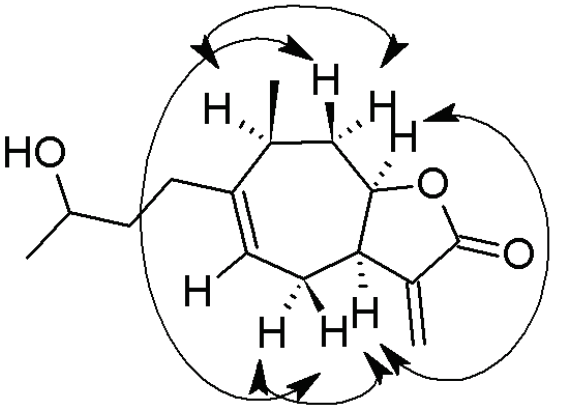

NOESY

MDR cancer cell lines with P-gp over-expression (NCI-H460/R, DLD1-TxR and U87-TxR) have been developed from their sensitive counterparts (NCI-H460, DLD1 and U87, respectively) by continuous exposure to increasing concentrations of chemotherapeutic drugs (Pešić et al., 2006; Podolski-Renić et al., 2011). COR-L23/R cell line is an MDR cancer cell line with MRP1 over-expression originating from corresponding sensitive cancer cell line (COR-L23/R). P-gp and MRP1 are ABC-type transporters (ATP-dependent drug efflux pumps) for xenobiotic compounds with broad substrate specificity. Isolated compounds were screened for their activity against non-small cell lung carcinoma (NCI-H460 and COR-L23), colorectal adenocarcinoma (DLD1), glioblastoma (U87), and their respective MDR cancer cell lines. Initially, 10 μM of each compound was tested by Sulforhodamine B assay (SRB) (Table 3).

Compound **2** was not assayed due to low purity (86%), as determined by HPLC at 230 nm. All other compounds were > 90% pure (data not shown). Compounds that achieved more than 50% inhibition (**7-10**) on the majority of cell lines after 10 μM application were selected for further testing. To compare their effects (the IC50 values) toward sensitive (NCI-H460) and MDR (NCI-H460/R) cancer cell lines as well as non-cancer cell line (HaCaT), SRB and MTT assays were applied (Table 4). Doxorubicin, a known anti-cancer drug, was used as a positive control. The results obtained by MTT and SRB assays were similar. Doxorubicin had approximately 100 times weaker activity against NCI-H460/R compared to corresponding sensitive NCI-H460 and 3 to 4 times stronger activity against NCI-H460 compared to non-cancer cell line – HaCaT. Contrary, no selectivity towards NCI-H460, NCI-H460/R or HaCaT was observed for **7-10,** suggesting that these compounds are generally cytotoxic. In addition, this data suggests that sesquiterpene lactones exhibit cytotoxic effects regardless of the presence of P-gp/MRP1.

Table 3. The percentage of cell growth inhibition induced by 10 μM (SRB assay)

Cell Lines	**1**	**3**	**4**	**5**	**6**	**7**	**8**	**9**	**10**
NCI-H460	25±9	35±5	n	20±5	13±9	32±6	71±15	83±13	81±6
NCI-H460/R	52±11	5±2	n	n	no	9±5	47±3	90±9	86±1
DLD1	14±6	12±5	n	n	26±9	25±5	86±4	78±2	87±9
DLD1-TxR	28±3	40±13	n	n	52±5	53±6	87±10	80±7	86±7
U87	24±6	20±4	10±4	25±10	26±6	67±4	74±6	63±6	66±2
U87-TxR	36±5	26±2	33±2	21±5	17±4	54±5	68±1	71±5	73±8
COR-L23	44±8	17±7	n	9±1	58±7	66±10	78±10	74±13	78±6
COR-L23/R	48±8	15±7	n	9±5	5±3	41±4	59±1	72±3	67±12

n = no inhibition.

Table 4. The IC50 values (μM) of **7**-**10** in NCI-H460, NCI-H460/R and HaCaT

	NCI-H460*		NCI-H460/R**		HaCaT***	
compounds	MTT	SRB	MTT	SRB	MTT	SRB
7	15.0±0.1	10.6±0.6	20.2±0.5	17.0±0.2	9.3±0.1	16.5±3.3
8	3.8±0.1	3.6±0.2	15.1±0.4	12.1±0.3	4.1±0.1	5.8±0.2
9	4.7±0.1	1.9±0.2	3.3±0.3	7.3±0.1	8.3±0.1	9.5±0.8
10	8.2±0.1	5.7±0.5	4.5±0.1	14.3±0.2	8.0±0.1	19.4±0.1
dox	0.036±0.001	0.037±0.003	4.42±0.17	2.04±0.05	0.146±0.01	0.09±0.01

*NCI-H460 were seeded at 1000 cells/well, **NCI-H460/R were seeded at 2000 cells/well, ***HaCaT were seeded at 4000 cells/well

Acknowledgement

The authors would like to thank the European Union Seventh Framework Program for funding the Terpmed project. Grant number 227448.

References

Adekenov, S., Abdykalykov, M., 1990. Pulchellin C from Inula caspica. Chemistry of Natural Compounds 26, 338–338.

Adekenov, S.M., Buděšínský, M., Abdikalikov, M.A., Turdybekov, C.M., Šaman, D., Błoszyk, E., Drożdż, B., Holub, M., 1990. Sesquiterpenic lactones of the Inula caspica BLUME species. Collection of Czechoslovak Chemical Communications 55, 1568–1579.

Artemova, N.P., Nikitina, L.E., Yushkov, D.A., Shigabutdinova, O.G., Plemenkov, V.V.,
Klochkov, V.V., Khairutdinov, B.I., 2005. Synthesis of S-Containing Derivatives of the Sesquiterpene Lactone Britanin. Chemistry of Natural Compounds 41, 45–47.

Bai, N., Lai, C.-S., He, K., Zhou, Z., Zhang, L., Quan, Z., Zhu, N., Zheng, Q.Y., Pan, M.-H., Ho, C.-T., 2006. Sesquiterpene lactones from Inula britannica and their cytotoxic and apoptotic effects on human cancer cell lines. Journal of Natural Products 69, 531–535.

Bohlmann, F., Mahanta, P.K., Jakupovic, J., Rastogi, R.C., Natu, A.A., 1978a. New sesquiterpene lactones from Inula species. Phytochemistry 17, 1165–1172.

Bohlmann, F., Mahanta, P.K., Jakupovic, J., Rastogi, R.C., Natu, A.A., 1978b. New sesquiterpene lactones from Inula species. Phytochemistry 17, 1165–1172.

Cheng, X., Zeng, Q., Ren, J., Qin, J., Zhang, S., Shen, Y., Zhu, J., Zhang, F., Chang, R., Zhu, Y., Zhang, W., Jin, H., 2011. Sesquiterpene lactones from Inula falconeri, a plant endemic to the Himalayas, as potential anti-inflammatory agents. European Journal of Medicinal Chemistry 46, 5408–5415.

Chugunov, P., Sheichenko, V., Ban'kovskii, A., Rybalko, K., 1971. The structure of britannin — A sesquiterpene lactone from Inula britannica. Chemistry of Natural Compounds 7, 265–268.

Dzhazin, K.A., Adekenov, S.M., 1996. Chemical modification of britanin and of inuchenolide C. Chemistry of Natural Compounds 32, 698–705.

Herz, W., Inayama, S., 1964. Constituents of Gaillardia species—II: Structures of pulchellin B and pulchellin C. Tetrahedron 20, 341–349.

Ito, K., Iida, T., 1981. Seven sesquiterpene lactones from Inula britannica var. chinensis. Phytochemistry 20, 271–273.

Khan, A.L., Hussain, J., Hamayun, M., Gilani, S.A., Ahmad, S., Rehman, G., Kim, Y.-H., Kang, S.-M., Lee, I.-J., 2010. Secondary Metabolites from Inula britannica L. and Their Biological Activities. Molecules 15, 1562–1577.

Kim, M.-R., Lee, S.-K., Kim, C.-S., Kim, K.-S., Moon, D.-C., 2004. Phytochemical constituents of Carpesium macrocephalum F(R). et S(AV). Archives of Pharmacal Research 27, 1029–1033.

Kupchan, S.M., Cassady, J.M., Bailey, J., Knox, J.R., 1965. Tumor inhibitors XII. Gaillardin, a new cytotoxic sesquiterpene lactone from Gaillardia pulchella. Journal of Pharmaceutical Sciences 54, 1703–1705.

Kupchan, S.M., Cassady, J.M., Kelsey, J.E., Schnoes, H.K., Smith, D.H., Burlingame, A.L., 1966. Structural Elucidation and High-Resolution Mass Spectrometry of Gaillardin, a New Cytotoxic Sesquiterpene Lactone. Journal of the American Chemical Society 88, 5292–5302.

Maruyama, M., Shibata, F., 1975. Stereochemistry of granilin isolated from Carpesium abrotanoides. Phytochemistry 14, 2247–2248.

Nikonova, L., Nikonov, G., 1972. Granilin — A new lactone from Inula grandis. Chemistry of Natural Compounds 8, 286–289.

Okhanov, V., Sheichenko, V., Miroshnikov, A., 1989. Structure of britannin. Use of two-dimensional 1H NMR spectroscopy. Chemistry of Natural Compounds 25, 672–676.

Park, E.J., Kim, J., 1998. Cytotoxic sesquiterpene lactones from Inula britannica. Planta Medica 64, 752–754.

Pesic, M., Markovic, J.Z., Jankovic, D., Kanazir, S., Markovic, I.D., Rakic, L., Ruzdijic, S., 2006. Induced resistance in the human non small cell lung carcinoma (NCI-H460) cell line in vitro by anticancer drugs. Journal of Chemotherapy 18, 66–73.

Podolski-Renić, A., Andelković, T., Banković, J., Tanić, N., Ruždijić, S., Pešić, M., 2011. The role of paclitaxel in the development and treatment of multidrug resistant cancer cell lines. Biomedicine & Pharmacotherapy 65, 345–353.

Qi, J.-L., Fu, Y., Shi, X.-W., Wu, Y.-B., Wang, Y.-Z., Zhang, D.-Q., Shi, Q.-W., 2008. Sesquiterpene Lactones and their Anti-Tumor Activity from the Flowers of Inula Britannica. Letters in Drug Design & Discovery 5, 433–436.

Rybalko, K., Sheichenko, V., Maslova, G., Kiseleva, E., Gubanov, I., 1968. Britannin — A lactone from Inula britannica. Chemistry of Natural Compounds 4, 215–215.

Serkerov, S., Mir-Babaev, N., 1988. Pulchellin C from Inula britannica. Chemistry of Natural Compounds 24, 752–753.

Skehan, P., Storeng, R., Scudiero, D., Monks, A., McMahon, J., Vistica, D., Warren, J.T., Bokesch, H., Kenney, S., Boyd, M.R., 1990. New colorimetric cytotoxicity assay for anticancer-drug screening. Journal of the National Cancer Institute 82, 1107–1112.

Vichnewski, W., Shuhama, I.K., Rasanske, R.C., Herz, W., 1976. Granilin and ivasperin from Ambrosia polystachya. 13C-NMR spectra of hydroxylated isoalantones. Phytochemistry 15, 1531–1532.

Yang, J.-L., Wang, R., Liu, L.-L., Shi, Y.-P., 2010. Sesquiterpenoids from Inula britannica. Planta Medica 77, 362–367.

Yoshioka, H., Mabry, T.J., Dennis, N., Herz, W., 1970. Constituents of Gaillardia species. IX. Structure and stereochemistry of pulchellin B, C, E, and F. The Journal of Organic Chemistry 35, 627–631.

Zhao, Y.-M., Zhang, M.-L., Shi, Q.-W., Kiyota, H., 2006. Chemical Constituents of Plants from the Genus Inula. Chemistry & Biodiversity 3, 371–384.

Zhou, B.-N., Bai, N.-S., Lin, L.-Z., Cordell, G.A., 1993. Sesquiterpene lactones from Inula britannica. Phytochemistry 34, 249–252.

Appendix Chapter 6

LC-MS

LC-MS with an Agilent 1100 series HPLC with a G1379A degasser, a G1312A binary pump, a G1367A WPALS (automated liquid sampler), a G1315B DAD detector, and a G1956 LC/MSD SL single quadropole mass spectrometer equipped with an atmospheric pressure chemical ionization probe (APCI) was used for initial mass determination. A 150 x 4.6 mm Luna 5 micron C18 (2) 100A column equipped with a guard column containing C18 4 x 3 mm cartridges was used for separation (Phenomenex Inc, Torrance, California, USA). Gradient elution with a flow of 0.5 mL/min consisted initially of 80% H_2O and 20% ACN which increased to 100% ACN in 20 min and remained at 100% ACN for 5 min. The DAD detector was set at 210 and 254 nm with a UV spectrum scan from 190-390 nm. Mass spectra were acquired in both positive and negative mode with a mass range of 50-500 amu and a fragmentor voltage of 150. The APCI spray chamber gas temperature was set to 350 °C, a vaporizer temperature of 325 °C, a drying gas flow rate of 5 L/min, and a nebulizer pressure of 40 psig. The VCap was set to 4000 V for positive scans and 3000 V for negative scans while the corona current was 5 µA for positive scans and 15 µA for negative scans.

LC-HRESIMS

High resolution mass spectrometry was performed on an LC-LTQ-Orbitrap FTMS system, (Thermo Scientific, Waltham, Massachusetts, USA) with an Accela HPLC, an Accela photodiode array detector, connected to a LTQ/Orbitrap hybrid mass spectrometer equipped with an electrospray (ESI) source. Chromatographic separation used a Phenomenex Luna C18(2) analytical column (150 x 2.0 mm, 3 µm particle size). Both H_2O and acetonitrile contained 0.1 % v/v formic acid, were run at a flow rate of 0.19 mL/min, and a column temperature of 40 °C. A linear gradient from 5 to 75% acetonitrile in 45 min was applied, which was followed by 15 min of washing and equilibration. FTMS full scans (*m/z* 100−1200) were recorded with a resolution of 60.000, whereas for MS^n scans a resolution of 15.000 was used. The FTMS was externally calibrated in negative mode using sodium formate clusters in the range *m/z* 150-1200 and automatic tuning was performed on *m/z* 384.93.

Typical NMR parameters

^{1}H-NMR: Solvent $CDCl_3$, Temperature 298.0, Pulse Sequence zg30, Experiment 1D, Number of Scans 128, Receiver Gain 181, Relaxation Delay 1.0000, Pulse Width 7.3000, Acquisition Time 3.1719, Spectrometer Frequency 500.13, Spectral Width 10330.6, Lowest Frequency -2090.8, Nucleus 1H, Acquired Size 32768, Spectral Size 65536; ^{1}H-^{1}H COSY: Parameter Value (f2, f1), Solvent $CDCl_3$, Temperature 298.0, Pulse Sequence cosygpqf, Experiment COSY, Number of Scans 4, Receiver Gain 256, Relaxation Delay 1.4869, Pulse Width 7.3000, Acquisition Time 0.2048, Spectrometer Frequency (500.13, 500.13), Spectral Width (5000.0, 5000.0),

Lowest Frequency (-263.4, -263.2), Nucleus (1H, 1H), Acquired Size (1024, 512), Spectral Size (1024, 1024); ^{13}C-APT: Solvent $CDCl_3$, Temperature 298.0, Pulse Sequence jmod, Experiment JMOD, Number of Scans 10240, Receiver Gain 23170, Relaxation Delay 2.0000, Pulse Width 9.5000, Acquisition Time 1.0912, Spectrometer Frequency 125.77, Spectral Width 30030.0, Lowest Frequency -2421.9, Nucleus 13C, Acquired Size 32768, Spectral Size 65536; HSQC: Parameter Value (f2, f1), Solvent $CDCl_3$, Temperature 298.1, Pulse Sequence hsqcetgp, Experiment HSQC, Number of Scans 4, Receiver Gain 20642, Relaxation Delay 1.5000, Pulse Width 7.3000, Acquisition Time 0.4096, Spectrometer Frequency (500.13, 125.77), Spectral Width (5000.0, 20833.3), Lowest Frequency (-312.0, -1044.5), Nucleus (1H, 13C), Acquired Size (2048, 512), Spectral Size (2048, 2048); HMBC: Parameter Value (f2, f1), Solvent $CDCl_3$, Temperature 298.0, Pulse Sequence hmbcgplpndqf, Experiment HMBC, Number of Scans 4, Receiver Gain 23170, Relaxation Delay 1.5000, Pulse Width 7.3000, Acquisition Time 0.2925, Spectrometer Frequency (500.13, 125.77), Spectral Width (7002.8, 26411.8), Lowest Frequency (-1315.3, -642.0), Nucleus (1H, 13C), Acquired Size (2048, 512), Spectral Size (2048, 2048); NOESY: Parameter Value (f2, f1), Solvent $CDCl_3$, Temperature 298.0, Pulse Sequence noesygpphpp, Experiment NOESY, Number of Scans 4, Receiver Gain 1626, Relaxation Delay 1.5000, Pulse Width 7.3000, Acquisition Time 0.2048, Spectrometer Frequency (500.13, 500.13), Spectral Width (5000.0, 5000.0), Lowest Frequency (-163.0, -163.5), Nucleus (1H, 1H), Acquired Size (1024, 400), Spectral Size (1024, 1024).

Gaillardin (**8**): white needles; $[\alpha]^{20}_{D}$ -2.1 (*c* 0.09, $CHCl_3$); APCIMS *m/z* 307 $[M + H]^+$ (35), 305 $[M - H]^-$ (5); HRESIMS *m/z* 307.1543 $[M + H]^+$ (calcd for $C_{17}H_{23}O_5$ 307.15455).

Britannin (**9**): clear crystals; $[\alpha]^{20}_{D}$ -15.1 (*c* 0.11, $CHCl_3$); APCIMS *m/z* 367 $[M + H]^+$ (100), 365 $[M - H]^-$ (100); HRESIMS *m/z* 367.1755 $[M + H]^+$ (calcd for $C_{19}H_{27}O_7$ 367.1757).

Table A1. ^{1}H-NMR and COSY data for compounds **8** and **9**

	8			**9**	
^{1}H	δ_H (J in Hz)	COSY	^{1}H	δ_H (J in Hz)	COSY
			1α	1.94, m*	2β
1β	2.46, br d	2β, 5, 9, 14			
2β	5.34, m	1, 3α,β	2β	4.9, br dd	1, 3α
3α	2.03, d (15.4)	3β	3α	2.07, m	2, 3β, 4
3β	1.93, dd (15.4, 4)	2β, 3α	3β	1.83, m	3α, 4
			4α	4.12, ddd (11.5, 8.2, 3.5)	3α,β, OH
5α	2.17, td (12.2, 3)	1, 6α,β			
6α	2.56, m	5, 6β, 7			
6β	1.41, m	5, 6α, 7	6β	5.06, d (8.3)	7
7	2.62, m	6α,β 8, 13a,b	7	3.03, m	6, 8, 13a,b
8	4.5, br d	7, 9, 14	8	4.53, m	7, 9α,β
9	5.94, br s	1, 8, 14	9α	2.45, m	8, 9β, 10
			9β	1.44, dt	8, 9α, 10
			10β	1.91, m*	9α,β, 14
13a	6.23, d (3.3)	7	13a	6.17, d (3.5)	7
13b	5.55, d (3.1)	7	13b	5.37, d (3.2)	7
14	1.83, br s		14	0.99, d (5.9)	10
15	1.26, s		15	1.02, s	
Ac	2.11, s		Ac	2.05, s	
			Ac	2.25, s	
			OH	2.38, d (3.5)	4

*Overlap

Figure A1. ^{1}H-NMR of 14-(3-methylpentanoyl)-6-deoxybritannilactone (**1**) ($CDCl_3$)

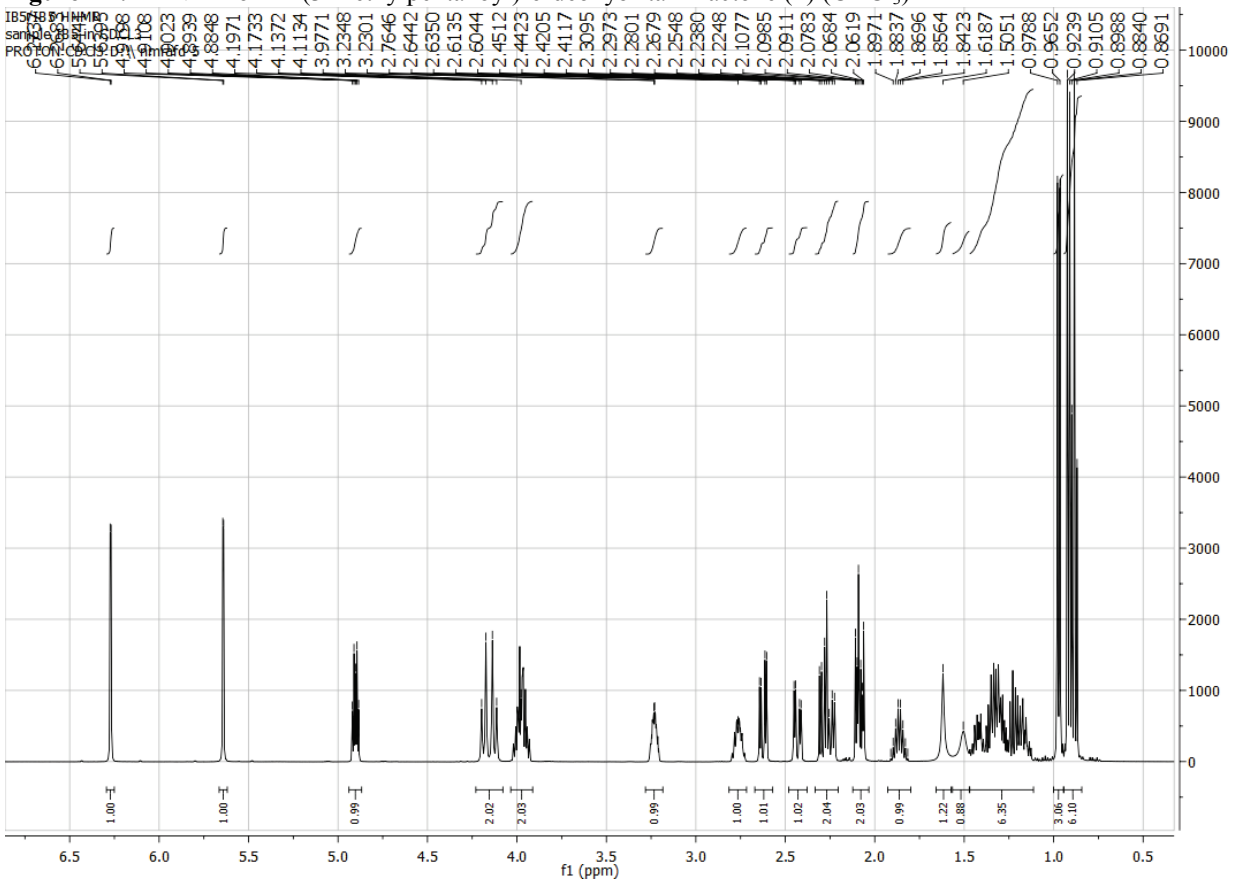

Figure A2. ^{1}H-NMR of 14-(3-methylbutanoyl)-6-deoxybritannilactone (**2**) ($CDCl_3$)

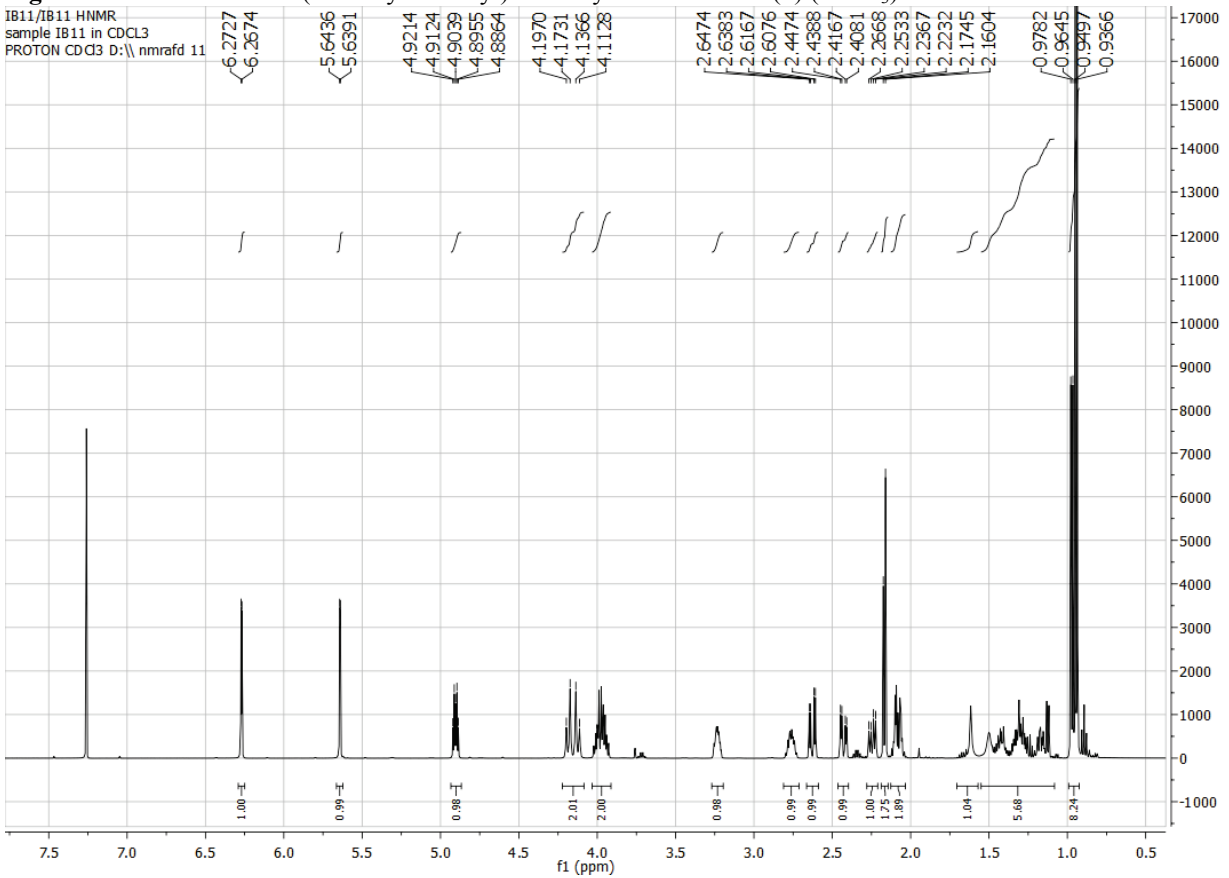

Figure A3. ^{1}H-NMR of 14-(2-methylpropanoyl)-6-deoxybritannilactone (**3**) ($CDCl_3$)

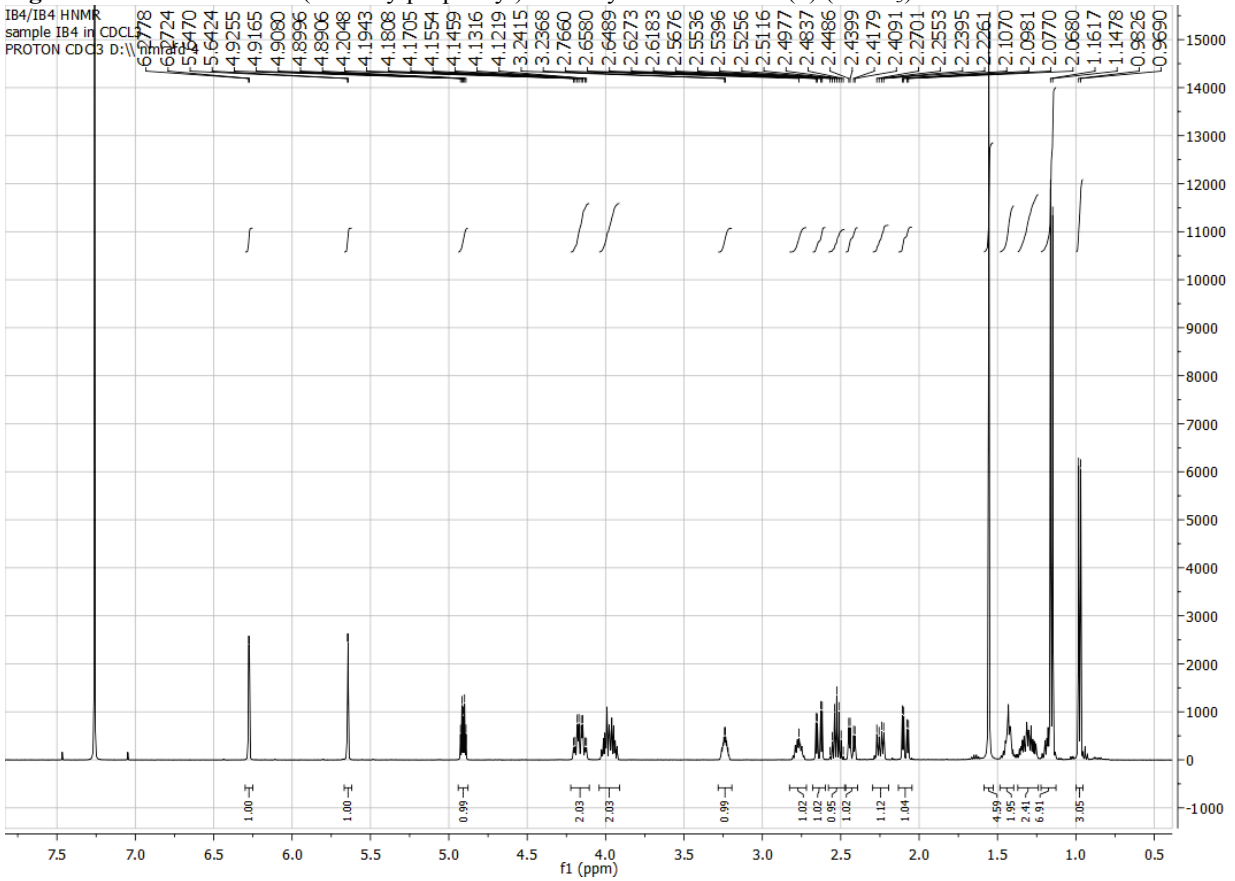

Figure A4. [1]H-NMR of 1,3-Epi-Granilin (**4**) (MeOD)

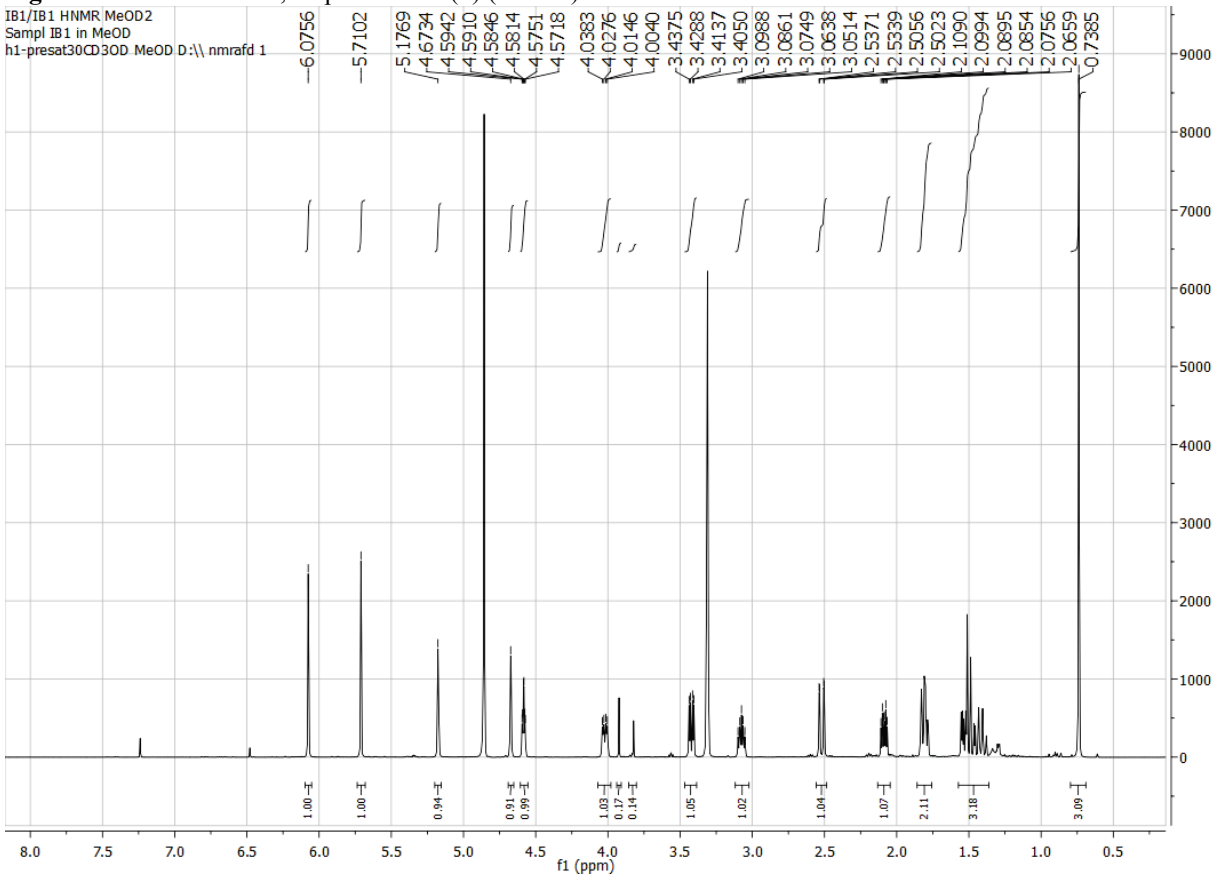

Figure A5. ^{1}H-NMR of 11,13-Dihydro-inuchinenolide B (**5**) ($CDCl_3$)

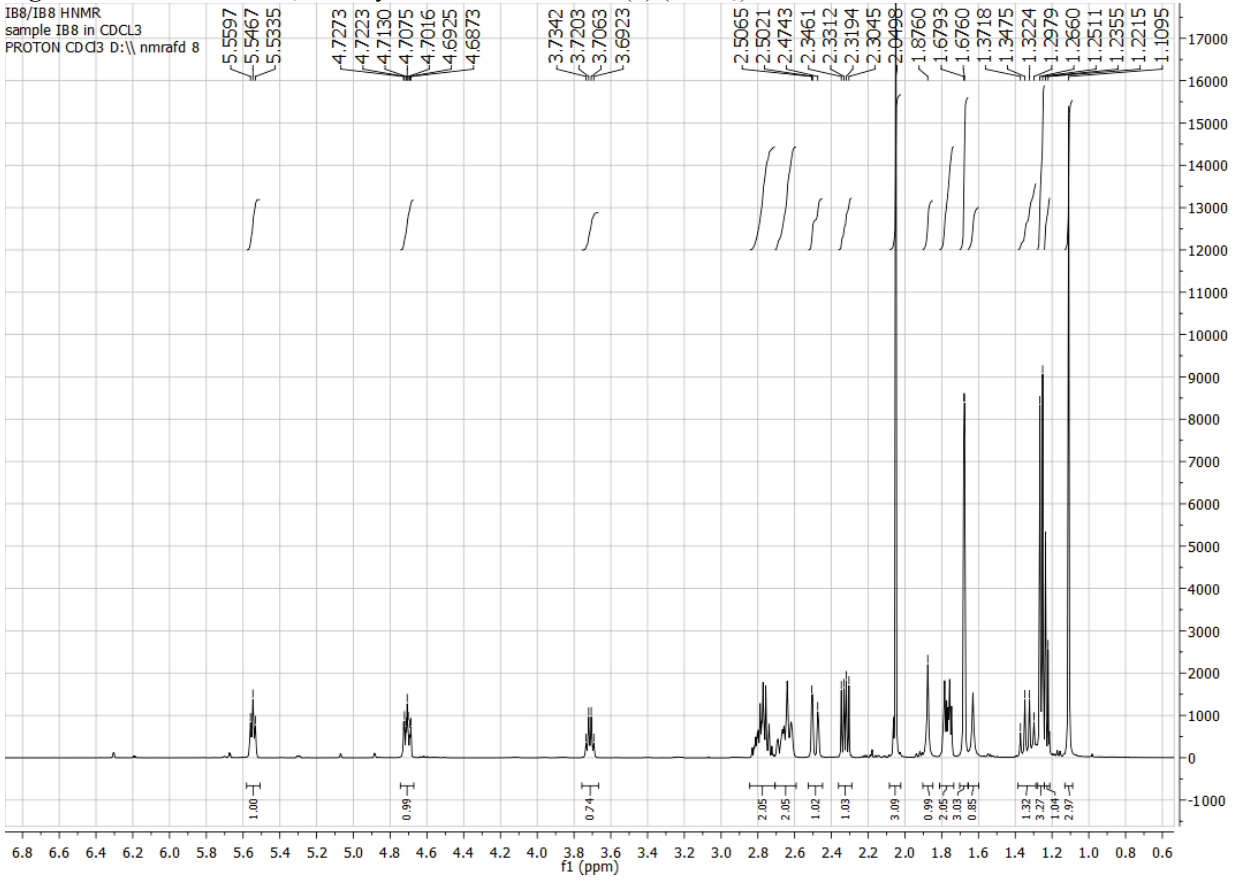

Figure A6. ^{1}H-NMR of Pulchellin C (**6**) (MeOD)

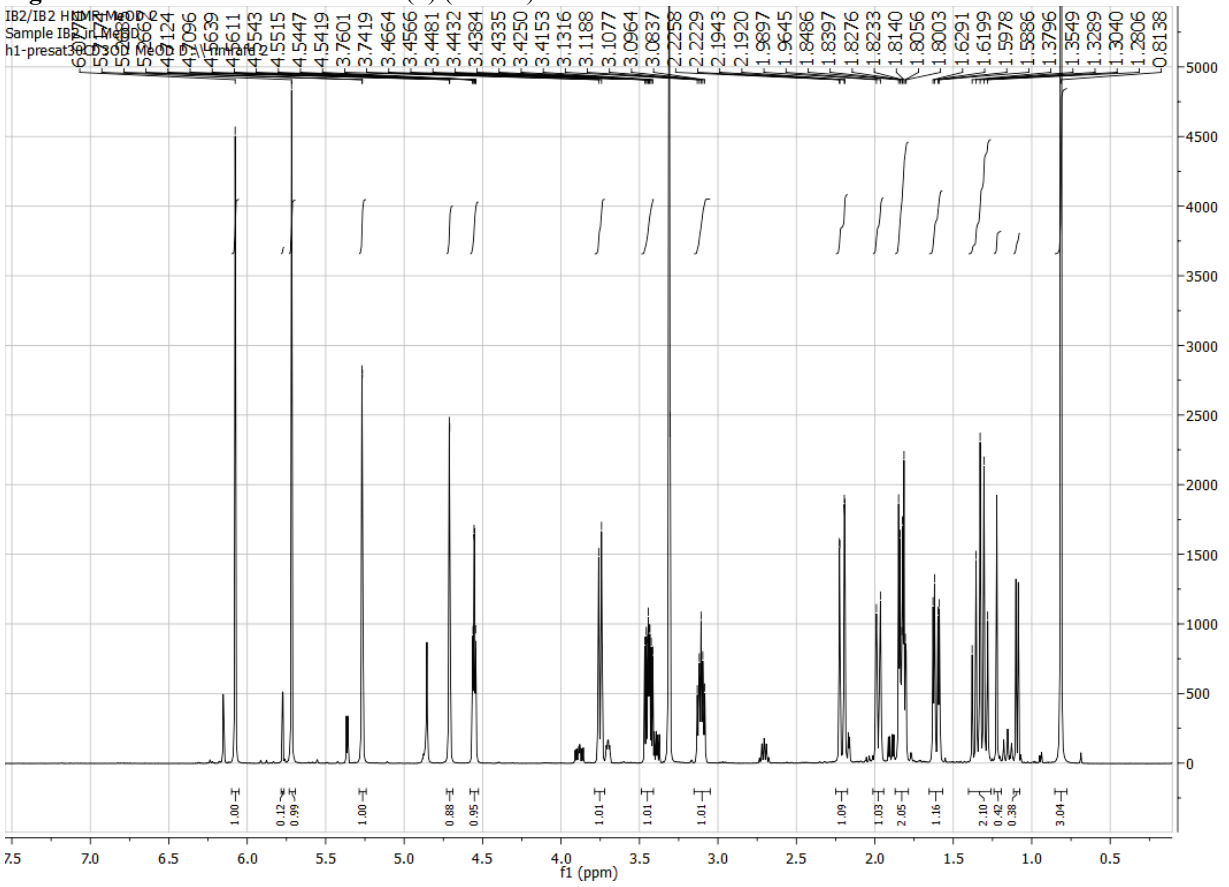

Figure A7. ^{1}H-NMR of 6-Deacetylbritanin (**7**) ($CDCl_3$)

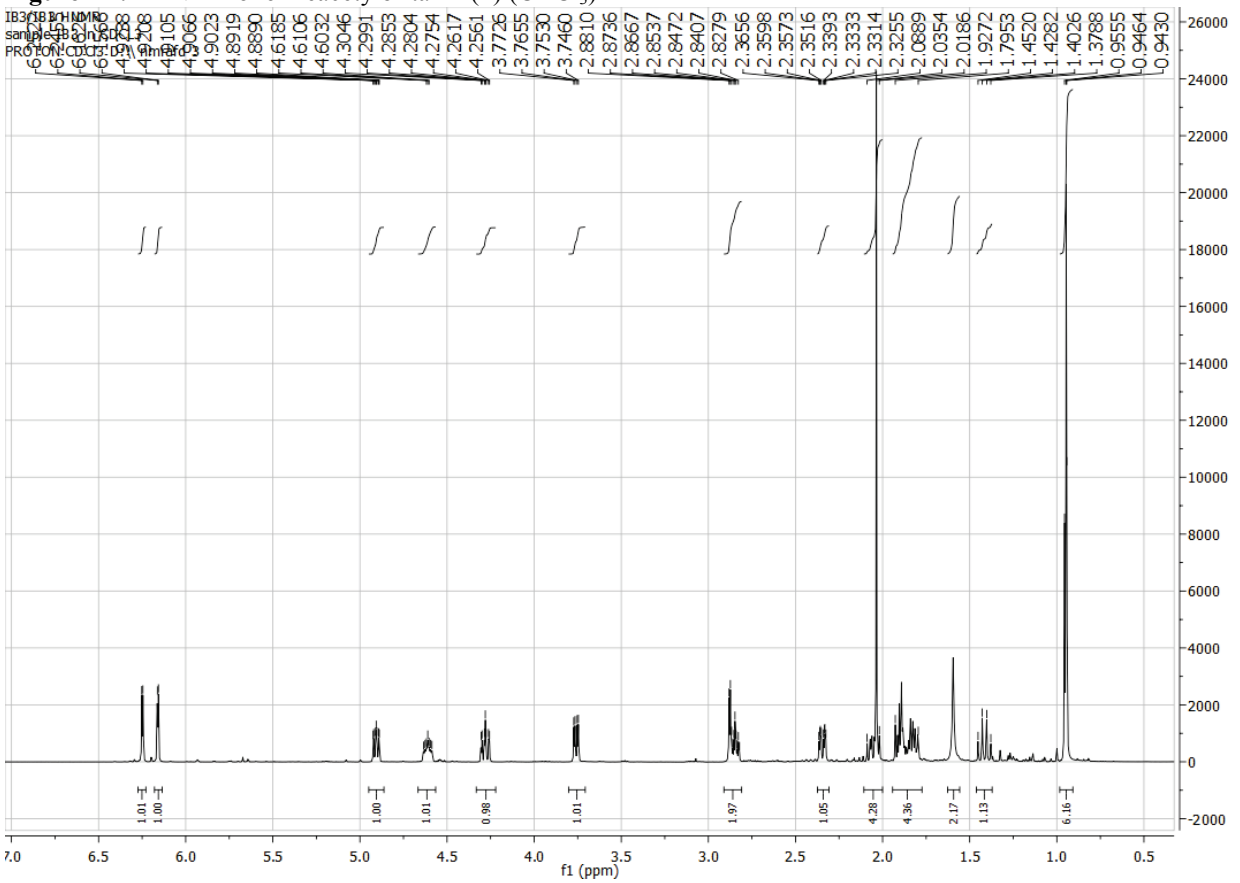

Figure A8. ^{1}H-NMR of Gaillardin (**8**) ($CDCl_3$)

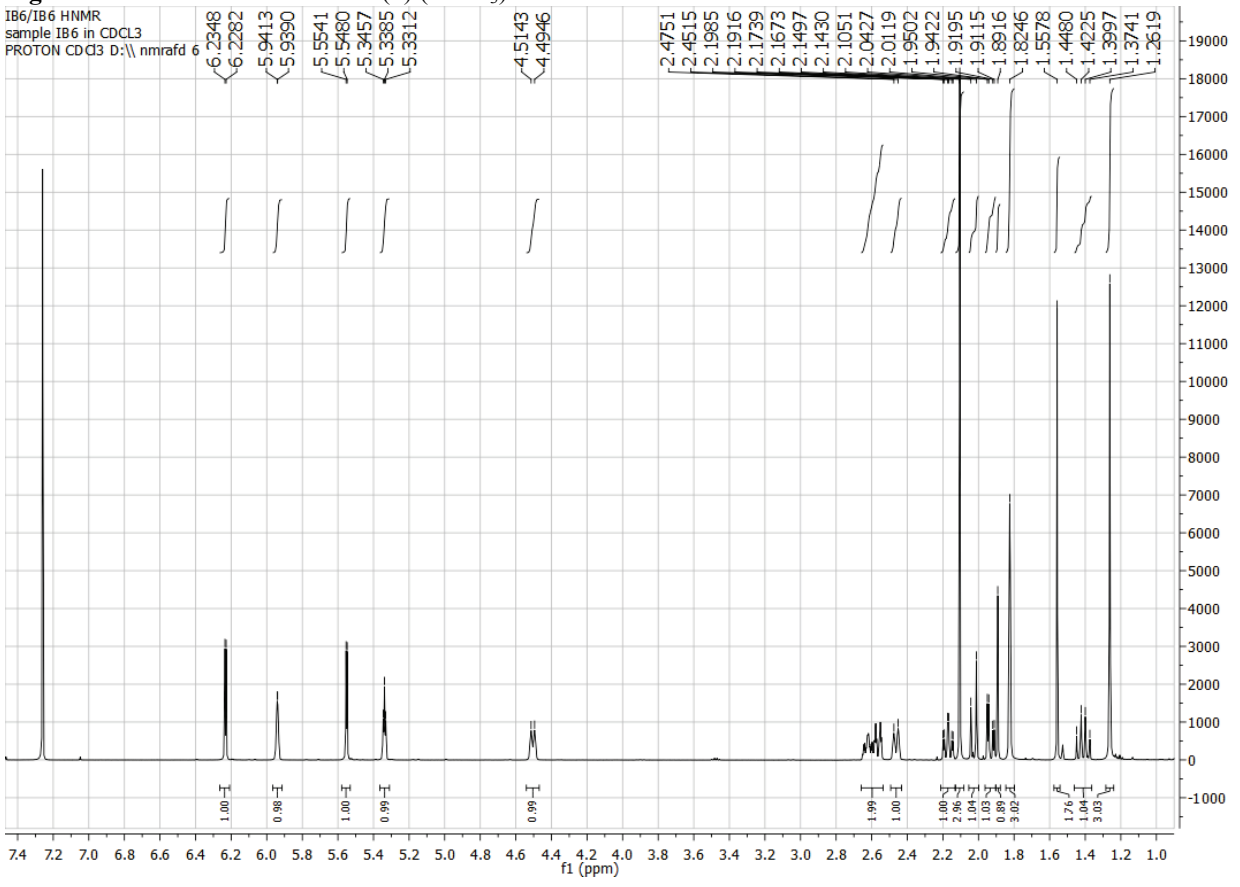

Figure A9. ^{1}H-NMR of Britannin (**9**) ($CDCl_3$)

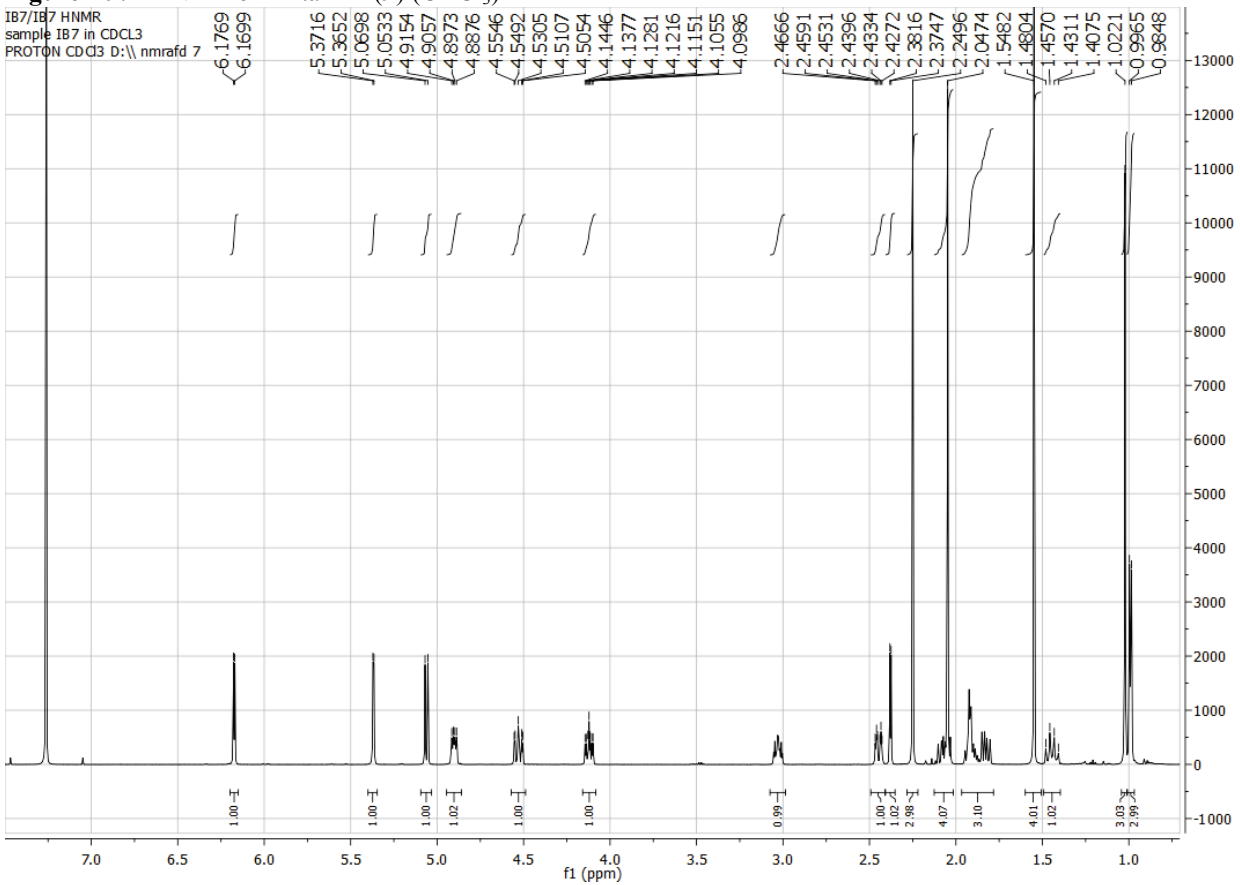

Figure A10. ^{1}H-NMR of 4H-Tomentosin (**10**) ($CDCl_3$)

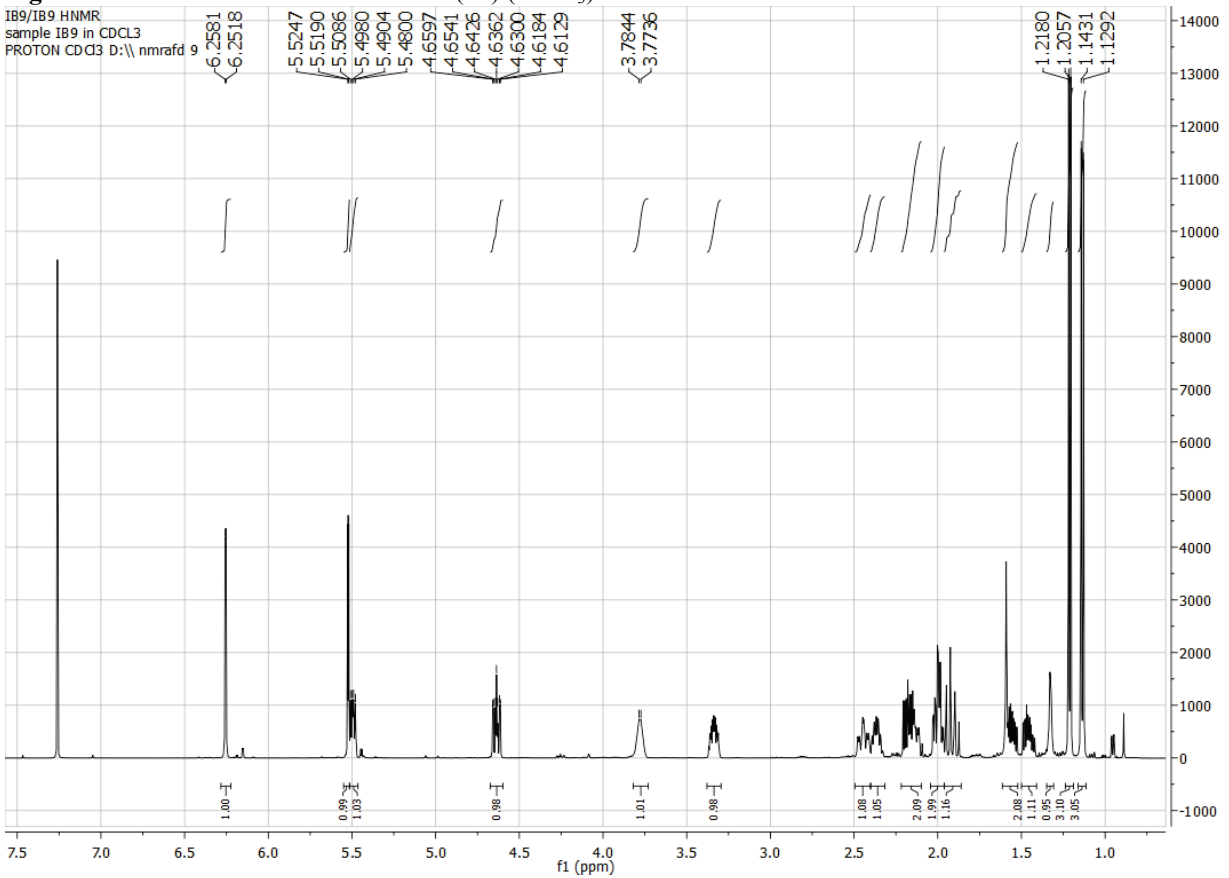

Chapter 7

Structure activity relationship of phenolic diterpenes from *Salvia officinalis* as activators of the antioxidant response element

Justin T Fischedick[a,b,*], Miranda Standiford[c], Delinda A. Johnson[c], Jeffrey A. Johnson[c]

[a]*PRISNA BV, Einsteinweg 55, 2300 RA Leiden, Netherlands*
[b]*Natural Products Laboratory, Institute of Biology, Leiden University, 2300 RA Leiden, The Netherlands*
[c]*Division of Pharmaceutical Sciences, School of Pharmacy, University of Wisconsin, Madison, WI, USA*

Abstract

Nuclear factor E2-related factor 2 is a transcription factor known to activate cytoprotective genes which may be useful in the treatment of neurodegenerative disease. In order to better understand the structure activity relationship of phenolic diterpenes from *Salvia officinalis* L., we isolated carnosic acid, carnosol, epirosmanol, rosmanol, 12-methoxy-carnosic acid, sageone, and carnosaldehyde using polyamide column, centrifugal partition chromatography, and semi-preparative high performance liquid chromatography. Isolated compounds were screened *in-vitro* for their ability to active the antioxidant response element and general cellular toxicity using mouse primary cortical cultures. All compounds except 12-methoxy-carnosic acid were able to activate the antioxidant response element. Rosmanol was able to dose dependently activate the antioxidant response element without cellular toxicity at the doses tested (12.5, 25, and 50 μM) and thus represents an interesting compound for further studies against neurodegenerative disease.

Submitted as part of larger publication: Bioorganic and Medicinal Chemistry

Introduction

Ethnobotanical investigations of English herbal texts, Indian Ayurvedic medicine, and Chinese traditional medicine report that *S. officinalis* has memory enhancing properties (Perry et al., 1999). *Rosmarinus officinalis* also has a reputation for treatment of nervous system related disorders in European traditional medicine (Heinrich et al., 2006). The essential oil of *Salvia* species including *S. officinalis*, *S. fruticosa*, and *S. lavandulaefolia* displays acetylcholinesterase inhibitory activities (Savelev et al., 2004), which may explain their effects on memory in healthy volunteers (Moss et al., 2010) and mild improvements in cognition shown in a small open labeled trial on patients with Alzheimer's disease (Perry et al., 2003). Extracts of *S. officinalis* have also been shown to improve memory and attention in older (> 65 years of age) healthy volunteers (Scholey et al., 2008).

A number of *Salvia* species and *R. officinalis* are well known to produce the phenolic diterpenes carnosic acid (**1)** and carnosol (**2**) (Abreu et al., 2008). Compounds **1** and **2** are strong antioxidants possessing anti-microbial, anti-cancer, anti-inflammatory, and lipid lowering properties (Bonito et al., 2011; Johnson, 2011). Recently a number of investigations have demonstrated that these compounds also exhibit biological activity which may be useful against neurodegenerative diseases. Protective effects of **2** on dopaminergic neuronal cell lines against rotenone induced toxicity and sodium nitroprusside toxicity in glial cells have been reported (Kim et al., 2006; Kim et al., 2010). Carnosic acid protects against glutamate toxicity in primary rat cortical cultures and against cerebral ischemia in mice by activating the nuclear factor E2-related factor 2 (Nrf2) / Kelch-like ECH-associated protein 1 (Keap1) pathway (Satoh et al., 2008a).

Nrf2 is a transcription factor known to induce a promoter sequence called the antioxidant response element (ARE) which leads to expression of various cytoprotective and antioxidant enzymes such as NQO1. Nrf2 localization and degradation is regulated by its cytoplasmic repressor protein Keap1. In conditions of oxidative stress or disruption by small molecules Nrf2 is freed from Keap1 and enters the nucleus activating the ARE (Itoh et al., 2004). Since many neurodegenerative diseases may be caused or exacerbated by oxidative stress, activation of the ARE is a potential therapeutic strategy (de Vries et al., 2008; Calkins et al., 2009).

Little information is available on the structure activity relationship of phenolic diterpenes for Nrf2/Keap1 activation. Comparisons have been made between **1**, **2**, and a series of alkyl-ester derivatives at carbon 11 and 12 of **1** in HT22 cell lines (Satoh et al., 2008b; Tamaki et al., 2010). Therefore in order to gain further insights into the structure activity of phenolic diterpenes for Nrf2/ARE activation we isolated **1**, **2**, epirosmanol (**3**), rosmanol (**4**), 12-methoxy-carnosic acid (**5**), sageone (**6**), and carnosaldehyde (**7**) from *S. officinalis* (Figure 1). Compounds were screened for Nrf2/ARE activation using transgenic primary mouse cortical cultures modified to express human placental alkaline phosphatase (hPAP) as a reporter gene for ARE. Potential toxicity of the isolated compounds was tested against the cultures using the 3-(4,5-dimethylthiazol-2-

yl)-5-(3-carboxymethoxyphenyl)-2-(4-sulfophenyl) 2H tetrazolium inner salt (MTS) assay.

Figure 1. Chemical structures of **1**-**7**

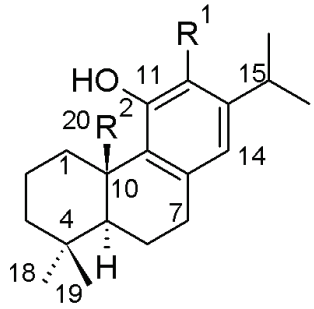

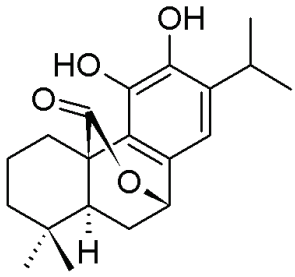

1 $R^1 = OH, R^2 = COOH$ **2**

5 $R^1 = OCH_3, R^2 = COOH$

7 $R^1 = OH, R^2 = CHO$

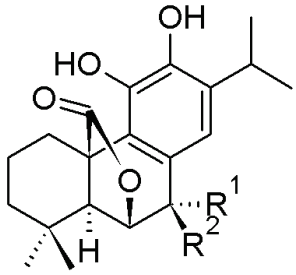

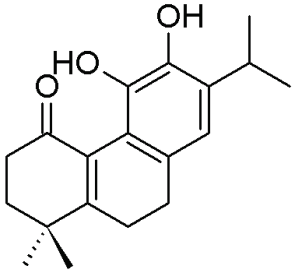

3 $R^1 = H, R^2 = OH$ **6**

4 $R^1 = OH, R^2 = H$

Materials and Methods

Plant material

Dried aerial parts of *Salvia officinalis* were purchased from De Groene Luifel BV, Sluis, Netherlands. A voucher specimen was deposited in the economic botany collection of the National Herbarium Nederland in Leiden under the following barcode: LamiaceaeSalviaofficinalisL.L 0991403J. FischedickNo. 192010.

Extraction

Plant material (100 g) was extracted with 2 L acetone for 2 hours to yield 9 g crude extract. The extract was extracted 2 times with 100 mL warm hexane and hexane solution added to polyamide column (100 g). The column was eluted with additional 300 mL of hexane to give 2 g hexane fraction and further eluted with 650 mL MeOH to give 2 g MeOH fraction.

CPC

The MeOH and hexane fractions were further purified using a Fast Centrifugal Partition Chromatograph with a 1 L internal volume rotor (Kromaton Technologies, Angers, France). The MeOH fraction was separated by using a two phase solvent system composed of 5 L heptane: acetone: H_2O (3: 5: 2). The MeOH fraction was dissolved in 30 mL 1:1 mixture of upper and lower layers of the solvent system. The CPC system was filled with the lower layer and the phase held in place with a rotor speed of 1000 rpm while the upper layer was pumped into the CPC at a flow rate of 10 mL/min in ascending mode. Equilibrium between the layers was reached when the upper layer began to elute from the CPC (lower layer displaced = 230 mL), after which the sample was immediately injected. After 250 mL of the mobile phase eluted 120 fractions (10 mL each) were collected. The system was then rinsed with 1 L of the remaining lower layer and the eluent collected as an additional rinse fraction. Pressure was stable between 63-65 bar throughout the run. The hexane fraction was separated using a 2 phase solvent system composed of 2.5: 6: 1.5 heptane: acetone: H_2O. All other CPC conditions were the same as for the MeOH fraction except the volume of the lower layer displaced during equilibration was 260 mL, the pressure 48 bar, and 80 (10 mL) fractions were collected. Fractions were analyzed by silica gel TLC (hexane: ethyl acetate: acetic acid, 7: 3: 0.1, vanillin/sulfuric acid reagent) and combined based on similarity of profile. Combined fractions from CPC experiment on MeOH fraction are referred to as CPC-M $Fr_{\#}$ and fractions from CPC on hexane fraction as CPC-H $Fr_{\#}$.

Semi-preparative HPLC

Final purification was performed on a Shimadzu semi-preparative HPLC. A Luna C18 (2) 100 A 5 micron 250 x 10 mm column was used for separations (Phenomenex, Torrance, CA, USA). H_2O (A) and MeOH (B) were used as mobile phase. Flow rates were 5 mL/min, 10 mL fractions were collected, and UV detector set to 230 and 280 nm. Samples were injected manually using a Rheodyne injector equipped with a 5 mL injection loop.

CPC-M $Fr_{40\text{-}75}$ (660 mg) was dissolved in 10 mL 70% aqueous MeOH and run twice using gradient from 70% B to 85% B in 60 min. Fractions 5, 8-15, and 18-20 were separately combined and MeOH removed under reduced pressure at 40 °C. Combined fractions were then dissolved in 100 mL H_2O and 150 mL EtOAc. The EtOAc layer was collected and solvent removed to yield 12.6 mg **2** from fraction 5, 506.7 mg **1** from fractions 8-15, and 31.4 mg **5** from fractions 18-20. CPC-M rinse

fraction (242 mg) was purified using gradient from 50% B to 100% B in 120 min. Solvent was removed from fractions 7, 9, and 24-25 to yield 2.1 mg **3**, 2.6 mg **4**, and 20.3 mg **2** respectively. CPC-H Fr_{26-40} (164 mg) was dissolved in 5 mL 70% aqueous MeOH and run with gradient from 70% B to 100% B in 120 min. Fractions 9-10 yielded 11.2 mg **6** and fractions 17-18 yielded 5.8 mg **7**. CPC-H Fr_{41-80} (50 mg) was purified under the same conditions as Fr_{26-40} to yield an additional 1.4 mg **6**.

Structure elucidation

The structure of isolated compounds was determined by ^{1}H-NMR and COSY on a Bruker DMX 500 MHz NMR (Karlsruhe, Germany). An Agilent single quadropole mass spectrometer equipped with an atmospheric pressure chemical ionization probe (APCI) was used for mass confirmation. A 150 x 4.6 mm Luna 5 micron C18 (2) 100A column was used for separation (Phenomenex Inc). Solvent system was composed of MeOH and H_2O plus 0.1% formic acid. The flow rate was 0.5 mL/min. Gradient of 70% MeOH to 100% MeOH in 20 min with 10 min hold at 100% MeOH was used. Mass spectra were acquired in both positive and negative mode with a mass range of 50-500 amu. APCI spray chamber gas temperature was set to 350 °C, a vaporizer temperature of 325 °C, a drying gas flow rate of 5 L/min, and a nebulizer pressure of 40 psig. The VCap was set to 4000 V for positive scans and negative scans while the corona current was 5 µA for positive scans and 15 µA for negative scans.

Cell cultures

Primary cortical neuronal cultures were derived from ARE-hPAP reporter mice as previously described (Johnson et al., 2002; Kraft et al., 2004). In brief cortices from E15 mouse pups were pooled in 10 mL ice-cold Ca^{2+} and Mg^{2+} free HBSS (Life Technologies, Carlsbad, CA, USA). Tissue was then minced, centrifuged, and digested in 0.05% trypsin containing no EDTA in HBSS for 15 min at 37 °C. Cells were rinsed 3 times with HBSS following digestion. Then cells were washed with CEMEM (minimum essential media with Earle's salts); (Life Technologies) 2 mM glutamine, 1% penicillin/streptomycin, 10% heat inactivated fetal bovine serum, and 10% horse serum (Atlanta Biologicals, Inc., Lawrenceville, Georgia, USA). Cells were triturated to a single-cell suspension and strained through a 70 µM cell strainer (BD Biosciences, San Jose, California, USA). Cells were counted, assayed for viability using trypan blue, and plated on poly-D-lysine coated plates at a density of 3 x 105 cell/cm^2. Cells were kept in CEMEM for 45 min, after which medium was changed with CEMEM. After two days, medium was changed from CEMEM to NBM (Neurobasal media; Life Technologies), supplemented with B27 with antioxidants, and 2 mM glutamine. These mixed cultures (~ 40% astrocytes and 60% neurons) were incubated at 37 °C in a tri-gas incubator with 5% O_2, 5% CO_2, and 90% N_2.

Bioassay

After 6 days in culture compounds were dissolved in 100% DMSO (final concentration DMSO 0.1%) and administered to cells for 48 hours. After 48 hours, Nrf2

activation was determined by measuring for hPAP activity as previously described (Kraft et al., 2004). In brief, cells were lysed in TMNC lysis buffer (50 mM Tris, 5 mM MgCl2, 100 mM NaCl, 1% 3-[(3-cholamidopropyl)dimethylammonio]-1-propanesulfonate (CHAPS)) and freeze-thawed at -20 ºC. To inactivate endogenous alkaline phosphatase activity extracts were incubated with 200 mM diethanolamine (DEA) buffer at 65 ºC. The hPAP activity was quantified in 200 mM DEA with 0.8 mM CSPD ((disodium 3-(4-methoxyspiro (1,2-dioxetane-3,2'-(5'-chloro)tricycle(3.3.1.1 ^{3,7})decan)-4-yl)phenyl phosphate) (Life technologies), 2x Emerald, and 5 mM $MgCl_2$). Using one second intergration luminescence was measured on a Berthold Orion microplate luminometer (Berthold Technologies GmbH & Co., Bad Wildbad, Germany). Baseline signals from hPAP negative control culture samples (n = 5 for each compound) were subtracted from all values. Cell viability was assayed using the MTS assay following the manufacturer's suggested protocol (Promega, Madison, WI, USA).

Data analysis

All data are represented as mean ± SEM (n = 5). Statistical analysis was performed using one-way ANOVA followed by Newman-Keuls multiple comparison (GraphPad Prism, version 4). A P value < 0.05 was considered statistically significant.

Results and Discussion

Isolation

Phenolic diterpenes **1**-**7** were isolated from an acetone extract of *S. officinalis* by first partitioning hexane soluble material over polyamide, followed by centrifugal partition chromatography, and finally with reverse phased semi-preparative HPLC. Isolated compounds were identified by comparison of ^{1}H-NMR with literature, confirmed with COSY, and LC-MS (Pukalskas et al., 2005; Cuvelier et al., 1994; Tada et al., 1994). Compound **7** is reported in *S. officinalis* for the first time. All compounds were > 95% pure, except **7** (91%) according to HPLC at 230 nm. Detailed structural data is available in the appendix.

Bioassay hPAP

The hPAP expressing primary cortical cultures used in this study have been previously validated as a model system for studying activation of the Nrf2/ARE pathway (Johnson et al., 2002). The positive control *tert*-Butylhydroquinone (tBHQ) has been demonstrated to show Nrf2/ARE dependant neuroprotective effects on such cultures (Kraft et al., 2004). Results of hPAP assays are expressed as the fold increase in hPAP activity over basal levels (Figure 2). The entire hPAP and MTS assay were performed twice with two separate batches of primary cortical cultures in order to understand batch to batch variation in activity. In general the trend in hPAP activity was the same between batches. However in the first batch cells appeared more responsive towards hPAP activation compared with the second batch. This observation could be the result of differences in cell density or ratio of cell types between batches.

Figure 2. Fold activation of hPAP levels (compounds **1-7)**. Top first batch, bottom second batch.

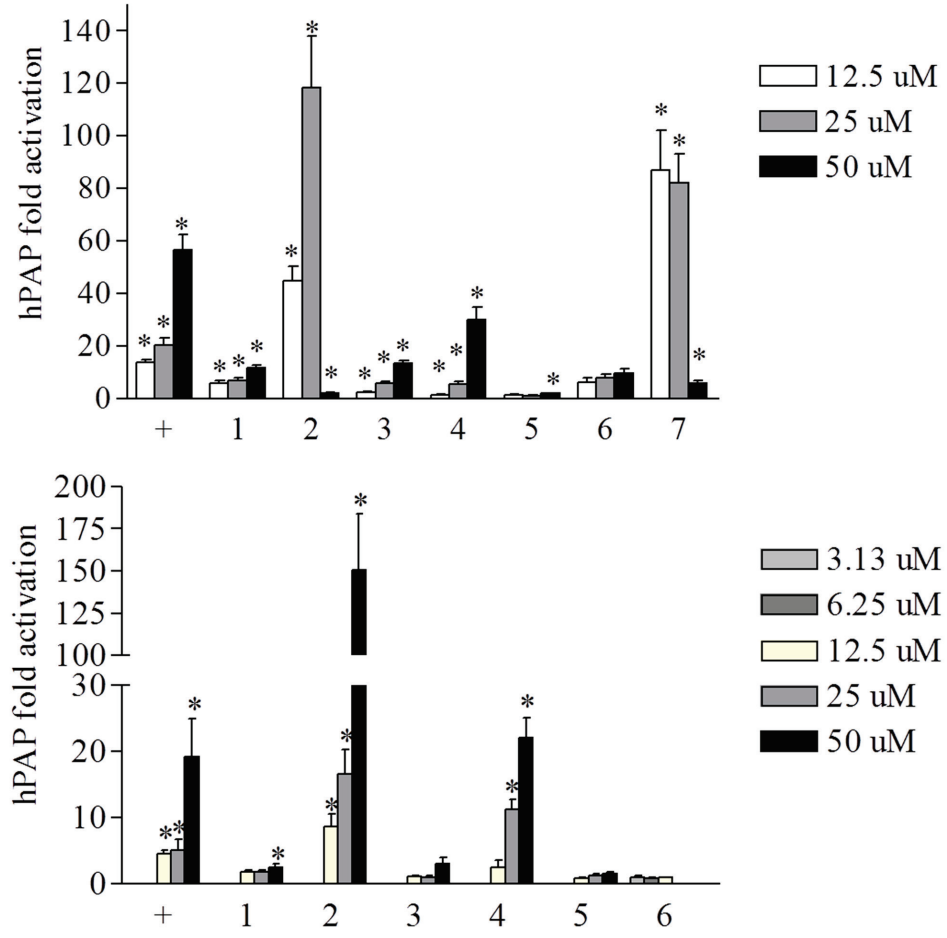

Compounds **2** and **7** were the most potent activators in both hPAP assays (Figure 2). In the first assay, **2** at 25 μM showed > 100 fold increase in hPAP activity and in the second assay at 50 μM > 100 fold increase. Compound **7** had similar levels of hPAP activity at 12.5 and 25 μM. A sharp decrease in hPAP activity was observed at 50 μM for **2** and **7** in the first experiment. Due to poor stability of **7** we were unable to assay this compound in the second batch of cultures. Compound **4** had a similar pattern of hPAP activation as the positive control, tBHQ in both assays. Compounds **1** and **3** had similar and weak patterns of hPAP activation while **5** and **6** were inactive.

Figure 3. Cell viability % (compounds **1**-**7**). Top first batch, bottom second batch.

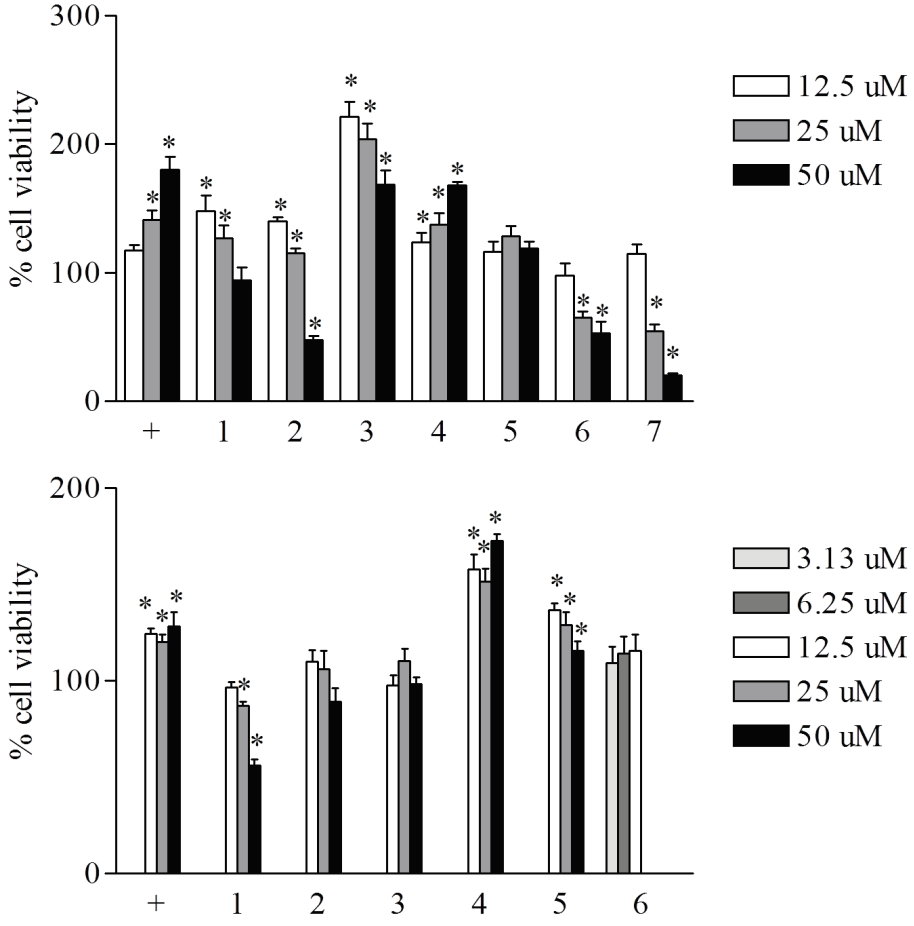

Bioassay MTS

Results from the MTS assay are expressed as % cell viability (Figure 3). Significant decrease in cell viability < 100% indicates cellular toxicity while > 100% indicates cell proliferation. Compounds **6** and **7** showed dose dependent decreases in cell viability in the first assay. In the second hPAP and MTS assay **6** was tested at lower doses, 3.13 and 6.25 μM. Although toxicity went away no significant hPAP activity was observed. Compound **2** caused a significant decrease in cell viability to 48% at 50 μM in the first culture batch (Figure 3). The sharp decreases in hPAP activity observed in compounds **2** and **7** at 50 μM in the first batch of cultures are explained by the MTS results demonstrating significant toxicity at such doses. Significant decreases in cell

viability were observed at 25 and 50 μM of **1** in the second batch while a non-significant decrease in viability (94%) at 50 μM was observed in the first batch. Therefore **1** and **2** at lower doses tended to increase or have no effect on cell proliferation while at higher doses decrease cell proliferation or cause toxicity. Compounds **6** and **7** were generally cytotoxic according to MTS results. Both the positive control tBHQ and **4** consistently had significant > 100% cell viability which tended to increase with dosage suggesting the compounds were inducing cell proliferation. Compound **3** was non-toxic in both assays and induced a strong increase in cell viability which decreased at higher doses in the first assay. This effect was not observed in the second assay for **3**. The hPAP inactive compound **5** had a similar pattern of activity as **3** in the MTS assay either dose dependently decreasing cell proliferation or having no effect on cell viability.

Structure activity relationship

Previous studies suggested that the mechanism of action of **1** to activate the Nrf2/ARE pathway was due to the catechol moiety initially acting as an antioxidant against reactive oxygen species. Upon oxidation **1** converts into an ortho quinone whose C-14 position can act as an electrophile, reacting with biological thiols such as the cysteine residues of Keap1 thus activating Nrf2 (Satoh et al., 2008a). Another study demonstrated that ester derivatives at both the C-11 and C-12 eliminated activity of **1** (Satoh et al., 2008b). In our experiments a methoxy group at position 12 as in **5** eliminated activity in the hPAP assay, confirming the importance of the catechol moiety for Nrf2/ARE activation. The lack of hPAP activity of **6** could be due to conjugation of the aromatic ring with the 1-carbonyl-5,10-diene functionality which would likely alter the oxidative products formed.

Replacement of the carboxylic acid functionality in **1** with an aldehyde as in **7** caused a dramatic increase in hPAP activity although this was accompanied by dose dependent loss in cell viability. Carnosol and **4** were also much more active than **1** in the hPAP assay. Compound **3**, a stereoisomer of **4**, had weaker activity suggesting that the stereochemistry of the hydroxyl group at position 7 is important. Together these results suggest that an electronegative functionality at the C-7 position can increase Nrf2/ARE activation compared to **1**. However, depending on the functionality it can either increase cell proliferation with higher doses as in **4** or decrease cell viability with higher doses as in **2**. It has been reported that **1** can induce nerve growth factor in human astrocytes and glioblastoma cells regulated by Nrf2 which may explain the potential increases in cell proliferation observed in our experiments (Mimura et al., 2011; Yoshida et al., 2011). A previous comparison of Nrf2/ARE mediated neuroprotection between **1** and **2** in HT22 cells demonstrated more potent activity of **1** compared with **2** (Satoh et al., 2008b). The differences in results are most likely due to differences in the cellular models used. Primary cortical cultures contain a mixture of astrocytes and neurons which are known to display differing patterns of Nrf2/ARE activation (Kraft et al., 2004). Immortalized neuronal cell lines such as HT22 may therefore be of limited use for studying phenolic diterpene mediated Nrf2/ARE activation.

Conclusions

In conclusion phenolic diterpenes isolated from *S. officinalis* can activate the Nrf/ARE pathway in mouse primary cortical cultures with varied potency. The balance between loss of cell viability and Nrf/ARE activation needs to be carefully considered when studying these compounds as drugs against neurodegenerative diseases. Compounds **1**, **2**, and **7** had a narrow window between doses that activated Nrf/ARE and doses that reduced cell viability. In contrast **4** showed dose dependent increases in Nrf2/ARE activity accompanied by dose dependent increases in cellular proliferation up to 50 μM. These results suggest that **4** is a compound worth further exploration as an agent against neurodegeneration. Finally our results in comparison with literature suggest that different cellular models of Nrf2/ARE activity may lead to different results. Therefore future studies should aim to test a range of active phenolic diterpenes in a variety of models used to study Nrf2/ARE mediated neuroprotection both *in vitro* and *in vivo*.

Acknowledgements

We would like to thank the European Union Seventh Framework Program for funding the Terpmed project, grant number 227448. This work was also partially funded by R01ES08089 and R01ES10042 from the National Institute of Environmental Health Sciences (JAJ).

References

Abreu, M.E., Müller, M., Alegre, L., Munné-Bosch, S., 2008. Phenolic diterpene and α-tocopherol contents in leaf extracts of 60 Salvia species. Journal of the Science of Food and Agriculture 88, 2648–2653.

Bonito, M.C., Cicala, C., Marcotullio, M.C., Maione, F., Mascolo, N., 2011. Biological activity of bicyclic and tricyclic diterpenoids from Salvia species of immediate pharmacological and pharmaceutical interest. Natural Product Communications 6, 1205–1215.

Calkins, M.J., Johnson, D.A., Townsend, J.A., Vargas, M.R., Dowell, J.A., Williamson, T.P., Kraft, A.D., Lee, J.-M., Li, J., Johnson, J.A., 2009. The Nrf2/ARE Pathway as a Potential Therapeutic Target in Neurodegenerative Disease. Antioxidants & Redox Signaling 11, 497–508.

Cuvelier, M.E., Berset, C., Richard, H., 1994. Antioxidant Constituents in Sage (Salvia officinalis). Journal of Agriculture and Food Chemistry 42, 665–669.

de Vries, H.E., Witte, M., Hondius, D., Rozemuller, A.J.M., Drukarch, B., Hoozemans, J., van Horssen, J., 2008. Nrf2-induced antioxidant protection: a promising target to counteract ROS-mediated damage in neurodegenerative disease? Free Radical Biology & Medicine 45, 1375–1383.

Heinrich, M., Kufer, J., Leonti, M., Pardo-de-Santayana, M., 2006. Ethnobotany and ethnopharmacology--interdisciplinary links with the historical sciences. Journal of Ethnopharmacology 107, 157–160.

Itoh, K., Tong, K.I., Yamamoto, M., 2004. Molecular mechanism activating Nrf2-Keap1 pathway in regulation of adaptive response to electrophiles. Free Radical Biology & Medicine 36, 1208–1213.

Johnson, D.A., Andrews, G.K., Xu, W., Johnson, J.A., 2002. Activation of the antioxidant response element in primary cortical neuronal cultures derived from transgenic reporter mice. Journal of Neurochemistry 81, 1233–1241.

Johnson, J.J., 2011. Carnosol: a promising anti-cancer and anti-inflammatory agent. Cancer Letters 305, 1–7.

Kim, S.-J., Kim, J.-S., Cho, H.-S., Lee, H.J., Kim, S.Y., Kim, S., Lee, S.-Y., Chun, H.S., 2006. Carnosol, a component of rosemary (Rosmarinus officinalis L.) protects nigral dopaminergic neuronal cells. Neuroreport 17, 1729–1733.

Kim, S.Y., Park, E., Park, J.A., Choi, B.-S., Kim, S., Jeong, G., Kim, C.-S., Kim, D.K., Kim, S.-J., Chun, H.S., 2010. The plant phenolic diterpene carnosol suppresses sodium nitroprusside-induced toxicity in c6 glial cells. Journal of Agriculture and Food Chemistry 58, 1543–1550.

Kraft, A.D., Johnson, D.A., Johnson, J.A., 2004. Nuclear Factor E2-Related Factor 2-Dependent Antioxidant Response Element Activation by tert-Butylhydroquinone and Sulforaphane Occurring Preferentially in Astrocytes Conditions Neurons against Oxidative Insult. Journal of Neuroscience 24, 1101–1112.

Mimura, J., Kosaka, K., Maruyama, A., Satoh, T., Harada, N., Yoshida, H., Satoh, K., Yamamoto, M., Itoh, K., 2011. Nrf2 regulates NGF mRNA induction by carnosic acid in T98G glioblastoma cells and normal human astrocytes. Journal of Biochemistry 150, 209–217.

Moss, L., Rouse, M., Wesnes, K.A., Moss, M., 2010. Differential effects of the aromas of Salvia species on memory and mood. Human Psychopharmacology 25, 388–396.

Perry, N.S.L., Bollen, C., Perry, E.K., Ballard, C., 2003. Salvia for dementia therapy: review of pharmacological activity and pilot tolerability clinical trial. Pharmacology, Biochemistry, and Behavior 75, 651–659.

Perry, E.K., Pickering, A.T., Wang, W.W., Houghton, P.J., Perry, N.S., 1999. Medicinal plants and Alzheimer's disease: from ethnobotany to phytotherapy. Journal of Pharmacy and Pharmacology 51, 527–534.

Pukalskas, A., van Beek, T.A., de Waard, P., 2005. Development of a triple hyphenated HPLC-radical scavenging detection-DAD-SPE-NMR system for the rapid identification of antioxidants in complex plant extracts. Journal of Chromatography A 1074, 81–88.

Savelev, S.U., Okello, E.J., Perry, E.K., 2004. Butyryl- and acetyl-cholinesterase inhibitory activities in essential oils of Salvia species and their constituents. Phytotherapy Research 18, 315–324.

Scholey, A.B., Tildesley, N.T.J., Ballard, C.G., Wesnes, K.A., Tasker, A., Perry, E.K., Kennedy, D.O., 2008. An extract of Salvia (sage) with anticholinesterase properties improves memory and attention in healthy older volunteers. Psychopharmacology 198, 127–139.

Satoh, T., Kosaka, K., Itoh, K., Kobayashi, A., Yamamoto, M., Shimojo, Y., Kitajima, C., Cui, J., Kamins, J., Okamoto, S., Izumi, M., Shirasawa, T., Lipton, S.A., 2008a. Carnosic acid, a catechol-type electrophilic compound, protects neurons both in vitro and in vivo through activation of the Keap1/Nrf2 pathway via S-alkylation of targeted cysteines on Keap1. Journal of Neurochemistry 104, 1116–1131.

Satoh, T., Izumi, M., Inukai, Y., Tsutsumi, Y., Nakayama, N., Kosaka, K., Shimojo, Y., Kitajima, C., Itoh, K., Yokoi, T., Shirasawa, T., 2008b. Carnosic acid protects neuronal HT22 Cells through activation of the antioxidant-responsive element in free carboxylic acid- and catechol hydroxyl moieties-dependent manners. Neuroscience Letters 434, 260–265.

Tada, M., Okuno, K., Chiba, K., Ohnishi, E., Yoshii, T., 1994. Antiviral diterpenes from Salvia officinalis. Phytochemistry 35, 539–541.

Tamaki, Y., Tabuchi, T., Takahashi, T., Kosaka, K., Satoh, T., 2010. Activated glutathione metabolism participates in protective effects of carnosic acid against oxidative stress in neuronal HT22 cells. Planta Medica 76, 683–688.

Yoshida, H., Mimura, J., Imaizumi, T., Matsumiya, T., Ishikawa, A., Metoki, N., Tanji, K., Ota, K., Hayakari, R., Kosaka, K., Itoh, K., Satoh, K., 2011. Edaravone and carnosic acid synergistically enhance the expression of nerve growth factor in human astrocytes under hypoxia/reoxygenation. Neuroscience Research 69, 291–298.

Appendix Chapter 7

Table A1. ^{1}H-NMR data [δ_H (J, Hz)] $CDCl_3$ 500 MHz (compounds **1**, **5**, **7**)

^{1}H	**carnosic acid**	**12-methoxy-carnosic acid**	**carnosaldehyde**
1α	1.25-1.3 m	1.23 m	1.13 m
1β	3.31 dt (3.6, 13.8)	3.56 m	3.22 m
2α	1.76 dddd (3.5, 8.7, 13.5, 17.1)	2.19 qt (4.5, 14.6)	1.48-1.59* m
2β	1.49 br d (13.3)	1.59 m	1.48-1.59* m
3α	1.57-1.65 m	1.54 m	1.15-1.36* m
3β	1.3-1.36 m	1.30 m	1.15-1.36* m
5	1.59 dd (1.7, 12.7)	1.56 m	1.62 dd (1.7, 12.7)
6α	1.88 m	1.85 m	2.03 m
6β	2.34 tdd (7.0, 10.8, 12.9)	2.28 tdd (6.5, 11.1, 12.9)	1.86 tt (8.7, 13.2)
7α	2.83 m	2.84 m	2.87 dd (3.6, 8.5)
7β	2.83 m	2.84 m	2.87 dd (3.6, 8.5)
14	6.57 s	6.53 s	6.60 s
15	3.19 hept (6.9)	3.17 hept (6.9)	3.23 m
16	1.21 d (6.9)	1.21 d (6.9)	1.21 d (6.9)
17	1.22 d (6.9)	1.21 d (6.9)	1.21 d (6.9)
18	1.01 s	0.98 s	1.04 s
19	0.92 s	0.89 s	0.9 s
20			9.9 d (1.5)
OH	~7.09 br s		7.13 s
OH	~5.71 br s	~6.11 br s	5.78 s
O-Me		3.73 s	

*Signals difficult to assign due to peak overlap. Calibrated to 7.26 ppm.

Table A2. ^{1}H-NMR data [δ_H (J, Hz)] $CDCl_3$ 500 MHz (compound **6**). Calibrated to 7.26 ppm.

^{1}H	sageone
2	2.69 t (7)
3	1.94 t (7)
6	2.39 dd (5.9, 8.1)
7	2.54 dd (5.9, 8)
14	6.58 s
15	3.29 hept (6.9)
16	1.24 d (6.9)
17	1.24 d (6.9)
18	1.27 s
19	1.27 s
OH	9.44 s
OH	6.16 s

Table A3. LC-MS data, APCI ion (percent abundance)

compound	APCI positive [M+H]	APCI negative [M-H]
carnosic acid	not detected	331 (100)
carnosol	331 (80)	329 (100)
epirosmanol	347 (10)	345 (100)
rosmanol	347 (10)	345 (100)
12-methoxy-carnosic acid	not detected	345 (100)
sageone	301 (100)	299 (100)
carnosaldehyde	317 (55)	315 (100)

Table A4. ^{1}H-NMR data [δ_H (J, Hz)] MeOD 500 MHz (compounds **2**-**4**)

^{1}H	**carnosol**	**epirosmanol**	**rosmanol**
1α	2.81 br dd (1.4, 14.3)	2.78 br d (14.3)	1.97 td (5.3, 14.1)
1β	2.57 td (4.4, 14)	2.57 td (4.4, 14)	3.30 *
2α	1.9 m	1.85 dtd (3.1, 10.8, 13.8)	1.62 m
2β	1.6 ddt (3.3, 7.2, 13.8)	1.6 m	1.52 m
3α	1.52 br dd (1.2, 13.1)	1.49 br d (13.2)	1.26 m
3β	1.32 td (3.3, 13.6)	1.32 dt (6.9, 13.6)	1.45 m
5	1.7 dd (5.7, 10.7)	1.38 d (4.1)	2.26 s
6α	1.85 m	4.3 dd (4.2, 4.3)	4.52 d (3.3)
6β	2.19 m		
7α	5.42 br d (2.9)	5.13 d (4.5)	
7β			4.59 d (3.3)
14	6.69 s	6.77 s	6.84 s
15	3.24 hept*	3.26 hept*	3.22 hept (7.1)
16	1.20 d (6.2)	1.22 d (6.1)	1.22 d (6.9)
17	1.19 d (6.5)	1.21 d (6.5)	1.19 d(6.9)
18	0.88 s	1.03 s	1.03 s
19	0.87 s	0.91 s	0.91 s
OH	~7.87 br		
OH	~4.57 br		

*Signals obscured by solvent. Calibrated to 3.31ppm

Figure A1. ^{1}H-NMR spectra of carnosic acid (**1**) 500 MHz $CDCl_3$

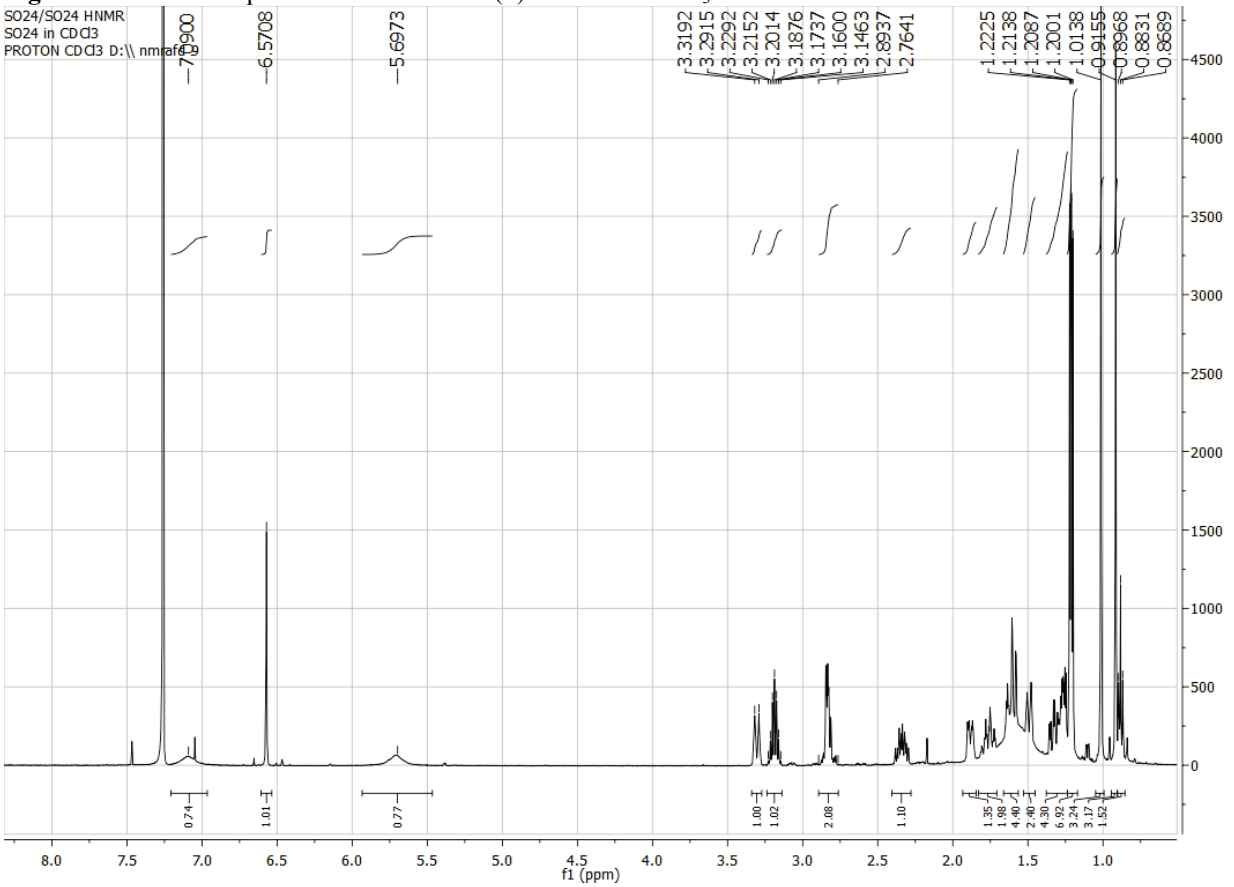

Figure A2. [1]H-NMR spectra of carnosol (**2**) 500 MHz MeOD

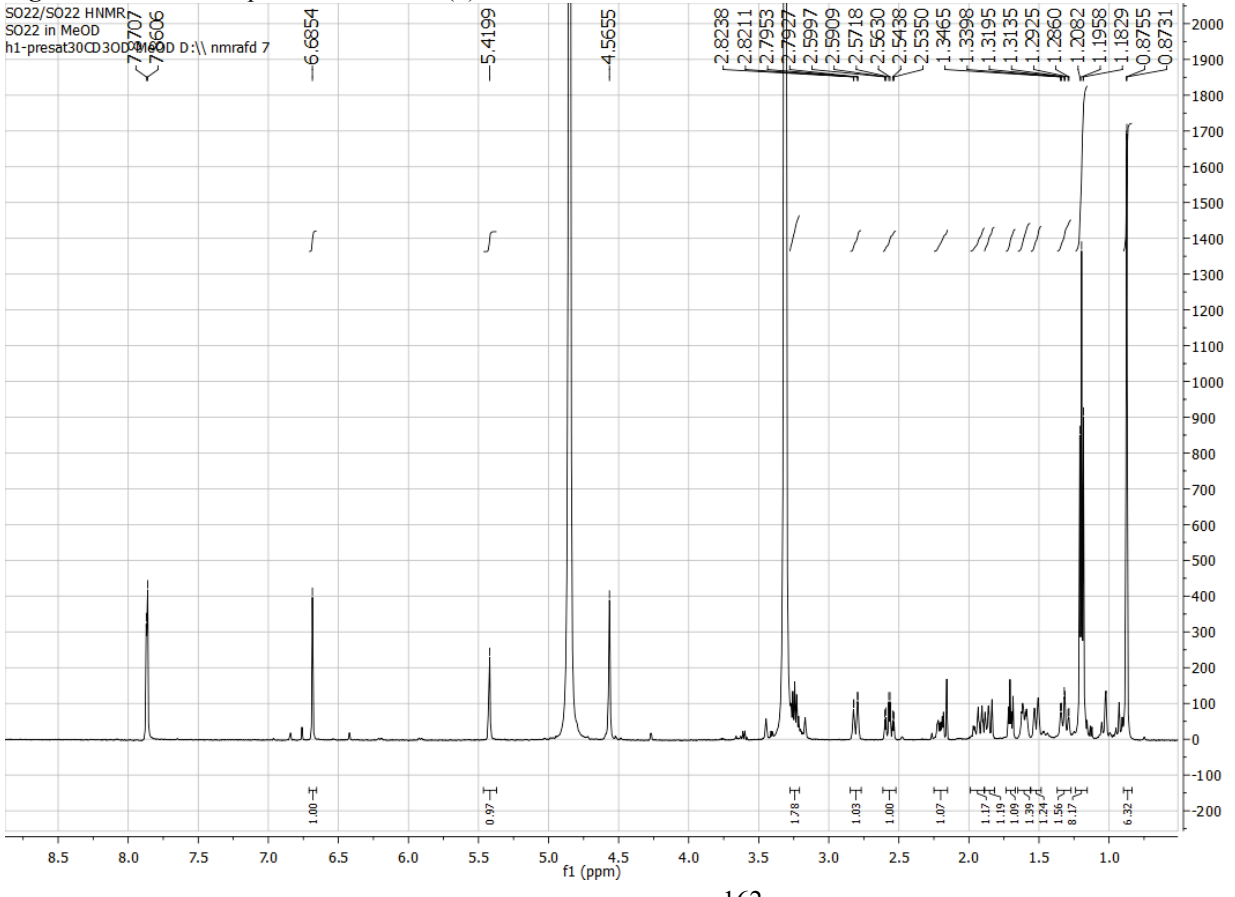

Figure A3. [1]H-NMR spectra of epirosmanol (**3**) 500 MHz MeOD

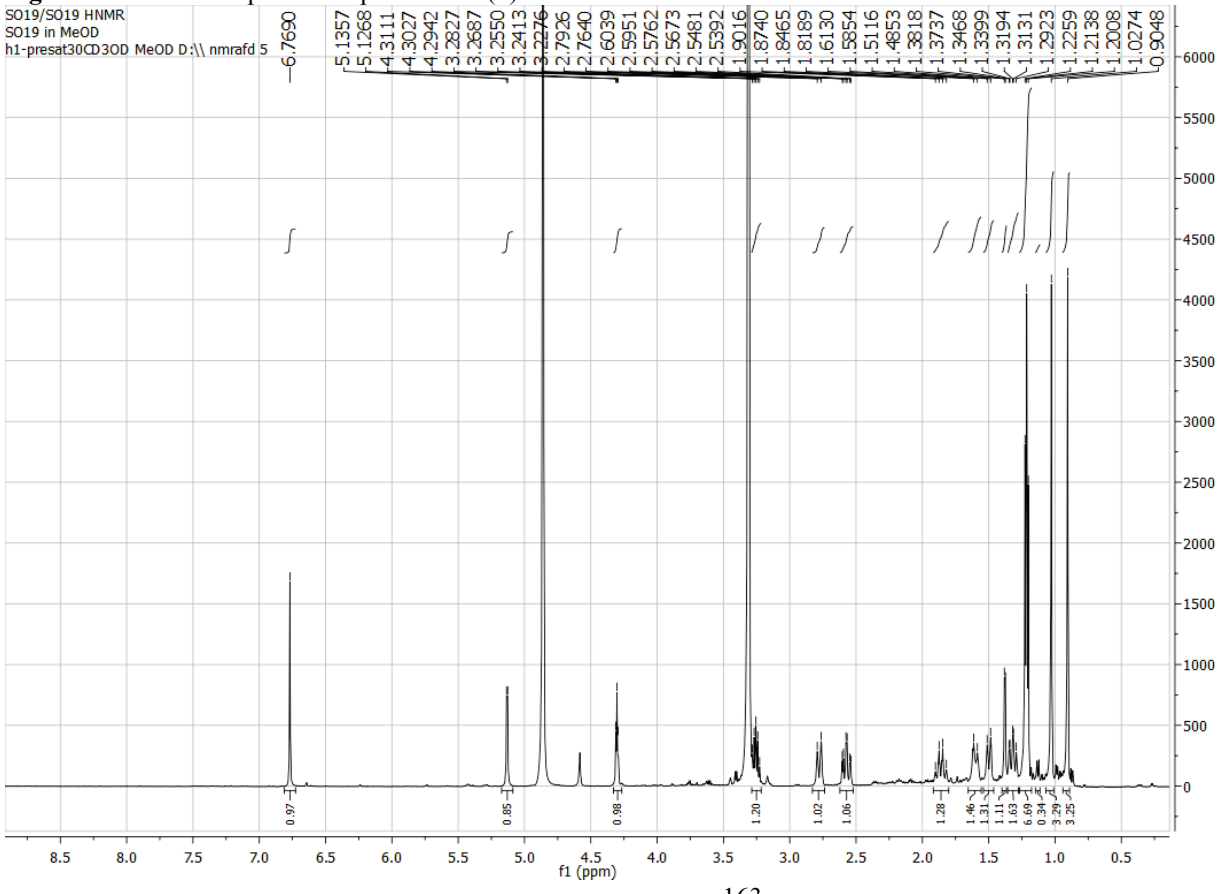

Figure A4. [1]H-NMR spectra of rosmanol (**4**) 500 MHz MeOD

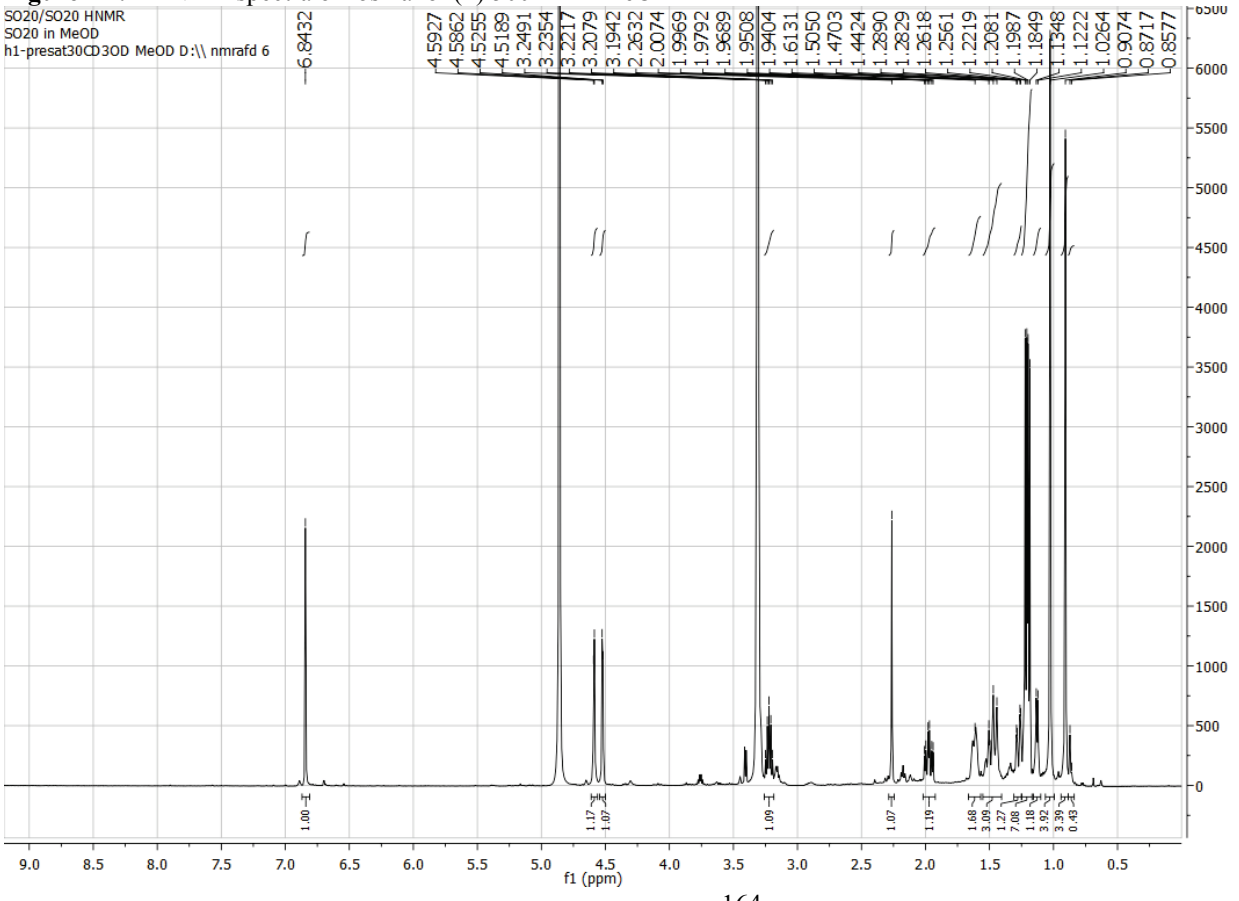

Figure A5. ^{1}H-NMR spectra of 12-methoxy-carnosic acid (**5**) 500 MHz $CDCl_3$

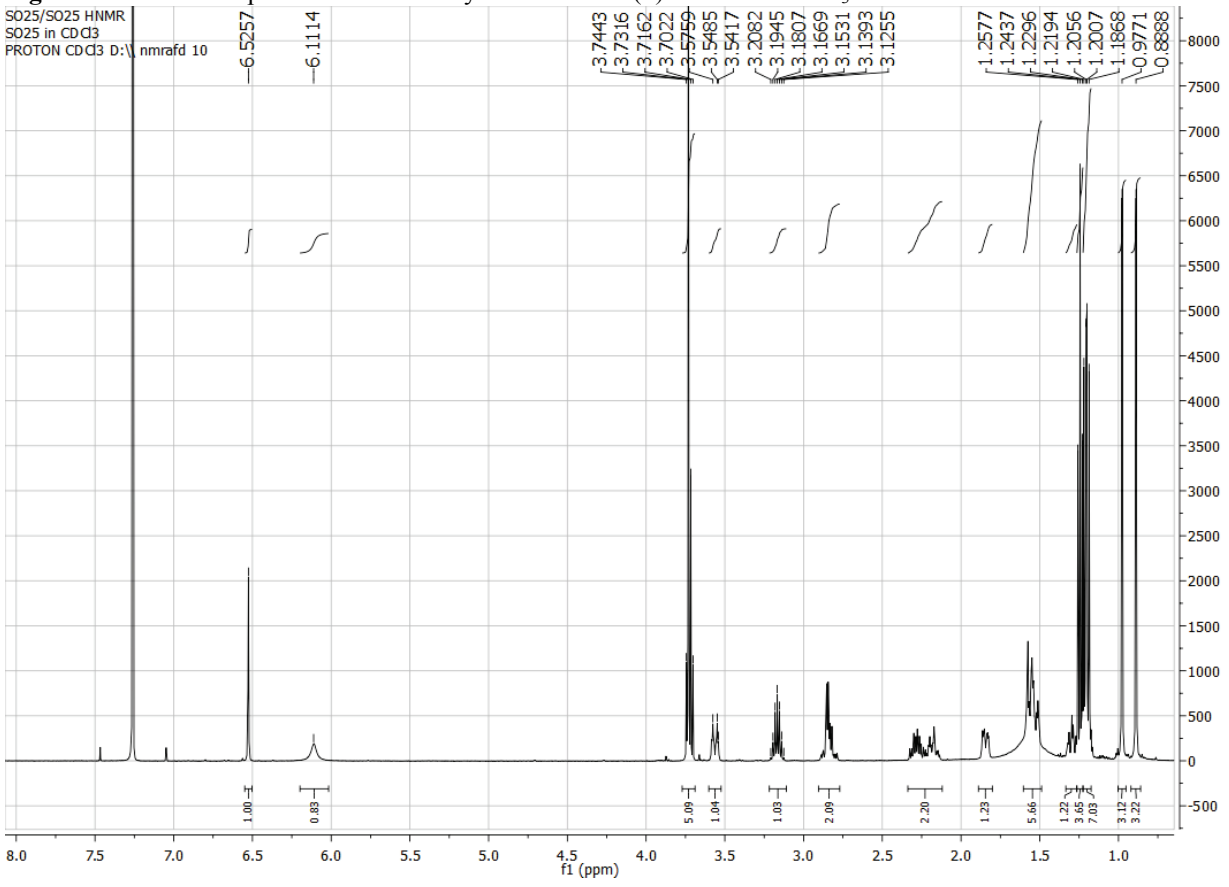

Figure A6. ^{1}H-NMR spectra of sageone (**6**) 500 MHz $CDCl_3$

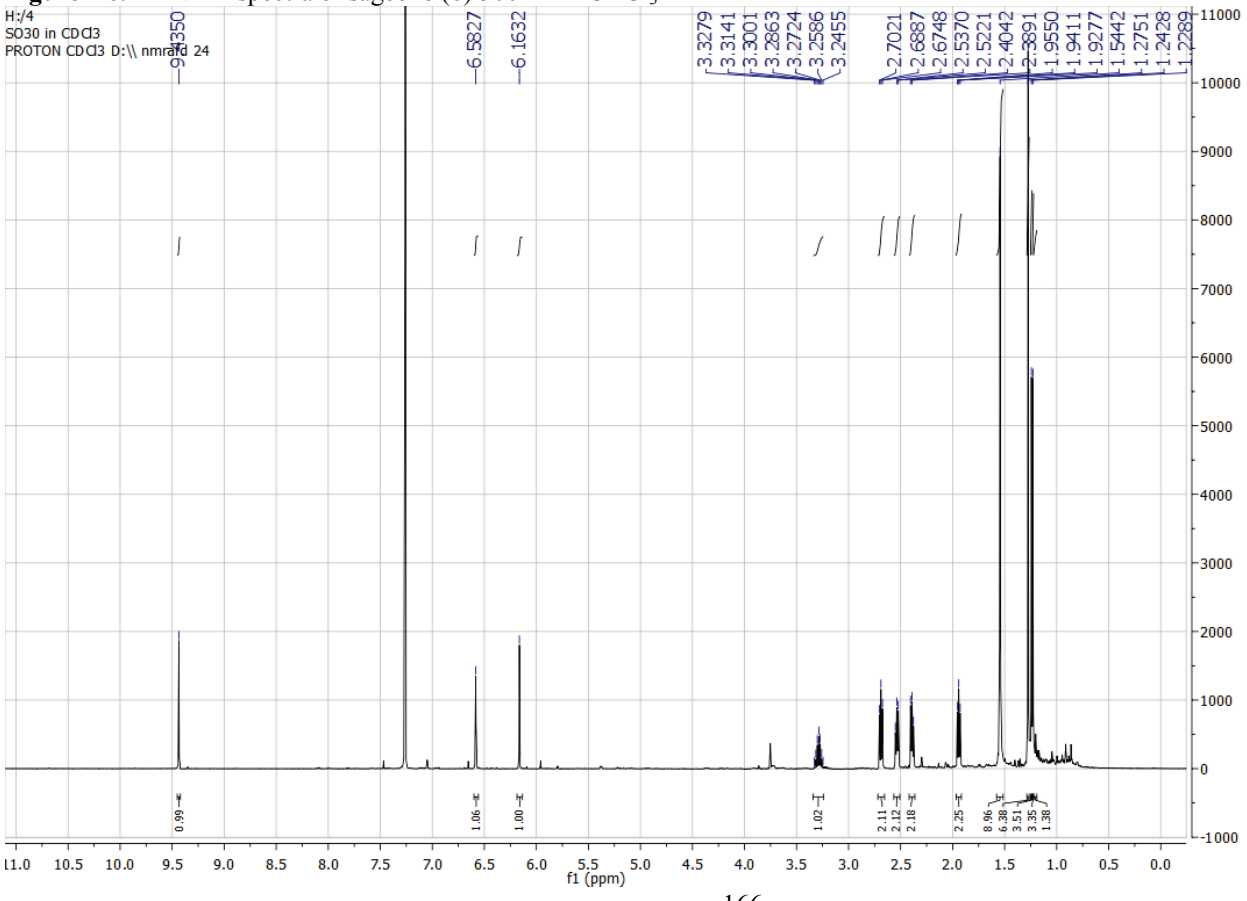

Figure A7. ^{1}H-NMR spectra of carnosaldehyde (**7**) 500 MHz $CDCl_3$

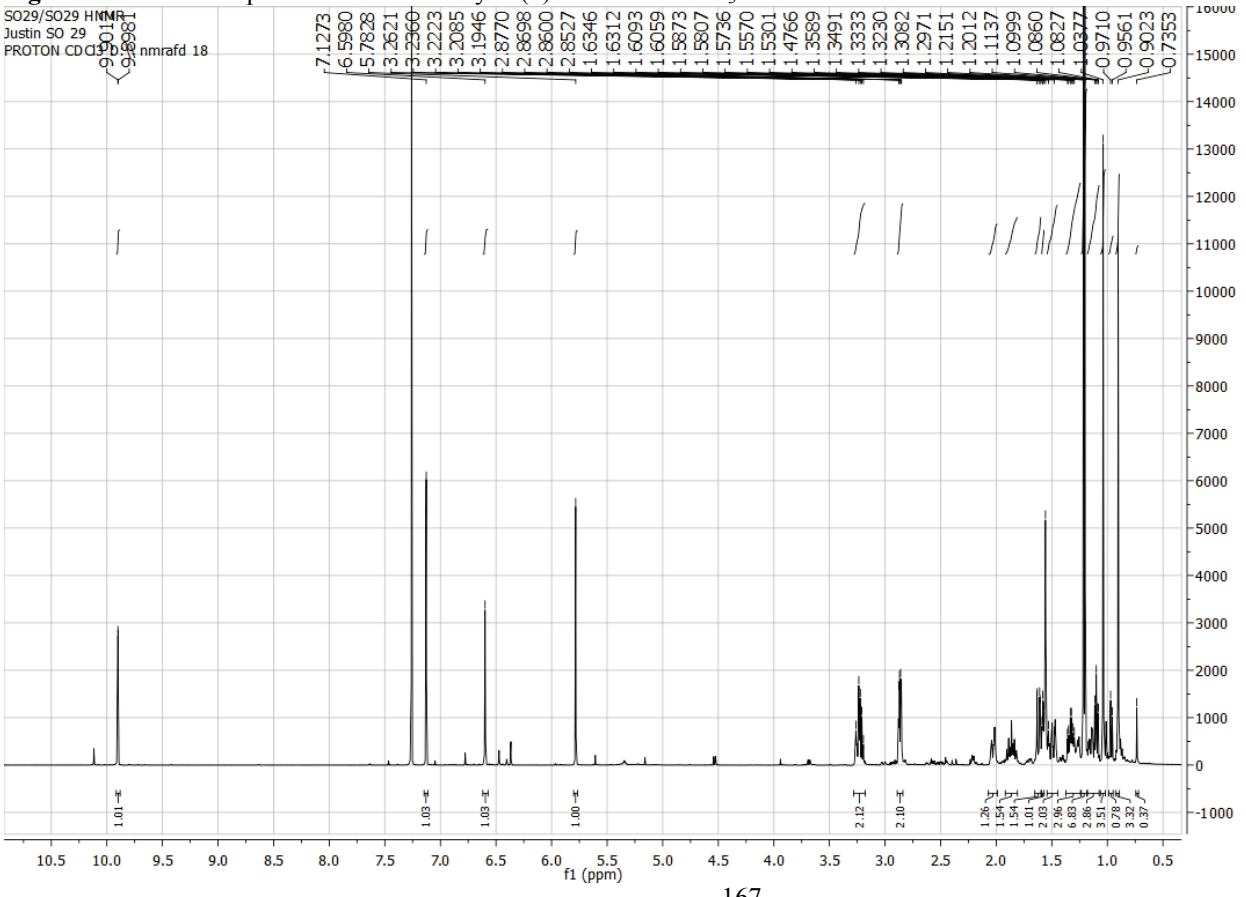

Chapter 8

Conclusions and Future Perspectives

Throughout this thesis numerous aspects of terpenoid chemistry as it relates to medicine were explored. In chapter 2 *Lavandula angustifolia, Thymus vulgaris, Matricaria recutita, Salvia officinalis*, *Eucalyptus globulus,* and *Melissa officinalis* were tested in the Volcano vaporizer. These results confirmed that the vaporizer is capable of volatilizing the main essential oil components from *L. angustifolia, T. vulgaris, M. recutita,* and *S. officinalis* in a reproducible manner. Plants producing essential oils in secretory cavities such as *E. globulus* and those containing low amounts of essential oils such as the batches of *M. officinalis* used in the study are not useful to administer in the vaporizer. However, vaporizers such as the Volcano contain a wire-mesh which allows pure terpenoids or essential oils to be used in the device and heated in the same manner as with plant material. Therefore such devices allow many possibilities for designing clinical protocols. This could improve study design when assessing potential therapeutic effects of essential oil bearing plants.

A more detailed analysis of the vaporizer was performed in chapter 3 using *Cannabis sativa* (cannabis) as a model plant. The cannabis vapor produced by the Volcano did not contain pyrolytic degradation products found in cannabis smoke confirming that the vaporizing is a safer administration method. Furthermore the *in-vitro* CB1 binding of Δ^9-THC was not altered by impurities found in the vapor, smoke, or between the strains. Any additional potential biological effects of other components in cannabis besides Δ^9-THC would be difficult or impossible to study *in-vitro*. The question of whether or not herbal cannabis contains more active ingredients than Δ^9-THC is still an ongoing discussion (Russo, 2011). This question of multiple active ingredients, which is a common question when studying a herbal drug, can only truly be answered with properly designed clinical trials in humans using standardized and chemically defined plant sources.

In chapter 4, cannabis was used as a model plant to determine if the chemical profile could distinguish different varieties. A targeted metabolic profiling approach was developed and validated to chemically classify 11 cannabis varieties according to the terpenoid and cannabinoid content. Indeed the results demonstrated that cannabis varieties can be distinguished based on cannabinoid and terpenoid profiles. Interestingly cannabis varieties with similar levels of Δ^9-THC could be differentiated based on mono and sesquiterpenoid content. Cannabis varieties of the same genotype, grown in multiple batches under the same environmental conditions had reproducible chemical profiles. Although alterations in growth period (number of days vegetative or flowering) seemed to increase quantitative differences in a variety's profile, the differences were minor and qualitatively they were the same. These results would be expected if terpenoid and cannabinoid production in cannabis is genetically regulated and influenced by the environmental conditions.

Figure 1. PCA plot (top) and loading plot (bottom) from Hazekamp and Fischedick, 2012 reprinted with permission. Amnesia samples represented as black triangles, white widow samples as black circles.

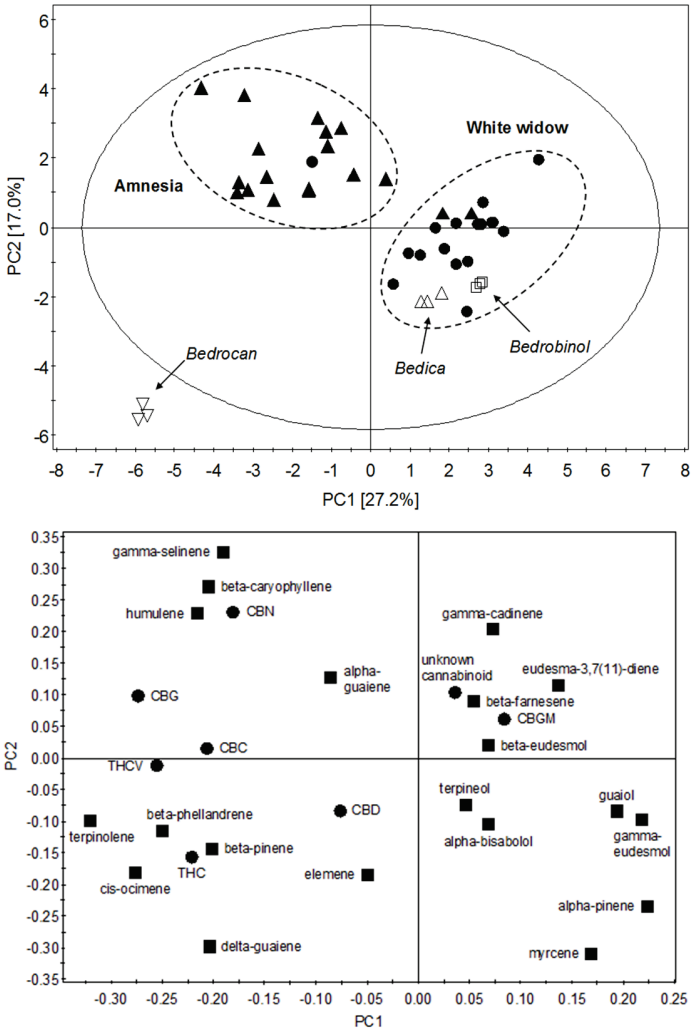

The approach outlined in chapter 4 for analyzing cannabis was extended to evaluate two common cannabis varieties sold in Dutch coffeeshops, known as 'white widow' and 'amnesia'. In this study two 1 gram samples of each variety purchased in 2 separate visits to each coffeeshop (10 coffeeshops total) spread throughout the Netherlands were obtained. By analyzing quantitative data for the terpenoid and cannabinoids both varieties and 3 additional cannabis varieties produced by Bedrocan

BV were clearly distinguished from each other by PCA (Figure 1). These results again demonstrated that cannabis varieties containing similar Δ^9-THC levels could be distinguished by terpenoid profile (Hazekamp and Fischedick, 2012).

Overall the results from chapters 3 and 4 demonstrate that it is possible to standardize a plant producing volatile terpenoids and its administration form. Although cannabis was chosen as a model example due to its complex chemical profile and ongoing clinical research it is in theory possible to take such an approach with any plant or herbal product as long as certain criteria can be met. These criteria include:

1. Standardization of the plant source material or extract
2. Appropriate chemical characterization of the product
3. Standardization of the plant or extracts administration form

Standardization of plant material would be more difficult with plants that cannot be cultivated or propagated asexually. In these cases homogenization of the used plant material or production of standardized extracts would be an alternative. Obviously if an herbal drug is administered as a tea or eaten whole as opposed to inhaled, chemical characterization should utilize an appropriate analytical method such as NMR or HPLC to standardize the procedure. If cannabis is used as an example the following clinical protocol could be envisioned; as treatments two or more cannabis varieties with unique chemical profiles, the isolated essential oil of each variety, equivalent doses of Δ^9-THC as a positive control, and a negative control with no drugs. Administered to humans with a relevant illness one could then conclusively address the question over whether herbal cannabis is more or less therapeutically effective compared with pure Δ^9-THC for that particular illness.

The second half of this thesis (chapters 5-7) focused on sesquiterpene lactones and phenolic diterpenoids as lead compounds for drug development. In chapter 5, eleven sesquiterpene lactones from *Tanacetum parthenium* were screened for their ability to activate the Nrf2/ARE pathway in mouse primary cortical cultures. The structure activity relationship of the compounds confirms the importance of the α-methylene-γ-lactone moiety for activity. Although the data also suggests that other functional groups and the shape or flexibility of the molecule contribute to the activity as well. This observation is consistent with literature concerning the structure activity relationship of sesquiterpene lactones and cytotoxicity (Ghantous et al., 2010). The considerable toxicity of sesquiterpene lactones on primary cortical cultures *in-vitro* as well as available toxicity information in the literature demonstrates that further research is needed to assess the toxicity and selectivity of these compounds *in-vivo*.

In chapter 6, the structure of 5 new sesquiterpene lactones is described along with the structure of 5 known sesquiterpene lactones isolated from *Inula britannica*. Screening the compounds on cancer cell lines, multi-drug resistant cancer cell lines, and human keratinocytes demonstrated again that biological activity was mainly dependent on the presence of α-methylene-γ-lactone moiety. Although no strong trends in

selectivity against any of the cell lines were observed the sesquiterpene lactones were capable of inhibiting drug resistant cancer cell lines. One of the main complications of cancer treatment is the development of resistance of cancer cells to the chemotherapeutic agents. Drugs such as taxol can induce cancer cells to overexpress membrane transporter permeability-glycoprotein-1 which increases the cells ability to pump out the drug and or inhibit its uptake (Podolski-Renić et al., 2011). There is evidence that constitutive activation of NF-$_{\kappa}$B contributes to resistance of cancer cell lines against anti-cancer drugs (Sethi et al., 2012). Inhibition of NF-$_{\kappa}$B by parthenolide was demonstrated as a mechanism by which parthenolide was able to potentiate the ability of taxol to induce cell death in lung cancer both *in-vitro* and *in-vivo* (Zhang et al., 2009). Therefore the relationship between the mechanisms by which anti-cancer drugs induce resistance in cancer cells and the mechanisms by which sesquiterpene lactones may be able to prevent or reverse this process is a promising area for further research.

Figure 2. Dimethylamino-parthenolide.

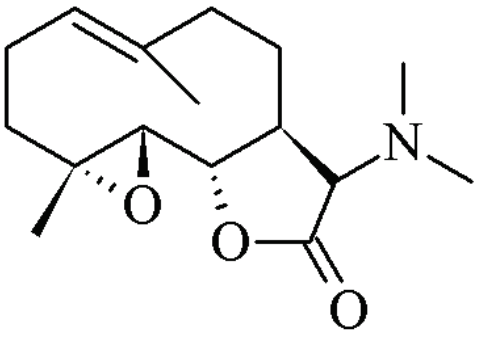

It is important to realize that for over 40 years it has been known that the cytotoxic activity of sesquiterpene lactones is often dependent on the α-methylene-γ-lactone moiety (Kupchan et al., 1971). Furthermore, no sesquiterpene lactones with the α-methylene-γ-lactone moiety have been approved as drugs to date. This is likely due to their lack of selective biological activity and toxicity concerns. In fact as mentioned in chapter 1 sesquiterpene lactones that do not contain the α-methylene-γ-lactone, yet contain other functional groups such as ester side chains or an endoperoxide moiety, such as thapsigargin and artemisinin respectively, are actively being investigated as anticancer drugs. Parthenolide, which shows promising antitumor activity *in-vivo*, suffers from poor pharmacokinetic properties such as low water solubility and poor bioavailability. In order to overcome this problem analogues of parthenolide have been synthesized, such as dimethylamino-parthenolide which shows improved pharmacokinetic properties and maintains antitumor activity *in-vivo* (Figure 2) (Shanmugam et al., 2011).

For these reasons future research into sesquiterpene lactones should avoid compounds with the α-methylene-γ-lactone moiety. The same problems demonstrated in

this thesis will continue to hinder drug development of these compounds. Bioactivity guided fractionation into plant families that often contain sesquiterpene lactones, such as the Asteraceae, may be biased towards sesquiterpene lactones due to the reactivity of the α-methylene-γ-lactone moiety. Researchers analyzing plant families rich in sesquiterpene lactones should aim early on in a bioactivity guided fractionation study to determine if they are present in a plant extract. Column material with active thiols or addition of biological thiols such as cysteine to the extract could potentially be used to remove or inactivate the α-methylene-γ-lactone moiety. This would make it easier for researchers to better assess if other components in the plant material have biological activity. Another area of future research is to chemically modify sesquiterpene lactones that have other interesting functional groups. For example tanaparthin-β-peroxide isolated in chapter 5 contains an endoperoxide moiety. Tanaparthin-β-peroxide was shown to potently activate the Nrf2/ARE pathway in mouse primary cortical cultures, but it was also toxic. Perhaps chemically reducing or modifying the α-methylene group would lead to a compound with more selective biological activity. Unfortunately the *T. parthenium* used in this study only produced low levels of tanaparthin- β-peroxide making such synthetic studies difficult. However, it has been reported that certain chemotypes of *T. parthenium* produce much larger amounts of tanaparthin peroxides (Begley et al., 1989).

In chapter 7, seven phenolic diterpenoids isolated from *S. officinalis* were screened for their ability to activate the Nrf2/ARE pathway in mouse primary cortical cultures. The catechol moiety was demonstrated as being necessary for activation of the pathway. Carnosaldehyde and sageone were toxic towards the cultures indicating structural features that are not desirable such as presence of an aldehyde at C-20 position. The presence of a functional group at the C-7 position also had an influence on activity, increasing hPAP activation in the case of carnosol and rosmanol when compared to carnosic acid. However further experiments are needed to determine which phenolic diterpenoids represent the most promising candidates for drug development. These experiments include determining if phenolic diterpenes are actually increasing cortical cell proliferation or if the MTS assay is giving false positives. Furthermore a direct demonstration of neuroprotection from the most promising compounds in our initial screening, carnosol and rosmanol, should be performed in both *in-vitro* and *in-vivo* experiments. At the time of this writing the follow up *in-vitro* experiments are being performed.

Finally many other *Salvia* species contain abietane diterpenoids with catechol moieties. Some examples include 16-hydroxycarnosic acid from *S. apiana* (Dentali and Hoffmann, 1990), euphraticol from *S. euphratica* (Ulubelen, 1989), and demethylcryptojaponol from *S. phlomoides* (Hueso-Rodríguez et al., 1983) (Figure 3). Another group of diterpenoids found in *Salvia* species that contain catechol moieties are the icetexanes, which include brussonol from *S. broussonetii* and przewalskin C from *S. przewalskii* (Figure 4) (Simmons and Sarpong, 2009). Future research should aim to investigate these and related compounds as potential neuroprotective agents as well. As discussed in previous chapters much of the research performed with *Salvia* species has

focused on the essential oil due to acetylcholinesterase inhibitory activity. Perhaps the phenolic diterpenoids in *Salvia* species may be essential for truly understanding the potential memory enhancing and neuroprotective effects of this valuable medicinal plant.

Figure 3. Abietane diterpenoids from *Salvia* species.

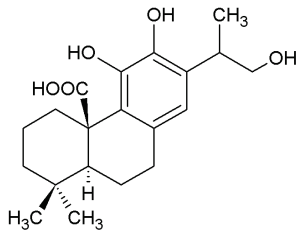

16-hydroxycarnosic acid

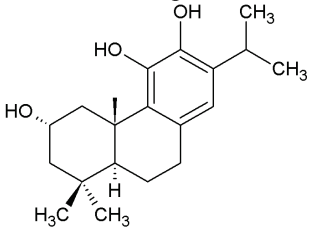

euphraticol

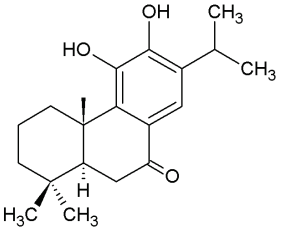

demethylcryptojaponol

Figure 4. Icetexanes from *Salvia* species.

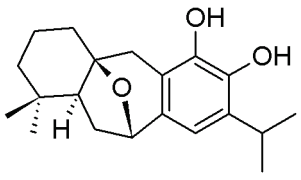

brussonol

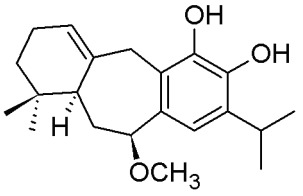

przewalskin C

References

Begley, M.J., Hewlett, M.J., Knight, D.W., 1989. Revised structures for guaianolide α-methylenebutyro-lactones from feverfew. Phytochemistry 28, 940–943.

Dentali, S.J., Hoffmann, J.J., 1990. 16-hydroxycarnosic acid, a diterpene from Salvia apiana. Phytochemistry 29, 993–994.

Ghantous, A., Gali-Muhtasib, H., Vuorela, H., Saliba, N.A., Darwiche, N., 2010. What made sesquiterpene lactones reach cancer clinical trials? Drug Discovery Today 15, 668–678.

Hazekamp, A., Fischedick, J.T., 2012. Cannabis - from cultivar to chemovar. Drug Testing and Analysis 4, 660–667.

Kupchan, S.M., Eakin, M.A., Thomas, A.M., 1971. Tumor inhibitors. 69. Structure-cytotoxicity relationships among the sesquiterpene lactones. Journal of Medicinal Chemistry 14, 1147–1152.

Podolski-Renić, A., Andelković, T., Banković, J., Tanić, N., Ruždijić, S., Pešić, M., 2011. The role of paclitaxel in the development and treatment of multidrug resistant cancer cell lines. Biomedicine & Pharmacotherapy 65, 345–353.

Hueso-Rodríguez, J.A., Jimeno, M.L., Rodríguez, B., Savona, G., Bruno, M., 1983. Abietane diterpenoids from the root of Salvia phlomoides. Phytochemistry 22, 2005–2009.

Russo, E.B., 2011. Taming THC: potential cannabis synergy and phytocannabinoid-terpenoid entourage effects. British Journal of Pharmacology 163, 1344–1364.

Sethi, G., Sung, B., Aggarwal, B.B., 2008. Nuclear factor-kappa B activation: from bench to bedside. Experimental Biology and Medicine 233, 21–31.

Shanmugam, R., Kusumanchi, P., Appaiah, H., Cheng, L., Crooks, P., Neelakantan, S., Peat, T., Klaunig, J., Matthews, W., Nakshatri, H., Sweeney, C.J., 2011. A water soluble parthenolide analogue suppresses in vivo tumor growth of two tobacco associated cancers, lung and bladder cancer, by targeting NF-κB and generating reactive oxygen species. International Journal of Cancer 128, 2481–2494.

Simmons, E.M., Sarpong, R., 2009. Structure, biosynthetic relationships and chemical synthesis of the icetexane diterpenoids. Natural Product Reports 26, 1195.

Ulubelen, A., 1989. Euphraticol and Euphracal, Two New Diterpenes from Salvia euphratica. Journal of Natural Products 52, 1313–1315.

Zhang, D., Qiu, L., Jin, X., Guo, Z., Guo, C., 2009. Nuclear factor-kappa B inhibition by parthenolide potentiates the efficacy of Taxol in non-small cell lung cancer in vitro and in vivo. Molecular Cancer Research 7, 1139–1149.

Summary

The purpose of this thesis was to investigate aspects of terpenoid chemistry relevant to medicine. Specifically, to test vaporizing as a viable administration form for volatile terpenoids, to determine if the chemical profile of *Cannabis sativa* volatiles is useful for chemotaxonomy and reproducible, and to screen sesquiterpene lactones and phenolic diterpenes as drug leads. In **chapter 2** the gas chromatographic analysis of the vapor's produced by the volcano vaporizing device from *Lavandula angustifolia, Thymus vulgaris, Matricaria recutita, Salvia officinalis*, *Eucalyptus globulus,* and *Melissa officinalis* plant material is described. *Lavandula. angustifolia, T. vulgaris, M. recutita,* and *S. officinalis* vapor contained >0.1 mg/g of major essential oil components which increased in concentration with increased temperature. **Chapter 3** compared the vapor, smoke, and ethanol extracts with gas chromatography of three medicinal cannabis varieties produced by Bedrocan BV. The varieties Bedrocan, Bedrobinol, and Bediol produced cannabinoids and mono-terpenoids as major components of their smoke and vapor. Pyrolytic breakdown products were detected in cannabis smoke while none were observed in the vapor. No statistically significant differences in CB1 binding affinity *in-vitro* between pure Δ^9-THC, smoke, and vapor were observed at equivalent concentrations of Δ^9-THC.

In **chapter 4** a quantitative gas chromatography flame ionization detection method is described as well as its validation for analysis of cannabis monoterpenoids, sesquiterpenoids, and cannabinoids. The method was used to quantitatively analyze 11 cannabis varieties. In total 36 compounds were quantified in the 11 varieties and multi-variant data analysis was used to analyze the quantitative data. By using principal component analysis the cannabis varieties could be chemically distinguished from each other. Furthermore, a number of the cannabis varieties were grown in multiple batches to test the reproducibility of the volatile chemical profile. Cannabis varieties that were grown under the same environmental conditions and were of the same genetic stock had a reproducible chemical profiles. Minor deviations in growth period had minor effects on the quantitative levels of volatile compounds.

Chapters 5 and **6** focused on the isolation, structure elucidation, and bioactivity screening of sesquiterpene lactones from *Tanacetum parthenium* and *Inula britannica* respectively. Centrifugal partition chromatography was used as the main fractionation technique. Solvent systems composed of heptane: ethyl acetate: methanol: and water proved effective in separating sesquiterpene lactones from both plants. From *T. parthenium*, 11 sesquiterpenes were isolated and identified by NMR and high resolution mass spectrometry. These compounds were screened *in-vitro* on mouse primary cortical cultures for the ability to activate the Nrf2 pathway. Sesquiterpene lactones with the α-methylene-γ-lactone moiety were able to activate the Nrf2 pathway however they were also toxic towards the cultures. From *I. britannica*, 10 sesquiterpene lactones were isolated and identified by NMR, high resolution mass spectrometry, and infrared spectroscopy. Five of these compounds were never reported previously. Isolated compounds were screened for cytotoxic activity *in-vitro* on human cancer cell

lines, their derived multi-drug resistant cell lines, and normal human keratinocytes. Cytotoxic activity was generally mild, in the micromolar range, and the activity was similar between the different cell types.

In **chapter 7** the isolation of phenolic diterpenoids from *Salvia officinalis* is reported. In total 7 compounds were isolated with polyamide and centrifugal partition chromatography as the main fractionation methods. Carnosic acid, carnosol, epirosmanol, rosmanol, 12-methoxy-carnosic acid, sageone, and carnosaldehyde were identified by NMR and mass spectrometry. Isolated compounds were screened *in-vitro* on mouse primary cortical cultures for the ability to activate the Nrf2 pathway. Carnosic acid, carnosol, epirosmanol, and rosmanol were able to activate the Nrf2 pathway with minimal or no observed toxicity. 12-Methoxy-carnosic acid was inactive while sageone was inactive and toxic. Carnosaldehyde was active but toxic.

The conclusions and future perspectives of this thesis are discussed in detail in **chapter 8**. The main conclusions are that vaporizing is a promising administration form for volatile terpenoids. The volatile chemical profile of cannabis can be used for discriminating between varieties and that if grown under controlled conditions the chemical profile cannabis is reproducible. Sesquiterpene lactones display many biological activities however they often lack the specificity and are generally cytotoxic due to the reactive α-methylene-γ-lactone moiety. Finally, carnosic acid, carnosol, and rosmanol from *S. officinalis* represent interesting lead compounds for development as drugs against neurodegenerative disease.

Samenvatting

Het doel van dit proefschrift was onderzoek te doen naar biochemische aspecten van terpenen die relevant zijn voor de medicinale toepassing en ontwikkeling van deze stoffen.
Meer in het bijzonder richtte het onderzoek zich op verdampen als efficiente toedieningsvorm van vluchtige terpenen, op het analyseren van het terpeen profiel van *Cannabis sativa* als methode voor chemotaxonomie en kwaliteitscontrole, en tenslotte op het screenen van sesquiterpeen-lactonen en fenolische diterpenen als *leads* voor nieuwe medicijnen.

In **hoofdstuk 2** wordt beschreven hoe de vluchtige stoffen van de plantensoorten *Lavandula angustifolia, Thymus vulgaris, Matricaria recutita, Salvia officinalis*, *Eucalyptus globulus,* en *Melissa officinalis* werden vrijgemaakt met behulp van de Volcano® verdamper, en geanalyseerd door middel van gas chromatografie (GC). Damp afkomstig van *L. angustifolia, T. vulgaris, M. recutita,* en *S. Officinalis* bevatte > 0.1 mg terpeen componenten per gram plant materiaal, en deze hoeveelheid nam toe bij toenemende verdamptemperatuur.

In **hoofdstuk 3** worden de damp, (verbrandings)rook, en ethanol extracten van drie verschillende typen medicinale cannabis, geproduceerd door Bedrocan BV, met elkaar vergeleken op basis van GC analyse. Cannabinoiden en monoterpenen waren hoofdbestanddelen in de rook en damp van alle drie de geanalyseerde cannabis varietëiten ‘Bedrocan’, ‘Bedrobinol’ en ‘Bediol’. Pyrolitische afbraakproducten waren wel detecteerbaar in cannabis rook na verbranding, maar niet in de onderzochte damp. In een daaropvolgende *in vitro* assay voor bindingsaffiniteit voor de CB1 receptor werd geen significant verschil gevonden tussen zuivere THC, en rook of damp afkomstig van cannabis met een equivalente concentratie aan THC.

In **hoofdstuk 4** wordt een kwantitatieve GC-FID methode beschreven en validatie voor de analyse van Cannabis monoterpenen, diterpenen en cannabinoiden. De ontwikkelde methode werd vervolgens gebruikt voor de analyse van 11 verschillende cannabis variëteiten. Hierbij werden in totaal 36 verschillende componenten gekwantificeerd, waarna de data werd geanalyseerd met behulp van multi-variate analyse software. Door toepassing van Principle Component Analysis (PCA) konden de verschillende variëteiten tenslotte efficient van elkaar worden onderscheiden op basis van hun chemisch profiel. Een aantal van de bestudeerde variëteiten werden bovendien geteeld in meerdere batches, met als doel om de reproduceerbaarheid van het terpeenprofiel tijdens de teelt vast te kunnen stellen. Cannabis variëteiten die werden gekweekt onder gelijke kweekomstandigheden en die afkomstig waren van dezelfde genetische basis vertoonden inderdaad een reproduceerbaar en herkenbaar chemisch profiel. Kleine afwijkingen in de teeltomstandigheden bleken geen significante invloed te hebben op de kwantitatieve hoeveelheden aan vluchtige terpenen.

Hoofdstukken 5 en 6 richten zich op de isolatie, structuuropheldering en bioactiviteitscreening van sesquiterpeen lactonen afkomstig van *Tanacetum parthenium* and *Inula britannica.* Centrifugale partitie chromatografie (CPC) werd daarbij gebruikt als de belangrijkste methode van fractioneren. Oplosmiddelsystemen bestaande uit specifieke mengsels van heptaan, ethylacetaat, methanol en water toonden zich daarbij het beste voor de scheiding van sesquiterpeen lactonen van beide plantensoorten. Uit *T. Parthenium* konden 11 sesquiterpenen worden geïsoleerd, en vervolgens geïdentificeerd door middel van NMR en hoge resolutie massaspectrometrie. Deze stoffen werden *in vitro* gescreend in muis primary cortical cultures op hun vermogen om de Nrf2 pathway te aktiveren. Sesquiterpeen lactonen met een α-methylene-γ-lacton structuur toonden een interessante activiteit, maar bleken tevens toxisch te zijn voor de gebruikte celcultures. Uit *I. Britannica* werden 10 sesquiterpeen lactonen geïsoleerd en geïdentificeerd met behulp van NMR, hoge resolutie massaspectrometrie en infrarood spectrometrie. Vijf van deze stoffen bleken nooit eerder gerapporteerd. De geïsoleerde verbindingen werden gescreend voor cytotoxische activiteit *in vitro* op humane kankercellijnen, daarvan afgeleide multi-drug resistente cellijnen, en op normale humane keratinocyten. De gevonden cytotoxische aktiviteiten waren over het algemeen beperkt, in de micromolair range, en de relatieve activiteit was vergelijkbaar tussen de verschillende cellijnen.

In **hoofdstuk 7** wordt de isolatie van fenolische diterpenen uit *Salvia officinalis* beschreven. In totaal konden 7 verschillende verbindingen worden geïsoleerd met polyamide kolom chromatografie en CPC als belangrijkste methoden van fractioneren. Carnosic acid, carnosol, epirosmanol, rosmanol, 12-methoxy-carnosic acid, sageone, en carnosaldehyde konden worden geïdentificeerd door middel van NMR en massa spectrometrie. De geïsoleerde verbindingen werden *in vitro* gescreend in muis primary cortical cultures op hun vermogen om de Nrf2 pathway te aktiveren. Carnosic zuur, carnosol, epirosmanol, en rosmanol toonden zich hierbij aktief met minimale of geen toxische werking op de cellen. 12-Methoxy-carnosic zuur en sageone waren niet aktief, en sageone was bovendien toxisch. Carnosaldehyde was actief maar toxisch.

De conclusies en perspectieven van dit proefschrift worden in detail besproken in **hoofdstuk 8**. Enkele van de belangrijkste conclusies daarbij zijn; dat verdampen een veelbelovende methode is voor het (medicinaal) toedienen van vluchtige terpenen; dat het terpeen profiel van cannabis kan worden benut voor het onderscheiden van verschillende variëteiten en dat gestandaardiseerde teelt van cannabis resulteert in een reproduceerbaar terpeen profiel; dat sesquiterpeen lactonen met een α-methylene-γ-lacton structuur verschillende interessante biologische aktiviteiten vertonen, maar dat ze vaak te weinig specifiek zijn en tegelijkertijd te toxisch zijn; en tenslotte dat carnosic zuur, carnosol, en rosmanol uit *S. Officinalis* interessante stoffen zijn voor het ontwikkelen van nieuwe medicijnen voor neurodegeneratieve aandoeningen.

Curriculum Vitae

Justin Fischedick was born January 1st 1984 on Long Island, New York in the United States of America. In 2002 he completed high-school at Sachem School disctrict on Long Island. In 2002 he began undergraduate education at the State University of New York College of Environmental Science and Forestry (SUNY-ESF). During this time he gained valuable lab experience by both working and doing undergraduate research project in biochemistry lab under the direction of Dr. Greg Boyer studying cyanobacterial toxins. In 2006 Justin Fischedick graduated from SUNY-ESF with a bachelor's of science with a focus on biotechnology. From 2006 to 2008 he earned a master's degree in science at the Leiden University, Institute of Biology, Natural Products Laboratory. His research project during this time focused on chemical characterization of *Cannabis sativa* and bioactivity of its essential oil. In 2008 he began a PhD at Leiden University, Institute of Biology, Natural Products Laboratory with a focus on the chemistry of terpenoids.

List of Publications:

Fischedick, J., Standiford, M., Johnson, D., De Vos, R., Todorović, S., Banjanac, T., Verpoorte, R., Johnson, J., 2012. Activation of Antioxidant Response Element in Mouse Primary Cortical Cultures with Sesquiterpene Lactones Isolated from Tanacetum parthenium. Planta Medica 78, 1725–1730.

Fischedick, J.T., Hazekamp, A., Erkelens, T., Choi, Y.H., Verpoorte, R., 2010. Metabolic fingerprinting of Cannabis sativa L., cannabinoids and terpenoids for chemotaxonomic and drug standardization purposes. Phytochemistry 71, 2058–2073.

Fischedick, J., Van Der Kooy, F., Verpoorte, R., 2010. Cannabinoid receptor 1 binding activity and quantitative analysis of Cannabis sativa L. smoke and vapor. Chemical Pharmaceutical Bulletin 58, 201–207.

Fischedick, J.T., Glas, R., Hazekamp, A., Verpoorte, R., 2009. A qualitative and quantitative HPTLC densitometry method for the analysis of cannabinoids in Cannabis sativa L. Phytochemical Analysis 20, 421–426.

Hazekamp, A., Fischedick, J.T., 2012. Cannabis - from cultivar to chemovar. Drug Testing and Analysis 4, 660–667.

Hazekamp, A., Fischedick, J.T., Díez, M.L., Lubbe, A., Ruhaak, R.L., 2010. 3.24 - Chemistry of Cannabis, in: Comprehensive Natural Products II. Elsevier, Oxford, pp. 1033–1084.

Acknowledgements

I would like to thank the European Union Seventh Framework Program for funding the Terpmed project, grant number 227448 and the Technologiestichting STW foundation for funding the GMP production of cannabinoids and their metabolites, project number 07426. Both of these projects funded the majority of my PhD research. I would also like to thank PRISNA BV for hiring me to work on the Terpmed project. Finally I thank all members of the Leiden University, Natural Products Laboratory both past and present for making this a very productive learning experience and a special time in my life.